博士論文

論文題目 Three Point Functions in AdS_5/CFT_4 Correspondence and Integrability (AdS_5/CFT_4 対応における三点関数と可積分性)

氏名　小松　尚太

Doctoral Dissertation

Three Point Functions in $\mathbf{AdS_5/CFT_4}$ Correspondence and Integrability

Shota Komatsu

A thesis submitted to
the University of Tokyo, Komaba,
Graduate school of Arts and Sciences

Tokyo, Japan, March, 2014

Abstract

This dissertation is devoted to the study of three-point functions in the $\mathrm{AdS}_5/\mathrm{CFT}_4$ correspondence, which is a conjectural duality between the $\mathcal{N} = 4$ super Yang-Mills theory in four dimensions and the type IIB superstring theory on a certain ten-dimensional curved space called $AdS_5 \times S^5$ spacetime. The main objective of the thesis is to explain how the integrability-based approaches help to simplify the computation of three-point functions and enable us to extract the structures common to both sides of the duality.

After a general introduction of the AdS/CFT correspondence, we begin with a brief review of the integrability structures in the gauge and the string theory found originally in the study of two-point functions. Then, in Part II, we review the perturbative computation of the three-point functions in the gauge theory and explain that it can be reformulated as a problem of evaluating the scalar products between two different states of a certain integrable spin chain. Next we summarize several existing expressions for such scalar products and discuss their behavior in the *semi-classical* limit, in which the length of the chain and the number of excitations are both large. Then we derive a new concise formula for such scalar products, which is expressed as a multiple integral akin to the eigenvalue integrals in the matrix models, and discuss that it is potentially useful to get a more physical picture of the semi-classical limit.

In Part III, which is a main part of this thesis, we explain the computation of three-point functions in the string theory. The strong coupling limit of the gauge theory is known to be described by the classical string theory on $AdS_5 \times S^5$. Thus the three-point functions in such a limit can be evaluated by computing the classical action of the three-pronged world-sheet plus the boundary terms, which come from the wave function of each string state. An important observation to be made is that both contributions are expressible in terms of the quantities, called *Wronskians*, which fit naturally into the framework of the integrability-based approach. We evaluate the Wronskians by setting up a certain Riemann-Hilbert problem and solving it. The resultant expression for the three-point function turns out to be remarkably simple in spite of the complexity of the contributions from various parts in the intermediate stages. In addition, it exhibits the structure similar to the one obtained in the gauge theory. We then perform a detailed comparison with the results in the gauge theory and discuss the implications.

Finally, in Part IV, we summarize the results explained in this thesis and conclude by mentioning open problems and future directions.

Acknowledgements

I would like to express my sincere gratitude to many people I met during my doctoral studies.

First and foremost, I would like to thank my advisor Yoichi Kazama for his guidance and assistance in my Ph.D. studies and, more importantly, for the fruitful collaborations and the stimulating discussions. It was always exciting experience for me to discuss with him various topics in string theory and physics in general. The discussion with him always deepened my understanding and broadened my perspective substantially. Second I would like to thank all the collaborators. I am particularly grateful to Daigo Honda and Takuya Nishimura as the works done in collaboration with them constitute important parts of this thesis.

I would also like to express my gratitude to all the former and current members of the particle theory group at Komaba for creating the enjoyable and at the same time stimulating environment. In particular, I feel indebted to Tetsuo Horigane and Toshifumi Noumi for innumerable discussions on the AdS/CFT correspondence.

I must also thank Pedro Vieira for giving wonderful lectures on three-point functions at the lecture series *Komaba 2013* and inviting me to the Perimeter Institute. Visiting the Perimeter Institute and working there in its stimulating scientific environment was an irreplaceable experience. My gratitude also goes to other members at the Perimeter Institute, in particular to João Caetano, Davide Gaiotto, Amit Sever, Jonathan Toledo and Tianheng Wang.

In the course of my Ph.D. studies, I have benefited also from discussions with various other people. As it is impossible to list them all, let me name a few of them, to whom I feel particularly indebted. I would like to thank Ivan Kostov, Didina Serban and Yunfeng Jiang for inspiring discussions on three-point functions and Io Kawaguchi, Kazuhiro Sakai, Ryo Suzuki and Kentaroh Yoshida for discussions on related topics.

Last but not least, I would like to thank my family for their support.

Contents

Part I

Introduction and Background

Chapter 1

General introduction

1.1 Prelude

String theory, first conceived in the late 1960s as a theory of hadrons, was once abandoned after the advent of quantum chromodynamics (QCD) because it predicted the existence of unrealistic massless particles and required the spacetime dimension to be 10. However, it was subsequently realized that these "unrealistic" massless particles could describe gravitons and the theory resurrected as a leading candidate for the unified theory of all interactions including gravity.

String theory, comprised not of zero-dimensional particles but of one-dimensional strings, has two main features which make it distinct from conventional quantum field theories (see Figure 1.1.1). The first feature, perhaps the most well-known one, is that a single string is capable of describing infinitely many kinds of particles including gravitons as vibration modes. This is often regarded as the most important and the most fundamental property which makes string theory a candidate for a theory of everything. However, this feature captures only a partial aspect of the theory as it tells just about the spectrum of the particles and nothing about their interactions. What is truly important for string theory to be a consistent theory of all interactions is the following second feature: Infinitely many types of interactions for infinitely many kinds of particles are described in a unified way by the geometric structure of the string worldsheet, which glues or splits when the interaction occurs. This is quite a remarkable property since it is inconceivable anyhow in conventional field theories that the interactions admit such sort of geometric interpretation.

Vigorous studies in the past thirty years have revealed another important but slightly bizarre facet of string theory, called *duality*. Duality is a phenomenon that two seemingly different theories secretly describe the same physical situation. Of course, duality itself is

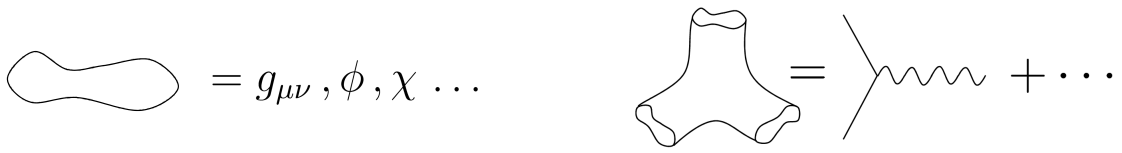

Figure 1.1.1: Two important characteristics of string theory: The realization of infinitely many particles as vibration modes (left) and the geometric realization of the interactions (right).

not peculiar to string theory as the longest-known example of duality is the century-old electric-magnetic duality. However, a distinctive feature of string theory is that it predicts various new dualities, some of which link theories in totally different guises; they often have completely different properties and sometimes are defined in different dimensions. Today, duality has become one of the essential ingredients in string theory, which helps to bring together diverse theoretical ideas.

Among numerous dualities found in string theory, the one which has been intensively studied in the past fifteen years is the *AdS/CFT correspondence* [1–3]. The AdS/CFT correspondence is a conjectural duality between a d-dimensional conformally invariant field theory and a $d+1$-dimensional quantum gravity on the anti-de Sitter space. It is a concrete realization of the old idea, called *holography* [4, 5], that the dynamics of quantum gravity is describable in terms of the degrees of freedom living on the boundary of the spacetime. As such, the AdS/CFT correspondence has had an immense impact on diverse areas of theoretical physics: On the one hand, it is considered to provide a non-perturbative formulation of quantum gravity in terms of conventional quantum field theories. On the other hand, it has enabled us to explore the strongly-coupled regime of interacting gauge theories via gravity. Looking back on the history of string theory, the discovery of the AdS/CFT correspondence marks a major milestone. It fulfills the dearest dream in the early days of string theory in rather an unexpected way: String theory indeed describes non-Abelian gauge theories, but only indirectly through the holography.

Despite its theoretical importance, fundamental understanding as to why and how the AdS/CFT correspondence holds is still missing even after fifteen years. To provide a motivational introduction for the rest of this thesis, below we shall attempt a brief but incomplete "derivation" of the duality. The object, which plays an important role in the heuristic derivation below, is a *D-brane*, a higher-dimensional membrane-like object at which strings can end. In the presence of the D-branes, the worldsheet of a closed string can have several holes, at which the string interacts with the D-branes (see Figure 1.1.2). Thus, the scattering amplitude of the string off the D-branes is evaluated by summing over all possible worldsheets with a different number, different positions and different sizes of the holes. In the low-energy

limit, such summation is known to reproduce the summation over the Feynmann diagrams of a certain non-Abelian gauge theory, and the scattering amplitude of the D-branes and the string is interpreted as a physical observable of the gauge theory. As a result of summation over the holes, the dynamics of the closed string will be substantially modified. Such a modified dynamics can often be described alternatively in terms of the "effective theory", in which the effect of the D-branes is replaced with some "effective potential". Since a D-brane warps the spacetime by emitting gravitons, which are massless and non-negligible even in the infrared limit, the effective description in the low-energy limit is provided by a certain curved geometry. The equivalence of the above two descriptions, the gauge theory and the curved geometry, is the gist of the AdS/CFT correspondence. The most difficult step to concretize the above heuristic argument is to perform the sum over the holes explicitly and prove the equivalence with the effective description in terms of the curved geometry. Such summation has been performed only in a few examples, most of which are simple "toy models" such as topological string [6–9] and non-critical string [10, 11]. The only known example in the ordinary string theory is the *imaginary D-branes* [12], the D-branes aligned along the imaginary time axis. In all these examples, owing to simple dynamics or as a result of Wick rotation, nontrivial contributions come mainly from holes of infinitesimal size. As an infinitesimal hole can be naturally replaced with some local operator insertion $\mathcal{W}$, the summation can be performed explicitly in such cases as follows[1]:

$$\sum_n \frac{g_s^n}{n!} \left(\int d^2z\, \mathcal{W} \right)^n \to \exp\left(g_s \int d^2z\, \mathcal{W} \right) . \tag{1.1.1}$$

This expression makes it clear that the summation modifies the action of the closed string by $g_s \int d^2z\, \mathcal{W}$ and deforms the background geometry[2]. However, in most of the nontrivial examples of the AdS/CFT correspondence, including the *AdS_5/CFT_4 correspondence* to be discussed in detail in this thesis, there is no a priori reason to expect that the sum is

[1] This explanation is intuitive but at the same time somewhat misleading. A more precise statement is as follows: In general, the contributions from holes can be decomposed into those from the on-shell closed strings and those from the off-shell closed strings. However, in all the solved examples, the off-shell contributions are absent. Then, we can replace the remaining on-shell contributions with the vertex operators $\mathcal{W}$ by using the standard state-operator correspondence. Owing to the marginality of the on-shell vertex operators, the position integration $\int d^2z\mathcal{W}$ is completely well-defined in such cases. Therefore, the summation can be performed explicitly as shown in (1.1.1). Note that although the integration over the size of the holes generally produces a propagator of the closed string, $1/(L_0 + \bar{L}_0)$, which diverges when the state is on-shell, such a factor cannot project away all the off-shell states. To realize the projection, we need the term of the form $\delta(L_0 + \bar{L}_0)$ instead of $1/(L_0 + \bar{L}_0)$. In the case of imaginary D-branes, $\delta(L_0 + \bar{L}_0)$ appears naturally from the propagator as a result of Wick rotation. However, for more general cases, a supplementary mechanism is necessary to realize such projection.

[2] To the author's knowledge, the first work which discussed such a possibility is the paper by Green and Polchinski [13].

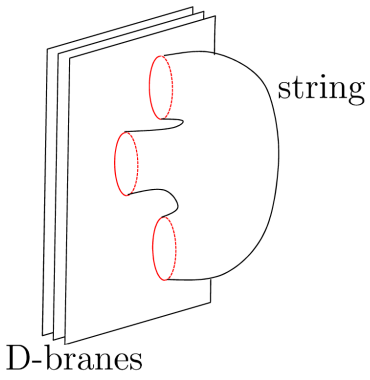

Figure 1.1.2: The worldsheet of a string in the presence of D-branes. The worldsheet has several boundaries (depicted in red) at which the string interacts with the D-branes.

dominated by infinitesimal holes[3] owing to the lack of any simplification mechanism. Thus, in most cases, the above heuristic argument is yet to be made rigorous and the duality is still to be proven.

In short of any rigorous arguments, the best thing we could try is to compute the observables on both sides of the duality and compare them. As the dual gauge theory is conformally invariant, there is no clear notion of particles or asymptotic states, with which we compute S-matrices. Instead, the most natural and the most fundamental objects in the theory are *local operators* and the counterparts of the S-matrices are provided by their *correlation functions*. Of particular interest among these are two- and three-point functions, which together constitute the building blocks of the dual gauge theory: One can express any correlation functions in the theory in terms of two- and three-point functions by performing the operator product expansion[4]. Remarkably enough, they are intimately related to the aforementioned two important characteristics of string theory; the realization of infinitely many kinds of particles as vibration modes and the geometric description of their interactions. In the AdS/CFT correspondence, the two-point function is considered to describe a free propagation of a vibrating string in the AdS spacetime and the strength and the direction of the vibration are reflected in the quantum numbers of the local operators. On the other hand, the three-point function is believed to describe their interactions and the interaction strength is encoded in the scalar factor, called the *structure constant*. Therefore,

[3]We should add that, in an attempt to sum over holes of the planar diagrams using the lightcone gauge [14], it was suggested that the sum may be dominated by small holes also in the case of the AdS_5/CFT_4 correspondence.

[4]Operator product expansion itself can be performed in any quantum field theory. However, in general, it is not clear if the expansion has a finite radius of convergence. In conformal field theories, it does have a finite radius of convergence thanks to the conformal symmetry the theory possesses.

although we lack a first-principle proof of the AdS/CFT correspondence, it would still be possible to gain new insights into the fundamental mechanism of the duality, which is yet enigmatic, by closely examining two- and three-point functions and clarifying their relations to the attributes of string theory.

In this thesis, we mostly focus on three-point functions, and explain the efficient methods to study them, which are based on the powerful techniques called integrability. As stated above, three-point functions are of crucial importance since they encode the dynamical information of the gauge theory and are considered to describe the interactions of the strings. However, it is not yet understood how the geometric structure of the worldsheet, which is an essential feature of the dual string theory, is realized in the three-point functions in the gauge theory. We believe that attempts made in this thesis will pave the way for deciphering such mysteries in the AdS/CFT correspondence.

1.2 Outline of the thesis

This thesis is devoted to the study of three-point functions in the most typical example of the AdS/CFT correspondence, called the $\mathrm{AdS}_5/\mathrm{CFT}_4$ correspondence, which is a conjectural duality between the $\mathcal{N} = 4$ super Yang-Mills theory in four dimensions and the type IIB superstring theory on a certain ten-dimensional curved space, called $AdS_5 \times S^5$ spacetime. The main objective of the thesis is to explain how the integrability-based approaches help to simplify the computation of three-point functions and enable us to extract the structures common to both sides of the duality.

In the rest of Part I, we first give a general introduction of the $\mathrm{AdS}_5/\mathrm{CFT}_4$ correspondence. Then, we review how the integrability-based techniques enabled us to compute two-point functions on each side of the duality. In Part II, we review the perturbative computation of three-point functions in the gauge theory and explain that the computation can be reformulated as a problem of evaluating the scalar products between two different states of a certain integrable spin-chain. Next we summarize several existing expressions for such scalar products and discuss their behavior in the *semi-classical* limit, in which the length of the chain and the number of excitations are both large. Then we derive a new concise formula for such scalar products, which is expressed as a multiple integral akin to the eigenvalue integrals in the matrix models, and discuss that it is potentially useful to get a more physical picture of the semi-classical limit.

In Part III, which is a main part of this thesis, we explain the computation of three-point functions on the string theory side. After recalling the well-known fact that the strong coupling limit of the gauge theory can be described alternatively by the classical string theory

on $AdS_5 \times S^5$, we explain that the three-point function in such a limit can be computed by evaluating the classical action of a three-pronged worldsheet plus the boundary terms, which come from the semi-classical wave function of each string. Then we describe the integrability-based method to compute these two contributions: First, we show that both of the contributions are expressible in terms of the important quantities, called *Wronskians*, which fit naturally into the framework of integrability. Next, we examine the analytic properties of the Wronskians and set up the Riemann-Hilbert problem. Then, we determine each Wronskian by solving the Riemann-Hilbert problem in terms of certain convolution integrals, and present a fairly general formula for three-point functions at strong couping. In spite of the complexity of the contributions from various parts in the intermediate stages, the final answer for the three-point function takes a remarkably simple form, exhibiting the structure reminiscent of the one obtained in the gauge theory. We then perform a detailed comparison with the results in the gauge theory and discuss the implications.

Finally, in Part IV, we summarize the results explained in this thesis and conclude by mentioning future directions.

Before ending this introductory chapter, let us clarify which parts of the thesis are based on the author's works. All of Part I and most of Part II are devoted to a review of known results and hence do not contain any original materials. An exception is chapter 5 in Part II, in which we derive a new integral formula for the scalar products of the XXX spin-chain, based on the author's work [15]. On the other hand, Part III is based heavily on the author's works [16–18] and most of the materials derived in this part are new and original.

Chapter 2

$\mathrm{AdS}_5/\mathrm{CFT}_4$ correspondence

The goal of this chapter is to introduce basic facts about the $\mathrm{AdS}_5/\mathrm{CFT}_4$ correspondence. In section 2.1, we present a heuristic argument connecting $\mathcal{N} = 4$ super Yang-Mills theory ($\mathcal{N} = 4$ SYM) and type IIB superstring theory on the $AdS_5 \times S^5$ spacetime based on the seminal paper [1]. In the course of discussion, we also explain the basics of the WKB analysis of quantum mechanics, which will play an important role later in Part III. Next, in section 2.2, we explain how the symmetry and the physical observables in two theories are related.

2.1 $\mathrm{AdS}_5/\mathrm{CFT}_4$ correspondence

In the ground-breaking paper [1], which appeared in late 1997, a remarkable duality between certain superconformal field theories with maximal supersymmetry and superstring theories on the anti-de Sitter spacetime was conjectured. The paper spurred rapid subsequent developments and an innumerable number of scientific articles discussing this duality have been written since then. Among numerous variants of such dualities, the most well-studied one is the duality between $\mathcal{N} = 4$ super Yang-Mills theory and type IIB superstring theory on the $AdS_5 \times S^5$ spacetime, which is often called the *AdS_5/CFT_4 correspondence*. In what follows, following the argument of [1], we will explain how to understand the existence of such a correspondence.

The starting point of discussion is to consider a stack of D3-branes, which are $3 + 1$-dimensional membrane-like objects existing in type IIB superstring theory. As briefly mentioned in section 1.1, the AdS/CFT correspondence can be understood by describing this physical system in two different ways. Below we shall explain two descriptions in order.

2.1.1 Low-energy excitation on D-branes

Type IIB superstring theory is a closed string theory defined in ten-dimensional spacetime. The only scale parameter in this theory is the *tension* of a string, T_s, which is related to the length scale of a string ℓ_s as

$$T_{\rm s} = \frac{1}{2\pi\ell_s^2}\,. \tag{2.1.1}$$

The tension and the length scale determine the strength of the quantum fluctuations on the world-sheet and, when ℓ_s goes to zero (and T_s goes to infinity), the string becomes infinitely rigid and the motion of strings becomes classical. The other important parameter in this theory is the *string coupling constant* g_s, which governs the interaction strength and determines the joining and splitting probability of strings. In string theories defined on a flat spacetime, a string acquires mass M depending on the strength of the oscillation as

$$M^2 = \frac{4N_{\rm osc}}{\ell_s^2}\,. \tag{2.1.2}$$

Here $N_{\rm osc}$ is an integer which describes the strength of the oscillation. Of particular importance in the following discussion are massless modes, namely the modes with $N_{\rm osc} = 0$, which govern the low-energy dynamics of the theory. In the case of type IIB superstring theory, massless modes consist of gravitons $g_{\mu\nu}$, NS-NS two-forms $B_{\mu\nu}$, a dialton ϕ, an axion χ, R-R two-forms $C_{\mu\nu}$ and R-R four-forms $C_{\mu\nu\rho\sigma}$ and their supersymmetric partners. The theory which consists only of these massless modes is known as type IIB supergravity and its action is schematically given as follows:

$$S_{IIB} = \frac{1}{16\pi G_N^{(10)}}\int d^{10}x\sqrt{-g}R + \cdots\,, \tag{2.1.3}$$

where $G_N^{(10)}$ is the ten-dimensional Newton constant. We can relate $G_N^{(10)}$ with the parameters in superstring theory by computing observables, such as tree-level scattering amplitudes, in two theories and comparing their results. As a result of such comparison, we obtain the following relation:

$$G_N^{(10)} = 8\pi^7\ell_s^8 g_s^2\,. \tag{2.1.4}$$

In the presence of N D3-branes, another kinds of excitations, the excitations of open strings whose ends are attached to D-branes, also exist. By quantizing such open strings, we obtain a set of modes akin to (2.1.2), whose massless part precisely coincides with the spectrum of the maximally supersymmetric U(N) gauge theory, known as $\mathcal{N} = 4$ SYM. The action of $\mathcal{N} = 4$ SYM is schematically given by

$$\frac{1}{2g_{\rm YM}^2}\int d^4x{\rm tr}\left[-\frac{1}{2}\left(F_{\mu\nu}\right)^2 + \cdots\right]\,, \tag{2.1.5}$$

where $g_{\rm YM}$ is the Yang-Mills coupling constant. $g_{\rm YM}$ can also be related with the parameters of string theory by comparing scattering amplitudes, and as a result we obtain the following relation:

$$g_{\rm YM}^2 = 4\pi g_s \,. \tag{2.1.6}$$

The full action describing N D3-branes in the flat $R^{1,9}$ spacetime is thus given by the sum of three parts; the action of closed strings, which include type IIB supergravity as a massless sector, the action of open strings on D3-branes, which include $\mathcal{N} = 4$ super Yang-Mills theory as a massless sector and the action for the interaction between them. Schematically, it is given by

$$S_{\rm total} = S_{\rm closed} + S_{\rm open} + S_{\rm int} \,. \tag{2.1.7}$$

$S_{\rm int}$ denotes the interaction between open strings, which describe field theoretical degrees of freedom, and closed strings, which describe gravitational degrees of freedom. Since the strength of such interaction is determined by the ten-dimensional Newton constant, $G_N^{(10)}$, we can separate out the open string sector and the close string sector by setting $G_N^{(10)}$ to zero. Now, owing to the relation (2.1.4), there are two possibilities to realize $G_N^{(10)} \to 0$ within type IIB superstring theory. One is to set g_s to zero and the other is to set ℓ_s to zero. However, in the former case, the whole system becomes non-interacting and we cannot expect any non-trivial dynamics. Thus, of particular interest is the limit where ℓ_s goes to zero while keeping g_s to be finite. In such a limit, the gravitational modes and the field theoretical modes completely decouple. Therefore, this limit is often called the *decoupling limit*. In the decoupling limit, all the massive modes become infinitely heavy owing to the relation (2.1.2) and become irrelevant in the low-energy physics. As a result, we are left with the following two mutually decoupled theories:

$$\text{4d } \mathcal{N} = 4 \text{ U}(N) \text{ SYM} \quad + \quad \text{Free type IIB supergravity} \,. \tag{2.1.8}$$

An important point here is that $\mathcal{N} = 4$ SYM still has a finite value of the coupling constant since we kept g_s finite in the limiting procedure.

2.1.2 Effective description of the D-brane background

Let us derive an alternative description of the above system, in which the effect of D-branes are replaced with some "effective potential". Since D-branes are sources of gravitons, such effective description is expected to be given by a certain curved geometry[1]. However, as

[1]Since D-branes are sources of other fields including the self-dual five-form flux, the effective description must also includes nontrivial configurations of such fields. However, as they will not play important roles in the subsequent discussion, we will not discuss them here.

discussed in section 1.1, it is extremely difficult to derive the effective theory from first principle starting from a complicated coupled system of open strings and closed strings.

Fortunately, in this case, a candidate of such effective description is already known in the study of supergravity. The geometry relevant here is the one called the *black 3-brane geometry*. The metric of this geometry is given by

$$ds^2 = H(r)^{-1/2}\left(-dt^2 + dx_i dx_i\right) + H(r)^{1/2}\left(dr^2 + r^2 d\Omega_5^2\right)\,, \qquad (i = 1, 2, 3) \tag{2.1.9}$$

where $d\Omega_5^2$ denotes the metric of the five sphere with a unit radius and $H(r)$ is defined by the characteristic size of the geometry, to be denoted by R, as

$$H(r) = 1 + \frac{R^4}{r^4}\,. \tag{2.1.10}$$

This background also includes R-R five-form flux and its macroscopic quantum numbers, most importantly the charge for the five-form flux, perfectly coincide with those of N D3-branes if we set the radius R as

$$R^4 = 4\pi N g_s \ell_s^4\,. \tag{2.1.11}$$

The use of the black 3-brane geometry as an effective description of closed string theory in the presence of N D3-branes is an important working hypothesis, which should, ideally, be proven rigorously from first principles. However, since such a rigorous argument is beyond our current reach, below we will instead discuss the consequences of this hypothesis.

Let us then consider the decoupling limit of this geometry in order to extract the degrees of freedom corresponding to $\mathcal{N} = 4$ SYM. As described above, the decoupling limit is the limit in which the string length ℓ_s goes to zero while the string coupling constant g_s is finite. In such a limit, the characteristic size of the geometry R goes to zero owing to the relation (2.1.11) and the black 3-brane geometry separates into two distinctive regions: In the first region $r \gg R$, $H(r)$ approaches unity and the metric (2.1.9) becomes that of the flat ten-dimensional spacetime. Then, because of the relation (2.1.2), all the stringy modes become infinitely heavy. In addition, the Newton constant vanishes in the decoupling limit and, as a consequence, we are left with free type IIB supergravity. On the other hand, in the second region $r \sim R$, which is close to the horizon, the background geometry remains highly curved. To describe this near-horizon region, it is convenient to introduce the coordinate $z \equiv R^2/r$ and express the metric in the limit as

$$ds^2 = R^2\left(\frac{-dt^2 + dx_i dx_i + dz^2}{z^2} + d\Omega_5^2\right)\,. \tag{2.1.12}$$

The geometry described by the metric (2.1.12) is nothing but the $AdS_5 \times S^5$ spacetime, a product of the five-dimensional anti-de Sitter space and the five-sphere, and the coordinate-system used is known as the Poincaré coordinate. This process of obtaining a nontrivial geometry by enlarging the region using a suitably scaled coordinate-system near the horizon is generally called the *near-horizon limit*. The above argument shows that the decoupling limit of the coupled system of open and closed strings naturally corresponds to the near-horizon limit of the black 3-brane geometry. In the near-horizon region, we cannot neglect massive stringy modes. This is because all the excitations in this region, including ones with arbitrarily high energy, experience a strong red-shift owing to the warp factor $H(r)^{-1/2}$, and are observed by a distant observer as the low-energy degrees of freedom. As a consequence, we obtain the following two decoupled theories:

$$\text{Type IIB superstring on } AdS_5 \times S^5 \quad + \quad \text{Free type IIB supergravity}\,. \tag{2.1.13}$$

Note that the theory on the left hand side in (2.1.13) is an *interacting* superstring theory since the string coupling constant g_s is kept finite in the limit.

2.1.3 Interlude: WKB analysis of quantum mechanics

A notable feature of the decoupling/near-horizon limit is that the system is decomposed into two sectors and one of them is described by a nontrivial theory including all the stringy modes while the other is simply given by free type IIB supergravity. It may seem slightly counter-intuitive that one sector remains interacting and includes all the massive modes even after the limit where the Newton constant $G_{\rm N}^{(10)}$ and the string length ℓ_s vanish. In the discussions above, this peculiarity was attributed to the strong red-shift produced by the black 3-brane geometry. To obtain a different perspective of this feature, let us now make a small detour and discuss a much simpler topic; the WKB analysis of the semi-classical quantum mechanics. Although the semi-classical limit of quantum mechanics certainly is quite different from the system we have been discussing, it shares some common qualitative features as we will see below. Another important purpose of making such a detour is to give a general introduction to the idea of the WKB analysis, which will be heavily used in Part III.

The WKB approximation is the approximation scheme for the semiclassical limit of quantum mechanics, which is valid when the state has a macroscopic quantum number. In most regions, such a state can be well-approximated by a simple plane-wave-like function as follows:

$$\psi \sim \exp\left[\frac{i}{\hbar}\int \sqrt{2m(E-V(x'))}dx'\right]\,. \tag{2.1.14}$$

However, the approximation (2.1.14) is known to break down in the vicinity of *turning points*, which are defined by $E - V(x) = 0$. To understand the behavior around the turning points, to be denoted by x_t, we need to introduce the rescaled coordinate as

$$z \equiv \left(\frac{2m|V'(x_t)|}{\hbar^2}\right)^{\frac{1}{3}} (x - x_t) \ , \tag{2.1.15}$$

and consider the scaling limit in which $\hbar$ goes to zero while z is kept finite. The Schrödinger equation in this scaling limit is given as follows:

$$-\frac{\hbar^2}{2m}\frac{d^2\psi}{dx^2} + V(x)\psi = E\psi \quad \longrightarrow \quad \frac{d^2\psi}{dz^2} \mp z\psi = 0 \, , \tag{2.1.16}$$

where the $\mp$ sign is chosen according to the sign of $V'(x_t)$. Then the behavior of the wave function in the vicinity of the turning points can be determined by solving the right equation of (2.1.16) *exactly*. The exact solution to (2.1.16) is known to be given in terms of the Airy function. From the asymptotic behavior of the Airy function, we can determine the behavior of the wave function ψ in the scaling limit. For instance, when $V'(x_t)$ is negative, we obtain

$$\begin{aligned} \psi(z) &\sim \frac{1}{2}\frac{1}{(-z)^{1/4}} \exp\left(-\frac{2}{3}(-z)^{3/2}\right) \quad \text{as } z \to +\infty \, , \\ \psi(z) &\sim \frac{1}{z^{1/4}} \sin\left(\frac{2}{3}z^{3/2} + \frac{\pi}{4}\right) \quad \text{as } z \to -\infty \, , \end{aligned} \tag{2.1.17}$$

The behavior of the wave function in the scaling limit (2.1.17) leads to the famous *connection formula* of the WKB approximation, which tells us how a single-exponential wave function transforms into a sum of exponentials such as sine or cosine after crossing a turning point. When combined with the plane-wave-like approximation (2.1.14), which is valid away from the turning points, the connection formula turns out to be very much powerful: It completely determines the global structure of the wave function in the semi-classical limit and enables us to compute various physical quantities, such as the Bohr-Sommerfeld quantization condition, the energy-splitting in the multi-well potential, the resonance energy and the tunneling probability. In Part III, we will also see that the method based on the WKB analysis can be used to compute three-point functions of classical strings.

An important feature of the above analysis is that, although we considered the semi-classical limit, we needed to solve the Schrödinger equation fully quantum-mechanically in the vicinity of turning points, (2.1.17). This is somewhat reminiscent of the decoupling/near-horizon limit, where we had to solve a non-trivial interacting theory near the horizon even after the limit where $G_N^{(10)}$ goes to zero. Given this apparent similarity[2], it is tempting to think that the quantum gravity in the near-horizon region is of crucial importance not just for

[2]To see the similarity more transparently, it is interesting to rewrite the classical action of a non-relativistic

the study of holography but also for understanding more general properties of the quantum gravity in a similar way the Schorödinger equation with a linear potential provided essential information on the global structure of general wave functions. Indeed, there is some evidence that the near horizon region contains major non-trivial information of quantum gravity. For instance, it is known that the entropy of a black hole, which is one of the universal and fundamental properties of quantum gravity, can be reproduced in some cases by studying their near-horizon regions [20–24]. Therefore, hopefully, the study of AdS/CFT will have a wider range of applicability, not just to holography, and will play a foundational role in the future study of quantum gravity.

2.1.4 Basic statement of AdS/CFT correspondence

Let us now go back to the original problem and examine the consequences of two different descriptions, given respectively in section 2.1.1 and section 2.1.2. By comparing (2.1.8) and (2.1.13), we notice that both desciptions have the same trivial sector, free type IIB supergravity. Thus, eliminating the trivial sector, we are led to the following conjectural relation,

$$\mathcal{N} = 4 \text{ SYM} \quad = \quad \text{Type IIB superstring theory on } AdS_5 \times S^5 \,, \tag{2.1.18}$$

which is the basic statement of the $\text{AdS}_5/\text{CFT}_4$ correspondence.

Let us now study the precise mapping of parameters in two theories. Owing to (2.1.6) and (2.1.11), the coupling constant on the gauge-theory side is mapped to the ratio between the size of $AdS_5 \times S^5$ and the string length as follows:

$$\lambda (\equiv g_{\text{YM}}^2 N) = \frac{R^4}{\ell_s^4} \,, \tag{2.1.19}$$

where λ is called 't Hooft coupling constant, which is often used in the large N expansion of the gauge theories. Since the coupling constants in both theories are related by (2.1.6), we can express the string coupling constant g_s in terms of 't Hooft coupling constant λ and the number of colors N as

$$g_s = \frac{\lambda}{4\pi N} \,. \tag{2.1.20}$$

particle into the form,

$$S = \int p_i dq_i - \int H dt = \left(\int \sqrt{2m(E - V(q)) dq_i dq_i} \right) - E(t_f - t_i) \,.$$

This expression is sometimes used to determine the trajectory of a classically moving particle by the variational principle [19]. In this form of action, we can explicitly see that the turning points correspond to horizon-like singularities of the "dynamical metric", $ds^2 = 2m(E - V(q)) dq_i dq_i$. It might be interesting to study this connection but we will not pursue it any further here.

Let us examine the consequences of the relations (2.1.19) and (2.1.20). Firstly, the relation (2.1.20) shows that the string theory in $AdS_5 \times S^5$ becomes non-interacting in the limit where the number of the colors N goes to infinity and the 't Hooft coupling constant λ is kept finite. This limit is known as the *'t Hooft* limit and is an ideal starting point for the detailed analysis. Even in this limit, both sides of the duality remains highly nontrivial. On the gauge theory side, the 't Hooft limit is also known as the *planar limit*, in which only a restricted class of Feymann diagrams, called planar diagrams[3], contribute. The 't Hooft coupling constant λ serves as the effective coupling constant in this limit and the interaction cannot be neglected as long as λ is kept finite. On the string theory side, the interaction between strings vanishes in this limit. However, since the theory is defined on a nontrivial curved geometry, the dynamics of a single string is still quite difficult to understand. Secondly, the relation (2.1.19) is the manifestation of the strong/weak nature of the AdS/CFT correspondence. For instance, when λ is close to zero, the string theory becomes highly quantum whereas the dual description is the weakly-coupled $\mathcal{N} = 4$ SYM, which can be studied by the conventional perturbation. On the other hand, when λ is sufficiently large, the gauge theory becomes strongly coupled and cannot be explored by any conventional means while it is described by classically moving strings in the dual description.

The inherent strong/weak nature of the duality is a mixed blessing: On the one hand, it enables us to explore the previously unaccessible region of each theory with relative ease. On the other hand, it stands as a great obstacle for checking or proving the correspondence. A powerful and promising framework which in principle can overcome such difficulties is the use of integrability. In the rest of the thesis, we will exclusively study the 't Hooft limit and see how integrability comes into play in the $\mathrm{AdS}_5/\mathrm{CFT}_4$ correspondence.

2.2 Correspondence of symmetries and observables

Before delving into the details of the integrability-based analysis, let us explain how the symmetries and observables in two theories are related with each other.

Since the action of $\mathcal{N} = 4$ SYM has no scale parameters, the theory is scale-independent and conformal at least at the classical level. The conformality is known to survive even at the quantum level since the β-function of the coupling constant in $\mathcal{N} = 4$ SYM vanishes to all orders[4] in perturbation theory [26]. Combined with the supersymmetry, it enhances to the *superconformal symmetry*, which in this case is given by $\mathrm{PSU}(2,2|4)$. On the other hand, this symmetry is realized geometrically on the string-theory side. For instance, the

[3]Planar diagrams are diagrams which can be drawn on a two-sphere. Other diagrams are called *non-planar* diagrams.

[4]For a non-perturbative argument, see [25].

isometry of the $AdS_5 \times S^5$ spacetime is known to be given by $\mathrm{SO}(4,2)\times\mathrm{SO}(6)$, which is a bosonic part[5] of $\mathrm{PSU}(2,2|4)$.

Let us next turn our attention to the correspondence of the observables. Since $\mathcal{N}=4$ SYM is conformal, natural observables in this theory are correlation functions of gauge-invariant operators. Of particular importance are two-point functions and three-point functions. This is because two-point functions encode the spectrum of the theory and three-point functions determine the essential dynamics. Furthermore, they together determine all the other correlation functions through the operator product expansion (OPE).

Given their importance, let us now take a closer look at these two quantities. Below we will exclusively discuss correlation functions of special composite operators, called *single-trace operators*, which consist of a single color-trace and are of the form $\mathrm{tr}\,(\Phi_1\Phi_2 D_\mu \Psi \cdots)$. Owing to conformal invariance, the spacetime dependence of two- and three-point functions of such operators are completely determined as follows:

$$G_{ij}(x_1,x_2) = \langle \mathcal{O}_i(x_1)\mathcal{O}_j(x_2)\rangle = \frac{\delta_{ij}}{|x_{12}|^{2\Delta_i}}\,, \tag{2.2.1}$$

$$\begin{aligned} G_{ijk}(x_1,x_2,x_3) &= \langle \mathcal{O}_i(x_1)\mathcal{O}_j(x_2)\mathcal{O}_k(x_3)\rangle \\ &= \frac{1}{N}\frac{C_{123}}{|x_{12}|^{\Delta_1+\Delta_2-\Delta_3}|x_{23}|^{\Delta_2+\Delta_3-\Delta_1}|x_{31}|^{\Delta_3+\Delta_1-\Delta_2}}\,. \end{aligned} \tag{2.2.2}$$

Note that, when the single-trace operators are defined such that they satisfy the normalized two-point functions (2.2.1), the universal prefactor, $1/N$, always appears in (2.2.2) to take into account the normalization condition. As the spacetime dependence is completely fixed, the dynamical details of the theory are encoded only in two observables, Δ_i and C_{ijk}.

The first quantity Δ_i is called the *conformal dimension* and represents the eigenvalue of the dilatation transformation, $x^\mu \to a x^\mu$. By conformal transformation, local operators in R^4 are mapped to certain states in $R\times S^3$. Under such a transformation, the dilatation transformation in R^4 is transformed into the "Hamiltonian" of $R\times S^3$, where R plays the role of the time axis. Therefore Δ_i's can also be interpreted as the energy of the state in $R\times S^3$. In general, Δ_i's receive quantum corrections and the difference between the exact conformal dimension and the bare (tree-level) conformal dimension is called the *anomalous dimension*. The second quantity C_{ijk} is called the *structure constant* and determines the "interaction" of the operators. More precisely, if we perform the OPE expansion of the first two operators $\mathcal{O}_i$ and $\mathcal{O}_j$, the third operator $\mathcal{O}_k$ appears in the expansion with a coefficient proportional to C_{ijk}.

[5] If we also consider the fermionic coordinates, we can explicitly see that the full symmetry $\mathrm{PSU}(2,2|4)$ is realized geometrically.

Let us next discuss the dual descriptions of these observables. In the AdS/CFT correspondence, the single-trace operators in the gauge theory are considered to be dual to the single string states in $AdS_5 \times S^5$. Since the conformal transformation SO(4,2) is realized as an isometry group on the string-theory side, the dimension of the operator Δ is naturally identified with the charge for the isometry transformation corresponding to the dilatation. This point of view is useful when we discuss general correlation functions of the dual gauge theory on R^4. However, when we focus on the conformal dimension alone, it is more convenient to take the boundary to be $R \times S^3$ and identify Δ with the energy E of the string state in the following way:

$$E = \Delta \,. \tag{2.2.3}$$

This is the key relation extensively used in the study of two-point functions. On the other hand, the structure constant is related to the interaction of three different string states. In the first-quantized formulation of string theory, a natural observable describing the interaction of strings is the worldsheet correlation functions given schematically as follows:

$$\int \frac{d^2 z_1 \cdots d^2 z_n}{\text{Möbius}} \langle \mathcal{V}_1(z_1) \cdots \mathcal{V}_n(z_n) \rangle \,, \tag{2.2.4}$$

where Möbius denotes the volume of the residual conformal Killing group, which is the Möbius group for spherical worldsheets. In flat spacetime, the worldsheet correlation functions of the form (2.2.4) describe the scattering amplitudes of strings. In this case, however, we expect that they correspond to the correlation functions in the gauge theory, which are the most natural observables in the present set-up. Of course, without any explicit construction of vertex operators $\mathcal{V}_i$, this is just a conjecture. However, as we will see in Part III, we can reproduce several important properties of the gauge theory correlation functions starting from the expression (2.2.4), at least in the classical limit of the string theory. In the case of three-point functions, (2.2.4) simplifies since we can fix the positions of three operators using the residual conformal Killing group. Thus, the correspondence relation for three-point functions is given by

$$G_{ijk}(x_1, x_2, x_3) = \langle \mathcal{V}_i(z_1) \mathcal{V}_j(z_2) \mathcal{V}_k(z_3) \rangle \,, \tag{2.2.5}$$

where z_1, z_2 and z_3 are arbitrary points on the worldsheet[6]. The detailed information of the gauge theory operators, including their insertion points, are expected to be contained in the detailed forms of the operators $\mathcal{V}_i$'s.

The relations (2.2.3) and (2.2.4) show that the two important characteristics of string theory, the existence of infinitely many kinds of particles and the geometrical realization of

[6]Since the vertex operators satisfy the physical-state condition, (2.2.5) will not depend on z_i's.

their interactions, are related with the two fundamental building blocks of $\mathcal{N} = 4$ SYM. In the subsequent chapters, we will explore these relations further using the powerful techniques of integrability.

Chapter 3

Two point functions and integrability

In this chapter, we summarize basic facts on integrability in the $\mathrm{AdS}_5/\mathrm{CFT}_4$ correspondence, which will be used in the subsequent chapters. In section 3.1, we discuss one-loop renormalization of the operators which consist only of scalar fields, following the paper [27]. As a result, we find that the mixing matrix, which determines the anomalous dimensions, coincides with the Hamiltonian of a certain integrable spin chain. Then we focus on a particular class of operators, belonging to the so-called SU(2)-sector, and explain the integrability-based method to diagonalize the Hamiltonian. Next in section 3.2, we review the classical integrability of the string theory. We first explain the full integrable structure of the string theory on $AdS_5 \times S^5$. Then, we focus on strings moving in a subspace S^3 and discuss a more detailed structure. In section 3.3, we then discuss a certain limit where we can compare the gauge theory side and the string theory side directly. Last in section 3.4, we briefly summarize the subsequent developments on two-point functions and explain the motivation to study three-point functions.

3.1 One-loop integrability in gauge theory

In this section, we review the one-loop integrability of gauge theory, found originally in [27], and show that the dilatation operator at one-loop can be naturally identified with the Hamiltonian of a certain integrable spin chain. We also explain an efficient method to diagonalize such spin chains, which is called the *algebraic Bethe ansatz*.

3.1.1 $\mathcal{N} = 4$ super Yang-Mills theory

Before starting to discuss the one-loop integrability, let us write down the action of the $\mathcal{N} = 4$ super Yang-Mills theory, which is a maximally supersymmetric gauge theory in

four-dimensional spacetime. The fundamental fields in this theory are six real scalars Φ_i ($i = 1, \ldots, 6$), gluons A_μ ($\mu = 0, \ldots, 3$) and four Weyl spinors ψ, all of which are in the adjoint representation of U(N). The four Weyl spinors can be expressed alternatively by sixteen component Majorana-Weyl spinor Ψ in ten dimensions and we will use this notation in what follows. Written explicitly, its action is of the following form:

$$S_{\rm YM} = \frac{1}{2g_{\rm YM}^2} \int d^4x \, {\rm tr} \left(-\frac{1}{2}(F_{\mu\nu})^2 + (D_\mu \Phi_i)^2 - \sum_{i<j} [\Phi_i, \Phi_j]^2 + i\bar{\Psi}\Gamma^\mu D_\mu \Psi - \bar{\Psi}\Gamma^i [\Phi_i \, , \Psi] \right) , \tag{3.1.1}$$

where the covariant derivative D_μ and the field strength $F_{\mu\nu}$ are defined in a usual way as

$$D_\mu \bullet = \partial_\mu - i \, [A_\mu, \bullet] \ , \quad F_{\mu\nu} = \partial_\mu A_\nu - \partial_\nu A_\mu + [A_\mu \, , A_\nu] \ , \tag{3.1.2}$$

and $\Gamma^A = (\Gamma^\mu, \Gamma^i)$ is the 16×16 Dirac matrices in ten dimensions normalized to ${\rm tr} \left(\Gamma^A \Gamma^B \right) = 16\delta^{AB}$. As mentioned in section 2.2, $\mathcal{N} = 4$ super Yang-Mills theory is known to be conformal and the coupling constant $g_{\rm YM}$ does not run under the renormalization group flow[1].

The main objects to study in the following discussions are the *single-trace operators*, which are gauge-invariant and are of the following form,

$$\mathcal{O}(x) = {\rm tr} \, \left(\Phi_{i_1} D_\mu \Phi_{i_2} D_\nu \Psi \Phi_{i_3} \cdots \right) (x) \, . \tag{3.1.3}$$

An important point in the expression (3.1.3) is that all the fields in the trace are inserted at the same point in the four-dimensional spacetime. Therefore, if we consider the quantum corrections, the naïve expression (3.1.3), to be called *bare operators*, gives divergent results unless we perform appropriate composite-operator renormalization.

3.1.2 SO(6) spin-chain from dilatation operator

As mentioned above, we need to renormalize composite operators in order to obtain finite correlation functions at loop levels. Renormalized operators are in general given by linear combination of bare operators as follows:

$$\mathcal{O}_A^{\rm ren} = Z_A{}^B \mathcal{O}_B^0 \, , \tag{3.1.4}$$

where $\mathcal{O}^{\rm ren}$ denotes a renormalized operator and $\mathcal{O}^0$ denotes a bare operator. The prefactor $Z_A{}^B$ in (3.1.4) is determined such that the renormalized operators give finite correlation functions and depends on the cut-off Λ. In the present context, it is convenient to take the

[1] By contrast, the wave-function renormalization exists in this theory.

renormalized operators such that they provide the orthonormal basis of two-point functions as

$$\langle \mathcal{O}_A^{\rm ren}(x_1)\mathcal{O}_B^{\rm ren}(x_2)\rangle \propto \delta_{AB}\,. \tag{3.1.5}$$

Since $\mathcal{N}=4$ SYM is a renormalizable field theory in four dimensions, the divergence we encounter is of the form $\ln\Lambda$ and $Z_A{}^B$ can in general be expressed as follows:

$$Z_A{}^B(\Lambda) = \left(e^{\hat{H}\ln\Lambda}\right)_A{}^B\,, \tag{3.1.6}$$

where the matrix $\hat{H}$ is defined by

$$\hat{H} = \frac{d\ln Z}{d\ln\Lambda}\,, \tag{3.1.7}$$

and is called the *mixing matrix* and the orthonormal basis for two-point functions can be obtained by diagonalizing this matrix.

Owing to the explicit cut-off dependence of $Z_A{}^B$, the renormalized operator has different conformal dimension from the corresponding bare operators. To see this explicitly, let us consider the eigenstate of $\hat{H}$ and denotes its eigenvalue by γ. Then, as the dilatation transformation $x^\mu \to ax^\mu$ also acts $\ln\Lambda$ as $\ln\Lambda \to \ln\Lambda - \ln a$, the renormalized operator is transformed as

$$\mathcal{O}^{\rm ren} \to a^{-(\Delta_0+\gamma)}\mathcal{O}^{\rm ren}\,, \tag{3.1.8}$$

where Δ_0 is the conformal dimension of the bare operator. The equation (3.1.8) clearly shows that the conformal dimension of the renormalized operator is given by $\Delta_0+\gamma$. Therefore, to compute the loop corrections to the conformal dimensions, we need to perform the following steps.

1. First, determine $Z_A{}^B$ by the perturbation such that the renormalize operators give finite correlation functions.
2. Then, diagonalize $Z_A{}^B$ and compute the eigenvalues of $\hat{H}$.

As two-point functions are determined completely by the conformal dimensions, these procedures also fix the quantum-corrected two-point functions.

Let us perform the above procedures to a special class of single-trace operators, which consist only of scalar fields. Such a class of operators, which have the following form, is called the *SO(6)-sector*:

$$\mathcal{O}_{i_1 i_2 i_3 \ldots} = \mathrm{tr}\,\left(\Phi_{i_1}\Phi_{i_2}\Phi_{i_3}\cdots\right)\,. \tag{3.1.9}$$

Since the details are given in [27], below we only explain the gist of the computation. At one-loop, there are three types of diagrams which contribute to two-point functions of operators in $SO(6)$-sector, the gluon-exchange diagram (Figure 3.1.1-(a)), the scalar-interaction diagram (Figure 3.1.1-(b)) and the wave function renormalization of the fields (Figure 3.1.1-(c)). Important simplification in the 't Hooft limit is that the diagrams connecting non-adjacent fields in the trace are suppressed by $1/N$. Therefore, only diagrams we need to consider are diagrams which connect neighboring two fields. To evaluate their contributions, let us examine scalar-interaction diagrams as an example. Scalar-interaction diagrams come from the commutator-squared term $[\Phi_i, \Phi_j]^2$ in the action (3.1.1). By expanding the squrare, we can see that such interactions consist of the following two different terms:

$$[\Phi_i, \Phi_j]^2 = 2\Phi_i\Phi_j\Phi_i\Phi_j - 2\Phi_i\Phi_i\Phi_j\Phi_j \,. \tag{3.1.10}$$

An important feature of (3.1.10) is that the relative weight of two terms depend on the ordering of SO(6)-indices. This feature, together with the aforementioned property that only neighboring two fields get quantum corrections, strongly indicate that the single-trace operator can be interpreted as a certain spin chain with the nearest-neighbor interaction.

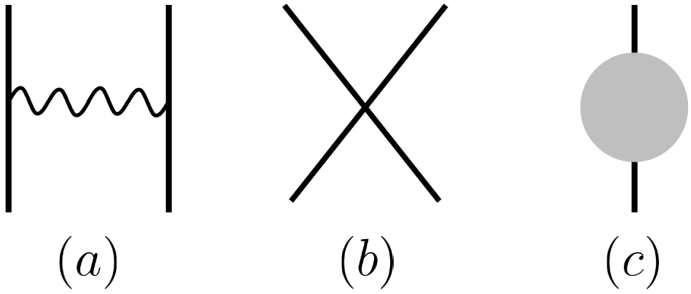

Figure 3.1.1: Diagrams which are relevant for the computation of the one-loop anomalous dimensions. (a) Gluon exchange diagram. (b) Scalar interaction diagram. (c) Wave function renormalization.

To explicitly compute the factor ${Z_A}^B$, we need to calculate the following correlation function,

$$\langle \mathcal{O}_{i_1 i_2 \cdots}(x)\Phi_{j_1}(x_1)\Phi_{j_2}(x_2)\cdots \rangle \,, \tag{3.1.11}$$

and determine ${Z_A}^B$ such that the correlation function after the renormalization,

$$\langle \mathcal{O}^{\rm ren}_{i_1 i_2 \cdots}(x)\Phi^{\rm ren}_{j_1}(x_1)\Phi^{\rm ren}_{j_2}(x_2)\cdots \rangle \,, \tag{3.1.12}$$

is completely finite. Here $\Phi^{\rm ren}_i$ is a renormalized scalar field defined by $\Phi^{\rm ren}_i = Z_\Phi^{-1/2}\Phi_i$.

Carrying out this procedure, we find, for instance, that the contribution from the scalar-interaction is given as follows:

$$Z^{(\text{scalar})}_{\cdots i_l i_{l+1}\cdots}{}^{\cdots j_l j_{l+1}\cdots} = 1 - \frac{\lambda}{16\pi^2}\left(2\delta_{i_l}{}^{j_{l+1}}\delta_{i_{l+1}}{}^{j_l} - \delta_{i_l}{}^{j_l}\delta_{i_{l+1}}{}^{j_{l+1}} - \delta_{i_l i_{l+1}}\delta^{j_l j_{l+1}}\right)\ln\Lambda\,, \tag{3.1.13}$$

where the term $2\delta_{i_l}{}^{j_{l+1}}\delta_{i_{l+1}}{}^{j_l}$ comes from the first term in (3.1.10) and and the terms $-\delta_{i_l}{}^{j_l}\delta_{i_{l+1}}{}^{j_{l+1}}$ and $-\delta_{i_l i_{l+1}}\delta^{j_l j_{l+1}}$ come from the second term in (3.1.15). Putting together all possible contributions, we obtain the full one-loop result as follows:

$$Z_{\cdots i_l i_{l+1}\cdots}{}^{\cdots j_l j_{l+1}\cdots} = 1 + \frac{\lambda}{16\pi^2}\left(-2\delta_{i_l}{}^{j_{l+1}}\delta_{i_{l+1}}{}^{j_l} + 2\delta_{i_l}{}^{j_l}\delta_{i_{l+1}}{}^{j_{l+1}} + \delta_{i_l i_{l+1}}\delta^{j_l j_{l+1}}\right)\ln\Lambda\,. \tag{3.1.14}$$

Therefore, the mixing matrix at one-loop is given by

$$\hat{H}_{\text{one-loop}} = \frac{\lambda}{16\pi^2}\sum_{n=1}^{\ell}\left(-2\mathbb{P}_{n,n+1} + 2\mathbb{I}_{n,n+1} + \mathbb{K}_{n,n+1}\right)\,, \tag{3.1.15}$$

where the matrices, $\mathbb{I}$, $\mathbb{P}$ and $\mathbb{K}$, act on the SO(6)-indices as

$$\begin{aligned}
\mathbb{I}|\ldots,i,j,\ldots\rangle &= |\ldots,i,j,\ldots\rangle\,,\\
\mathbb{P}|\ldots,i,j,\ldots\rangle &= |\ldots,j,i,\ldots\rangle\,,\\
\mathbb{K}|\ldots,i,j,\ldots\rangle &= \delta_{ij}\sum_{k=1}^{6}|\ldots,k,k,\ldots\rangle\,,
\end{aligned} \tag{3.1.16}$$

where we denoted the SO(6)-indices as $|\ldots,i,j,\ldots\rangle$ in order to make clear the connection with the spin chain. A crucial feature of the mixing matrix (3.1.15) is that it coincides with the Hamiltonian of the SO(6) integrable spin chain [28, 29]. Making use of this connection, we can diagonalize the mixing matrix using the standard techniques in integrability. In the next subsection, we will explain one such technique, called the *algebraic Bethe ansatz*.

In the above computation, we have *not* heavily used the features peculiar to $\mathcal{N}=4$ SYM. This suggests that the identification of the mixing matrix with the Hamiltonian of the integrable spin chain may work also in other theories. In fact, in [30], it was shown that the one-loop mixing matrix in a sub-sector of the large N QCD can also be identified with the integrable spin chains. However, a distinctive feature of $\mathcal{N}=4$ SYM is that such identification works for all the single-trace operators and can be extended to higher-loop orders, as we will mention shortly. Such features do not exist in most theories.

3.1.3 SU(2)-sector and algebraic Bethe ansatz

Having seen that the single-trace operators composed only of the scalar fields are identified with SO(6) spin chains, let us now consider a more special class of operators, which are made

up of two complex scalars,

$$Z = \Phi_1 + i\Phi_2\,, \quad X = \Phi_3 + i\Phi_4\,. \tag{3.1.17}$$

This class of operators is called the *SU(2)-sector* and the mixing is known to be closed within this sector at all orders in perturbation theory. This is simply because the dilatation only mixes the operators with the same bare conformal dimensions at the level of perturbation theory and there are no scalar operators outside the SU(2)-sector which have the same bare dimension and the same R-charges. This is why operators in the SU(2)-sector are widely studied in the literature. However, let us stress that the notion of "sectors" exists only at the level of perturbation theory and there is an indication that the SU(2)-sector is not closed non-perturbatively [31].

The operators in the SU(2)-sector can be naturally identified with the states in the ordinary SU(2) spin chain in the following way:

$$\mathrm{tr}\,(ZXZXZZ\cdots) \quad \leftrightarrow \quad |\uparrow\downarrow\uparrow\downarrow\uparrow\uparrow\cdots\rangle\,. \tag{3.1.18}$$

Then, the mixing matrix reduces to the Hamiltonian of the well-known Heisenberg spin-chain,

$$\hat{H}_{\mathrm{one-loop}} = \frac{\lambda}{8\pi^2}\sum_{n=1}^{\ell}\left(\mathbb{I}_{n,n+1} - \mathbb{P}_{n,n+1}\right)\,, \tag{3.1.19}$$

which is known also as the *XXX spin chain*. The Hamiltonian (3.1.19) can be recast into a more familiar form as

$$\hat{H}_{\mathrm{one-loop}} = \frac{\lambda}{4\pi^2}\sum_{n=1}^{\ell}\sum_{i=\{x,y,z\}}\left(\frac{1}{4} - S_n^i S_{n+1}^i\right)\,, \tag{3.1.20}$$

where $S_n^{x,y,z}$ are local spin operators.

There are several ways to diagonalize the Hamiltonian (3.1.19). The most intuitive one is called the *coordinate Bethe ansatz*, in which we first assume a rough form of the wave function and later determine unfixed constants such that the wave function becomes the eigenvector of $\hat{H}$. A more sophisticated method, which we will explain below, is called the *algebraic Bethe ansatz*. In this method, we use certain algraic relations and systematically construct the eigenvectors. The third method is *Sklyanin's separation of variables*[2], which we will fully describe in chapter 5.

Let us now explain the algebraic Bethe ansatz. The basic ingredient in the framework of the algebraic Bethe ansatz is the so-called *Lax operator* acting on the product of the

[2]Originally, it was called the *functional Bethe ansatz*.

spin-chain Hilbert space $\mathcal{H}$ and an auxiliary vector space. In the case of the XXX spin 1/2 chain with L sites, $\mathcal{H}$ is the tensor product of L copies of a two-dimensional vector space, consisting of the up-spin state $|\uparrow\rangle$ and the down-spin state $|\downarrow\rangle$ at each site, and the auxiliary space has the structure of $\mathbb{C}^2$. The Lax operator $L_n(u)$ acting on the n-th site is then given by

$$L_n(u) \equiv u\mathbf{1} + i \sum_{k=x,y,z} S_n^k \sigma^k = \begin{pmatrix} u + iS_n^z & iS_n^- \\ iS_n^+ & u - iS_n^z \end{pmatrix}, \tag{3.1.21}$$

where S_n^k are the local spin operators[3] and u is the complex spectral parameter. We will impose the periodic boundary condition so that $S_{n+L}^k = S_n^k$. Going around the spin chain, we define the monodromy matrix $\Omega(u)$ as

$$\begin{aligned} \Omega(u) &\equiv L_1(u-\theta_1)\cdots L_\ell(u-\theta_\ell) \equiv \begin{pmatrix} A(u) & B(u) \\ C(u) & D(u) \end{pmatrix} \\ &= u^\ell \mathbf{1} + iu^{\ell-1}\left(\sum_{k=x,y,z} S^k\sigma^k + i\sum_{j=1}^{\ell}\theta_j\right) + \mathcal{O}(u^{\ell-2})\,. \end{aligned} \tag{3.1.22}$$

Here $S^k = \sum_n S_n^k$ are the total spin operators and we have introduced the *inhomogeneity parameters* $\boldsymbol{\theta} = \{\theta_1, \ldots, \theta_\ell\}$ at each site, which preserve the integrability. As will be discussed in Part II, they are necessary for avoiding certain degeneracies in the intermediate steps of computing three-point functions and are also useful for other purposes[4]. However, for the purpose of this section, we can simply set them to zero.

Although the actions of the operators $A(u)$–$D(u)$ on $\mathcal{H}$ are in general quite complicated and non-local, they are known to satisfy rather simple exchange relations, which we call

[3] We define $S_n^\pm$ as $S_n^\pm \equiv S_n^x \pm iS_n^y$.

[4] Although the physical meaning of the inhomogeneity parameters in the context of the three-point functions has not been fully clarified, they are useful in generating loop corrections from the tree-level contributions [32, 33]. See also the discussion part, Part IV.

Yang-Baxter algebra [34]. Written explicitly, they are given by

$$
\begin{aligned}
&(u-v)A(v)B(u) = (u-v+i)B(u)A(v) - iB(v)A(u)\,,\\
&(u-v)B(v)A(u) = (u-v+i)A(u)B(v) - iA(v)B(u)\,,\\
&(v-u)D(v)B(u) = (v-u+i)B(u)D(v) - iB(v)D(u)\,,\\
&(v-u)B(v)D(u) = (v-u+i)D(u)B(v) - iD(v)B(u)\,,\\
&(v-u)C(v)A(u) = (v-u+i)A(u)C(v) - iA(v)C(u)\,,\\
&(v-u)A(v)C(u) = (v-u+i)C(u)A(v) - iC(v)A(u)\,,\\
&(u-v)C(v)D(u) = (u-v+i)D(u)C(v) - iD(v)C(u)\,,\\
&(u-v)D(v)C(u) = (u-v+i)C(u)D(v) - iC(v)D(u)\,,\\
&[C(v),B(u)] = \frac{i}{u-v}\left[A(v)D(u) - A(u)D(v)\right] = \frac{i}{u-v}\left[D(u)A(v) - D(v)A(u)\right]\,,\\
&[D(v),A(u)] = \frac{i}{u-v}\left[B(v)C(u) - B(u)C(v)\right] = \frac{i}{u-v}\left[C(u)B(v) - C(v)B(u)\right]\,,\\
&[B(u),B(v)] = [C(u),C(v)] = [A(u),A(v)] = [D(u),D(v)] = 0\,.
\end{aligned}
\tag{3.1.23}
$$

Let us sketch the derivation of the algebra (3.1.23). Of extreme importance in the derivation are the commutativity of the Lax operators defined at different sites,

$$
[L_n(u), L_m(v)] = 0 \quad (n \neq m)\,, \tag{3.1.24}
$$

and the following "commutation relations" of the Lax operators defined at the same site:

$$
[R(u-v)]^{ab}{}_{ik}\,[L_n(u)]^{i}{}_{j}\,[L_n(v)]^{k}{}_{l} = [L_n(v)]^{b}{}_{k}\,[L_n(u)]^{a}{}_{i}\,[R(u-v)]^{ik}{}_{jl}\,, \tag{3.1.25}
$$

where $[L_n(u)]^{i}{}_{j}$ is a (i,j) component of the 2×2 matrix (3.1.21). $R(u-v)$ is the operator acting on the tensor product of the auxiliary vector spaces, $\mathbb{C}^2\otimes\mathbb{C}^2$, and is given by

$$
[R(u)]^{ik}{}_{jl} = u\delta^{i}{}_{j}\delta^{k}{}_{l} + i\delta^{i}{}_{l}\delta^{k}{}_{j}\,. \tag{3.1.26}
$$

Using the identity operator $\mathbb{I}$, which preserves the structure of the auxiliary spaces, and the permutation operator $\mathbb{P}$, which exchanges the two auxiliary spaces, $R(u)$ can be schematically written as

$$
R_{12}(u) = u\mathbb{I}_{12} + i\mathbb{P}_{12}\,, \tag{3.1.27}
$$

where the subscript 12 signifies the first and the second auxiliary space respectively. Among the aforementioned two important relations, (3.1.24) and (3.1.25), the commutativity (3.1.24)

immediately follows from the explicit form of the Lax operators (3.1.21). On the other hand, to prove (3.1.25), we need to re-express the Lax operator as follows:

$$L_n(u) = \left(u - \frac{i}{2}\right) \mathbb{I}_{a\, s_n} + i\mathbb{P}_{a\, s_n}\,, \tag{3.1.28}$$

where $\mathbb{I}_{a\, s_n}$ and $\mathbb{P}_{a\, s_n}$ are the identity operator and the permutation operator acting on the tensor product of the auxiliary space, denoted by a, and the spin space at the n-th site, denoted by s_n. One can verify that the expression (3.1.28) is equivalent to the original definition (3.1.21) by direct computation. Then, the left hand side of (3.1.25) can be schematically written as

$$((u-v)\mathbb{I}_{12} + i\mathbb{P}_{12}) \left(\left(u - \frac{i}{2}\right) \mathbb{I}_{1\, s_n} + i\mathbb{P}_{1\, s_n}\right) \left(\left(v - \frac{i}{2}\right) \mathbb{I}_{2\, s_n} + i\mathbb{P}_{2\, s_n}\right)\,, \tag{3.1.29}$$

whereas the right hand side can be written as

$$\left(\left(u - \frac{i}{2}\right) \mathbb{I}_{2\, s_n} + i\mathbb{P}_{2\, s_n}\right) \left(\left(u - \frac{i}{2}\right) \mathbb{I}_{1\, s_n} + i\mathbb{P}_{1\, s_n}\right) ((u-v)\mathbb{I}_{12} + i\mathbb{P}_{12})\,. \tag{3.1.30}$$

Now it is straightforward to show that the two expressions (3.1.29) and (3.1.30) are equivalent. The matrix $R(u)$, which governs the commutation relations of the Lax operators, is called *R-matrix* and is the crux of the matter in the algebraic Bethe ansatz. An important property of the R-matrix is that it satisfies the following *Yang-Baxter relation*:

$$R_{12}(u)R_{13}(u+v)R_{23}(v) = R_{23}(v)R_{13}(u+v)R_{12}(u)\,. \tag{3.1.31}$$

This can be expressed also pictorially as in Figure 3.1.2. Since the Lax operator (3.1.28) itself is a variant of the R-matrix in this case, (3.1.25) can be understood simply as a consequence of the Yang-Baxter relation. Now, using (3.1.24) and (3.1.25), we can derive the commutation relations of the monodromy as

$$[R(u-v)]^{ab}{}_{ik}\, [\Omega(u)]^{i}{}_{j}\, [\Omega(v)]^{k}{}_{l} = [\Omega(v)]^{b}{}_{k}\, [\Omega(u)]^{a}{}_{i}\, [R(u-v)]^{ik}{}_{jl}\,, \tag{3.1.32}$$

which can be schematically written as

$$R_{12}(u-v)\Omega^{(1)}(u)\Omega^{(2)}(v) = \Omega^{(2)}(v)\Omega^{(1)}(u)R_{12}(u-v)\,. \tag{3.1.33}$$

The commutation relation (3.1.32) is indeed equivalent to (3.1.23). To see why (3.1.32) holds, let us consider a two-site chain. In this case, the monodromy matrix is a product of two Lax operators, $\Omega^{(i)}(u) = L^{(i)}_a(u)L^{(i)}_b(u)$, where we denoted two sites by a and b. Then,

$R_{12}(u-v)\Omega^{(1)}(u)\Omega^{(2)}(v)$ can be computed by a repeated use of (3.1.24) and (3.1.25) as

$$\begin{aligned} R_{12}(u-v)\Omega^{(1)}(u)\Omega^{(2)}(v) &= R_{12}(u-v)L_a^{(1)}(u)L_b^{(1)}(u)L_a^{(2)}(v)L_b^{(2)}(v) \\ &= R_{12}(u-v)L_a^{(1)}(u)L_a^{(2)}(v)L_b^{(1)}(u)L_b^{(2)}(v) \\ &= L_a^{(2)}(v)L_a^{(1)}(u)R_{12}(u-v)L_b^{(1)}(u)L_b^{(2)}(v) \\ &= L_a^{(2)}(v)L_a^{(1)}(u)L_b^{(2)}(v)L_b^{(1)}(u)R_{12}(u-v) \\ &= L_a^{(2)}(v)L_b^{(2)}(v)L_a^{(1)}(u)L_b^{(1)}(u)R_{12}(u-v) \\ &= \Omega^{(2)}(v)\Omega^{(1)}(u)R_{12}(u-v)\,, \end{aligned} \tag{3.1.34}$$

where we used the commutativity at different sites (3.1.24) in the equalities denoted in red and we used the R-matrix commutation relation (3.1.25) in the equalities denoted in blue. In this way, we have proved (3.1.32) for the two-site chain. For a longer chain, (3.1.32) can be proven using the mathematical induction.

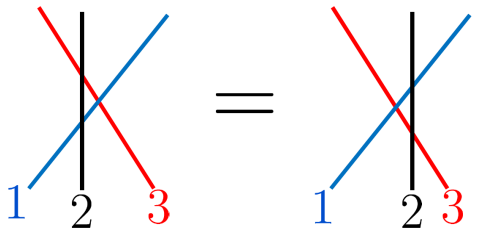

Figure 3.1.2: A pictorial expression of Yang-Baxter relation.

The asymptotic form of the monodromy matrix (3.1.22) reveals that $B(u)$ and $C(u)$ are proportional respectively to S^- and S^+ when u is large. Thus they can be naturally interpreted as a "creation" and an "annihilation" operator with respect to the *vacuum* state $|\uparrow^\ell\rangle \equiv \underbrace{|\uparrow\rangle \otimes \cdots \otimes |\uparrow\rangle}_{\ell}$, in which all the spins are up. The excitations in this case are called *magnons* and their number corresponds to the number of spins down. These features allow one to construct the Hilbert space $\mathcal{H}$ as the Fock space spanned by the M-magnon states, of the form $|\boldsymbol{u}\rangle = B(u_1)B(u_2)\cdots B(u_M)|\uparrow^\ell\rangle$ while $C(v)|\uparrow^\ell\rangle = 0$. Here u_i's are called the *rapidities* of the magnons. The physical meaning of the rapidities is not clear in the algebraic Bethe ansatz. However, if we compare the resultant states with the coordinate Bethe ansatz, it becomes clear that the rapidities are related to the momenta of magnons by

$$p_{\text{magnon}} = \ln\left(\frac{u+i/2}{u-i/2}\right)\,. \tag{3.1.35}$$

Similarly, the bra-states are generated by the operator $C(v)$'s as $\langle \boldsymbol{v}| = \langle \uparrow^\ell | C(v_1)C(v_2)\cdots C(v_M)$, built upon the dual vacuum $\langle \uparrow^\ell |$ satisfying $\langle \uparrow^\ell | B(u) = 0$ and $\langle \uparrow^\ell | \uparrow^\ell \rangle = 1$. These Fock states will be referred to as generic Bethe states.

Of particular importance is the *transfer matrix* given by $T(u) \equiv \operatorname{tr} \Omega(u) = A(u) + D(u)$. Owing to the algebra (3.1.23), $T(u)$'s mutually commute as follows:

$$[T(u), T(v)] = 0\,. \tag{3.1.36}$$

Therefore, when expanded in powers of u, the transfer matrix generates infinitely many mutually commuting quantities including the Hamiltonian of the spin chain. More explicitly, the Hamiltonian (3.1.19) can be obtained from $T(u)$ in the following way (when θ_i's are set to zero):

$$\hat{H} = \frac{\lambda L}{8\pi^2} + \frac{\lambda}{8\pi i} \left. \frac{d \ln T(u)}{du} \right|_{u=0, \boldsymbol{\theta}=0} . \tag{3.1.37}$$

We can also express the total momentum of the system P as

$$e^{iP} = (-i)^\ell T(0)\big|_{\boldsymbol{\theta}=0}\,. \tag{3.1.38}$$

The (dual) vacuum is known to be the eigenstate of $T(u)$ in the manner

$$A(u)|\uparrow^\ell\rangle = Q^+_{\boldsymbol{\theta}}(u)|\uparrow^\ell\rangle\,, \qquad D(u)|\uparrow^\ell\rangle = Q^-_{\boldsymbol{\theta}}(u)|\uparrow^\ell\rangle\,, \tag{3.1.39}$$

$$\langle\uparrow^\ell|A(u) = \langle\uparrow^\ell|Q^+_{\boldsymbol{\theta}}(u)\,, \qquad \langle\uparrow^\ell|D(u) = \langle\uparrow^\ell|Q^-_{\boldsymbol{\theta}}(u)\,, \tag{3.1.40}$$

where $Q_{\boldsymbol{\theta}}$ functions are defined as[5]

$$Q_{\boldsymbol{\theta}}(u) \equiv \prod_{k=1}^{\ell} (u - \theta_k)\,, \qquad Q^\pm_{\boldsymbol{\theta}}(u) \equiv \prod_{k=1}^{\ell} \left(u - \theta_k \pm \frac{i}{2}\right)\,. \tag{3.1.41}$$

Using this fact, the action of $T(u)$ on the generic Bethe state $|\boldsymbol{u}\rangle = \prod_{i=1}^M B(u_i)|\uparrow\rangle$ can be computed by pushing $A(u)$ and $D(u)$ through $B(u_i)$'s using the exchange relations in (3.1.23). One then finds that $|\boldsymbol{u}\rangle$ becomes the eigenstate of $T(u)$ if and only if the following sets of equations, called the *Bethe ansatz equations*, for the rapidities are satisfied:

$$\prod_{k=1}^{\ell} \left(\frac{u_j - \theta_k + \frac{i}{2}}{u_j - \theta_k - \frac{i}{2}}\right) = \prod_{l\neq j}^{M} \left(\frac{u_j - u_l + i}{u_j - u_l - i}\right)\,. \tag{3.1.42}$$

In the coordinate Bethe ansatz, this equation arise as a periodicity condition for the phases of the magnon excitations as we go around the chain. When this equation is satisfied, the

[5] As in these definitions, each $+$ (respectively $-$) superscript on a function signifies that its argument is shifted by $+\frac{i}{2}$ (respectively $-\frac{i}{2}$). According to this convention, $Q^{++}_{\boldsymbol{\theta}}(u)$ means $Q_{\boldsymbol{\theta}}(u+i)$, etc. When $\theta_k = 0$, the functions $Q^\pm_{\boldsymbol{\theta}}(u)$ are often referred to as $a(u)$ (for $+$) and $d(u)$ (for $-$).

Bethe state is said to be *on-shell* (otherwise called *off-shell*). In that case, the eigenvalue $t_{\boldsymbol{u}}(u)$ of the transfer matrix $T(u)$ is given by

$$t_{\boldsymbol{u}}(u) = Q^{+}_{\boldsymbol{\theta}}(u)\frac{Q^{--}_{\boldsymbol{u}}(u)}{Q_{\boldsymbol{u}}(u)} + Q^{-}_{\boldsymbol{\theta}}(u)\frac{Q^{++}_{\boldsymbol{u}}(u)}{Q_{\boldsymbol{u}}(u)}\,, \tag{3.1.43}$$

which is sometimes called the Baxter equation (3.1.42) for the Q-function defined as

$$Q_{\boldsymbol{u}}(u) = \prod_{k=1}^{M}(u-u_k)\,. \tag{3.1.44}$$

The equation (3.1.43) is in fact equivalent to the Bethe ansatz equation. To see this, note that $t_{\boldsymbol{u}}(u)$ has no poles despite the presence of $Q_{\boldsymbol{u}}(u)$ in the denominator of (3.1.43). Then the condition that $Q^{+}_{\boldsymbol{\theta}}(u)Q^{--}_{\boldsymbol{u}}(u) + Q^{-}_{\boldsymbol{\theta}}(u)Q^{++}_{\boldsymbol{u}}(u)$ vanishes at $u = u_k$ leads to the Bethe ansatz equation.

Before closing this section, let us make two additional remarks:

- The energy and the momentum of the on-shell Bethe states can be expressed in terms of the rapidities as follows:

$$E = \frac{\lambda}{4\pi^2}\sum_{j=1}^{M}\left(\frac{i}{u_j+\frac{i}{2}} - \frac{i}{u_j-\frac{i}{2}}\right)\,, \quad e^{iP} = \prod_{j=1}^{M}\frac{u_j+\frac{i}{2}}{u_j-\frac{i}{2}}\,, \tag{3.1.45}$$

  where E and P are eigenvalues of (3.1.37) and (3.1.38) respectively. As a spin-chain state, the momentum P can be arbitrary. However, only the spin-chain states with $e^{iP} = 1$ correspond to the single-trace operators in the gauge theory, owing to the cyclicity of the trace.

- The properties of the operators $A(u), \ldots, D(u)$ under the global SU(2) generators S^i are often quite informative. For instance, from the transformation properties

$$\begin{aligned}[S^z, B(u)] &= -B(u)\,,\\ [S^+, B(u)] &= A(u) - D(u)\,,\end{aligned} \tag{3.1.46}$$

  and the algebra (3.1.23), one can show that if the Bethe state $|\boldsymbol{u}\rangle$ is on-shell it is the highest weight state with spin $\frac{\ell}{2} - M$. On the other hand, if it is off-shell, although having the same spin $\frac{\ell}{2} - M$, it is a direct sum of states belonging to various representations and is not a highest weight state.

3.2 Classical integrability in string theory

The aim of this section is to summarize basic facts on the classical integrability of the string theory. First in subsection 3.2.1, we briefly review the classical integrability of a superstring

on $AdS_5 \times S^5$, reviewing the papers [35–37]. Then in subsection 3.2.2, we describe a string moving in the S^3-subspace of $AdS_5 \times S^5$ more in detail.

3.2.1 Superstring on $AdS_5 \times S^5$ as Z_4 super-coset

In this subsection, we write down the action of superstring on $AdS_5 \times S^5$ in terms of Z_4-symmetric super-coset and briefly describe its integrability structure following mainly [37]. First note that the $AdS_5 \times S^5$ space can be realized as a coset space,

$$\frac{\mathrm{SO}(4,2) \times \mathrm{SO}(6)}{\mathrm{SO}(4,1) \times \mathrm{SO}(5)}\,, \tag{3.2.1}$$

where $\mathrm{SO}(4,2)(\simeq \mathrm{U}(2,2))$ is the isometry group of AdS_5 and $\mathrm{SO}(6)(\simeq \mathrm{U}(4))$ is the isometry group of S^5. Since we are considering *super*string theory, the string moves not only in the bosonic space but also in the fermionic space. The full super-space in which the string moves is given by the following super-coset,

$$\frac{\mathrm{PSU}(2,2|4)}{\mathrm{SO}(4,1) \times \mathrm{SO}(5)}\,. \tag{3.2.2}$$

Before writing down the action using the coset structure, let us briefly explain the basic properties of this super-coset. The elements of superalgebra $su(2,2|4)$ are given by $(4|4) \times (4|4)$ supermatrices,

$$M = \left(\begin{array}{c|c} A & B \\ \hline C & D \end{array}\right)\,, \tag{3.2.3}$$

satisfying the following three conditions: First, the bosonic parts A and D belong to $u(2,2)$ and $u(4)$ respectively. Second the fermionic parts C and D satisfy

$$C = B^\dagger \begin{pmatrix} 1_{2\times 2} & 0 \\ 0 & -1_{2\times 2} \end{pmatrix} \tag{3.2.4}$$

Third, M satisfies the supertraceless condition,

$$\mathrm{str} M = \mathrm{tr}\, A - \mathrm{tr}\, D = 0\,. \tag{3.2.5}$$

Modding by the matrices proportional to the identity, we obtain the $psu(2,2|4)$ superalgebra from $su(2,2|4)$. The $su(2,2|4)$ has the following automorphism,

$$\mathcal{S}\,[M] = \begin{pmatrix} EA^tE & -EC^tE \\ EB^tE & ED^tE \end{pmatrix}\,, \quad E = \begin{pmatrix} 0 & -1 & 0 & 0 \\ 1 & 0 & 0 & 0 \\ 0 & 0 & 0 & -1 \\ 0 & 0 & 1 & 0 \end{pmatrix}\,, \tag{3.2.6}$$

which satisfies

$$\mathcal{S}^4 = 1\,. \tag{3.2.7}$$

Using this Z_4-automorphism, one can decompose the elements of the algebra as

$$M = \sum_{i=1}^{3} M^{(i)}\,, \qquad \left(\mathcal{S}\left[M^{(n)}\right] = i^n M^{(n)}\right)\,. \tag{3.2.8}$$

Written explicitly, they are given by

$$M^{(0)} = \frac{1}{2}\begin{pmatrix} A + EA^tE & 0 \\ 0 & D + ED^tE \end{pmatrix}\,,\; M^{(1)} = \frac{1}{2}\begin{pmatrix} 0 & B + iEC^tE \\ C - iEB^tE & 0 \end{pmatrix}\,, \tag{3.2.9}$$

$$M^{(2)} = \frac{1}{2}\begin{pmatrix} A - EA^tE & 0 \\ 0 & D - ED^tE \end{pmatrix}\,,\; M^{(3)} = \frac{1}{2}\begin{pmatrix} 0 & B - iEC^tE \\ C + iEB^tE & 0 \end{pmatrix}\,. \tag{3.2.10}$$

From the explicit forms of $M^{(0)}$, one can conclude that $M^{(0)}$ precisely corresponds to the degrees of freedom projected out upon taking the coset, namely the denominator of (3.2.2), SO(4,1)×SO(5).

Now we are in a position to write down the action of the superstring in $AdS_5 \times S^5$. For this purpose, let us consider the current,

$$J = -g^{-1}dg\,, \tag{3.2.11}$$

where $g(\tau, \sigma)$ is a group element of PSU(2,2|4), and decompose it using the aforementioned Z_4-symmetry as $J = \sum_{i=1}^{4} J^{(i)}$. Then, the Green-Schwartz-type action for the superstring in $AdS_5 \times S^5$, first constructed by Metsaev and Tseytlin in [38], is given by[6]

$$S = \frac{\sqrt{\lambda}}{4\pi}\int \mathrm{str}\left(J^{(2)} \wedge *J^{(2)} - J^{(1)} \wedge *J^{(3)}\right) + \Lambda \wedge \mathrm{str}J^{(2)}\,, \tag{3.2.12}$$

where we have introduced the Lagrange multiplier Λ to enforce the supertraceless condition $\mathrm{str}J^{(2)} = 0$. Here $J^{(2)}$ corresponds to the bosonic coordinates of $AdS_5 \times S^5$ whereas $J^{(1,3)}$ correspond to the fermionic corrdinates. Note that $J^{(0)}$ does not appear in the action (3.2.2) as it represents the degrees of freedom projected out upon taking the coset. The equation of motion can be derived by considering the first-order variation of this action. The easiest

[6]The action for the string usually contains the prefactor, $1/(2\pi\ell_s^2)$. Such a prefactor, combined with the radius of $AdS_5 \times S^5$, give the prefactor in (3.2.12), owing to the relation (2.1.19).

way is to consider an infinitesimal left transformation[7], $g \to \delta G_L g$, and see how the action changes. Then the result is given as the following conservation law:

$$d * k = 0\,, \tag{3.2.13}$$

where k is the Noether current associated with the global left-transformation symmetry defined as

$$\begin{aligned} k &= gKg^{-1}\,, \\ K &= J^{(2)} + \frac{1}{2} * J^{(1)} - \frac{1}{2} * J^{(3)} - \frac{1}{2} * \Lambda\,. \end{aligned} \tag{3.2.14}$$

Let us now discuss the integrable structures of the superstring in $AdS_5 \times S^5$. Using the equation of motion (3.2.13) and the flatness condition,

$$dJ - J \wedge J = 0\,, \tag{3.2.15}$$

which trivially follows from the definition of J, $J = g^{-1}dg$, we can show that the connection

$$A(x) = J^{(0)} + \frac{x^2+1}{x^2-1} J^{(2)} - \frac{2x}{x^2-1}\left(*J^{(2)} - \Lambda\right) + \sqrt{\frac{x+1}{x-1}} J^{(1)} + \sqrt{\frac{(x-1)}{(x+1)}} J^{(3)} \tag{3.2.16}$$

is flat regardless of the value of the complex number x, which is called the *spectral parameter*. This property is the clearest manifestation of the integrability the system possesses. To see the integrability more explicitly, consider the following path-ordered exponential of $A(x)$, called the *monodromy matrix*, along a nontrivial closed cycle of the worldsheet:

$$\Omega(x; z_0) = \mathrm{P} \exp\left(\oint A(x)\right)\,. \tag{3.2.17}$$

As indicated, the matrix $\Omega(x)$ depends on the base-point of the cycle z_0. Owing to the flatness of $A(x)$, the monodromy matrix will not be affected by the local deformation of the cycle and its expansion as a function of x around some point yields an infinite number of conserved charges. Quantities independent of the base-point z_0 can be extracted from the eigenvalues of the monodromy matrix, called the *quasi-momenta*. In the present case, there are the following eight quasi-momenta:

$$u(x; z_0)\Omega(x; z_0)u(x; z_0)^{-1} = \mathrm{diag}\{e^{i\hat{p}_1}, e^{i\hat{p}_2}, e^{i\hat{p}_3}, e^{i\hat{p}_4} | e^{ip_1}, e^{ip_2}, e^{ip_3}, e^{ip_4}\}\,, \tag{3.2.18}$$

where $\hat{p}_i$'s denote the eigenvalues corresponding to $u(2,2)$-part and describe the dynamics in AdS_5 whereas p_i's denote the eigenvalues corresponding to $u(4)$-part and describe the

[7]By performing an infinitesimal *right* transformation, we can derive the conservation laws for the right Noether current. However, as it is not independent of (3.2.13), we will not write it down here.

dynamics in S^5. Expansions of $\hat{p}_i$ and p_i as functions of x yield an infinite number of mutually commutative charges. For instance, the expansions around $x = \infty$ give the global charges associated the Cartan generators at the leading order,

$$\begin{pmatrix} \hat{p}_1 \\ \hat{p}_2 \\ \hat{p}_3 \\ \hat{p}_4 \\ \hline p_1 \\ p_2 \\ p_3 \\ p_4 \end{pmatrix} = \frac{2\pi}{x\sqrt{\lambda}} \begin{pmatrix} +\Delta - S_1 + S_2 \\ +\Delta + S_1 - S_2 \\ -\Delta - S_1 - S_2 \\ -\Delta + S_1 + S_2 \\ \hline +J_1 + J_2 - J_3 \\ +J_1 - J_2 + J_3 \\ -J_1 + J_2 + J_3 \\ -J_1 - J_2 - J_3 \end{pmatrix} + O(x^{-2}) \,, \tag{3.2.19}$$

where Δ is the dilatation charge and S_i and J_i are angular momenta for AdS_5 and S^5 respectively. For the string moving in S^3, more detailed descriptions, including the explicit definitions of charges, will be given in the next subsection.

3.2.2 Classical integrability of string on S^3

In the previous subsection, we have explained that the superstring theory in $AdS_5 \times S^5$ possesses classical integrability. However, the argument above was somewhat abstract. Below we give a detailed description of a string which does not have angular momenta in AdS_5 and moves in the S^3-subspace[8] of the full S^5. The goal of this section is to provide necessary backgrounds for the computation of three-point functions, which will be discussed in Part III. A more specific details will be explained in section 7.1.

Let us first write down the action and the equation of motion for the string on S^3. The Polyakov action of a string on S^3 is given by[9]

$$S_{S^3} \equiv \frac{\sqrt{\lambda}}{\pi} \int_\Sigma d^2z \partial Y^I \bar{\partial} Y_I \,, \tag{3.2.20}$$

where the contraction of indices is defined by $V^I V_I \equiv \sum_{i=1}^4 (V_i)^2$ and Y^I are the embedding coordinates of S^3, which satisfy

$$Y^I Y_I = 1 \,. \tag{3.2.21}$$

[8] In the following discussions, we will concentrate on the bosonic degrees of freedom since the fermionic part does not give the leading contribution in the classical limit.

[9] In the study of the spectrum of the string, the worldsheet is often taken to be Minkowskian. However, to study three-point functions, the worldsheet must be Euclidean.

Since our main focus in this thesis is on the large N limit of the gauge theory, which corresponds to the $g_s \to 0$ limit in the string theory, we take the worldsheet of the string, Σ, to be a sphere. We also allow the worldsheet to have several punctures, which correspond to the insertion points of the vertex operators. Owing to the constraint (3.2.21), the equation of motion becomes

$$\partial\bar{\partial}Y^I + \left(\partial Y^J \bar{\partial} Y_J\right) Y^I = 0\,. \tag{3.2.22}$$

In addition to the equation of motion (3.2.22), the solutions which describe physical string states must obey an additional constraint called the *Virasoro constraint*, which requires the sum of the AdS contribution and the S contribution to the stress-energy tensor to vanish, $T_{AdS} + T_S = 0$.

T_{AdS} and T_S become singular at the punctures. Near such points, the behavior of the solution will be determined solely by the operators inserted there and will not depend on other operators inserted at different points. This means that, for any solutions, the behavior near the puncture is the same as that of the solution for the two-point function, which is known explicitly. Since we take the external states to be those without AdS spin, the AdS part of the solutions for two-point functions can be easily obtained: It is given by an appropriate SO(4,2) global transformation of the following simple solution[10]:

$$z_{\rm AdS} = e^{2\kappa\tau}\,, \tag{3.2.23}$$

where τ is the cylinder-coordinate, $\ln z = \tau + i\sigma$, and $z_{\rm AdS}$ is the radial coordinate[11] of AdS, which we denoted previously by z in (2.1.12). Since the dilatation charge of the solution (3.2.23) is computed as

$$\Delta = \frac{\sqrt{\lambda}}{\pi}\int_0^{2\pi} d\sigma \frac{\partial_\tau z_{\rm AdS}}{2 z_{\rm AdS}} = 2\sqrt{\lambda}\kappa\,, \tag{3.2.24}$$

we can express the constant κ in terms of the conformal dimension Δ as

$$\kappa = \frac{\Delta}{2\sqrt{\lambda}}\,, \tag{3.2.25}$$

Using the solution (3.2.23), we can compute the AdS part of the stress-energy tensor for two-point functions $T_{AdS,2\rm pt}$ as follows:

$$T_{AdS,2\rm pt} = \frac{\partial z_{\rm AdS}\bar{\partial} z_{\rm AdS}}{z_{\rm AdS}^2} = \frac{\kappa^2}{z^2}\,. \tag{3.2.26}$$

[10]The solution (3.2.23) describes the trajectory of the string which starts from the boundary of AdS at $\tau = -\infty$ and is absorbed by the horizon at $\tau = \infty$. The general solution describing two-point functions can be obtained by performing a SO(4,2) transformation which maps the point at the horizon to an arbitrary point on the boundary. For details, see [39].

[11]Since we denote the worldsheet coordinate by z in this section, we used a slightly different notation for the radius coordinate here.

Thus, near each puncture z_i, T_{AdS} and T_S behave generally as

$$T_{AdS}(z) \sim \frac{\kappa_i^2}{(z-z_i)^2}\,, \quad T_S(z) \sim \frac{-\kappa_i^2}{(z-z_i)^2} \quad \text{as } z \to z_i\,, \tag{3.2.27}$$

where κ_i is related to the conformal dimension of each operator Δ_i as $\kappa_i = \Delta_i/(2\sqrt{\lambda})$.

The embedding coordinates of S^3 can be conveniently assembled into a 2×2 matrix with unit determinant as

$$\mathbb{Y} = \begin{pmatrix} Z & X \\ -\bar{X} & \bar{Z} \end{pmatrix}\,, \qquad \det \mathbb{Y} = 1\,. \tag{3.2.28}$$

where Z and X are given by $Z = Y_1 + iY_2$ and $X = Y_3 + iY_4$ and $\bar{Z}$ and $\bar{X}$ are their conjugates. Under the isometry group $\mathrm{SO}(4,2) = \mathrm{SU}(2)_L \times \mathrm{SU}(2)_R$, they transform as follows:

$$\mathbb{Y} \to U_L \mathbb{Y} U_R\,, \qquad U_R \in \mathrm{SU}(2)_R\,, \quad U_L \in \mathrm{SU}(2)_L\,. \tag{3.2.29}$$

The quantities of central importance in the following discussion are the *right current* j and the *left current* l, defined respectively by

$$j = \mathbb{Y}^{-1} d\mathbb{Y}\,, \quad l = d\mathbb{Y}\mathbb{Y}^{-1}\,. \tag{3.2.30}$$

Evidently, two currents are related by $l = \mathbb{Y} j \mathbb{Y}^{-1}$. Under the transformation (3.2.29), they transform covariantly as

$$j \to U_R^{-1} j U_R\,, \quad l \to U_L l U_L^{-1}\,. \tag{3.2.31}$$

Then, owing to the equation of motion (3.2.22), we can define two one-parameter families of flat connections,

$$\left[\partial + \frac{j_z}{1-x}, \bar{\partial} + \frac{j_{\bar{z}}}{1+x}\right] = 0\,, \tag{3.2.32}$$

$$\left[\partial + \frac{x l_z}{1-x}, \bar{\partial} - \frac{x l_{\bar{z}}}{1+x}\right] = 0\,, \tag{3.2.33}$$

which we call the *right connection* and the *left connection* respectively in the rest of this thesis. The two connections are related by the gauge transformation of the form

$$\mathbb{Y}\left(\partial + \frac{j_z}{1-x}\right)\mathbb{Y}^{-1} = \partial + \frac{x l_z}{1-x}\,, \quad \mathbb{Y}\left(\bar{\partial} + \frac{j_{\bar{z}}}{1+x}\right)\mathbb{Y}^{-1} = \bar{\partial} - \frac{x l_{\bar{z}}}{1+x}\,. \tag{3.2.34}$$

One of the manifestations of integrability is the existence of an infinite number of conserved charges. As we have seen in the previous section, they are constructed from path-

ordered exponentials of the connections (3.2.32) and (3.2.33), which are called the monodromy matrix[12],

$$\Omega(x;z_0) \equiv \mathrm{P}\exp\left(-\oint dz\frac{j_z}{1-x}+d\bar{z}\frac{j_{\bar{z}}}{1+x}\right). \tag{3.2.35}$$

Here we only displayed the monodromy matrix constructed from the right connection since the monodromy matrix constructed from the left connection $\tilde{\Omega}$ is related to Ω as $\tilde{\Omega}=\mathbb{Y}\Omega\mathbb{Y}^{-1}$. In the present case, the integration path is taken to be a contour encircling a puncture. By virtue of the flatness of the connection, an expansion of $\Omega(x)$ as a function of x around some point yields an infinite number of conserved charges as coefficients. In particular, expansions around $x=\infty$ and $x=0$ yield global charges, corresponding to $\mathrm{SU}(2)_R$ and $\mathrm{SU}(2)_L$ respectively, at the leading order in the following way:

$$\Omega(x;z_0) = \mathbf{1}-\frac{4\pi i}{\sqrt{\lambda}x}Q_R+O(x^{-2}) \quad (x\to\infty), \tag{3.2.36}$$

$$\mathbb{Y}(z_0)\Omega(x;z_0)\mathbb{Y}^{-1}(z_0) = \mathbf{1}+\frac{4\pi i x}{\sqrt{\lambda}}Q_L+O(x^2) \quad (x\to 0). \tag{3.2.37}$$

where the matrices Q_R and Q_L are given by

$$Q_R \equiv \frac{i\sqrt{\lambda}}{4\pi}\oint(j_z dz - j_{\bar{z}}d\bar{z}), \qquad Q_L \equiv \frac{i\sqrt{\lambda}}{4\pi}\oint(l_z dz - l_{\bar{z}}d\bar{z}). \tag{3.2.38}$$

To characterize the string states, it is often more convenient to use quantities independent of the base point z_0. Such quantities can be extracted from the eigenvalues of the monodromy matrix:

$$u(x;z_0)\,\Omega(x)\,u(x;z_0)^{-1} = \begin{pmatrix} e^{ip(x)} & 0 \\ 0 & e^{-ip(x)} \end{pmatrix}, \tag{3.2.39}$$

where $u(x;z_0)$ is the matrix which diagonalizes Ω and the function $p(x)$ is called *quasi-momentum*. Reflecting the asymptotics of Ω around $x=\infty$ and $x=0$, $p(x)$ exhibits the following behavior:

$$p(x)-p(\infty) = -\frac{4\pi}{\sqrt{\lambda}x}R+O(x^{-2}) \qquad (x\to\infty), \tag{3.2.40}$$

$$p(x)-p(\infty) = 2\pi m+\frac{4\pi x}{\sqrt{\lambda}}L+O(x^2) \qquad (x\to 0). \tag{3.2.41}$$

Here the conserved charges R and L are the (upper) eigenvalues of Q_R and Q_L respectively and m is an integer. Let us now make comments on the definition of $p(x)$. Since $p(x)$ is

[12]Mathematically speaking, the monodromy matrix should be defined using the *anti-path-ordered* exponential. It would be more appropriate to call the object defined in (3.2.35) the *holonomy matrix*. However, here we adopted the convention extensively used in the literature on integrability in AdS/CFT.

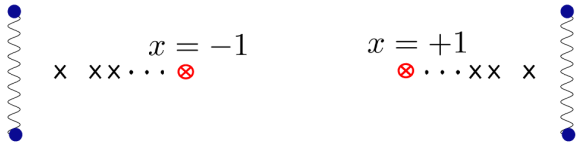

Figure 3.2.1: Analytic structure of the spectral curve of a string in S^3. The wavy lines denote square-root cuts. There are essential singularities at $x = \pm 1$, corresponding to simple poles of $p(x)$. The node-like points, denoted by crossed accumulate to these points.

defined as a logarithm of the eigenvalue of Ω, it is ambiguous by a multiple of 2π. However, since most of the important quantities to be discussed below will be defined solely in terms of the differential dp, such ambiguity is inessential. In addition to the 2π-ambiguity, there is Z_2 ambiguity, $p(x) \leftrightarrow -p(x)$, which comes from the exchange of two different eigenvalues of Ω. Such ambiguity will be fixed when we discuss the pole structure of $p(x)$ shortly.

To discuss other nontrivial conserved charges, it is important to study the analytic properties of $p(x)$. Such analytic structures are encoded in the *spectral curve* defined by

$$\Gamma : \quad \Gamma(x, y) \equiv \det\left(y\mathbf{1} - \Omega(x; z_0)\right) = 0\,, \tag{3.2.42}$$

which is equivalent to $\left(y - e^{ip(x)}\right)\left(y - e^{-ip(x)}\right) = 0$. As we shall show, the spectral curve Γ has three kinds of analytic structures, namely *essential singularities*, *cusp-like points* and *node-like points* (see Figure 3.2.1).

Let us first focus on the essential singularities. It is known that the essential singularities arise at $x = \pm 1$, where the Lax connection (3.2.32) becomes singular [40]. To see this, recall the definition of the monodromy matrix (3.2.35). Near $x = \pm 1$, it behaves as

$$\Omega(x; z_0) = \mathrm{P}\exp\left[-\oint dz \frac{j_z}{1-x} + O((x-1)^0)\right] \qquad (x \to 1)\,, \tag{3.2.43}$$

$$\Omega(x; z_0) = \mathrm{P}\exp\left[-\oint dz \frac{j_{\bar{z}}}{1+x} + O((x+1)^0)\right] \qquad (x \to -1)\,. \tag{3.2.44}$$

Since the stress-energy tensor can be expressed in terms of the right currents as

$$T_S(z) = -\frac{1}{2}\mathrm{Tr}\,(j_z j_z)\,, \quad \bar{T}_S(\bar{z}) = -\frac{1}{2}\mathrm{Tr}\,(j_{\bar{z}} j_{\bar{z}})\,, \tag{3.2.45}$$

we can determine the behavior of the eigenvalues from the behavior of $T_S(z)$ around the puncture (3.2.27) as

$$u(x; z_0)\Omega(x; z_0)u(x; z_0)^{-1} = \exp\left[\frac{2i\pi\kappa}{x \mp 1}\sigma_3 + O((x \mp 1)^0)\right] \qquad (x \to \pm 1)\,, \tag{3.2.46}$$

where we dropped the subscript i since, in the rest of this section, we focus on the properties of one particular operator neglecting other operators. The behavior (3.2.46) clearly shows the existence of essential singularities at $x = \pm 1$ (see Figure 3.2.1). Evidently, they correspond to the simple pole singularities of $p(x)$ of the form

$$p(x) = -\frac{2\pi\kappa}{x \mp 1} + O(1) \quad (x \to \pm 1^{+}) \,, \tag{3.2.47}$$

where the superscript $+$ signifies the point on the first sheet of the spectral curve. Note that requiring $p(x)$ to behave as (3.2.47), not as $\sim +2\pi\kappa/(x \mp 1)$, completely fixes the aforementioned Z_2 ambiguity.

Next, let us discuss the remaining analytic structures, *i.e.* the cusp-like points and the node-like points. These points are collectively called *singular points*. Both of them are defined as the zeros of the discriminant Δ_Γ of the spectral curve given by

$$\Delta_\Gamma \equiv \left(e^{ip(x)} - e^{-ip(x)}\right)^2 \,. \tag{3.2.48}$$

Note that, although they are singular points of the spectral curve, the quasi-momentum $p(x)$ is not singular at these points. They are classified according to the order of the zero. If the order of the zero is odd, *i.e.* $\Delta_\Gamma \sim (x - x_i^{(c)})^{2r+1}$, then such a point is called cusp-like. If it is even, like $\Delta_\Gamma \sim (x - x_i^{(n)})^{2r}$, it is called node-like. Around such a zero, the quasi-momentum is approximated as

$$e^{ip(x)} \sim \pm\left(1 + \frac{\sqrt{\Delta_\Gamma}}{2}\right) \quad \Rightarrow \quad p(x) \sim m\pi + \frac{\sqrt{\Delta_\Gamma}}{2i} \qquad m \in \mathbb{Z} \,. \tag{3.2.49}$$

This shows that, at the cusp-like points, the spectral curve develops branch cuts. Another important property of a cusp-like point is that, as shown in Proposition 7.3 in [41], the monodromy matrix at such a point always takes the form of a Jordan block, namely

$$\Omega(x_i^{(c)}) \sim \pm \begin{pmatrix} 1 & * \\ 0 & 1 \end{pmatrix} \,. \tag{3.2.50}$$

Now consider the properties of the node-like points. The formula (3.2.49) shows that in this case the spectral curve does not develop a branch cut and such a point is characterized simply by some integer m_i as

$$p(x_i^{(n)}) = m_i\pi \,. \tag{3.2.51}$$

As concerns the form of the monodromy matrix, there are two possibilities at a node-like point. It either takes the form of a Jordan block or is proportional to the identity matrix:

$$\Omega(x_i^{(n)}) \sim \pm \begin{pmatrix} 1 & * \\ 0 & 1 \end{pmatrix} \quad \text{or} \quad \pm \mathbf{1} \,. \tag{3.2.52}$$

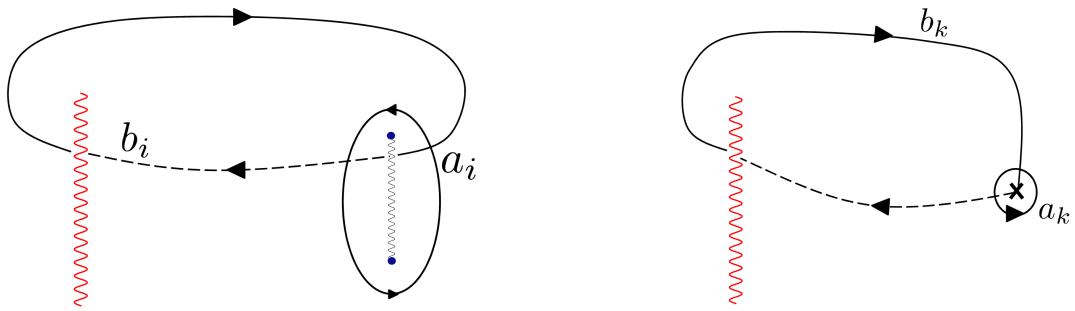

Figure 3.2.2: The definition of the a- and b-cycles. On the left figure, we depicted the case where the branch cut has a finite size while, on the right figure, we depicted the case where the branch cut shrinks to a point. The reference cut is depicted in red.

As we will see in Part III, in the case of three-point functions, the monodromy matrix necessarily takes the form of a Jordan block at node-like points, owing to the global consistency of the monodromy on the worldsheet. On the other hand, in the *finite gap method*, which is a powerful method to construct the solutions for two-point functions and is briefly reviewed in section 7.1, the monodromy matrix is assumed to be proportional to the identity matrix at node-like points.

It is often convenient to regard the node-like points as infinitesimal branch cuts. In fact, it is known that the node-like points correspond to unexcited modes of the string [41–43] and one can perturb the classical string solution by inserting a small cut at the position of the node-like points [37]. This perspective will play a crucial role also when we discuss three-point functions in Part III.

To extract nontrivial information from the spectral curve, we now introduce a basis of cycles on the spectral curve. As shown in Figure 3.2.2, a convenient choice is to define the a-cycles as those which surround branch cuts (including node-like points) counterclockwise and the b-cycles as those connecting some "reference cut" and the other cuts. Under an appropriate choice of the branch of the logarithm and the positions of the branch cuts, the integrals of the differential dp along a- and b-cycles take the following form [42, 43]:

$$\oint_{a_i} dp = 0\,, \qquad \int_{b_i} dp = 2\pi n_i\,, \qquad n_i \in \mathbb{Z}\,. \tag{3.2.53}$$

In addition to these cycles, it is convenient to introduce four more cycles a_0, a_∞, b_0 and b_∞. The cycles a_0 and a_∞ surround the points $x = 0$ and $x = \infty$ counterclockwise respectively, while b_0 and b_∞ connect the reference cut with $x = 0$ and $x = \infty$. As discussed in [41], one can treat these cycles essentially on equal footing with the other cycles. Now using the a-type cycles, one can define a set of conserved charges called *filling fractions* as

$$S_i \equiv \frac{i}{2\pi} \oint_{a_i} p(x)dz \left(= \oint_{a_i} \frac{zdp}{2\pi i} \right)\,, \tag{3.2.54}$$

where

$$z = \frac{\sqrt{\lambda}}{4\pi}\left(x + \frac{1}{x}\right) \tag{3.2.55}$$

is called the *Zhukovsky variable*. As will be discussed in section 7.1, when interpreted appropriately as dynamical variables of a string system, $p(x)$ and z are canonically conjugate and hence the definition (3.2.54) is nothing but that of an action variable. For this reason the filling fractions are of extreme importance and we will construct the angle variables as their conjugates in section 7.1. In addition, as will be explained in section 3.3, the filling fractions can be naturally identified with the number of Bethe roots in the spin chain in certain limits. Among the S_i's, S_0 and S_∞ are of special interest since they correspond to the global charges R and L in the following way:

$$S_0 = L\,, \qquad S_\infty = -R\,. \tag{3.2.56}$$

It should be remarked that the filing fractions for the node-like points vanish, since $p(x)$ is not singular at those points:

$$S_k = \frac{i}{2\pi}\oint_{x_k} p(x)dz = 0\,. \tag{3.2.57}$$

This is consistent with the interpretation of the node-like points as representing unexcited modes of the string.

3.3 Weak/strong match: Frolov-Tseytlin limit

In the preceding two sections, we have seen that the integrable structures exist both at one loop in the gauge theory and at the classical limit of string theory. However, these two descriptions work well in a totally different range of validity, $\lambda \to 0$ and $\lambda \to \infty$ respectively. Thus it is hard to directly relate these two structures. The key to overcome this difficulty is to consider the states with a sufficiently large R-charge J. Then, we can formally expand both sides of the duality in powers of λ/J^2 and compare the leading terms[13] directly. Physically, this is due to the fact that any quantum system, whether it is spin chain or string, can be well-approximated by the WKB-approximation when the quantum number is sufficiently large.

To see this more explicitly, below we take the following steps. First, in subsection 3.3.1, we discuss the semi-classical limit of the XXX spin chain and its Bethe equation, and show that the dynamics in such a limit can be well-described by the so-called *Landau-Lifshitz*

[13]The comparison of the subleading terms will be briefly mentioned in section 3.5.

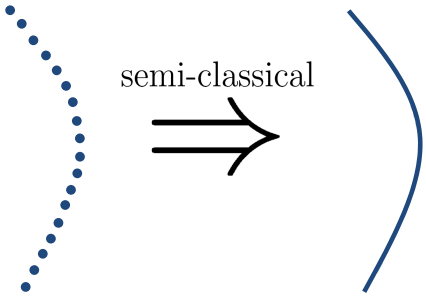

Figure 3.3.1: Condensation of the Bethe roots. In the semi-classical limit, the Bethe roots align on a certain curve on the rapidity plane and form a branch cut

sigma model. Then, in subsection 3.3.2, we discuss strings with large angular momenta and show that, in such a limit, the string sigma model on S^3 coincides with the Landau-Lifshitz sigma model at the level of integrable structures.

3.3.1 Semi-classical limit of the XXX spin chain

We have seen that the integrable structure governs both the gauge theory side and the string theory side. However, an important difference is that the system is inherently defined on a discretized lattice on the gauge theory side whereas it is defined on a continuous worldsheet on the string theory side. In order to directly compare the results on both sides and extract the common structures, it is useful to consider the particular low-energy limit of the spin chain when the length of the spin waves are large and magnon excitations exhibit collective motion. In such a limit, one can effectively neglect the discrete lattice structure and describe the system in terms of the classical motion of collective fields.

To be more precise, we consider the limit where the length of the chain ℓ and the number of the magnons M are both large and the ratio M/ℓ is finite. In addition, we scale the rapidities of the Bethe roots with the length of the chain as $u \sim L$. Since the rapidities are related to the momenta of magnons by (3.1.35), this corresponds to considering the excitations whose wave lengths are comparable to the length of the chain.

Let us first examine the Bethe equation in such a limit. Setting inhomogeneities to zero and taking the logarithm, (3.1.42) can be rewritten as follows:

$$\ell \ln\left(\frac{u_j+\frac{i}{2}}{u_j-\frac{i}{2}}\right) + 2m_j\pi i = \sum_{l\neq j} \ln\left(\frac{u_j-u_l+i}{u_j-u_l-i}\right) , \tag{3.3.1}$$

where an integer m_j corresponds to the *mode number* of the magnon excitation. In order to study the collective behavior of the magnon excitations, we need to consider a solution

to the Bethe equations in which a macroscopic number of Bethe roots have the same mode number. If we take the scaling limit of such solutions, where ℓ goes infinity and M and u_j are of the order ℓ, the Bethe roots condense into several cuts on the rapidity plane as shown in Figure 3.3.1. To study such situations, it is convenient to introduce the the resolvent,

$$G(u) = \sum_{j=1}^{M} \frac{1}{u - u_j} \,, \tag{3.3.2}$$

and define the "density" of the Bethe roots as

$$\rho(u) = \frac{1}{2\pi i} \left(G(u - \epsilon) - G(u + \epsilon) \right) \quad \text{for } u \in \mathcal{C} \,. \tag{3.3.3}$$

Here ϵ is an infinitesimally small positive number and $\mathcal{C} = \mathcal{C}_1 \cup \mathcal{C}_2 \cup \dots$ is a set of contours on which Bethe roots condense, where, on $\mathcal{C}_j$, the roots have the mode number m_j. Then, the logarithmic Bethe equation (3.3.1) in the scaling limit takes the following form[14]:

$$2m_j\pi = G(u + \epsilon) + G(u - \epsilon) - \frac{\ell}{u} \qquad \text{for } u \in \mathcal{C}_j \,. \tag{3.3.4}$$

The equations (3.3.3) and (3.3.4) can be compactly expressed using the *quasi-momentum*,

$$p(u) = G(u) - \frac{\ell}{2u} \,, \tag{3.3.5}$$

as

$$\begin{aligned} &p(u + \epsilon) - p(u - \epsilon) = -2\pi i \rho(u) \,, \\ &p(u + \epsilon) + p(u - \epsilon) = 2\pi m_j \,, \end{aligned} \qquad \text{for } u \in \mathcal{C}_j \,. \tag{3.3.6}$$

Then, the end points of the cut $\mathcal{C}_j$, at which the density $\rho(u)$ vanishes, can be characterized by

$$p(u_*) = \pi m_j \,. \tag{3.3.7}$$

Notice that the equation (3.3.7) is of the same form as the equation characterizing the branch points of the quasi-momentum of the classical string (3.2.49). Later in this section, we will see that the two quasi-momenta are directly related. Note also that the number of magnons can be read off from the asymptotic behavior of $p(x)$ as

$$p(x) \sim \frac{M - \ell/2}{x} \quad \text{as } x \to \infty \,. \tag{3.3.8}$$

[14] Although we take the rapidities to be large, the difference between two rapidities, $u_j - u_l$ on the left hand side of (3.3.1), is not necessarily large. Therefore, precisely speaking, we cannot simply replace the logarithm on the right hand side of (3.3.1) with $2i/(u_i - u_j)$ on the right hand side of (3.3.2). However, such an effect, called the *anomaly* in the literature, is known to be suppressed by $1/\ell$.

The similarity with the classical string signa model indicates that the XXX spin chain in this limit can be described by a certain classical system. Such an expectation is natural in view of the fact that any quantum system has a semi-classical (WKB) description when the quantum number is sufficiently large. However, the problem in the present case is that the fundamental degrees of freedom in the XXX spin chain are given by the spin variables $S_n^{x,y,z}$, which do not have direct classical counterparts. This difficulty can be overcome by the use of the coherent states of the spin chain. Since the coherent-state description is very effective to explore the connection with the string sigma model, below we shall review it slightly in detail.

As a first step, let us discuss the coherent-state description of a single spin-1/2 state. In what follows, we will use the following definition of the coherent state,

$$|\vec{n}\rangle = \exp\left[i\frac{\theta}{\sin\theta}(\vec{n}_0 \times \vec{n})\cdot\vec{S}\right]|\uparrow\rangle\,, \tag{3.3.9}$$

where $\vec{n}_0$ is a unit vector along 3-axis and θ is defined by

$$\vec{n}_0\cdot\vec{n} = \cos\theta\,. \tag{3.3.10}$$

The definition, (3.3.9), can also be expressed in a more explicit manner:

$$|\vec{n}\rangle = \cos\frac{\theta}{2}|\uparrow\rangle - e^{i\phi}\sin\frac{\theta}{2}|\downarrow\rangle\,, \tag{3.3.11}$$

where ϕ is defined by $n_1 + in_2 = \sin\theta e^{i\phi}$. Then the inner product between two coherent states can be calculated as

$$\begin{aligned}\langle\vec{n}'|\vec{n}\rangle &= \cos\frac{\theta}{2}\cos\frac{\theta'}{2} + e^{i(\phi-\phi')}\sin\frac{\theta}{2}\sin\frac{\theta'}{2}\\ &= \exp\left(i\frac{\Phi(\vec{n}',\vec{n})}{2}\right)\sqrt{1-\frac{(\vec{n}-\vec{n}')^2}{4}}\,,\end{aligned} \tag{3.3.12}$$

where $\Phi(\vec{n}',\vec{n})$ is the area of the triangle drawn on a unit sphere with vertices at $\vec{n}_1$, $\vec{n}_2$ and $\vec{n}_0$:

$$\begin{aligned}\tan\frac{\Phi(\vec{n}',\vec{n})}{2} &\equiv \frac{\sin(\theta/2)\sin(\theta'/2)\sin(\phi-\phi')}{\cos(\theta/2)\cos(\theta'/2)+\sin(\theta/2)\sin(\theta'/2)\cos(\phi-\phi')}\\ &= \frac{\det\,(\vec{n}',\vec{n},\vec{n}_0)}{1+\vec{n}_0\cdot\vec{n}+\vec{n}_0\cdot\vec{n}'+\vec{n}\cdot\vec{n}'}\left(=\frac{(\vec{n}'\times\vec{n})\cdot\vec{n}_0}{1+\vec{n}_0\cdot\vec{n}+\vec{n}_0\cdot\vec{n}'+\vec{n}\cdot\vec{n}'}\right)\,.\end{aligned} \tag{3.3.13}$$

The (over)completeness of coherent states is given by

$$1 = \frac{1}{2\pi}\int d^3n\,\delta(\vec{n}^2-1)|\vec{n}\rangle\langle\vec{n}|\,, \tag{3.3.14}$$

which can be verified as follows:

$$\frac{1}{2\pi}\int d^3n\delta(\vec{n}^2-1)|\vec{n}\rangle\langle\vec{n}| = \frac{1}{2\pi}\int d\theta d\phi \sin\theta \left(\cos\frac{\theta}{2}|\uparrow\rangle - e^{i\phi}\sin\frac{\theta}{2}|\downarrow\rangle\right)\left(\cos\frac{\theta}{2}\langle\uparrow| - e^{i\phi}\sin\frac{\theta}{2}\langle\downarrow|\right)$$
$$= |\uparrow\rangle\langle\uparrow| + |\downarrow\rangle\langle\downarrow|\,. \tag{3.3.15}$$

Finally the diagonal matrix element of $\vec{S}$ is given by

$$\langle\vec{n}|\vec{S}|\vec{n}\rangle = \frac{1}{2}\vec{n} \tag{3.3.16}$$

We are now in a position to derive the semi-classical description of the XXX spin chain. In what follows, we denote the one-loop dilatation operator in SU(2)-sector,

$$\hat{H}_{\rm one-loop} = \frac{\lambda}{4\pi^2}\sum_{i=1}^{L}\left(\frac{1}{4} - \vec{S}_i\vec{S}_{i+1}\right)\,, \tag{3.3.17}$$

simply by H to keep the expressions short. First, we re-express the time evolution operator e^{-iHt} as an infinite product of discrete time evolutions,

$$e^{iHt} = \lim_{\epsilon\to 0}(1-i\epsilon H)^{t/\epsilon}\,, \tag{3.3.18}$$

and insert the decomposition of unity (3.3.14) at each step. This leads to the following expression of the transition amplitude[15]

$$\langle\vec{\boldsymbol{n}}_{\rm final}|e^{-iHt}|\vec{\boldsymbol{n}}_{\rm initial}\rangle = \lim_{\delta\to 0}\int \mathcal{D}\vec{\boldsymbol{n}}\prod_{I=1}^{t/\epsilon}\langle\vec{\boldsymbol{n}}_I|\left(1-i\epsilon H\right)|\vec{\boldsymbol{n}}_{I-1}\rangle\,, \tag{3.3.19}$$
$$(\vec{\boldsymbol{n}}_{I=0}\equiv\vec{\boldsymbol{n}}_{\rm initial}\,,\quad \vec{\boldsymbol{n}}_{I=t/\delta}\equiv\vec{\boldsymbol{n}}_{\rm final})\,.$$

Here and below, $\vec{\boldsymbol{n}}_I$ denotes a tensor product of ℓ coherent states at I-th discretized time, $\vec{\boldsymbol{n}}_I = |\vec{n}_1^{(I)}\rangle\otimes\cdots\otimes|\vec{n}_\ell^{(I)}\rangle$. Each factor $\langle\vec{\boldsymbol{n}}_I|\left(1-i\epsilon H\right)|\vec{\boldsymbol{n}}_{I-1}\rangle$ can be evaluated as

$$\langle\vec{\boldsymbol{n}}_I|\left(1-i\epsilon H\right)|\vec{\boldsymbol{n}}_{I-1}\rangle = \exp\left(i\sum_{i=1}^{\ell}\frac{\Phi(\vec{n}_i^{(I)},\vec{n}_i^{(I-1)})}{2}\right)\sqrt{1-\frac{(\vec{n}_I-\vec{n}_{I-1})^2}{4}} - i\epsilon\langle\vec{n}_I|H|\vec{n}_{I-1}\rangle$$
$$= \exp\left(i\frac{\sum_{i=1}^{\ell}\delta\Phi(\vec{n}_i^{(I)},\vec{n}_i^{(I-1)})}{2}\right) - i\epsilon\langle\vec{n}_I|H|\vec{n}_{I-1}\rangle + O(\epsilon^2)\,, \tag{3.3.20}$$

where $\delta\Phi$ is the infinitesimal change of the area of the spherical triangle given by

$$\frac{\delta\Phi(\vec{n}_i^{(I-1)},\vec{n}_i^{(I)})}{2} \simeq \frac{\epsilon\left(\vec{n}_i^{(I)}\times\partial_t\vec{n}_i^{(I)}\right)\cdot\vec{n}_0}{2(1+\vec{n}_i^{(I)}\cdot\vec{n}_0)}\,. \tag{3.3.21}$$

[15] We use an uppercase letter to denote a discretized time whereas we use a lowercase letter to denote a site number.

Therefore, the transition amplitude can be re-expressed as

$$\langle \vec{n}_{\text{final}}|e^{-iHt}|\vec{n}_{\text{initial}}\rangle = \int \mathcal{D}\vec{\boldsymbol{n}}(t)e^{iS}\,, \tag{3.3.22}$$

where S is defined by

$$S = \sum_{i=1}^{\ell}\int dt\left[\frac{(\vec{n}_i\times\partial_t\vec{n}_i)\cdot\vec{n}_0}{2(1+\vec{n}_i\cdot\vec{n}_0)} - \frac{\lambda}{32\pi^2}(\vec{n}_i-\vec{n}_{i-1})^2\right]. \tag{3.3.23}$$

Note that the first term on the right hand side of (3.3.23) can be re-written as the Wess-Zumino term as follows:

$$\frac{1}{2}\sum_{i=1}^{\ell}\int dt\int_0^1 ds\,\vec{n}_i\cdot(\partial_t\vec{n}_i\times\partial_s\vec{n}_i)\,, \tag{3.3.24}$$

where s-dependence of $\vec{n}_i$ is defined such that $\vec{n}_i(s=1)=(0,0,1)$ and $\vec{n}_i(s=0)=\vec{n}$. The equivalence of two expressions can be confirmed in the following way. First let us take s-dependence of $\vec{n}$ to be

$$\vec{n}(s) = (\sin((1-s)\theta)\cos\phi\,,\sin((1-s)\theta)\sin\phi\,,\cos((1-s)\theta))^t\,. \tag{3.3.25}$$

Then the expression (3.3.24) can be rewritten as

$$\frac{1}{2}\int dt\int_0^1 ds\,\theta\partial_t\phi\sin((1-s)\theta) = -\frac{1}{2}\int dt\cos\theta\partial_t\phi\,. \tag{3.3.26}$$

On the other hand, the first term in (3.3.23) can be expressed as

$$\int dt\sin^2\frac{\theta}{2}\partial_t\phi = -\frac{1}{2}\int dt\cos\theta\partial_t\phi + (\text{surface term}) \tag{3.3.27}$$

Since the surface term does not change the dynamics of the system, we thus conclude that the two expressions are exactly equivalent.

Let us next consider the long wave-length limit of (3.3.23). By taking the naïve continuum limit of (3.3.23), we obtain the action

$$S_{\text{Landau}-\text{Lifshitz}} = \int dt\int_0^{\ell} d\sigma\left[\frac{(\vec{n}\times\partial_t\vec{n})\cdot\vec{n}_0}{2(1+\vec{n}\cdot\vec{n}_0)} - \frac{\lambda}{32\pi^2}\partial_\sigma\vec{n}\cdot\partial_\sigma\vec{n}\right], \tag{3.3.28}$$

which is nothing but the action of the famous Landau-Lifshitz model. Although we cannot usually take the continuum limit in such a naïve way, in this case, the naïve continuum limit correctly reproduces the scaling limit of the quantum results as we will see shortly. From (3.3.28), we can derive the following equation of motion:

$$\frac{(\partial_t\vec{n}\times\vec{n}_0)}{2(1+\vec{n}\cdot\vec{n}_0)} - \partial_t\left(\frac{(\vec{n}_0\times\vec{n})}{2(1+\vec{n}\cdot\vec{n}_0)}\right) - \frac{\vec{n}_0}{1+\vec{n}\cdot\vec{n}_0}\frac{(\vec{n}\times\partial_t\vec{n})\cdot\vec{n}_0}{2(1+\vec{n}\cdot\vec{n}_0)} + \frac{\lambda}{16\pi^2}\partial_\sigma^2\vec{n} + C\vec{n} = 0\,, \tag{3.3.29}$$

where the constant C is the Lagrange multiplier necessary to incorporate the normalization condition, $\vec{n}\cdot\vec{n}=1$. Although the equation (3.3.29) looks complicated, we can simplify it by writing the first three terms in terms of the basis of vectors, $\vec{n}$, $\partial_t\vec{n}$ and $\partial_t\vec{n}\times\vec{n}$:

$$(\text{First 3-terms in (3.3.28)}) = \frac{1}{2}\left(\partial_t\vec{n}\times\vec{n}\right) + (\text{Complicated factor})\,\vec{n}\ \ (+0\times\partial_t\vec{n})\ . \tag{3.3.30}$$

The coefficients in (3.3.30) can be determined by calculating the inner product between first three terms in (3.3.29) and $\vec{n}$, $\partial_t\vec{n}$ and $\partial_t\vec{n}\times\vec{n}$. Since the complicated factor in front of $\vec{n}$ in (3.3.30) can be absorbed into the Lagrange multiplier C, (3.3.29) can be re-expressed as

$$\frac{1}{2}\partial_t\vec{n}\times\vec{n}+\frac{\lambda}{16\pi^2}\partial_\sigma^2\vec{n}+C'\vec{n}=0\,. \tag{3.3.31}$$

By taking the cross product of $\vec{n}$ and (3.3.31), we finally arrive at the familiar form of the equation of motion of the Landau-Lifshitz model.

$$\partial_t\vec{n}=\frac{\lambda}{8\pi^2}\vec{n}\times\partial_\sigma^2\vec{n}\,. \tag{3.3.32}$$

The Landau-Lifshitz model is by itself classically integrable and has the following one-parameter family of connections[16]:

$$[\partial_\sigma - J_\sigma\,,\partial_t - J_t]=0\,, \tag{3.3.33}$$

$$J_\sigma = \frac{i}{2x}\vec{n}\vec{\sigma}=\frac{i}{2x}\begin{pmatrix} n_3 & n_1-in_2\\ n_1+in_2 & -n_3\end{pmatrix}\,, \tag{3.3.34}$$

$$J_t = \frac{i\lambda}{8\pi^2x^2}\vec{n}\vec{\sigma}+\frac{i\lambda}{8\pi^2x}\left(\vec{n}\times\partial_\sigma\vec{n}\right)\vec{\sigma}\,. \tag{3.3.35}$$

From the above connection, one can construct the monodromy matrix as follows.

$$\Omega(x)\equiv \mathrm{P}\exp\left(\int_0^\ell d\sigma J_\sigma\right)\,. \tag{3.3.36}$$

The quasi-momenta can be defined similarly as in the string sigma model. Namely, we define the quasi-momenta as the logarithm of the eigenvalue of the monodromy matrix as follows

$$\Omega(x)\sim\begin{pmatrix} e^{ip_{\mathrm{LL}}(x)} & 0\\ 0 & e^{-ip_{\mathrm{LL}}(x)}\end{pmatrix}\,. \tag{3.3.37}$$

The main difference from the string sigma model is the singularity of the quasi-momentum: In the case of the string sigma model, the connection and the quasi-momenta have the

[16]For a more compact representation, see [40].

singularity at $x = \pm 1$. On the other hand, since the connection of the Landau-Lifshitz sigma model is singular at $x = 0$, the quasi-momenta has the singularity at $x = 0$ as follows:

$$p_{\rm LL}(x) = -\frac{\ell}{2x} + O(1)\,. \tag{3.3.38}$$

In addition to the singularity at $x = 0$, there are cusp-like points (branch points) and the node-like points, characterized by

$$p_{\rm LL}(x_j^{(c,n)}) = \pi m_j \quad m_j \in \mathbb{Z}\,. \tag{3.3.39}$$

The total spin of the system can be read off from the behavior at infinity as

$$p_{\rm LL}(x) = -\frac{S^z_{\rm tot}}{x} + O(x^{-2})\,. \tag{3.3.40}$$

The above three features of $p_{\rm LL}(x)$, (3.3.38)–(3.3.40), exactly coincide with those of the quasi-momentum in the scaling limit of the XXX spin chain, (3.3.5)–(3.3.8). Since the above three features can also be regarded as defining relations of the spectral curve, the equivalence of these features means that the spectral curves of the Landau-Lifshitz model and the scaling limit of the XXX spin chain coincide.

Before ending this subsection, let us make one extra comment regarding the semi-classical limit. It may seem slightly bizarre that the low energy limit of the XXX spin chain is describable by such a naïve continuum limit since we usually need to take into account the effect of nontrivial renormalization in order to derive the low-energy effective action correctly. This peculiarity is partly due to the simplicity of the model considered. In [45], it was shown that the Landau-Lifshitz model is *quantum*-integrable and the resultant Bethe equation precisely matches with the continuum limit of the Bethe equation of the XXX spin chain. In the course of analysis, certain non-renormalization properties have been found and played an important role. Such non-renormalization properties probably accounts for the aforementioned peculiarity, although details needs to be worked out.

3.3.2 String with large angular momentum

Having seen that the semi-classical limit of the XXX spin chain is described by the classical Landau-Lifshitz sigma model, we now move our focus onto the string theory side. The limit we will discuss below was first discussed by Frolov and Tseytlin [44] and is known as the *Frolov-Tseytlin limit*.

In [46], it was shown that the dynamics of fluctuations around such a fast-moving string can be directly mapped to the dynamics of the Landau-Lifshitz model. In such a limit, the angular momentum J for the S^3 rotation becomes quite large so that the ratio $\sqrt{\lambda}/J$

becomes vanishingly small. This limit is useful since we can expand the string-theory result with respect to the small parameter $\sqrt{\lambda}/J$ and compare it with the gauge-theory result. At the level of the quasi-momentum, the limit corresponds to taking κ to be sufficiently large with the mode numbers, $\oint_{b_i} dp$, fixed. In order to keep the mode numbers finite, we need to scale the positions of the branch cuts with κ.

Let us see the relation with the Landau-Lifshitz model at the level of the integrable structures following the argument of [40]. For this purpose, we consider a string solution whose left and right SU(2) charges are both proportional to σ_3, and subtract off the center of mass motion in the following way:

$$\begin{aligned} Z &= e^{2\kappa\tau} U_1 \,, \quad X = e^{2\kappa\tau} U_2 \,, \\ \bar{Z} &= e^{-2\kappa\tau} \bar{U}_1 \,, \quad \bar{X} = e^{-2\kappa\tau} \bar{U}_2 \,. \end{aligned} \tag{3.3.41}$$

In terms of the variables $U_{1,2}$ and $\bar{U}_{1,2}$, one can express the Frolov-Tseytlin limit as follows:

$$\kappa \to \infty \quad \text{with} \quad \kappa \partial_\tau U_{1,2} \,, \ \kappa \partial_\tau \bar{U}_{1,2} \text{: fixed} \,. \tag{3.3.42}$$

Let us next study the currents and the connections in the limit. Using (3.3.41), one can write down the time component of the right current in the Frolov-Tseytlin limit:

$$j_\tau = \mathbb{Y}^{-1} \partial_\tau \mathbb{Y} = 2\kappa \left[\begin{pmatrix} n_3 & n_+ \\ n_- & -n_3 \end{pmatrix} + O(1/\kappa) \right] = 2\kappa \left[\vec{n} \cdot \vec{\sigma} + O(1/\kappa) \right] \,, \tag{3.3.43}$$

where 3-vector $\vec{n}$ is related to $U_{1,2}$ in the following way:

$$n_3 = U_1 \bar{U}_1 - U_2 \bar{U}_2 \,, \tag{3.3.44}$$

$$n_+ \equiv n_1 + i n_2 = 2 U_2 \bar{U}_1 \,, \tag{3.3.45}$$

$$n_- \equiv n_1 - i n_2 = 2 U_1 \bar{U}_2 \,. \tag{3.3.46}$$

The sigma component of the right current can be determined by the flatness condition,

$$[\partial_\tau + j_\tau \,, \partial_\sigma + j_\sigma] = 0 \,. \tag{3.3.47}$$

Owing to the scaling behavior (3.3.42), the flatness condition (3.3.47) can be expressed as

$$\partial_\sigma j_\tau - [j_\tau \,, j_\sigma] = O(1) \,, \tag{3.3.48}$$

where the left hand side is of the order κ whereas the right hand side of of the order 1 and thus can be neglected. By expressing j_τ as $2\kappa \vec{n} \cdot \vec{\sigma}$ and solving (3.3.48), one can express j_σ as

$$j_\sigma = i \left(\vec{n} \times \partial_\sigma \vec{n} \right) \cdot \vec{\sigma} + O(1/\kappa) \,. \tag{3.3.49}$$

Therefore, the flat connection in the limit takes the following form:

$$\partial_\tau + \frac{2\kappa}{1-x^2}\vec{n}\cdot\vec{\sigma} + \frac{x}{1-x^2}\left(\vec{n}\times\partial_\sigma\vec{n}\right)\cdot\vec{\sigma}\,, \quad \partial_\sigma + \frac{1}{1-x^2}\left(\vec{n}\times\partial_\sigma\vec{n}\right)\cdot\vec{\sigma} + i\frac{\kappa x}{1-x^2}\vec{n}\cdot\vec{\sigma}\,.$$

To explicitly see the relation with the Landau-Lifshitz model, we introduce rescaled coordinates as

$$\tilde{\sigma} = \frac{\sqrt{\lambda}\kappa}{\pi}\sigma\,, \qquad \tilde{\tau} = \kappa\tau\,, \tag{3.3.50}$$

and identify the parameters as

$$2\sqrt{\lambda}\kappa = \ell\,. \tag{3.3.51}$$

Note that the rescaling (3.3.50) changes the periodicity of the space-coordinate from 2π to ℓ. Then, scaling x with κ and neglecting the subleading term, the connection takes the following form:

$$\begin{aligned} &\partial_{\tilde{\tau}} - \frac{\lambda}{8\pi^2 z^2}\vec{n}\vec{\sigma} - \frac{\lambda}{8\pi^2 z}\left(\vec{n}\times\partial_{\tilde{\sigma}}\vec{n}\right)\,, \\ &\partial_{\tilde{\sigma}} - i\frac{1}{2z}\vec{n}\cdot\vec{\sigma}\,, \end{aligned} \tag{3.3.52}$$

where z is the Zhoukovsky variable defined by

$$z = \frac{\sqrt{\lambda}}{4\pi}\left(x + \frac{1}{x}\right)\,. \tag{3.3.53}$$

The connection (3.3.52) coincides in form with that of the Landua-Lifshitz model (3.3.34) and (3.3.35) under the Wick rotation, $t \to -i\tilde{\tau}$. From the relation (3.3.51), we can conclude that the Frolov-Tseytlin limit $\kappa \to \infty$ is essentially equivalent to the semi-classical limit $\ell \to \infty$, which we discussed earlier. Therefore, from the results of this and the previous subsections, we conclude that the classical string and the quantum XXX spin chain coincide in the Frolov-Tseytlin/semi-classical limit at the level of the integrable structure. This limit also plays an important role in the study of three-point functions in Part III.

Before ending this section, let us now make two comments. First, under the identification (3.3.51) and (3.3.53), the quasi-momentum on the string theory side is mapped directly to the quasi-momentum on the gauge theory side as

$$p_{\text{string}}(x) \simeq p_{\text{LL}}(z(x))\,. \tag{3.3.54}$$

In particular, the behavior at infinity is mapped correctly as

$$p_{\text{string}}(x) \sim -\frac{\sqrt{\lambda}R}{4\pi x} \quad \longrightarrow \quad p_{\text{LL}}(z) \sim -\frac{S^z_{\text{tot}}}{z}\,, \tag{3.3.55}$$

under the identification $R \leftrightarrow S^z_{\rm tot}$. The correspondence of the spectral parameters in two theories, $x \leftrightarrow z(x)$, is motivated also by the form of the all-loop asymptotic Bethe ansatz, which we will briefly describe in the next section. Second, in the limit we discussed above, the time component of the left current is given trivially by

$$l_\tau = 2\kappa \left[\begin{pmatrix} 1 & 0 \\ 0 & 1 \end{pmatrix} + O(1/\kappa) \right] . \tag{3.3.56}$$

Thus, we cannot construct a nontrivial flat connection from the left currents in this limit.

3.4 Further developments

In this section, we briefly review the subsequent developments of the integrability-based approach to two-point functions[17]. Although they are not directly relevant to the materials discussed in the rest of this thesis, it would be important to know the past developments on two-point functions to motivate the study of three-point functions.

Soon after the seminal work by Minahan and Zarembo [27], one-loop integrability was extended to include all sorts of single-trace operators in the gauge theory. Subsequently, the main subject of study gradually shifted to the search of integrability at higher-loop. At higher-loop, the dilatation operator is described by a long-range spin-chain, with a range of interaction proportional to the loop order. In [49], it was shown that the dilatation operator in SU(2)-sector up to three-loop order can be matched with the Hamiltonian of an existing integrable spin-chain, called *Inozemtzev model* [50]. In seek of a spin-chain description at even higher loop order, another integrable spin-chain which also reproduces the three-loop results in SU(2)-sector, called *BDS spin-chain*, was found in [51]. The Hamiltonians of these spin-chains are diagonalizable by the Bethe ansatz when the chain is infinitely long. The resultant equations, which are correct only in the infinite-length limit, are often referred to as *asymptotic Bethe ansatz equations*. Based on the explicit result up to three-loop order, the all-loop asymptotic Bethe ansatz equation, known today as the *BDS equation*, was

[17] It is impossible to cover all the developments so far in this single section. For a comprehensive review including a number of references, see [47].

conjectured[18] in [51]. Its explicit form is given as follows:

$$\left(\frac{x^+(u_i)}{x^-(u_i)}\right)^\ell = \prod_{j\neq i}\frac{u_i-u_j-i}{u_i-u_j+i}\,,$$
$$u = x(u) + \frac{g^2}{x(u)}\,, \quad g^2 \equiv \frac{\lambda}{16\pi^2}\,, \quad f^\pm(u) \equiv f(u\pm i/2)\,, \tag{3.4.1}$$

However, it was later recognized that the equation needs to be supplemented by an extra scalar factor σ^2 called the *dressing phase* in the following way:

$$\left(\frac{x^+(u_i)}{x^-(u_i)}\right)^\ell = \prod_{j\neq i}\sigma^2(u_i,u_j)\frac{u_i-u_j-i}{u_i-u_j+i}\,. \tag{3.4.2}$$

The corrected equation (3.4.2) was generalized to all the sectors [52]. The equations thus obtained are nowadays called the *Beisert-Staudacher equations*.

The discovery of the dressing phase is a major achievement in the development of integrability in AdS/CFT. To fully appreciate its importance, let us for the moment turn our eyes to the relation with the string theory. As explained in section 3.2, when the operator (or the string) has a large R-charge J, a consistent expansion in powers of λ/J^2 seems to exist on both sides of the duality. Indeed, the leading contribution on both sides completely coincide [40, 44]. Such comparison was subsequently performed at the subleading orders and discrepancy was found at three-loop order [49]. This is the notorious *three-loop discrepancy*, which puzzled people for a considerable time. In [49], it was already suggested that such discrepancy may occur because two different limits, the weak coupling limit and the large charge limit, do not commute with each other. However, detailed understanding as to how such non-commutativity arises was missing for a while. Only after the discovery of the dressing phase, it became clear that the origin of such non-commutativity precisely is the dressing phase.

The Beisert-Staudacher equations, first conjectured in [52], were later re-derived by Beisert based on a firmer group-theoretical argument [53]. His approach is to consider the S-matrix of magnons without specifying details of the underlying spin-chain and constrain it using the symmetry. In the case of $\mathcal{N}=4$ SYM, this indeed determines the S-matrix uniquely up to a scalar factor, which is nothing but the dressing phase. Owing to these works, the existence and the importance of the dressing phase became widely known. However, a complete expression of the phase was not available at that time. A breakthrough was brought about by Janik, who first wrote down so-called *crossing equations* which the

[18] The relation between $x(u)$ and u in (3.4.1) is essentially the same as the relation between the spectral parameter x and the Zhukowski variable $z(x)$ used in the study of classical string in section 3.2. However, owing to the difference in normalization of rapidities, here it takes a slightly different form.

dressing phase must satisfy [54]. The solution to the equation was then obtained in [55, 56] and the fully explicit form of the Beisert-Staudacher equations finally became available.

Although the Beisert-Staudacher equations work remarkably well on both sides of the duality, it is applicable only to sufficiently long operators. When the operators have finite size, another type of corrections, called *wrapping corrections*, are known to appear. They represent contributions from the Feyman diagrams which wrap around the spin-chain. In [59], it was shown that such corrections can be computed by generalizing the method which was developed by Lüscher to study the relations between S-matrices and finite size corrections in general quantum field theories [57, 58]. In the case of integrable field theories, there exists a more systematic integrability-based approach, called *Thermodynamic Bethe Ansatz* (TBA). This method is called "Thermodynamic" because it was originally invented to compute observables at finite temperature in [60] before it was utilized to compute the finite size corrections of integrable field theories by exchanging roles of space and time in [61]. By three different groups [62–66], TBA was applied to the spectrum problem of the AdS_5/CFT_4 correspondence and a complete interpolation between the gauge theory result and the string theory result was obtained. The result obtained in this approach was recently checked against the perturbative computation of the gauge theory up to five loops [67]. Subsequently, the method of TBA was refined and applied to various observables [68, 69]. Quite recently, it was further reformulated in terms of quantized spectral curves [70] and the anomalous dimension at nine-loop order is now in hand.

3.5 What have we learned?

The developments reviewed in the previous section is truly remarkable: This is the first time in the long history of theoretical physics that people succeeded in exactly computing anomalous dimensions of a fairly large class of operators in a 4d interacting gauge theory. However, we should also keep in mind that our ultimate objective is not to exactly compute quantities in a theory far distant from the real world, but to deepen our understanding of the AdS/CFT correspondence through such computation. Therefore, it seems appropriate to pause here, and ask the following question: Do the remarkable achievements reviewed above give any new insight into the understanding of the AdS/CFT correspondence?

The answer is, unfortunately, not so clear because of the following reasons: Firstly, the method of computation relies heavily on the integrability of the system, whose existence is not yet proven neither on the gauge theory side nor on the string theory side. Secondly, in the computation, we utilized the properties of both the gauge theory and the string theory at the same time. For instance, the idea of characterizing the states as a collection of magnon excitations on top of a certain vacuum state came originally from the perturbative

computation of the gauge theory while we needed to resort to a continuous worldsheet picture to exchange roles of space and time and apply the TBA. These two features to some extent obscure the implication of the whole computation.

Nevertheless, there *are* several important observations we can make. First, a remarkable success of the integrability-based approach provides strong evidence that it is highly effective to regard the composite operators in the gauge theory as certain 1+1-dimensional spin-chains when we explore the connection with strings in AdS. Although such an idea was put forward originally in the paper by Berenstein, Maldacena and Nastase [71] shortly before all the above developments, the subsequent success of the integrability-based approach have revealed unexpected power and profoundness of such an idea. Second, the most pertinent way to interpret the aforementioned results would be to regard them as giving a new framework to quantize the string sigma-model, which is based on integrability (in particular on the TBA). Unlike the conventional methods of quantization, the integrability-based approach does not tell the details of the quantization procedures, such as the operator-ordering or the detailed form of states. Instead, it indirectly confirms the existence of a quantization scheme which preserves the integrable structure, by checking a set of nontrivial consistency conditions required for the existence of integrability.

To further explore the underlying mechanism of the AdS/CFT correspondence based upon the above two observations, it is important to see if the integrability-based approach can be generalized to compute other observables. This is because of the following two inter-related reasons: First computing other observables serves as a further consistency check of the integrability-based quantization of the string sigma-model. Second, since we only considered the cylindrical worldsheet in the computation of the spectrum, it is of crucial importance to consider observables defined on other worldsheet geometry, in order to fully understand the 2d CFT structures of the string sigma-model. One such observable is a three-point function, which is described by the worldsheet with three long legs.

Studying three-point functions is by itself important for several reasons: First, two- and three-point functions are building blocks of conformally invariant theories since they determine all the other correlation functions through the operator product expansion. Second, the three-point function on the string theory side corresponds to the interaction of strings, which is an important building block for the string theory in $AdS_5 \times S^5$. Third, the fact that the interaction of strings is encoded in the geometry of the worldsheet is one of the most important characteristics of string theory, as mentioned in section 1.1. Thus, to understand the mysterious relation between the gauge theory and the string theory, it would be crucial to examine the gauge theory three-point functions and try to uncover how the geometric properties of the worldsheet are realized in a perturbative computation of the gauge theory.

These are the main reasons we study three-point functions in the AdS_5/CFT_4 correspondence in the rest of this thesis. In the next part, we will start off the exploration with the computation on the gauge-theory side.

Part II

Three Point Functions in Perturbative Gauge Theory

Chapter 4

Three-point functions and spin-chains

Having discussed the integrable structures of the spectrum problem, we are now in a position to discuss three-point functions, which are the main subject of study in this thesis. In this chapter, we review the computation of three-point functions on the gauge-theory side. In section 4.1, we first review the basic facts on the three-point functions and explain the basic set-up to be used throughout this chapter. Then, in section 4.2, we describe how the computation of the structure constants in the gauge theory is mapped to the computation of the scalar products of the XXX spin chain. Finally, in section 4.3, we review various formulas to compute such scalar products and discuss their semi-classical limit. The structure constants in the semi-classical limit turn out to be expressed by certain integrals on the spectral curve. We will see in Part III that similar expressions can be derived on the string theory side.

4.1 Basic set-up

On the gauge theory side, the structure constants are expanded in powers of the 't Hooft coupling as

$$C_{123}(\lambda) = C_{123}^{(0)} + C_{123}^{(1)}\lambda + C_{123}^{(2)}\lambda^2 + \cdots , \tag{4.1.1}$$

The leading term $C_{123}^{(0)}$ is the tree-level result, which in principle can be computed by counting the number of Wick contractions among three operators. However, in practice, such computation is quite involved for the following reasons: At $\lambda = 0$, a large number of operators have the identical conformal dimension. Since such degeneracy will be lifted by the one-loop corrections, we need to compute the tree-level Wick contractions using the eigenstates of the one-loop dilatation operator to obtain a consistent expansion (4.1.1). Note that this is just a standard statement of the degenerate perturbation of the quantum mechanics. As a result of

such diagonalization, the explicit forms of the single-trace operators become quite nontrivial especially when the operator is long. Thus, it becomes an extremely difficult combinatorial problem to compute all the Wick contractions. In the subsequent sections, we will see that such computation greatly simplifies by mapping the problem to the computation of the scalar products in the spin chain. Here we will review the basics of the three-point functions and explain the set-up.

Three-point functions of $\mathcal{N} = 4$ SYM were systematically studied in the context of the AdS/CFT correspondence first by [72]. They studied the three-point functions of half-BPS operators and found that the tree-level results in the gauge theory precisely agree with the results in the supergravity. This led them to conjecture that such BPS three-point functions are tree-level exact. This conjecture was later proven[1] in the papers [74–76]. The integrability-based approach to the three-point functions were first proposed in the pioneering papers [77–79]. In [77], it was shown that the algebraic Bethe ansatz can be used to compute tree-level three-point functions. In [78] and [79], it was found that the one-loop correction to the three-point functions in the so-called SO(6)-sector can be computed by inserting the Hamiltonian of the spin chain at the *splitting points*, which separates the operator into two parts depending on with which operator they are contracted. Building on these earlier works, the integrability techniques to compute three-point functions were developed in [80].

The three-point functions studied in [80] consist of the following three types of operators:

$$\mathcal{O}_1 = \mathrm{tr}\,(ZZXZ\cdots)\,, \quad \mathcal{O}_2 = \mathrm{tr}\,\left(\bar{Z}\bar{Z}\bar{X}\bar{Z}\cdots\right)\,, \quad \mathcal{O}_3 = \mathrm{tr}\,\left(ZZ\bar{X}Z\cdots\right)\,,$$

where roles of the scalar fields for the operators $\mathcal{O}_i$ are summarized as follows:

	vacuum	excitation
$\mathcal{O}_1$	Z	X
$\mathcal{O}_2$	$\bar{Z}$	$\bar{X}$
$\mathcal{O}_3$	Z	$\bar{X}$

(4.1.2)

They are the simplest three-point functions that can produce *non-extremal* three-point functions[2], which satisfy $\Delta_i \neq \Delta_j + \Delta_k$, and are usually referred to as three-point functions in "SU(2)-sector"[3]. The Wick contractions for such three-point functions are depicted in Figure 4.1.1. A special feature of this class of three-point functions is that all $\bar{X}$ fields in $\mathcal{O}_3$

[1] Recently, the proof was simplified in [73].

[2] When the conformal dimensions of three operators satisfy the extremal condition, $\Delta_i = \Delta_j + \Delta_k$, it is known that the $1/N$ correction is not suppressed and one needs to take into account the mixing with the double-trace operators [81, 82].

[3] Precisely speaking, each operator is in a different SU(2)-subsector and three-point functions as a whole are not contained in a single SU(2)-sector. This is the reason we study the string moving on the S^3 subspace in Part III, which has the $\mathrm{SU}(2)_R \times \mathrm{SU}(2)_L$ isometry, not just a single SU(2).

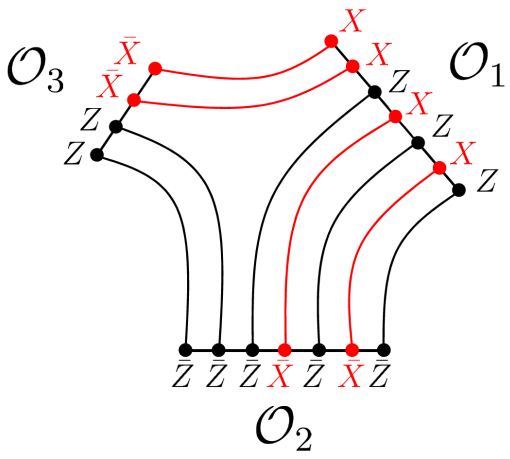

Figure 4.1.1: Tree-level Wick contraction for an example of the simplest non-extremal three-point functions of SU(2) operators.

are contracted with X fields in $\mathcal{O}_1$ and all Z fields in $\mathcal{O}_3$ are contracted with $\bar{Z}$ fields in $\mathcal{O}_2$. On the other hand, the contractions between $\mathcal{O}_1$ and $\mathcal{O}_2$ are complicated since they consist of both X-$\bar{X}$ contractions and Z-$\bar{Z}$ contractions.

To deal with such complicated contractions, it is useful to translate the computation into the computation in the spin-chain. To carry this out, first recall that the single-trace operators can be mapped to the states in the XXX spin chain,

$$\mathrm{tr}\,(ZZXZ) \mapsto |\uparrow\uparrow\downarrow\uparrow\rangle\,. \tag{4.1.3}$$

Here we only wrote down the mapping of the operator made of Z and X, but we can do the same also for other operators showin in (4.1.2), by mapping the "vacuum" field to $\uparrow$ and the "excitation" field to $\downarrow$. Then the three-point functions can be computed by going through the following steps:

1. We start with three closed spin chains with length ℓ_1, ℓ_2 and ℓ_3 respectively. Then we consider the eigenstate $|\Psi_i\rangle$ of the Hamiltonian on each of the chains.

2. Next we break each chain into two parts. To be more explicit, we break the i-the closed chain into left and right open sub-chains of length $(\ell_i+\ell_j-\ell_k)/2$ and $(\ell_i+\ell_k-\ell_j)/2$. Then, the state defined on the closed chain can be expressed as an *entangled* state of left and right open sub-chains as

$$|\Psi_i\rangle = \sum_a |\Psi_i^{(a)}\rangle_l \otimes |\Psi_i^{(a)}\rangle_r\,. \tag{4.1.4}$$

3. To perform the Wick contraction, we first flip[4] the kets on the left sub-chains into the bras as $|\Psi_i^{(a)}\rangle_l \otimes |\Psi_i^{(a)}\rangle_r \to |\Psi_i^{(a)}\rangle_l \otimes {}_r\langle\tilde{\Psi}_i^{(a)}|$ and then compute the scalar products as ${}_r\langle\tilde{\Psi}_i^{(a)}|\Psi_j^{(b)}\rangle_l$.

4. Finally we need to divide the resultant expressions by the norm of each state to obtain correctly normalized three-point functions.

As a result of such computation, we obtain the following expressions of the structure constants at tree-level:

$$C_{ijk}^{(0)} = \frac{\ell_i \ell_j \ell_k \sum_{a,b,c} {}_r\langle\tilde{\Psi}_i^{(a)}|\Psi_j^{(b)}\rangle_{lr}\langle\tilde{\Psi}_j^{(b)}|\Psi_k^{(c)}\rangle_{lr}\langle\tilde{\Psi}_k^{(c)}|\Psi_i^{(a)}\rangle_l}{\sqrt{\ell_i\langle\Psi_i|\Psi_i\rangle}\sqrt{\ell_j\langle\Psi_j|\Psi_j\rangle}\sqrt{\ell_k\langle\Psi_k|\Psi_k\rangle}} \,. \tag{4.1.5}$$

Here the factors of ℓ_i, ℓ_j and ℓ_k come from the summation over all possible ways of cutting closed chains into two open sub-chains. In the next section, we will evaluate the expression (4.1.5) more explicitly and explain how the integrability-based approach is useful for such computation.

Before ending this section, let us make several comments. First, by examining Figure 4.1.1, we can conclude that the contractions do not exist and the structure constant vanish unless the following "conservation laws" are satisfied:

$$M_1 = M_2 + M_3 \,, \tag{4.1.6}$$

$$\ell_1 + \ell_3 - \ell_2 = 2M_3 \,, \tag{4.1.7}$$

where ℓ_i and M_i denote the length and the number of magnons of each spin chain respectively. On the gauge theory side, they seems to be a consequence of simplicity of the tree-level contractions. However, as we see in Part III, the same conditions can be reproduced on the string theory side as a consequence of the structures of the global symmetry. Second, the above computation is a structurally similar to the interaction vertex of string field theory. This is of course quite natural since the three-point functions in the gauge theory are expected to be dual to the interaction vertex of three strings in $AdS_5 \times S^5$ spacetime. The action of string field theory is known to be severely constrained by the gauge-invariance and the algebraic structure. Thus it would be interesting to see how the perturbative computation of the gauge theory, which is based on the Feynman diagrams, fit into such a framework. Third, the aforementioned procedures of computing three-point functions are somewhat reminiscent of the computation of the entanglement entropy. In fact, the entanglement entropy of the

[4]Such a flipping operation is defined such that it reproduces the contraction rule of the gauge theory. Therefore, precisely speaking it is not completely the same as the Hermitian conjugation of the spin-chain state. However, we will not delve into the details of the flipping operation in this thesis as we will not use it directly. For details of the flipping operation, see [80].

spin chain can be computed by first expressing the state as an entangled state of two sub-chains, then introducing the reduced density matrix defined as

$$\hat{\rho} = \sum_a {}_r\langle \Psi_i^{(a)} | \Psi_i^{(a)} \rangle_r | \Psi_i^{(a)} \rangle_l \otimes {}_l\langle \Psi_i^{(a)} | \,,$$

and finally computing the entropy by $S_{\rm EE} = -\ln(\hat{\rho}\ln\hat{\rho})$. From this point of view, the structure constant can be regarded as an observable defined for three spin-chain states which measures how strongly the three states are entangled with each other. The entanglement entropy is now widely studied in condensed matter physics to characterize exotic quantum properties of strongly correlated materials [83–86]. It would be interesting if some analogue of the structure constant plays an important role also in such a context.

4.2 Connection to the scalar products of the XXX spin-chain

Let us now discuss how to compute (4.1.5) using the integrability techniques. The key observation is that the contractions between $\mathcal{O}_3$ and the other two operators are trivial for a particular set of three operators described in the previous section. Then, instead of cutting open three chains and summing over all possible intermediate states, the structure constants for such operators can be computed in the following simpler way:

1. The operator $\mathcal{O}_3$ is given by a complicated linear combination of simple spin-chain states, $|\uparrow\uparrow\downarrow\cdots\rangle$ *etc.* However, in the present case, only the state of the form

$$|\ \underbrace{\downarrow\cdots\downarrow}_{(\ell_3+\ell_1-\ell_2)/2}\ \underbrace{\uparrow\cdots\uparrow}_{(\ell_3+\ell_2-\ell_1)/2}\ \rangle\,, \tag{4.2.1}$$

   which corresponds to tr $\left(\bar{X}\cdots\bar{X}Z\cdots Z\right)$, can be contracted with the other operators. Thus, $\mathcal{O}_3$ contributes to the structure constant only through the coefficient of the state (4.2.1), which can be computed by the following scalar product:

$$\langle\downarrow\cdots\downarrow\uparrow\cdots\uparrow|\Psi_3\rangle\,. \tag{4.2.2}$$

2. On the other hand, the contractions between the other two operators are quite complicated. However, owing to the simplicity of the contractions involving $\mathcal{O}_3$, they can be computed alternatively by going through the following steps: First, identify a string of letters

$$\underbrace{\bar{Z}\cdots\bar{Z}}_{(\ell_2+\ell_3-\ell_1)/2}\,, \tag{4.2.3}$$

in the operator $\mathcal{O}_2$ and remove it. Next, insert the following string of letters into the position where we removed (4.2.3):

$$\underbrace{\bar{X}\cdots\bar{X}}_{(\ell_1+\ell_3-\ell_2)/2}\,. \tag{4.2.4}$$

If we denote the spin-chain state obtained in this way by $|\Psi_2'\rangle$, the contractions between $\mathcal{O}_1$ and $\mathcal{O}_2$ can be computed by

$$\langle\Psi_2'|\Psi_1\rangle\,. \tag{4.2.5}$$

3. When the operator $\mathcal{O}_2$ is characterized by a set of magnons $\boldsymbol{v}$, the aforementioned state $\langle\Psi_2'|$ can be obtained by creating those magnon excitations on top of the "deformed vacuum" $\langle\downarrow\cdots\downarrow\uparrow\cdots\uparrow|$ as

$$\langle\Psi_2'| = \langle\, \underbrace{\downarrow\cdots\downarrow}_{(\ell_1+\ell_3-\ell_2)/2}\ \underbrace{\uparrow\cdots\uparrow}_{(\ell_1+\ell_2-\ell_3)/2}\ |\prod_j C(v_j)\,. \tag{4.2.6}$$

This statement would perhaps be understood at relative ease pictorially using Figure 4.1.1.

Going through the above procedures, one can compute the structure constants as a product of two scalar product, $\langle\downarrow\cdots\downarrow\uparrow\cdots\uparrow|\Psi_3\rangle$ and $\langle\Psi_2'|\Psi_1\rangle$. We can further simplify the computation by expressing the deformed vacuum as a off-shell Bethe state. For this purpose, it is convenient to introduce inhomogeneities to the spin chain. Then the deformed vacuum can be expressed as

$$\langle\downarrow^K\uparrow^{\ell-K}| \propto \prod_{j=1}^{K}\langle\uparrow^\ell|C(\theta_j+\frac{i}{2})\,. \tag{4.2.7}$$

The relation (4.2.7) was shown in [87] by using the correspondence between the scalar products of the XXX spin chain and the partition functions of a certain two dimensional integrable lattice model, called the six-vertex model. As the derivation is somewhat technical, here we will instead confirm that the relation (4.2.7) indeed holds for the two-site spin chain. For two-site spin chains, the operator $C(u)$ can be written explicitly as

$$i(u-\theta_2+iS_2^z)S_1^+ + i(u-\theta_1-iS_1^z)S_2^+\,. \tag{4.2.8}$$

When acted upon the vacuum state $\langle\uparrow\uparrow|$, it produces

$$i(u-\theta_1-\frac{i}{2})\langle\uparrow\downarrow| + i(u-\theta_2+\frac{i}{2})\langle\downarrow\uparrow|\,. \tag{4.2.9}$$

Then it is easy to see[5] that we obtain $i(\theta_1 - \theta_2 + i)\langle\downarrow\uparrow|$ upon setting $u = \theta_1 + i/2$.

As a result of such manipulations, we finally arrive at the following simple expression for the structure constant, which was derived in [87]:

$$C_{123}^{(0)} = \sqrt{\ell_1\ell_2\ell_3}\frac{\langle \boldsymbol{v} \cup \boldsymbol{z}|\boldsymbol{u}\rangle_{\boldsymbol{\theta}_{(1)}}\langle \boldsymbol{z}|\boldsymbol{w}\rangle_{\boldsymbol{\theta}_{(3)}}}{\sqrt{\langle \boldsymbol{u}|\boldsymbol{u}\rangle_{\boldsymbol{\theta}_{(1)}}\langle \boldsymbol{v}|\boldsymbol{v}\rangle_{\boldsymbol{\theta}_{(2)}}\langle \boldsymbol{w}|\boldsymbol{w}\rangle_{\boldsymbol{\theta}_{(3)}}}}\,, \tag{4.2.10}$$

where $\boldsymbol{u}$, $\boldsymbol{v}$ and $\boldsymbol{w}$ denote the rapidities of $\mathcal{O}_1$, $\mathcal{O}_2$ and $\mathcal{O}_3$ respectively and $\boldsymbol{\theta}_{(i)}$ denote the total inhomogeneities associated with the i-th chain. The rapidities $\boldsymbol{z}$ are given in terms of the inhomogeneities common to the first and the third operators $\boldsymbol{\theta}^{(13)}$ as

$$\boldsymbol{z} = \boldsymbol{\theta}^{(13)} + \frac{i}{2}\,. \tag{4.2.11}$$

Note that all the inhomogeneities are set to zero at the end of the calculation.

The expression (4.2.10) allows us to evaluate the structure constant in terms of the scalar products between an on-shell and an off-shell Bethe states. As we will see in the next section, simple formulas for such quantities are already known and we can employ them to efficiently compute the structure constants.

4.3 Determinant formulas for the scalar products and the semi-classical limit

As we have seen in the previous section, the computation of the structure constant reduces to the computation of the scalar products between an on-shell and an off-shell Bethe states,

$$\langle \boldsymbol{v}|\boldsymbol{u}\rangle = \langle\uparrow^\ell|\prod_{i=1}^{M} C(v_i)\prod_{j=1}^{M} B(u_j)|\uparrow^\ell\rangle\,. \tag{4.3.1}$$

Traditionally, the computation of such a product has been pursued in the framework of the algebraic Bethe ansatz reviewed in section 3.1.3. Although the computation is conceptually quite straightforward as one simply needs to move $C(v_i)$'s all the way through $B(u_j)$'s, using the exchange algebra, and act on the vacuum $|\uparrow^\ell\rangle$, in practice this procedure produces a multitude of terms which grow exponentially in the number of magnons and becomes intractable. Fortunately, in the case of the product between an on-shell and an off-shell Bethe states, Slavnov discovered a much more concise expression in the form of a determinant, which was to be called Slavnov's determinant formula [88]. More recently, various other types of determinant formulas have been developed, which are intimately related to the

[5] We can continue this line of argument and prove (4.2.7) by mathematical induction.

Slavnov's determinant. Below we shall review these variants of determinant formulas and explain their semi-classical limit. As the derivations will be technically complicated and lengthy, we basically present the formulas without detailed proofs although we make several important comments on the physical interpretation of such formulas.

As stated above, let us consider the case where either one of the set of rapidities $\boldsymbol{u}$ or $\boldsymbol{v}$ are on-shell. For definiteness, let us take $\boldsymbol{v}$ to be on-shell. Then the original Slavnov's formula computes the scalar product $\langle \boldsymbol{v}|\boldsymbol{u}\rangle$ as a $M\times M$ determinant of the form

$$\begin{aligned}\langle \boldsymbol{v}|\boldsymbol{u}\rangle &= \frac{\prod_{i=1}^M Q^+_{\boldsymbol{\theta}}(u_i)Q^-_{\boldsymbol{\theta}}(v_i)}{\prod_{i<j}(u_i-u_j)(v_j-v_i)} \\ &\times \det\left(\frac{1}{u_m-v_n}\left(\prod_{k\neq n}^M(u_m-v_k-i)-\prod_{k\neq n}^M(u_m-v_k+i)\prod_{l=1}^{\ell}\frac{u_m-\theta_l-\frac{i}{2}}{u_m-\theta_l+\frac{i}{2}}\right)\right)_{1\le m,n\le M}.\end{aligned} \tag{4.3.2}$$

Very recently, Kostov and Matsuo [89] showed that this expression is equivalent to an alternative determinantal expression of the form

$$\langle \boldsymbol{v}|\boldsymbol{u}\rangle = (-1)^M Z^{\mathrm{KM}}(\boldsymbol{z}|\boldsymbol{\theta}), \qquad \boldsymbol{z}\equiv \boldsymbol{u}\cup\boldsymbol{v} \tag{4.3.3}$$

where $Z^{\mathrm{KM}}(\boldsymbol{z}|\boldsymbol{\theta})$ is now a $2M\times 2M$ determinant given by

$$Z^{\mathrm{KM}}(\boldsymbol{z}|\boldsymbol{\theta}) = \frac{\prod_{i=1}^{2M}Q^-_{\boldsymbol{\theta}}(z_i)}{\prod_{i<j}(z_i-z_j)}\det\left(z_m^{n-1}-\prod_{l=1}^{\ell}\frac{z_m-\theta_l+i/2}{z_m-\theta_l-i/2}(z_m+i)^{n-1}\right)_{1\le m,n\le 2M}. \tag{4.3.4}$$

They also pointed out that this equivalence is due essentially to the following equality valid when $\boldsymbol{u}$ or $\boldsymbol{v}$ are on-shell:

$$\langle\uparrow^\ell|\prod_{i=1}^M C(v_i)\prod_{j=1}^M B(u_j)|\uparrow^\ell\rangle \propto \langle\downarrow^\ell|(S^-)^{\ell-2M}\prod_{i=1}^M B(v_i)\prod_{j=1}^M B(u_j)|\uparrow^\ell\rangle. \tag{4.3.5}$$

Intuitively this can be understood in the following way. Suppose the set of rapidities $\boldsymbol{v}$ are on-shell. Then the Bethe state $\prod_{i=1}^M B(v_i)|\uparrow^\ell\rangle$ built on the up vacuum is the highest weight state of global SU(2) with spin $\frac{\ell}{2}-M$. On the other hand, the state $\prod_{i=1}^M C(v_i)|\downarrow^\ell\rangle$ generated by the action of $C(v)$ on the down pseudovacuum has the same eigenvalue for the transfer matrix $T(u)$. Generally, an on-shell state corresponding to the same solution of the Bethe ansatz equations is expected to belong to the same SU(2) multiplet. Since $\prod_{i=1}^M C(v_i)|\downarrow^\ell\rangle$ is a lowest weight state with spin $-\frac{\ell}{2}+M$, we can make it into the highest weight state with spin $\frac{\ell}{2}-M$ by the action of $(S^+)^{\ell-2M}$. Therefore we should have the equality

$$\prod_{i=1}^M B(v_i)|\uparrow^\ell\rangle \propto (S^+)^{\ell-2M}\prod_{i=1}^M C(v_i)|\downarrow^\ell\rangle. \tag{4.3.6}$$

Taking the conjugate of this relation, we obtain (4.3.5). This identification will be of crucial importance when we develop the method based on the separation of variables (SoV) for the computation of the scalar product in section 5.3.

Another variant of the determinant formula was found by Foda and Wheeler [90]. They showed that the Kostov-Matsuo expression $Z^{\mathrm{KM}}(\boldsymbol{z})$ can be identified with the so-called partial domain wall partition function (pDWPF) $Z^{\mathrm{pDWPF}}(\boldsymbol{z}|\boldsymbol{\theta})$, which naturally arises in the context of the six vertex model:

$$Z^{\mathrm{pDWPF}}(\boldsymbol{z}|\boldsymbol{\theta}) = \frac{\prod_{\alpha=1}^{2M} Q^{+}_{\boldsymbol{\theta}}(z_\alpha) Q^{-}_{\boldsymbol{\theta}}(z_\alpha)}{\prod_{\alpha<\beta}(z_\alpha - z_\beta)\prod_{i<j}(\theta_j-\theta_i)} \times \det \begin{pmatrix} \frac{i}{(z_1-\theta_1+i/2)(z_1-\theta_1-i/2)} & \cdots & \frac{i}{(z_1-\theta_\ell+i/2)(z_1-\theta_\ell-i/2)} \\ \vdots & & \vdots \\ \frac{i}{(z_{2M}-\theta_1+i/2)(z_{2M}-\theta_1-i/2)} & \cdots & \frac{i}{(z_{2M}-\theta_\ell+i/2)(z_{2M}-\theta_\ell-i/2)} \\ \theta_1^{\ell-2M-1} & \cdots & \theta_\ell^{\ell-2M-1} \\ \vdots & & \vdots \\ \theta_1^{0} & \cdots & \theta_\ell^{0} \end{pmatrix}. \tag{4.3.7}$$

These determinant formulas are remarkably compact as compared to the results of the brute force computation, for which the number of terms increases exponentially in the number of magnons. However, they are still impractical for the purpose of studying the semi-classical limit, in which the length of the chain and the number of magnons are both large. This difficulty was overcome for the case of one non-BPS and two BPS correlation functions in [91]. They studied the limiting form of the determinant expressions carefully and managed to derive a simple integral expression for the logarithm of the structure constant. Their computation was generalized to the case of three non-BPS correlation functions in [92, 93]. In [92,93], the determinant expression was first rewritten as a correlator of the chiral fermions and then bosonized. The resultant expression is given by the expectation value of a product of two operators, which completely factorizes in the semi-classical limit. Then by approximating the expectation values of the operators by their classical counterparts, we arrive at the following intriguingly simple formula for the scalar products[6]:

$$\ln\langle \boldsymbol{v}|\boldsymbol{u}\rangle \simeq \oint_{\mathcal{A}_{\boldsymbol{u}}\cup\mathcal{A}_{\boldsymbol{v}}} \frac{du}{2\pi} \mathrm{Li}_2\left(e^{ip_{\boldsymbol{u}}(u)+ip_{\boldsymbol{v}}(u)}\right), \tag{4.3.8}$$

where $\mathcal{A}_{\boldsymbol{u}}$ and $\mathcal{A}_{\boldsymbol{v}}$ are contours which respectively encircle the distributions of the Bethe roots $\boldsymbol{u}$ and $\boldsymbol{v}$ counter-clockwise and $p_{\boldsymbol{u}}$ and $p_{\boldsymbol{v}}$ are the quasi-momenta for $|\boldsymbol{u}\rangle$ and $|\boldsymbol{v}\rangle$ defined as

[6] Precisely speaking, we sometimes need to deform the integration contour to avoid the singularities in the integrands. For details, see [93].

the semi-classical limit of the following quantities:

$$
\begin{aligned}
p_{\boldsymbol{u}}(u) &= \sum_{i=1}^{M} \frac{1}{u-u_i} - \sum_{k=1}^{\ell} \frac{\ell}{2(u-\theta_k)}\,, \\
p_{\boldsymbol{v}}(u) &= \sum_{i=1}^{M} \frac{1}{u-v_i} - \sum_{k=1}^{\ell} \frac{\ell}{2(u-\theta_k)}\,,
\end{aligned}
\tag{4.3.9}
$$

where ℓ is the length of the chain and θ_k's are the inhomogeneities. Using the formula (4.3.8), the semi-classical limit of the structure constants (4.2.10) can be evaluated as follows:

$$
\begin{aligned}
\ln C_{123}^{(0)} \simeq & \oint_{\mathcal{A}_{\boldsymbol{u}}\cup\mathcal{A}_{\boldsymbol{v}}} \frac{du}{2\pi} \mathrm{Li}_2\left(e^{ip_{\boldsymbol{u}}+ip_{\boldsymbol{v}}+i\ell_3/(2u)}\right) + \oint_{\mathcal{A}_{\boldsymbol{w}}} \frac{du}{2\pi} \mathrm{Li}_2\left(e^{ip_{\boldsymbol{w}}+i(\ell_3-\ell_1)/(2u)}\right) \\
& - \frac{1}{2}\oint_{\mathcal{A}_{\boldsymbol{u}}} \frac{du}{2\pi} \mathrm{Li}_2\left(e^{2ip_{\boldsymbol{u}}}\right) - \frac{1}{2}\oint_{\mathcal{A}_{\boldsymbol{v}}} \frac{du}{2\pi} \mathrm{Li}_2\left(e^{2ip_{\boldsymbol{v}}}\right) - \frac{1}{2}\oint_{\mathcal{A}_{\boldsymbol{w}}} \frac{du}{2\pi} \mathrm{Li}_2\left(e^{2ip_{\boldsymbol{w}}}\right)\,.
\end{aligned}
\tag{4.3.10}
$$

Note that the prefactor $\sqrt{\ell_1\ell_2\ell_3}$ is negligible in the semi-classical limit.

It is quite remarkable that the semi-classical limit of the seemingly complicated determinant formulas can be expressed so concisely as shown in (4.3.10). In addition, the fact that the result is given only in terms of the quasi-momenta of the spin chains suggests that we can derive a similar expression from the Frolov-Tseytlin limit of the string theory side since the quasi-momenta on both sides coincide in the Frolov-Tseytlin limit as discussed in section 3.3. This expectation will turn out to be partially correct. In Part III, we will derive an expression which is structurally quite similar to (4.3.10). However, the resultant expression does not precisely match with (4.3.10) even after taking the Frolov-Tseytlin limit.

Before ending this section, let us stress that although the semi-classical expression for the structure constant is remarkably simple, the derivation is, unfortunately, technically complicated. To better understand the structure of three-point functions and explore the connection with the string theory, it is important to derive the above formulas in a more physical way and uncover the physical mechanism behind such computation. As a first step toward this goal, we will derive a new formula for the scalar products in the next chapter based on the so-called Sklyanin's separation of variables.

Chapter 5

A new integral expression for the scalar products

In the previous chapter, we have seen that the computation of the structure constants, in some cases, reduces to the computation of the scalar products of the spin chain, and the semi-classical limit of the structure constants can be computed by taking the limit of determinant formulas for the scalar products. In this chapter, however, we shall take a different route for the calculation of this scalar product. This alternative is the method of separation of variables (SoV), which was advanced substantially by Sklyanin [94]. The resultant expression is given by a multiple-integral over the separated variables and is akin to the eigenvalue integrals of a matrix model.

In section 5.1, we review the preceding works on the application of SoV to the computation of scalar products, giving a brief overview of our methods of computation. Then in section 5.2, we give a general introduction to the idea of the separation of variables without delving into the specific details. After that, in section 5.3, we discuss the separation of variables of the XXX spin chain and derive the integral expression for the scalar products. Lastly in section 5.4, we briefly discuss that the multiple-integral formula may be useful to derive a semi-classical result in a more intuitive way.

5.1 Overview on the application of Sklyanin's separation of variables

The concept of SoV represents the most primitive and fundamental form of integrability, where one reduces the interacting many-body system to mutually decoupled set of dynamical systems, each with a single degree of freedom. Of course the highly non-trivial question is

how to actually construct such separated variables $\{x_k\}$ and the corresponding canonically conjugate momenta $\{p_k\}$. For the integrable systems which admit the formulation with Lax operators, Sklyanin proposed a powerful concrete recipe for the construction. Relegating more detailed description to section 5.2, the prescription applied to the case of XXX spin 1/2 chain says that the solutions x_k of the operator equation $B(x_k) = 0$ provide the separated coordinates, while their conjugate momenta p_k are given essentially by $D(x_k)$. One can indeed check that they satisfy (with appropriate ordering in the quantum case) the canonical Poisson-Lie commutation relations. Therefore if one can diagonalize and factorize $B(u)$ as $B(u) \propto \prod_{k=1}^{\ell}(u - x_k)$, with precisely ℓ zeros, x_k provide a complete basis of separated coordinates. Once this is achieved, one can figure out the measure factor $\mu(x_1, \ldots, x_\ell)$ and compute the scalar products between various states in the x-representation.

Indeed such a method has been applied successfully to some cases where the conventional algebraic Bethe ansatz is not readily applicable. One example is the non-compact SL(2) spin chain in the unitary representation, studied in [95]. One gratifying feature of this case is that in such a unitary representation the hermitian conjugate of $B(u)$ operator is basically itself and hence can be easily diagonalized. The integration measure is found and the scalar product is thus defined in the SoV framework. More recently, the results were applied to the computation of three-point functions in the so-called *SL(2)-sector* [96]. Another system for which the SoV analysis has been performed is the SU(2) spin chain with anti-periodic boundary condition [97, 98]. In this case, due to the insertion of the twisting matrix $K = \begin{pmatrix} 0 & 1 \\ 1 & 0 \end{pmatrix}$ which flips the spin at the boundary, the operator which should be diagonalized to yield separated variables changes from $B(u)$ to $D(u)$. Since this operator is hermitian and naturally diagonalizable the subsequent analysis à la Sklyanin is straightforward.

Now for the more fundamental case of the SU(2) spin chain with the periodic boundary condition, there are two apparent obstacles in computing the scalar products using the Sklyanin's procedure. The first problem is that because the hermitian conjugate of $B(u)$ is $C(u)$, the basis in which $B(u)$ is diagonal is different from the one in which $C(u)$ is diagonal. Hence the scalar product of our interest $\langle \boldsymbol{v} | \boldsymbol{u} \rangle = \langle \uparrow^\ell | \prod_{i=1}^{M} C(v_i) \prod_{i=1}^{M} B(u_i) | \uparrow^\ell \rangle$ cannot be easily computed in $B(u)$-diagonal basis. The second problem is that $B(u)$ operator as it stands is actually not a good operator in the SoV framework, since the coefficient of the highest power u^ℓ in the expansion of $B(u)$ is proportional to $S^- = S^x - iS^y$ belonging to the global SU(2), which is obviously not diagonalizable. It is perhaps for these reasons that this important basic model has not been treated in the SoV basis. In the subsequent sections, we will see how these two problems are overcome by making use of the observation made by Kostov and Matsuo [89] that the scalar products can be rewritten in the

form $\langle\downarrow^\ell|(S_-)^{\ell-2M}\prod_{i=1}^M B(v_i)B(u_i)|\uparrow^\ell\rangle$, and by the introduction of an appropriate twisting matrix at the boundary.

5.2 Separation of variables for integrable models

As explained in section 3.1.3, excited states in the XXX spin chain $\prod_i B(u_i)|\uparrow^\ell\rangle$ are characterized as a collection of magnon excitations on top of the ground state and they are distinguished by a set of complex parameters called the Bethe roots, $\{u_i\}$, which are normally interpreted as *the rapidities of the magnons*. Then the periodicity condition for such excitations leads to the Bethe equation (3.1.42). In this chapter, however, we advocate an alternative view of the excited states, namely that the states are characterized by the nodes (zeros) of their wave functions and the Bethe roots are interpreted instead as *the positions of the nodes*. In this perspective, the Bethe equation arises as a consistency condition for the nodes of the wave function.

To illustrate the basic idea, let us first discuss a simpler example, a one-dimensional harmonic oscillator[1]. As is well-known, the Schrödinger equation for the harmonic oscillator can be explicitly solved in terms of the Hermite polynomials. However, here we shall take a slightly different route and try to determine the spectrum without explicitly solving the equation. For this purpose, let us first re-express the Schrödinger equation by dividing both sides by the wave function $\psi(x)$:

$$-\frac{\hbar^2}{2m\psi(x)}\frac{d^2}{dx^2}\psi(x)+\frac{m\omega^2x^2}{2}=E\,. \tag{5.2.1}$$

Then, by studying the behavior of (5.2.1) at large x, we conclude that $\psi(x)$ should behave as $\psi(x)\sim\exp\left(-m\omega x^2/2\hbar\right)$ when x is large. For excited states, $\psi(x)$ must also contain a polynomial prefactor, which gives rise to nodes of the wave functions. Therefore, to characterize $\psi(x)$ by the position of the nodes, let us write down the following ansatz for $\psi(x)$,

$$\psi(x)=\prod_{i=1}^N(x-x_i)e^{-m\omega x^2/2\hbar}\,. \tag{5.2.2}$$

Substituting this ansatz into (5.2.1), we obtain the following equation

$$\sum_{i<j}\frac{2}{(x-x_i)(x-x_j)}+\hbar\omega\left(\sum_i\frac{x}{x-x_i}+\frac{1}{2}\right)=E\,. \tag{5.2.3}$$

[1]This toy model is discussed in a similar manner also in [37]

Then from its large x behavior, the energy E is determined in terms of the number of nodes as $E = \hbar\omega(N + 1/2)$. In addition, since the RHS of (5.2.3) is a constant and free of poles, we must demand that the residue of the poles at $x = x_i$ on the LHS must vanish. This leads to a Bethe-ansatz-like equation for the positions of the nodes of the wave function,

$$x_i = \frac{\hbar}{2m\omega} \sum_{j \neq i} \frac{1}{x_i - x_j} \,. \tag{5.2.4}$$

Although this idea of characterizing the excited states in terms of the number and the positions of the nodes is quite elementary and intuitive, it is technically difficult to apply this idea directly to the system with many degrees of freedom. However, in the case of the integrable models, it is often possible to decompose the system into a set of mutually decoupled one dimensional problems. The systematic method to carry this out is the method of separation of variables developed by Sklyanin, which we will explain in the rest of this section. By applying this method, we will see explicitly in section 5.3 that the Bethe equation for the XXX spin chain can indeed be interpreted as a consistency equation for the nodes of the wave function as in (5.2.4).

5.2.1 Basic notions of the separation of variables

Before delving into the details of the method developed by Sklyanin, here we briefly summarize the basic notion of the separation of variables. In classical mechanics, separation of variable is applicable only if there are as many number of conserved charges, $h_1, \ldots, h_d$, as the dynamical variables. In such a case, by a judicious choice of canonical variables, it is often possible to write down a set of equations, each of which contains only one canonical pair $\{x_k, p_k\}$:

$$W_k(x_k, p_k; h_1, \ldots, h_d) = 0 \,, \qquad k = 1 \ldots d \,. \tag{5.2.5}$$

This type of equation is analogous to the expression of the energy of the harmonic oscillator, $E = p^2/2m + m\omega^2 x^2/2$, and one can determine the classical motion of the system in much the same way as in that case.

When we consider the quantum system, the equations (5.2.5) are replaced by the following equations for the eigenstates of the conserved charges,

$$W_k(\hat{x}_k, \hat{p}_k; h_1, \ldots, h_d)|\Psi\rangle = 0 \,, \qquad k = 1 \ldots d \,. \tag{5.2.6}$$

In terms of the wave function in the coordinate representation, $\Psi(x_1, \ldots, x_d)$, (5.2.6) can be re-expressed as

$$W_k\left(x_k, \frac{\hbar}{i}\frac{\partial}{\partial x_k}; h_1, \ldots, h_d\right) \Psi(x_1, \ldots, x_d) = 0 \,, \qquad k = 1 \ldots d \,. \tag{5.2.7}$$

It is easy to see that (5.2.7) admits a completely factorized solution, $\Psi = \prod_k \psi_k(x_k)$, each factor of which satisfies the following one dimensional equation,

$$W_k\left(x_k, \frac{\hbar}{i}\frac{\partial}{\partial x_k}; h_1, \ldots, h_d\right)\psi_k(x_k) = 0\,. \tag{5.2.8}$$

In this way, the original system with many degrees of freedom can be reduced to a set of mutually decoupled one dimensional systems.

5.2.2 Sklyanin's magic recipe

The most nontrivial step in the procedure above is the construction of the separated variables satisfying the equations of the form (5.2.5) or (5.2.6). This is indeed a difficult problem for interacting many-body systems. However, for the integrable models which can be formulated in terms of the Lax operators, Sklyanin proposed a systematic method for the construction, often referred to as the Sklyanin's magic recipe. In what follows, we sketch the essence of this recipe[2] applied to systems with a 2×2 monodromy matrix. More precise analysis for the case of the XXX spin chain will be given in the next section.

For simplicity, let us first consider the classical case. In a classically integrable system with a 2×2 monodromy matrix

$$\Omega(u) = \begin{pmatrix} A(u) & B(u) \\ C(u) & D(u) \end{pmatrix}, \tag{5.2.9}$$

there is an immediate candidate for the set of equations (5.2.5). It is the *characteristic equation* for the monodromy matrix

$$\det\,(z - \Omega(x)) = 0\,, \tag{5.2.10}$$

where z is the eigenvalue of the matrix $\Omega(x)$. Since the expansion of $\Omega(x)$ in powers of x yields a set of conserved charges as its coefficients, (5.2.10) is indeed of the form of (5.2.5) if we can somehow identify x and z with dynamical variables. The recipe proposed by Sklyanin is to use the solutions x_k's to the equation $B(u) = 0$ as x-variables:

$$B(u) = (u - x_1)(u - x_2)\cdots\,. \tag{5.2.11}$$

In the case of the lattice models, such as the XXX spin chain discussed in the previous section, $B(u)$ is a polynomial in u, whose order basically equals the lattice size. Therefore, this prescription indeed provides the correct number of variables. Furthermore, owing to the

[2]The discussion here is basically restricted to the simplest class of the integrable models, called *rational* models. For *trigonometric* or *elliptic* models, nontrivial modification of the method is required [94].

Poisson commutativity among $B(u)$'s, x_k's also commute with each other and thus they are mutually independent separated variables. On the other hand, the z-variables, which are the eigenvalues of $\Omega(x)$, are provided by the diagonal components, $A(x_k)$ or $D(x_k)$, since $\Omega(x_k)$ becomes a lower triangular matrix owing to $B(x_k) = 0$. Then the remaining task is to understand the relation of $A(x_k)$ and $D(x_k)$ to the conjugate momenta p_k, which satisfy the standard commutation relations:

$$\{x_k, x_l\} = 0\,, \qquad \{p_k, p_l\} = 0\,, \qquad \{x_k, p_l\} = \delta_{kl}\,. \tag{5.2.12}$$

In most cases, by explicitly computing the Poisson brackets of $A(x_k)$ and $D(x_k)$ with x_k, we can show that they are related to p_k roughly as

$$A(x_k) \sim e^{ip_k}\,, \qquad D(x_k) \sim e^{-ip_k}\,. \tag{5.2.13}$$

In the case of the quantum integrable models, separated variables x_k's become a set of commuting operators $\hat{x}_k$'s, which are characterized as the roots of the *operator* equation $B(u) = 0$. Just as for the classical case, the conjugate operators, $e^{i\hat{p}_k}$ and $e^{-i\hat{p}_k}$, are given[3] essentially by $A(\hat{x}_k)$ or $D(\hat{x}_k)$. To derive a set of one dimensional equations of the type (5.2.7), let us consider the wave function in the x_k-basis:

$$\Psi(x_1, \ldots, x_d) = \langle x_1, \ldots, x_d | \Psi \rangle\,, \tag{5.2.14}$$

where $\langle x_1, \ldots, x_d|$ is an eigenstate of the operators $\hat{x}_k$'s. Now if the state $|\Psi\rangle$ is an eigenstate of $T(u) = A(u) + D(u)$, a generating function of the commuting set of Hamiltonians, we can compute $\langle x_1, \ldots, x_d|T(\hat{x}_k)|\Psi\rangle$ as

$$\langle x_1, \ldots, x_d|T(\hat{x}_k)|\Psi\rangle = t(x_k)\Psi(x_1, \ldots, x_d)\,, \tag{5.2.15}$$

where $t(u)$ is the eigenvalue of $T(u)$ for $|\Psi\rangle$. We can evaluate the same quantity also by acting $T(\hat{x}_k)$ to the left on $\langle x_1, \ldots, x_d|$. To carry this out we use the relation of $T(\hat{x}_k)$ with the momenta $\hat{p}_k$, *i.e.*

$$T(\hat{x}_k) = A(\hat{x}_k) + D(\hat{x}_k) \sim e^{i\hat{p}_k} + e^{-i\hat{p}_k}\,. \tag{5.2.16}$$

Then we find

$$\langle \ldots, x_k, \ldots | T(\hat{x}_k) \sim \langle \ldots, x_k + 1, \ldots | + \langle \ldots, x_k - 1, \ldots |\,. \tag{5.2.17}$$

In this way we arrive at the following equation for the wave function Ψ:

$$t(x_k)\Psi(\ldots, x_k, \ldots) \sim \Psi(\ldots, x_k + 1, \ldots) + \Psi(\ldots, x_k - 1, \ldots)\,, \quad k = 1, \ldots, d\,. \tag{5.2.18}$$

[3]Note, in the quantum case, we need to consider the ordering of the operators. In the case of the XXX spin chain, this is explicitly worked out in section 5.3.

Assuming the factorized form of the wave functions $\Psi(x_1, \ldots, x_d) = \prod_k \psi_k(x_k)$, we can decompose (5.2.18) into a set of mutually decoupled one dimensional equations:

$$t(x_k)\psi_k(x_k) \sim \psi_k(x_k + 1) + \psi_k(x_k - 1)\,. \tag{5.2.19}$$

This equation is the analogue of the Schrödinger equation for the harmonic oscillator. Therefore, as in that case, we can derive a consistency condition for the nodes of the wave function. Assuming a form of ψ_k as $\psi_k(x) = \prod_l (x - u_l)$ and setting $x_k = u_j$ in (5.2.19), we obtain the algebraic relations for the positions u_j of the nodes:

$$1 \sim \prod_{l \neq j} \frac{u_j - u_l + 1}{u_j - u_l - 1}\,. \tag{5.2.20}$$

Note that this is identical with the Bethe equation. Therefore, as mentioned at the beginning of this section, the Bethe roots can be interpreted as the nodes of the wave function in this approach. In the next section, we will see that the logic outlined here is explicitly realized in the case of the XXX spin chain.

5.3 Integral representation of the scalar products for XXX spin chain

In the preceding section, we sketched the basic idea of the method of separated variables for integrable models. In this section, we will apply it to the periodic SU(2) XXX spin chain and derive a multiple integral representation of the scalar products in the basis where the separated variables are diagonal. The resultant expression can be brought to a form which resembles the integral over the eigenvalues of a matrix model.

5.3.1 Construction of the separated variables

Recall the definition of the monodromy matrix $\Omega(u)$ for the XXX spin chain with inhomogeneity parameters θ_k:

$$\Omega(u) = \begin{pmatrix} A(u) & B(u) \\ C(u) & D(u) \end{pmatrix} \equiv L_1(u - \theta_1)L_2(u - \theta_2)\cdots L_\ell(u - \theta_\ell)\,, \tag{5.3.1}$$

$$L_k(u) \equiv \begin{pmatrix} u + iS_k^z & iS_k^- \\ iS_k^+ & u - iS_k^z \end{pmatrix}\,. \tag{5.3.2}$$

As outlined in the previous section, the separated variables for integrable models with a 2×2 monodromy matrix are usually given by the roots of the operator equation, $B(u) = 0$.

However, as already pointed out in section 5.1, in the case of the periodic SU(2) spin chain, the operator $B(u)$ is proportional to S^- in the large u limit as $B(u) \sim iS^- u^{\ell-1} + \cdots$, and is not diagonalizable. This problem can be circumvented by introducing a twisting matrix $K_\epsilon = \begin{pmatrix} 1 & \epsilon \\ -\epsilon & 1 \end{pmatrix}$, which changes the boundary condition and modifies the monodromy matrix as

$$\Omega_\epsilon(u) = K_\epsilon \Omega(u) \equiv \begin{pmatrix} A_\epsilon(u) & B_\epsilon(u) \\ C_\epsilon(u) & D_\epsilon(u) \end{pmatrix} . \tag{5.3.3}$$

Although such a twisting changes the dynamical properties of the spin chain, it does not affect the computation of the scalar products since, as we shall show explicitly later in this section, they can be re-expressed in terms of quantities independent of the twisting parameter ϵ. After twisting, the large u behavior of $B_\epsilon(u)$ is modified to $B_\epsilon(u) \sim \epsilon u^\ell + i(S^- - \epsilon S^z + i\sum_j \theta_j) u^{\ell-1} + \cdots$ and $B_\epsilon(u)$ becomes diagonalizable. Then it can be factorized as

$$B_\epsilon(u) = \epsilon \prod_{k=1}^{\ell} (u - \hat{x}_k) \,, \tag{5.3.4}$$

where $\hat{x}_k$'s are the roots of the operator equation, $B_\epsilon(u) = 0$. As the twisting preserves the algebra among the elements $A(u), \cdots, D(u)$, the operators B_ϵ's continue to commute with each other, namely $[B_\epsilon(u), B_\epsilon(v)] = 0$, and this implies that $\hat{x}_k$'s also mutually commute: $[\hat{x}_k \,, \hat{x}_l] = 0$. These operators are the "coordinates" of the separated variables and one can consider their left eigenstates and right eigenstates, $\langle x_1, \ldots, x_\ell|$ and $|x_1, \ldots, x_\ell\rangle$, upon which $B_\epsilon(u)$ acts in the following way:

$$\langle x_1, \ldots, x_\ell | B_\epsilon(u) = \left(\epsilon \prod_{k=1}^{\ell} (u - x_k) \right) \langle x_1, \ldots, x_\ell | \,, \tag{5.3.5}$$

$$B_\epsilon(u) | x_1, \ldots, x_\ell \rangle = \left(\epsilon \prod_{k=1}^{\ell} (u - x_k) \right) | x_1, \ldots, x_\ell \rangle \,. \tag{5.3.6}$$

As explained in the Appendix A.1, the eigenvalue of the operator $\hat{x}_k$ takes only two values given by $\theta_k \pm \frac{i}{2}$. As a consequence, the dimension of the Hilbert space spanned by the eigenstates of the separated variables is 2^ℓ, which precisely matches that of the spin chain Hilbert space. This assures the completeness of the separated variable basis.

At $\hat{x}_k$ the operator B_ϵ vanishes and the form of the monodromy matrix becomes lower triangular. Therefore the two eigenvalues are given by $A_\epsilon(\hat{x}_k)$ and $D_\epsilon(\hat{x}_k)$, which are expected to be identified as $e^{\pm i\hat{p}_k}$, where $\hat{p}_k$ is the momentum operator conjugate to $\hat{x}_k$. To see this more precisely, since $A_\epsilon(u)$ and $D_\epsilon(u)$ are polynomials in u with operator-valued coefficients, we need to specify the ordering of $\hat{x}_k$ and the coefficients, which are also operators in general.

The ordering appropriate for the left eigenstates, to be denoted by $:\bullet:_L$, turns out to be placing all the $\hat{x}_k$'s to the left of the coefficients, namely

$$:F(\hat{x}_k):_L \equiv \sum_n \hat{x}_k^n \hat{F}_n\,, \qquad \text{for} \quad F(u) = \sum_n u^n \hat{F}_n\,. \tag{5.3.7}$$

Then the commutation relation between $A_\epsilon(u)$ and $B_\epsilon(u)$, given by $(u-v)A_\epsilon(v)B_\epsilon(u) = (u-v+i)B_\epsilon(u)A_\epsilon(v) - iB_\epsilon(v)A_\epsilon(u)$, leads to

$$:(u-\hat{x}_k)A_\epsilon(\hat{x}_k)B_\epsilon(u):_L = :(u-\hat{x}_k+i)B_\epsilon(u)A_\epsilon(\hat{x}_k):_L - i:B_\epsilon(\hat{x}_k)A_\epsilon(u):_L\,. \tag{5.3.8}$$

Since the second term on the RHS of (5.3.8), containing $B_\epsilon(\hat{x}_k)$, vanishes, and since $B_\epsilon(u)$ commutes with $\hat{x}_k$, we can simplify (5.3.8) to

$$(u-\hat{x}_k):A_\epsilon(\hat{x}_k):_L B_\epsilon(u) = (u-\hat{x}_k+i)B_\epsilon(u):A_\epsilon(\hat{x}_k):_L\,, \tag{5.3.9}$$

where the normal-ordering is now imposed only on $A_\epsilon(\hat{x}_k)$. Then by acting (5.3.9) to the left eigenstate, we obtain

$$(u-x_k)\langle x_1,\ldots,x_\ell|:A_\epsilon(\hat{x}_k):_L B_\epsilon(u) = \epsilon(u-x_k+i)\prod_{l=1}^{\ell}(u-x_l)\langle x_1,\ldots,x_\ell|:A_\epsilon(\hat{x}_k):_L\,.$$

Dividing both sides by $(u-x_k)$, we see that $B(u)$ acting on the state $\langle x_1,\ldots,x_\ell|:A_\epsilon(\hat{x}_k):_L$ vanishes at $u = x_k - i$. This means that the operator $:A_\epsilon(\hat{x}_k):_L$ indeed effects the shift of the eigenvalue of $\hat{x}_k$ by $-i$, namely[4]

$$\langle\ldots,x_k,\ldots|:A_\epsilon(\hat{x}_k):_L \propto \langle\ldots,x_k-i,\ldots|\,. \tag{5.3.10}$$

A similar argument for $D_\epsilon(u)$ leads to the conclusion that $:D_\epsilon(\hat{x}_i):_L$ shifts the eigenvalue of $\hat{x}_k$ by $+i$,

$$\langle\ldots,x_k,\ldots|:D_\epsilon(\hat{x}_k):_L \propto \langle\ldots,x_k+i,\ldots|\,. \tag{5.3.11}$$

The constants of proportionality in (5.3.10) and (5.3.11) can be determined by the analysis detailed in the Appendix A.1. Since these results, together with the spectrum of $\hat{x}_k$ already quoted, are basic to the rest of the analysis, we shall display them as a theorem:

Theorem

[4]For the literal identification of $:A_\epsilon(\hat{x}_k):_L$ with $e^{i\hat{p}_k}$, it is more natural to rename $\hat{x}_k$ as $-i\hat{x}_k$. Then, the new $\hat{x}_k$ gets shifted by $+1$ and its spectrum becomes real at $\theta_k = 0$. But we shall not do this and stick to the customary definition.

(*i*) The spectrum of $\hat{x}_k$ is given by the two values[5]

$$x_k = \theta_k + \frac{i}{2}\,, \quad \theta_k - \frac{i}{2}. \tag{5.3.12}$$

(*ii*) The operators $:A_\epsilon(\hat{x}_k):_L$ and $:D_\epsilon(\hat{x}_k):_L$ act on the left eigenstates in the following manner

$$\langle \dots, x_k, \dots | :A_\epsilon(\hat{x}_k):_L = \sqrt{1+\epsilon^2}\, Q^+_{\boldsymbol{\theta}}(x_k) \langle \dots, x_k - i, \dots |\,, \tag{5.3.13}$$

$$\langle \dots, x_k, \dots | :D_\epsilon(\hat{x}_k):_L = \sqrt{1+\epsilon^2}\, Q^-_{\boldsymbol{\theta}}(x_k) \langle \dots, x_k + i, \dots |\,. \tag{5.3.14}$$

For the right eigenstates, an appropriate ordering prescription is to put all x_k's to the right of the coefficients of $A_\epsilon(u)$ and $D_\epsilon(u)$:

$$:F(\hat{x}_k):_R \equiv \sum_n \hat{F}_n \hat{x}_k^n\,, \qquad \text{for} \quad F(u) = \sum_n u^n \hat{F}_n\,. \tag{5.3.15}$$

Then the action of $:A_\epsilon(\hat{x}_k):_R$ and $:D_\epsilon(\hat{x}_k):_R$ on the right eigenstates are expressible as

$$:A_\epsilon(\hat{x}_k):_R | \dots, x_k, \dots \rangle = \sqrt{1+\epsilon^2}\, Q^-_{\boldsymbol{\theta}}(x_k) | \dots, x_k + i, \dots \rangle\,, \tag{5.3.16}$$

$$:D_\epsilon(\hat{x}_k):_R | \dots, x_k, \dots \rangle = \sqrt{1+\epsilon^2}\, Q^+_{\boldsymbol{\theta}}(x_k) | \dots, x_k - i, \dots \rangle\,. \tag{5.3.17}$$

Since $A_\epsilon(u)$ and $D_\epsilon(u)$ are ℓ-th order polynomials in u with a unit leading coefficient, the action of these operators at ℓ distinct values of u, (5.3.13) and (5.3.14), completely determines the explicit forms of the operators as follows:

$$A_\epsilon(u) = \prod_{k=1}^{\ell}(u - \hat{x}_k) + \sum_{k=1}^{\ell} \left(\prod_{j\neq k} \frac{u - \hat{x}_j}{\hat{x}_k - \hat{x}_j} \right) :A_\epsilon(\hat{x}_k):_L\,, \tag{5.3.18}$$

$$D_\epsilon(u) = \prod_{k=1}^{\ell}(u - \hat{x}_k) + \sum_{k=1}^{\ell} \left(\prod_{j\neq k} \frac{u - \hat{x}_j}{\hat{x}_k - \hat{x}_j} \right) :D_\epsilon(\hat{x}_k):_L\,. \tag{5.3.19}$$

They are expressible also in terms of the right-ordered operators, $:A_\epsilon(\hat{x}_k):_R$ and $:D_\epsilon(\hat{x}_k):_R$, as

$$A_\epsilon(u) = \prod_{k=1}^{\ell}(u - \hat{x}_k) + \sum_{k=1}^{\ell} :A_\epsilon(\hat{x}_k):_R \left(\prod_{j\neq k} \frac{u - \hat{x}_j}{\hat{x}_k - \hat{x}_j} \right)\,, \tag{5.3.20}$$

$$D_\epsilon(u) = \prod_{k=1}^{\ell}(u - \hat{x}_k) + \sum_{k=1}^{\ell} :D_\epsilon(\hat{x}_k):_R \left(\prod_{j\neq k} \frac{u - \hat{x}_j}{\hat{x}_k - \hat{x}_j} \right)\,. \tag{5.3.21}$$

[5] As shown in Appendix A.1, what one can show is that the spectrum of each $\hat{x}_j$ is of the form $\theta_k \pm \frac{i}{2}$ for some k. Here and hereafter we adopt the natural convention to associate the spectrum $\theta_k \pm \frac{i}{2}$ with $\hat{x}_k$.

From (5.3.18) and (5.3.19), we can derive a difference equation for the eigenstate $|\psi\rangle$ of the (twisted) transfer matrix, $T_\epsilon(u) \equiv A_\epsilon(u) + D_\epsilon(u)$. This is done by computing $\langle x_1, x_2, \ldots, x_\ell | T_\epsilon(u) | \psi \rangle$ in two different ways: First by acting $T_\epsilon(u)$ on $\langle x_1, x_2, \ldots, x_\ell|$ using (5.3.18) and (5.3.19), and second by acting it on $|\psi\rangle$. By setting $u = x_k$ in the resulting equation, we obtain the following simple equation for the wave function of the eigenstate, $\Psi(x_1, \ldots, x_\ell) \equiv \langle x_1, \ldots, x_\ell | \psi \rangle$:

$$\frac{t_\epsilon(x_k)}{\sqrt{1+\epsilon^2}} \Psi(\ldots, x_k, \ldots) = Q^+_{\boldsymbol{\theta}}(x_k) \Psi(\ldots, x_k - i, \ldots) + Q^-_{\boldsymbol{\theta}}(x_k) \Psi(\ldots, x_k + i, \ldots) \,. \tag{5.3.22}$$

Here $t_\epsilon(u)$ is the eigenvalue of $T_\epsilon(u)$, *i.e.* $T_\epsilon(u)|\psi\rangle = t_\epsilon(u)|\psi\rangle$. Assuming a factorized form of the wave function, $\Psi(x_1, x_2, \ldots, x_\ell) = \psi_1(x_1)\psi_2(x_2)\ldots\psi_\ell(x_\ell)$, (5.3.22) can be decomposed into a set of ℓ one-dimensional equations, which can be regarded as the "Schrödinger equations" for the separated variables:

$$\frac{t_\epsilon(x_k)}{\sqrt{1+\epsilon^2}} \psi_k(x_k) = Q^+_{\boldsymbol{\theta}}(x_k) \psi_k^{--}(x_k) + Q^-_{\boldsymbol{\theta}}(x_k) \psi_k^{++}(x_k) \,. \tag{5.3.23}$$

In the $\epsilon \to 0$ limit, the equation (5.3.23) for ψ_k apparently takes the same form as the Baxter equation (3.1.43) for the Q-function, $Q_{\boldsymbol{u}}(u)$. However one should keep in mind that $Q_{\boldsymbol{u}}$ and $\psi_k(x_k)$ are conceptually quite different: While $Q_{\boldsymbol{u}}$ is introduced as a polynomial with zeros at the rapidities of the magnon excitations and can be defined on the whole complex plane, ψ_k is the wave function in the separated variable basis and is defined only on the discrete eigenvalues $x_k = \theta_k \pm i/2$. Therefore it is *a priori* not clear whether we can identify ψ_k with $Q_{\boldsymbol{u}}$. Nevertheless, as we shall later see explicitly, the factor representing the wave function in the multiple integral formula is given indeed by the Q-function. Therefore, as far as the multiple integral formula is concerned, ψ_k can be identified with $Q_{\boldsymbol{u}}$ and the Bethe equation can be interpreted as the consistency condition for the zeros of the wave function. This evidently parallels the case of the harmonic oscillator discussed in section 5.2.

5.3.2 Multiple integral representation for scalar products

Having constructed the separated variables, our next goal is to express the scalar product between an off-shell and an on-shell Bethe states given by $\langle \boldsymbol{v} | \boldsymbol{u} \rangle = \langle \uparrow^\ell | \prod_{i=1}^M C(v_i) \prod_{i=1}^M B(u_i) | \uparrow^\ell \rangle$ as the overlap between two wave functions of separated variables. Our basic strategy for deriving such a expression is to insert into the scalar product a resolution of unity in the SoV basis, namely

$$1 = \sum_{x_k = \theta_k \pm i/2} \mu(\boldsymbol{x}) \, |\boldsymbol{x}\rangle\langle\boldsymbol{x}| \,, \tag{5.3.24}$$

where $\boldsymbol{x}$ stands for $\{x_1, \dots, x_\ell\}$ and $\mu(\boldsymbol{x})$ is the measure factor for the summation, to be specified later. Unfortunately, this procedure cannot be carried out straightforwardly because the scalar product of our interest contains the operator $C(u)$ and its action on the B-diagonal SoV basis is quite complicated. In addition, to employ the SoV basis, we need to introduce the twist in the boundary condition as in (5.3.3), which is not present in the original scalar product as above.

The first problem can be circumvented by the trick due to Kostov and Matsuo [89], which converts $C(v_i)$ to $B(v_i)$ within the scalar product provided v_i's satisfy the Bethe equation. Although not explicitly given in [89], one can work out the precise factors in the conversion formula and obtain the expression

$$\langle\uparrow^\ell | \prod_{i=1}^{M} C(v_i) \prod_{j=1}^{M} B(u_j) | \uparrow^\ell\rangle = \frac{(-1)^M}{(\ell-2M)!} \langle\downarrow^\ell | (S^-)^{\ell-2M} \prod_{i=1}^{M} B(v_i) \prod_{j=1}^{M} B(u_j) | \uparrow^\ell\rangle\,, \tag{5.3.25}$$

which contains only the operator $B(u)$. This rewriting has another gratifying feature: It allows us to introduce the twist of the boundary condition without changing the value of the scalar product. This is done by replacing the right hand side of (5.3.25) with

$$\langle\downarrow^\ell | (S^- - \epsilon S^z + i\sum_{l=1}^{\ell} \theta_l)^{\ell-2M} \prod_{i=1}^{M} B_\epsilon(v_i) \prod_{j=1}^{M} B_\epsilon(u_j) | \uparrow^\ell\rangle\,. \tag{5.3.26}$$

Although (5.3.26) has apparent dependence on ϵ as well as an extra dependence on θ_l's, such unwanted terms actually vanish[6] thanks to the conservation of the total spin S^z along the z-axis.

Then, inserting a resolution of unity (5.3.24) into (5.3.26) and using the action of $B_\epsilon(u)$ on the SoV basis (5.3.5) and (5.3.6), we obtain the following expression[7]

$$\begin{aligned}
&\langle\downarrow^\ell | (S^- - \epsilon S^z + i\sum_{l=1}^{\ell} \theta_l)^{\ell-2M} \prod_{i=1}^{M} B_\epsilon(v_i) \prod_{j=1}^{M} B_\epsilon(u_j) | \uparrow^\ell\rangle \\
&= \sum_{x_k=\theta_k\pm i/2} \epsilon^\ell \mu(\boldsymbol{x}) f_L(\boldsymbol{x}) f_R(\boldsymbol{x}) \left(\sum_{j=1}^{\ell} x_j\right)^{\ell-2M} \prod_{k=1}^{\ell} Q_{\boldsymbol{u}}(x_k) Q_{\boldsymbol{v}}(x_k)\,,
\end{aligned} \tag{5.3.27}$$

where $f_{L,R}$ are given by

$$f_L(\boldsymbol{x}) \equiv \langle\downarrow^\ell | \boldsymbol{x}\rangle\,, \qquad f_R(\boldsymbol{x}) \equiv \langle\boldsymbol{x}| \uparrow^\ell\rangle\,. \tag{5.3.28}$$

[6] To see this, it suffices to recall that $B_\epsilon(u)$ is composed of $B(u) + \epsilon D(u)$ and S^- and that $B(u)$ lowers the eigenvalue of S^z by $1/2$ while S^z and $D(u)$ leave it unchanged.

[7] Note that the combination $S^- - \epsilon S^z + i\sum_j \theta_j$ appears in $B_\epsilon(u)$ as $B_\epsilon(u) \sim \epsilon u^\ell + i(S^- - \epsilon S^z + i\sum_j \theta_j) u^{\ell-1} + \dots$ and its action on the SoV basis is thus given by $(S^- - \epsilon S^z + i\sum_j \theta_j)|x_1, \dots, x_\ell\rangle = \epsilon \sum_i x_i |x_1, \dots, x_\ell\rangle$.

Note that both the measure $\mu(\boldsymbol{x})$ and the functions $f_{L,R}(\boldsymbol{x})$ depend on the twist parameter ϵ but the total expression (5.3.27) should be ϵ-independent as argued above.

Let us now determine $\mu(\boldsymbol{x})$ and $f_{L,R}(\boldsymbol{x})$. To determine $\mu(\boldsymbol{x})$, we consider the overlap[8] between the left and the right eigenstates in the SoV basis, $\langle \boldsymbol{x'}|\boldsymbol{x}\rangle$. First, since $\langle \boldsymbol{x'}|$ and $|\boldsymbol{x}\rangle$ are both eigenstates of the operators $\hat{x}_k$'s, the overlap vanishes unless the eigenvalues coincide. Therefore, we conclude that $\langle \boldsymbol{x'}|\boldsymbol{x}\rangle$ is proportional to $\delta_{x'_1,x_1}\delta_{x'_2,x_2}\dots\delta_{x'_\ell,x_\ell}$. Second, when we act the right hand side of (5.3.24) on the state $\langle \boldsymbol{x'}|$, the state should not change as the left hand side of (5.3.24) is just an identity operator. Owing to this condition, we can express $\langle \boldsymbol{x'}|\boldsymbol{x}\rangle$ in terms of the measure factor $\mu(\boldsymbol{x})$ as

$$\langle \boldsymbol{x'}|\boldsymbol{x}\rangle = \mu^{-1}(\boldsymbol{x})\,\delta_{x'_1,x_1}\dots\delta_{x'_\ell,x_\ell}\,. \tag{5.3.29}$$

This suggests that $\mu(\boldsymbol{x})$ can be determined by computing the matrix element

$$\langle \boldsymbol{x'}|A_\epsilon(u)|\boldsymbol{x}\rangle \tag{5.3.30}$$

in two different ways: First, by acting $A_\epsilon(u)$ on the bra using (5.3.13) and (5.3.18) and setting $x'_j = x_j$ for $j \neq k$ and $x'_k = x_k + i$, we obtain

$$\mu^{-1}(\dots,x_k,\dots)\left(\prod_{j\neq k}\frac{u-x_j}{x_k-x_j+i}\right)Q^{+++}_{\boldsymbol{\theta}}(x_k)\,. \tag{5.3.31}$$

Second, by acting $A_\epsilon(u)$ on the ket using (5.3.16) and (5.3.20) and setting $x'_j = x_j$ for $j \neq k$ and $x'_k = x_k + i$, we obtain

$$\mu^{-1}(\dots,x_k+i,\dots)\left(\prod_{j\neq k}\frac{u-x_j}{x_k-x_j}\right)Q^{-}_{\boldsymbol{\theta}}(x_k)\,. \tag{5.3.32}$$

By equating (5.3.31) and (5.3.32), we arrive at the following recursion relation for $\mu(\boldsymbol{x})$:

$$\frac{\mu(\dots,x_k+i,\dots)}{\mu(\dots,x_k,\dots)} = \frac{Q^{-}_{\boldsymbol{\theta}}(x_k)}{Q^{+++}_{\boldsymbol{\theta}}(x_k)}\prod_{j\neq k}\frac{x_k-x_j+i}{x_k-x_j}\,. \tag{5.3.33}$$

The solution to this equation can be obtained as

$$\mu(\boldsymbol{x}) \propto \prod_{i<j}(x_i-x_j)\prod_k e^{-\pi(x_k-\theta_k)}\prod_{l\neq m}\frac{1}{(x_l-\theta_m+\frac{i}{2})(x_l-\theta_m-\frac{i}{2})}\,. \tag{5.3.34}$$

Similarly, we can derive the recursion relations for $f_{L,R}(\boldsymbol{x})$ by computing $\langle\downarrow^\ell|A_\epsilon(u)|\boldsymbol{x}\rangle$ and $\langle\boldsymbol{x}|A_\epsilon(u)|\uparrow^\ell\rangle$ in two different ways. First, by acting $A_\epsilon(u)$ on the bra using the formula,

$$\langle\downarrow^\ell|A_\epsilon(u) = \langle\downarrow^\ell|\,(A(u)+\epsilon C(u)) = Q^{-}_{\boldsymbol{\theta}}(u)\langle\downarrow^\ell|\,, \tag{5.3.35}$$

[8]Note $\langle \boldsymbol{x'}|\boldsymbol{x}\rangle$ cannot be regarded as a norm since the left and the right eigenstates are not Hermitian conjugate to each other. Therefore $\langle \boldsymbol{x'}|\boldsymbol{x}\rangle$ can be in general complex-valued.

and (5.3.18), we obtain

$$\langle\downarrow^{\ell}|A_{\epsilon}(u)|\boldsymbol{x}\rangle = Q^{-}_{\boldsymbol{\theta}}(u)f_L(\boldsymbol{x})\,, \tag{5.3.36}$$

$$\begin{aligned}\langle\boldsymbol{x}|A_{\epsilon}(u)|\uparrow^{\ell}\rangle =& \prod_{k=1}^{\ell}(u-x_k)f_R(\boldsymbol{x}) \\ &+\sqrt{1+\epsilon^2}\sum_{k=1}^{\ell}\left(\prod_{j\neq k}\frac{u-x_j}{x_k-x_j}\right)Q^{+}_{\boldsymbol{\theta}}(x_k)f_R\left(\dots,x_k-i\,,\dots\right)\,.\end{aligned} \tag{5.3.37}$$

Second, by acting $A_{\epsilon}(u)$ on the ket using (5.3.20) and the formula

$$A_{\epsilon}(u)|\uparrow^{\ell}\rangle = \left(A(u)+\epsilon C(u)\right)|\uparrow^{\ell}\rangle = Q^{+}_{\boldsymbol{\theta}}(u)|\uparrow^{\ell}\rangle\,, \tag{5.3.38}$$

we obtain

$$\begin{aligned}\langle\downarrow^{\ell}|A_{\epsilon}(u)|\boldsymbol{x}\rangle =& \prod_{k=1}^{\ell}(u-x_k)f_L(\boldsymbol{x}) \\ &+\sqrt{1+\epsilon^2}\sum_{k=1}^{\ell}\left(\prod_{j\neq k}\frac{u-x_j}{x_k-x_j}\right)Q^{-}_{\boldsymbol{\theta}}(x_k)f_L\left(\dots,x_k+i\,,\dots\right)\,,\end{aligned} \tag{5.3.39}$$

$$\langle\boldsymbol{x}|A_{\epsilon}(u)|\uparrow^{\ell}\rangle = Q^{+}_{\boldsymbol{\theta}}(u)f_R(\boldsymbol{x})\,. \tag{5.3.40}$$

By equating (5.3.36) with (5.3.39) and (5.3.37) with (5.3.40) and setting $u=x_k$, we can derive the following recursion relations for $f_{L,R}(\boldsymbol{x})$:

$$f_L(\dots,x_k+i\,,\dots) = \frac{1}{\sqrt{1+\epsilon^2}}f_L(\boldsymbol{x})\,, \tag{5.3.41}$$

$$f_R(\dots,x_k-i\,,\dots) = \frac{1}{\sqrt{1+\epsilon^2}}f_R(\boldsymbol{x})\,. \tag{5.3.42}$$

Solving these recursion relations, $f_{L,R}(\boldsymbol{x})$ can be determined as

$$f_L(\boldsymbol{x})\propto\exp\left(\frac{i}{2}\ln(1+\epsilon^2)\sum_{k=1}^{\ell}x_k\right)\,,\quad f_R(\boldsymbol{x})\propto\exp\left(-\frac{i}{2}\ln(1+\epsilon^2)\sum_{k=1}^{\ell}x_k\right)\,. \tag{5.3.43}$$

Let us now convert the summation over the discrete spectrum of $\hat{x}_k$'s to contour integrals over the continuous variables x_k. To carry this out, we utilize the following relations:

$$e^{-\pi(x_k-\theta_k)} = \mathrm{Res}_{z=x_k}\left[\frac{1}{(z-\theta_k+\frac{i}{2})(z-\theta_k-\frac{i}{2})}\right]\,. \tag{5.3.44}$$

Note that x_k takes only two values, $\theta_k\pm\frac{i}{2}$, and (5.3.44) is either $+i$ or $-i$ depending on which value x_k takes. Then, by re-expressing the factor $\prod_k e^{-\pi(x_k-\theta_k)}$ in (5.3.34) using the

relations (5.3.44), we can rewrite the whole measure as the residue of the following simple function:

$$\mu(\boldsymbol{x}) \propto \mathrm{Res}_{\{z_k\}=\{x_k\}} \left[\frac{\prod_{i<j}(z_i - z_j)}{\prod_l Q^+_{\boldsymbol{\theta}}(z_l) Q^-_{\boldsymbol{\theta}}(z_l)} \right] , \tag{5.3.45}$$

where $Q_{\boldsymbol{\theta}}$ is given by $\prod_{k=1}^{\ell}(u - \theta_k)$ as defined previously in (3.1.41). The constants of proportionality in (5.3.43) and (5.3.45), which are left undetermined, are functions of the twist parameter ϵ and the inhomogeneity parameters θ_k's. These constants are related to the overall normalization of the scalar products and will be fixed by the analysis presented in the Appendix A.2, which compares it with the other known formula for the scalar product. Taking into account the constants of proportionality in (5.3.43) and (5.3.45), we finally arrive at the following multiple integral formula[9] for the scalar product between an off-shell Bethe-state and an on-shell Bethe state:

$$\begin{aligned} \langle \uparrow^{\ell} | \prod_{i=1}^{M} C(v_i) \prod_{j=1}^{M} B(u_j) | \uparrow^{\ell} \rangle = \frac{\prod_{j<k}(\theta_j - \theta_k)(\theta_j - \theta_k + i)(\theta_j - \theta_k - i)}{(\ell - 2M)!} \\ \times \prod_{n=1}^{\ell} \oint_{\mathcal{C}_n} \frac{dx_n}{2\pi i} \left(\sum_{j=1}^{\ell} x_j \right)^{\ell - 2M} \prod_{k<l}(x_k - x_l) \prod_{m=1}^{\ell} \frac{Q_{\boldsymbol{u}}(x_m) Q_{\boldsymbol{v}}(x_m)}{Q^+_{\boldsymbol{\theta}}(x_m) Q^-_{\boldsymbol{\theta}}(x_m)} . \end{aligned} \tag{5.3.46}$$

In this formula, $\mathcal{C}_n$ denotes the integration contour which encloses $\theta_n \pm i/2$ counterclockwise. Actually the prefactors in front of the integral are unimportant when computing physical observables, since they drop out upon normalizing the Bethe states.

5.3.3 Symmetrization and simplification of the multiple integral

The multiple integral formula (5.3.46) derived in the last subsection has one unsatisfactory feature: This expression becomes singular as we take the homogeneous limit, $\theta_n \to 0$. There are two sources for the singular behavior. One is that the integration contours $\mathcal{C}_n$ get pinched and collide when all the θ_n's move to the origin. Another source is that at the same time the prefactor $\prod_{j<k}(\theta_j - \theta_k)$ will vanish. To get around this difficulty, we wish to deform each integration contour into the one, to be denoted by $\mathcal{C}_{\mathrm{all}}$, which encloses all the singularities in the integrand. However, if we naïvely make such deformations, obviously we will pick up unwanted contributions coming from different integration variables encircling the poles from the same group $\theta_n \pm i/2$. We can avoid such contributions by inserting a factor of the form $\prod_{k<l}(e^{2\pi x_k} - e^{2\pi x_l})$, which vanishes for all the undesired cases. For the genuine contributions for which this factor does not vanish, we must normalize properly to reproduce the original

[9] In the Appendix A.2, we will give a direct analytical proof of the equivalence between (5.3.46) and the known determinant formulas.

value of the integral. In this way, with the factor $\ell!$ coming from the permutation of x_n's, we obtain the following more symmetric expression for the scalar product:

$$\langle\uparrow^\ell|\prod_{i=1}^{M}C(v_i)\prod_{j=1}^{M}B(u_j)|\uparrow^\ell\rangle=\frac{\Xi}{\ell!(\ell-2M)!}$$
$$\times\prod_{n=1}^{\ell}\oint_{\mathcal{C}_{\rm all}}\frac{dx_n}{2\pi i}\left(\sum_{j=1}^{\ell}x_j\right)^{\ell-2M}\prod_{k<l}(x_k-x_l)(e^{2\pi x_k}-e^{2\pi x_l})\prod_{m=1}^{\ell}\frac{Q_{\boldsymbol{u}}(x_m)Q_{\boldsymbol{v}}(x_m)}{Q^+_{\boldsymbol{\theta}}(x_m)Q^-_{\boldsymbol{\theta}}(x_m)}\,, \quad (5.3.47)$$

where the prefactor Ξ is given by

$$\Xi\equiv\prod_{j<k}\frac{(\theta_j-\theta_k)(\theta_j-\theta_k+i)(\theta_j-\theta_k-i)}{(e^{2\pi\theta_j}-e^{2\pi\theta_k})}\,. \quad (5.3.48)$$

Note that for this expression the prefactor Ξ is indeed finite in the homogeneous limit.

Although the expression above is symmetric in all the variables and hence quite useful, it is of interest to point out that actually we can integrate out one of the x_k's and obtain a slightly simpler expression containing $\ell-1$ integration variables. To derive it, let us first re-express the factor $\prod_{k<l}(e^{2\pi x_k}-e^{2\pi x_l})$ as a determinant of Vandermonde type:

$$\prod_{k<l}(e^{2\pi x_k}-e^{2\pi x_l})=\det\left(e^{2\pi(j-1)x_k}\right)_{1\le j,k\le\ell}\,. \quad (5.3.49)$$

Then, by using the basic definition of the determinant, we can rewrite it into a sum over permutations of the form $\sum_\sigma(-1)^\sigma e^{2\pi(\sigma(j)-1)x_j}$. Now note that the remaining terms in the integrand is completely antisymmetric with respect to permutations. Hence, all the terms in the above sum contribute equally and we arrive at the following expression:

$$\frac{\Xi}{(\ell-2M)!}\prod_{n=1}^{\ell}\oint_{\mathcal{C}_{\rm all}}\frac{dx_n}{2\pi i}\left(\sum_{j=1}^{\ell}x_j\right)^{\ell-2M}\prod_{k<l}(x_k-x_l)\prod_{m=1}^{\ell}\frac{Q_{\boldsymbol{u}}(x_m)Q_{\boldsymbol{v}}(x_m)e^{2\pi(m-1)x_m}}{Q^+_{\boldsymbol{\theta}}(x_m)Q^-_{\boldsymbol{\theta}}(x_m)}\,. \quad (5.3.50)$$

Notice that the integral is over meromorphic factors, except for $\exp(2\pi(m-1)x_m)$. However for x_1 this factor is absent. Hence we can easily integrate out this variable by closing its contour at infinity. At infinity all the factors become power functions and the only non-vanishing integral to be performed is $\oint dx_1/(2\pi i x_1)=1$. After this procedure, we may convert the factor $e^{2\pi(m-1)x_m}$ back to the determinant and further to the original expression $\prod_{k<l}(e^{2\pi x_k}-e^{2\pi x_l})$. In this way we obtain the following simple formula with $\ell-1$ integration variables:[10]

$$\langle\uparrow^\ell|\prod_{i=1}^{M}C(v_i)\prod_{j=1}^{M}B(u_j)|\uparrow^\ell\rangle=\frac{\Xi}{(\ell-1)!(\ell-2M)!}$$
$$\times\prod_{n=1}^{\ell-1}\oint_{\mathcal{C}_{\rm all}}\frac{dx_n}{2\pi i}\prod_{k<l}(x_k-x_l)(e^{2\pi x_k}-e^{2\pi x_l})\prod_{m=1}^{\ell-1}\frac{Q_{\boldsymbol{u}}(x_m)Q_{\boldsymbol{v}}(x_m)e^{2\pi x_m}}{Q^+_{\boldsymbol{\theta}}(x_m)Q^-_{\boldsymbol{\theta}}(x_m)}\,. \quad (5.3.51)$$

[10]For simplicity, we have renamed $x_2,\ldots,x_\ell$ as $x_1,\ldots,x_{\ell-1}$.

Note that the factor, $(\sum_j x_j)^{\ell-2M}$, which was present in the previous expressions, disappeared upon integration over x_1. Therefore (5.3.51) is structurally similar to the eigenvalue integral of a matrix model. Namely, Q-functions correspond to a potential term for the eigenvalues and $\prod_{k<l}(x_k - x_l)(e^{2\pi x_k} - e^{2\pi x_l})$ can be interpreted as a modified Vandermonde factor. It is intriguing to note that this modified Vandermonde factor is a hybrid of the ordinary Vandermonde factor for the Hermitian matrix model, $\prod_{k<l}(x_k - x_l)^2$, and the generalized Vandermonde factor for the unitary matrix model and the Chern-Simons matrix model [99], which is essentially given by $\prod_{k<l}(e^{2\pi x_k} - e^{2\pi x_l})^2$. This resemblance to a matrix model strongly suggests that the semi-classical limit for the scalar product can be analyzed by applying the method of large N expansion familiar for matrix models as we shall discuss in the next section.

5.4 Attempt to derive the semi-classical limit

Having derived the integral formula, let us now turn our eyes to how the formula can be put to use. Below, we describe our so-far unsuccessful attempt to derive the semi-classical limit of the scalar products. Although we have not succeeded in deriving the expression (4.3.8), we believe the argument below partially clarifies the physical mechanism behind it.

For this purpose, it is instructive to first consider the semi-classical limit of a one-dimensional harmonic oscillator, whose Schödinger equation is given in (5.2.1), and consider the expectation value,

$$\langle \mathcal{O}(x) \rangle = \frac{\langle \psi | \mathcal{O}(x) | \psi \rangle}{\langle \psi | \psi \rangle} \,. \tag{5.4.1}$$

As discussed in section 2.1.3, the wave function in the semi-classical limit can be approximated by the WKB wave function. In the present case, it is given as follows:

$$\begin{aligned}
\psi(x) &\sim \frac{1}{p(x)^{1/2}} \cos\left[\frac{1}{\hbar}\int_{x_1}^{x} p(x')dx' - \frac{\pi}{4}\right] \quad \text{for } x_1 \geq x \geq x_2 \,, \\
\psi(x) &\sim \frac{1}{\rho(x)^{1/2}} \exp\left[-\frac{1}{\hbar}\int_{x}^{x_1} \rho(x')dx'\right] \qquad \text{for } x < x_1 \,, \\
\psi(x) &\sim \frac{1}{\rho(x)^{1/2}} \exp\left[-\frac{1}{\hbar}\int_{x_2}^{x} \rho(x')dx'\right] \qquad \text{for } x_2 < x \,,
\end{aligned} \tag{5.4.2}$$

where $x_1 < x_2$ are two real solutions for

$$E - V(x) = E - \frac{m\omega^2 x^2}{2} = 0 \,, \tag{5.4.3}$$

and $p(x)$ and $\rho(x)$ are given respectively by $p(x) = \sqrt{2m(E - V(x))}$ and $\rho(x) = \sqrt{2m(V(x) - E)}$. Owing to the exponential suppression factor, we can neglect the contributions from the two

regions, $x < x_1$ and $x_2 < x$, in the semi-classical limit. Furthermore, since the argument of the cosine-function in (5.4.2) is rapidly oscillating in the semi-classical limit, we can replace the square of the cosine-function by

$$\cos^2\left[\frac{1}{\hbar}\int_x^{x_1} p(x')dx' - \frac{\pi}{4}\right] \sim \frac{1}{2}\,, \tag{5.4.4}$$

in the limit. Therefore, (5.4.1) can be approximated as

$$\frac{\int_{x_1}^{x_2} \mathcal{O}(x)p(x)^{-1}dx}{\int_{x_1}^{x_2} p(x)^{-1}dx}\,. \tag{5.4.5}$$

Since, classically, the momentum p can be expressed by the velocity of the particle as

$$p = mv = m\frac{dx}{dt}\,, \tag{5.4.6}$$

the expression (5.4.5) can be recast into the following form:

$$\langle \mathcal{O}(x) \rangle \simeq \frac{\oint \mathcal{O}(x(t))dt}{\oint dt}\,, \tag{5.4.7}$$

which is nothing but the classical time average.

This elementary example shows clearly how the classical motion emerges from the quantum observable. What is more interesting is that the branch cut of $p(x)$ originates from the condensation of poles. To see this, let us consider the exact wave function, given in (5.2.2),

$$\psi(x) = \prod_{i=1}^{N}(x - x_i)e^{-m\omega x^2/2\hbar}\,. \tag{5.4.8}$$

We can define the quantum analogue of $p(x)$ as the logarithmic derivative of the wave function as

$$p_{\text{exact}}(x) = -i\frac{d\ln\psi}{dx} = \sum_{i=1}^{N}\frac{-i}{x - x_i} + \frac{im\omega x}{\hbar}\,. \tag{5.4.9}$$

This expression makes it clear that the branch cut of $p(x)$ originates from the condensation of poles. This feature is reminiscent of the semi-classical limit of the XXX spin chain, in which the condensation of the Bethe roots results in the branch cuts in the spectral curve. This analogy indeed goes further and the formula (5.4.5) can also be expressed as the integration around the branch cut just like the semi-classical formula for the scalar products of the XXX spin chain (4.3.8):

$$\frac{\oint \mathcal{O}(x)p(x)^{-1}dx}{\oint p(x)^{-1}dx}\,. \tag{5.4.10}$$

The above observations suggest the possibility that we can directly derive the semi-classical limit of the scalar products starting from our integral formula. In fact, the following combination of the Q-functions can be approximated as follows in the semi-classical limit:

$$\frac{Q_{\boldsymbol{u}}(x)}{\sqrt{Q_{\boldsymbol{\theta}}(x)}} \simeq \exp\left(\int^{x} p_{\boldsymbol{u}}(x')dx'\right) , \tag{5.4.11}$$

where $p_{\boldsymbol{u}}$ is the quasi-momentum defined in (4.3.9). Let us study the norm of the scalar product $\langle \boldsymbol{u}|\boldsymbol{u}\rangle$ using this approximation. Unfortunately the discussion below is very much hand-waving and far from a rigorous proof. We nevertheless explain it since it gives us certain insights into the semi-classical limit of the scalar products. Substituting (5.4.11) into the expression (5.3.50), which we derived in the intermediate step of the symmetrization of the scalar products, and setting $\boldsymbol{v} = \boldsymbol{u}$, we obtain the following expression:

$$\prod_{n=1}^{\ell} \oint_{\mathcal{C}_{\rm all}} \frac{dx_n}{2\pi i} \left(\ast\right) \prod_{m=1}^{\ell} e^{2\int^{x_m} p_{\boldsymbol{u}}(x')dx' + 2\pi(m-1)x_m} , \tag{5.4.12}$$

where various other factors are denoted by $\left(\ast\right)$. If we perform a saddle-point approximation to (5.4.12) neglecting the factor $\left(\ast\right)$, we arrive at the following saddle point equation:

$$p_{\boldsymbol{u}}(x_m) = \pi(m-1) . \tag{5.4.13}$$

Note that the equation (5.4.13) is the same in form as the defining equations for the branch points and the node-like points (3.3.39). This is consistent with the observation to be made in section 7.1 that most of the separated variables are confined in the node-like points in the classical solutions describing two-point functions. By evaluating the integrand on the saddle point and neglecting the contributions from $\left(\ast\right)$, we obtain the following expression for the semi-classical limit:

$$\ln\langle \boldsymbol{u}|\boldsymbol{u}\rangle \simeq \oint \left(2\int^{x} p_{\boldsymbol{u}}(x')dx' - 2p_{\boldsymbol{u}}(x)x\right) \frac{d\ln\sin p_{\boldsymbol{u}}(x)}{dx} dx . , \tag{5.4.14}$$

where the integration contour is taken to encircle all the poles in the integrand counterclockwise. Let us explain the meaning of each factor on the right hand side of (5.4.14). The terms in the big parenthesis simply denote the logarithm of the integrands in (5.4.12). On the other hand, the term $(\ln\sin p_{\boldsymbol{u}})'$ produces poles at $p_{\boldsymbol{u}}(x) = n\pi$. Therefore, upon integration, we obtain the values of the integrands in (5.4.12) evaluated on the saddle points (5.4.13). Since the integration contour of (5.4.13) encircles all the poles in the integrand, we can deform it such that the contour after integration only encircles the branch cuts of $p_{\boldsymbol{u}}(x)$, $\mathcal{A}_{\boldsymbol{u}}$, as follows:

$$\ln\langle \boldsymbol{u}|\boldsymbol{u}\rangle \simeq \oint_{-\mathcal{A}_{\boldsymbol{u}}} \left(2\int^{x} p_{\boldsymbol{u}}(x')dx' - 2p_{\boldsymbol{u}}(x)x\right) \frac{d\ln\sin p_{\boldsymbol{u}}(x)}{dx} \frac{dx}{2\pi i} . \tag{5.4.15}$$

By partial integration, this expression can be further converted as

$$= 2\oint_{-\mathcal{A}_{\boldsymbol{u}}} x\frac{p_{\boldsymbol{u}}(x)}{dx}\ln\sin p_{\boldsymbol{u}}(x)\frac{dx}{2\pi i} = \oint_{\mathcal{A}_{\boldsymbol{u}}}\frac{dx}{2\pi}\mathrm{Li}_2\left(e^{2ip_{\boldsymbol{u}}(x)}\right)\ , \tag{5.4.16}$$

where we neglected terms, which only changes the overall phase of the norm, on the right hand side. In this way, the semi-classical limit of the norm (4.3.8) can be reproduced.

We should keep in mind that the above derivation is far from rigorous since we deliberately neglected various important terms including the Vandermonde factor $\prod_{i<j}(x_i - x_j)$, which plays a crucial role in the large N limit of the ordinary matrix model. However, the fact that the known semi-classical result can be reproduced by neglecting such terms indicate that their contributions are in fact suppressed in the semi-classical limit. This of course should be validated by some rigorous argument but, at present, we have no convincing proof. Thus, the rigorous derivation of the semi-classical limit starting from the integral formula still remains an important open question.

Part III

Three Point Functions in Classical String Theory

Chapter 6

Correlation functions and classical strings

Having seen that the three-point functions at weak coupling can be computed using the integrability-based techniques, let us start discussing the main theme of this thesis: The computation of three-point functions at strong coupling using the classical string and integrability.

The aim of this chapter is to give a general overview of the computation of three-point functions in the classical string theory. In section 6.1, we explain how the correlation functions in the strong coupling limit of the gauge theory can be computed by the classical string. In particular, we explain how various types of the operators in the gauge theory are described on the string theory side. Then in section 6.2, we review various previous works on the computation of three-point functions at strong coupling, and motivate the discussions in the next chapter.

6.1 Correlation functions at strong coupling from the saddle-point approximation

Let us get started by overviewing the computation of three-point functions in the classical string theory.

As explained in section 2.2, the correlation function in the gauge theory is computed on the string theory side by the worldsheet correlation function given as follows:

$$\langle \mathcal{O}_1(x_1) \cdots \mathcal{O}_n(x_n) \rangle = \int \frac{d^2 z_1 \cdots d^2 z_n}{\text{Möbius}} \langle \mathcal{V}_1(z_1) \cdots \mathcal{V}_n(z_n) \rangle \,. \tag{6.1.1}$$

In terms of the path integral, the right hand side of (6.1.1) is re-expressed schematically as

$$\int \frac{d^2z_1 \cdots d^2z_n}{\text{Möbius}} \int \mathcal{D}X e^{-\sqrt{\lambda}S[X]} \mathcal{V}_1[X(z_1)] \cdots \mathcal{V}_n[X(z_n)] \,. \tag{6.1.2}$$

Owing to the $\sqrt{\lambda}$ factor in front of the action $S[X]$, the path integral (6.1.2) will be dominated by the saddle-point contribution when the 't Hooft coupling constant λ goes to infinity. Then, the saddle-point equation is given by

$$\frac{\delta S[X]}{\delta X(z)} = \frac{1}{\sqrt{\lambda}} \sum_{i=1}^{n} \frac{\delta \ln \mathcal{V}_i[X(z_i)]}{\delta X(z)} \,. \tag{6.1.3}$$

If we take the $\lambda \to \infty$ limit assuming that $\ln \mathcal{V}_i$'s are much smaller than $\sqrt{\lambda}$, the right hand side of (6.1.3) simply vanishes and the saddle point equation becomes identical with the one without any vertex operator insertions. Then the dominant contribution is provided by a point-like worldsheet with zero area, irrespective of the vertex operators. In such a case, the leading semi-classical result is trivial and one needs to compute the quantum correction in order to take into account the detailed information of the vertex operators. On the other hand, when $\ln \mathcal{V}_i$ is of order $\sqrt{\lambda}$, the right hand side of (6.1.3) cannot be neglected even in the limit. Then the dominant contribution is provided by a nontrivial worldsheet configuration, which in general has a long leg at each insertion point. Unlike the previous case, the detailed information of the vertex operators is already reflected in the saddle-point configuration and we just need to evaluate the integrand of (6.1.3) on the saddle point to obtain the leading result in the $\lambda \to \infty$ limit.

To estimate the magnitude of the logarithm of the vertex operator $\ln \mathcal{V}_i$, let us first recall the form of the vertex operator of the rotating string in the flat spacetime,

$$\mathcal{V} = (X_1 + iX_2)^J e^{ik_\mu X^\mu} \,, \tag{6.1.4}$$

where J is the angular momentum on the X_1-X_2 plane whereas k_μ is the spacetime momentum. The equation (6.1.4) shows clearly that $\ln \mathcal{V}$ is proportional to the charges (quantum numbers), J and k_μ. This property is quite universal and is true also for the string theory on the $AdS_5 \times S^5$ spacetime. To see this clearly, it is convenient to map the vertex operator to the wave function using the state-operator correspondence. Then as we will see in section 7.3, the semi-classical limit of the wave function, which is related to the vertex operator through the state-operator mapping, can be expressed as

$$\mathcal{V}_i \mapsto \Psi \sim \exp\left(i \sum_i S_i \phi_i \right) \,, \tag{6.1.5}$$

where S_i's are charges of the string state and ϕ_i's are the conjugate angle variables. The expression (6.1.5) makes it clear that the logarithm of the vertex operator is of the order of

the charges S_i's. Since the charges are typically of the order of conformal dimension Δ in the string theory on $AdS_5 \times S^5$, we conclude that $\ln \mathcal{V}_i$ is roughly proportional to Δ. This means that only the vertex operators whose conformal dimension are of the order of $\sqrt{\lambda}$ affect the saddle point configuration.

Let us now give a more physical description of the above statement. When λ goes to infinity, the string becomes infinitely rigid and the ratio between the string length ℓ_s and the AdS radius R scales as

$$\frac{\ell_s}{R} \sim \lambda^{-1/4} \to 0\,. \tag{6.1.6}$$

In such a situation, it is convenient to classify the string states depending on their conformal dimensions.

- First, the strings with zero oscillation number $N_{\rm osc}$ (see (2.1.2)), which correspond to the supergravity modes, typically have the $O(1)$ energy (conformal dimension):

$$E \sim \Delta \sim O(1)\,. \tag{6.1.7}$$

  Since such states cannot modify the saddle point, the quantum correction needs to be considered. In what follows, we call these states the *light* states. It is known that these light supergravity states are dual to the 1/2-BPS operators in the gauge theory.

- On the other hand, if the string has a finite number of oscillation modes, its energy scales as

$$E = \Delta \sim \frac{1}{\ell_s} \sim \lambda^{1/4}\,. \tag{6.1.8}$$

  Although this is divergent in the limit $\lambda \to \infty$, it is still much smaller than $\sqrt{\lambda}$. Therefore, such states do not affect the saddle point either. These states are often called the *medium* states and are considered to be dual to the short non-BPS operators in the gauge theory.

- The string states which do modify the saddle points are called the *heavy* states, whose oscillation number scales as $N_{\rm osc} \sim \lambda^{1/4}$ and whose energy is given by

$$E = \Delta \sim \frac{N_{\rm osc}}{\ell_s} \sim \sqrt{\lambda}\,. \tag{6.1.9}$$

  Since the angular momenta of such states are of the same order as Δ, the string can extend macroscopically owing to the strong centrifugal force. The operators dual to these states are given by long non-BPS operators in the gauge theory.

A summary of the above classification is given as follows:

	Δ	String theory	Gauge theory
Light	$\Delta \sim 1$	Supergravity	BPS operator
Medium	$\Delta \sim \lambda^{1/4}$	String with finite excitations	Short non-BPS operator
Heavy	$\Delta \sim \lambda^{1/2}$	Macroscopic string	Long non-BPS operator

(6.1.10)

In the next chapter, we focus on three-point functions of heavy string states. In the case of three-point functions, we can fix the insertion points of the vertex operators using the Möbius transformation and the path integral expression is schematically given by

$$\int \mathcal{D}X\, \mathcal{V}_1[X_1]\, \mathcal{V}_2[X_2]\, \mathcal{V}_3[X_3]\, e^{-\sqrt{\lambda}S}\,. \tag{6.1.11}$$

The saddle point of such a path integral is provided by the worldsheet with three long legs (see Figure 6.1.1). However it is practically impossible to determine the precise shape of the saddle point owing to the complicated dynamics of the string on $AdS_5 \times S^5$. In addition, since we do not know the explicit way to quantize the string sigma model on $AdS_5 \times S^5$, we cannot construct the exact form of the vertex operator. In the next chapter, we will see how these two difficulties can be overcome by an ingenious use of integrability.

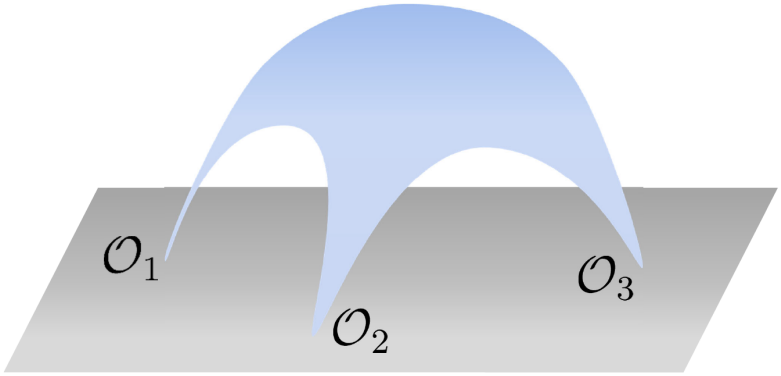

Figure 6.1.1: A typical saddle-point configuration in AdS spacetime for the three-point function.

6.2 Various attempts on the string-theory side

Before we move on to the actual computation, let us review various preceding works on the three-point functions on the string-theory side.

The most well-studied three-point functions at strong coupling are those with three light states. Since the light states are nothing but the supergravity modes, one can compute such

three-point functions using the supergravity and it was found that the result completely matches the one obtained in the gauge theory [72]. Another class of well-studied three-point functions are the so-called "Heavy-Heavy-Light" three-point functions, which were first studied in [100–102]. Since the third operator is light in this case, we can compute such three-point functions by using the known saddle-point trajectory of two heavy states and evaluating the third supergravity mode on that trajectory. In [91], it was found that such three-point functions completely agree with the gauge-theory results if we take the Frolov-Tseytlin limit. Recently, a method to compute the three-point functions of the medium states was proposed in [103, 104]. They assumed that the medium states are insensitive to the curvature of the AdS spacetime since they are almost point-like. Then they approximated the states by those on the flat space and computed three-point functions using the flat-space scattering amplitude. Although it is not clear at present to what extent we can approximate the medium state by the string state on the flat spacetime, it is certainly a direction worth to be explored.

We should also mention that there is a number of works studying three-point functions in the *BMN limit* using the light-cone string field theory. The string states in the BMN limit are the states with an angular momentum much larger than $\sqrt{\lambda}$ and with a finite number of mode excitations. They share common properties with all three aforementioned states: First, they are certainly heavy since the conformal dimension Δ is larger than $\sqrt{\lambda}$. Second, they have a finite number of mode excitations similarly as the medium states. Third, since the number of excitations is negligibly small as compared to Δ, the string is of infinitesimal size as the light state. Therefore, studying such three-point functions is certainly interesting and will probably be rewarding. However, a crucial limitation in this approach is that only near-extremal three-point functions, which satisfy $\Delta_i + \Delta_j \sim \Delta_k$, can be computed. The near-extremal limit is a singular and degenerate limit and the trajectory of the string approaches to that of the two-point function in such a limit.

To explore the genuine characteristics of three-point functions of the string theory on $AdS_5 \times S^5$, we need to consider three-point functions of heavy states. However, as stated at the end of the previous subsection, the computation of such three-point functions is known to be extremely difficult and only a few papers were written regarding this topic. In the first of such attempts [105], the contribution from the AdS_2 part was evaluated for the string in $AdS_2 \times S^k$, where the string is assumed to be rotating only in S^k. Since the contribution from the sphere part was not computed in [105], the complete answer for the three-point function was not given. In this context, the computation to be explained in the next chapter can be regarded as the completion of the work initiated by [105].

At about the same time, computation of the three-point functions for different type of external states was attempted in [16]. We took as the external states the so-called Gubser-

Klebanov-Polyakov (GKP) strings [106] spinning within AdS_3 with large spins. In this work, the contribution to the three-point function from the action evaluated on the saddle point configuration was computed by a method similar to the one in [105]. However, unlike the case of [105], the GKP string is not point-like on the boundary, and hence the contributions from the non-trivial vertex operators were needed to give the complete answer. Since the precise form of such vertex operators were not known, again the computation had to be left unfinished. This difficulty was later overcome by the development of a new integrability-based method built on the state-operator correspondence and the contribution of the non-trivial wave functions of the external states was obtained [17]. Combined with the contribution from the action evaluated previously, this gave the full answer for the three-point function of the GKP strings in the large spin limit [17].

However, three-point functions of the operators dual to the GKP strings are not well studied on the gauge theory side. This made it impossible to compare the results on both sides and extract a common structure. Thus, in the next chapter, we set out to discuss a class of three-point functions which were well-studied in the gauge theory side; three-point functions in "SU(2)-sector", discussed in Part II.

Chapter 7

Three-point functions in SU(2)-sector at strong coupling

In the previous chapter, we have seen that the three-point functions in the strong coupling limit of the gauge theory can be computed by the classical string on the three-pronged worldsheet and that the contribution can be split into two parts, the action and the vertex operators. In this chapter, we explicitly carry out such computation. More precisely, we study three-point functions of strings which do not have angular momenta in AdS_5 and move in the S^3-subspace of the full S^5. In particular, we discuss the three-point functions of one-cut string solutions, which have only one branch cut on the spectral parameter plane. They include the ones, which are dual to the three-point functions in the "SU(2)-sector" of the gauge theory discussed in detail in Part II.

First in section 7.1, we summarize several known facts on the classical strings in S^3, to be used in the subsequent discussions. Then in section 7.2, we begin with the computation of the action-part and show that the contribution from the action can be re-expressed in terms of the Wronskians of the auxiliary linear problem. Next, in section 7.3, we discuss the contribution from the vertex operators and find that this contribution can also be expressed in terms of the Wronskians. Based on these observations, we next proceed to evaluate the Wronskians in section 7.4. We first determine the analytic property of the Wronskian using an appropriate generalization of the WKB analysis. Using this information, we next set up the Riemann-Hilbert problem and solve it in terms of certain convolution integrals on the spectral curve. In section 7.5, we then put together all the results obtained up to this point and write down the general formula for three-point functions of strings rotating in S^3. The resulting formula is surprisingly simple and highly resembles the result in the gauge theory before taking any limits. Lastly in section 7.6 we examine the formula using several explicit examples and perform a detailed comparison with the results in the gauge theory. As a result,

we find a small mismatch between the string theory and the gauge theory even after taking the Frolov-Tseytlin limit. We then briefly discuss the possible origin and interpretation of this mismatch.

7.1 Classical strings in S^3 and three-point functions

Let us begin by setting up the formalism to deal with the three-point functions in the classical string theory.

7.1.1 A word on the set-up

The three-point function we wish to compute in the semi-classical approximation has the following structure[1]:

$$G_{123}(x_1, x_2, x_3) = \langle \mathcal{V}_1 \mathcal{V}_2 \mathcal{V}_3 \rangle \sim e^{-S[X_*]_\epsilon} \prod_{i=1}^{3} \mathcal{V}_i[X_*; x_i, Q_i]_\epsilon \,. \tag{7.1.1}$$

It consists of the contribution of the action and that of the vertex operators, evaluated on the saddle point configuration denoted by X_*. The subscript ϵ signifies a small cut-off which regulates the divergences contained in S and $\mathcal{V}_i$. As we shall show, these divergences cancel against each other and the total three-point function is completely finite. The vertex operator $\mathcal{V}_i[X_*; x_i, Q_i]_\epsilon$ is assumed to carry a large charge Q_i of order $O(\sqrt{\lambda})$ and is located at x_i on the boundary of the AdS space.

In this chapter, we will consider the string propagating in the product space of the Euclidean AdS_3 subspace of AdS_5 (to be denoted by $EAdS_3$) and the sphere S^3. The external string states we use are those with nontrivial S^3 angular momenta but without $EAdS_3$ angular momenta. Therefore, we will mostly concentrate on the S^3 part in the subsequent discussions. An exception is section 7.5.2, where we take into account the contributions from the $EAdS_3$-part.

In the case of a string in $EAdS_3 \times S^3$, the action and the vertex operators are split into the $EAdS_3$ part and the S^3 part. Their contributions are connected solely through the Virasoro constraint $T(z)_{EAdS_3} + T(z)_{S^3} = 0$ (and its anti-holomorphic counterpart). In the semi-classical approximation, an external state is characterized by the asymptotic behavior of a classical solution, which should be the saddle point configuration for its two-point function. However, a conformally invariant vertex operator which creates such a state is practically impossible to construct at present. Moreover, even if one had the vertex operator, it is of

[1] A more detailed explanation on the structure will be given in subsection 7.1.7.

no use since the explicit saddle point solution X_* on which to evaluate the vertex operator (and the action) cannot be obtained by existing technology.

Such difficulties, although seemingly insurmountable, can be overcome with the aid of the integrable structure of the system as we will see in the following sections. In the rest of this section, we recall several known facts on the classical integrability, which we did not explain in section 3.2.2, in order to provide enough background knowledge for the subsequent computation.

7.1.2 More on the classical integrability of the string in S^3

Let us explain several necessary facts on the classical integrability of the string in S^3 for the analysis in the subsequent sections.

The auxiliary linear problem

Of crucial importance in the analysis in the following sections is the so-called *auxiliary linear problem*, to be abbreviated as ALP. They are the following coupled linear differential equations for vector functions:

$$\text{right ALP}: \quad (\partial + \frac{j_z}{1-x})\psi = 0\,, \qquad (\bar{\partial} + \frac{j_{\bar{z}}}{1+x})\psi = 0\,, \tag{7.1.2}$$

$$\text{left ALP}: \quad (\partial + \frac{xl_z}{1-x})\tilde{\psi} = 0\,, \qquad (\bar{\partial} - \frac{xl_z}{1+x})\tilde{\psi} = 0\,. \tag{7.1.3}$$

Compatibility of the system of the ALP implies the original equations of motion. Since the left and the right connections are related by the gauge transformation, the solutions to the ALP, ψ and $\tilde{\psi}$, are also related with each other as follows:

$$\tilde{\psi} = \mathbb{Y}\psi\,. \tag{7.1.4}$$

Pohlmeyer reduction

The formulation of the classical integrability in terms of the left and the right currents l and j is convenient for analyzing the property of the system under the global symmetry transformations. Hence it will be used as the basis of the construction of the wave function corresponding to the vertex operators in section 7.3. On the other hand, for the analysis of the contribution of the action, which is invariant under the global transformation, the formalism of the *Pohlmeyer reduction* [107, 108] will be more convenient.

The essential idea of the Pohlmeyer reduction is to describe the motion of the string in a suitably defined moving frame. This then leads to the Lax equations in terms of the connections which are invariant under the global symmetry transformations. Below we shall only sketch the procedures and then summarize the basic equations we will need later. Further details will be given in Appendix C.2.

In what follows we shall denote a 4-component field A^I simply as A and use the notations $A \cdot B = A^I B_I, A^2 = A^I A_I$. The basic moving frame of 4-component fields, to be called $q_i, (i = 1, 2, 3, 4)$, are taken as $q_1 \equiv Y, q_2 \equiv a\partial Y + b\bar{\partial} Y, q_3 \equiv c\partial Y + d\bar{\partial} Y$ and $q_4 \equiv N$, where N is the unit vector orthogonal to $Y, \partial Y$ and $\bar{\partial} Y$, and the (field-dependent) coefficients a, b, c, d are chosen so that the simple conditions $q_2 \cdot q_3 = -2, q_2^2 = q_3^2 = 0$ are satisfied. (Note that since $Y^2 = 1$, we automatically have $q_1^2 = 1, q_1 \cdot q_2 = q_1 \cdot q_3 = 0$.) Let us define an SO(4)-invariant field γ by the relation

$$\partial Y \cdot \bar{\partial} Y = \sqrt{T\bar{T}} \cos 2\gamma \,. \tag{7.1.5}$$

Then, the coefficients a, b, c, d can be expressed in terms of $T, \bar{T}$ and γ, giving q_2 and q_3 of the form

$$q_2 = -\frac{i}{\sin 2\gamma} \left[\frac{e^{i\gamma}}{\sqrt{T}} \partial Y + \frac{e^{-i\gamma}}{\sqrt{\bar{T}}} \bar{\partial} Y \right] , \tag{7.1.6}$$

$$q_3 = \frac{i}{\sin 2\gamma} \left[\frac{e^{i\gamma}}{\sqrt{\bar{T}}} \bar{\partial} Y + \frac{e^{-i\gamma}}{\sqrt{T}} \partial Y \right] . \tag{7.1.7}$$

Once the moving frame is prepared, one can compute the derivatives of q_i and express them in terms of q_i again. The result can be assembled into the following equations

$$\partial W + B_z^L W + W B_z^R = 0 \,, \qquad \bar{\partial} W + B_{\bar{z}}^L W + W B_{\bar{z}}^R = 0 \,, \tag{7.1.8}$$

where W is given by

$$W = \frac{1}{2} \begin{pmatrix} q_1 + iq_4 & q_2 \\ q_3 & q_1 - iq_4 \end{pmatrix} , \tag{7.1.9}$$

and $B_{z,\bar{z}}^{L,R}$ are matrices whose components are expressed in terms of $T, \bar{T}$ and γ. (Explicit forms are given in Appendix C.2.) From the equations (7.1.8) one deduces that the left and the right connections B^L and B^R, given in (C.2.21)–(C.2.24), are flat, namely

$$[\partial + B_z^L, \bar{\partial} + B_{\bar{z}}^L] = 0 \,, \qquad [\partial + B_z^R, \bar{\partial} + B_{\bar{z}}^R] = 0 \,. \tag{7.1.10}$$

These relations give the equations of motion for the invariant fields in the form

$$\begin{aligned} &\partial\bar{\partial}\gamma + \frac{\sqrt{T\bar{T}}}{2} \sin 2\gamma + \frac{2\rho\tilde{\rho}}{\sqrt{T\bar{T}}} \frac{1}{\sin 2\gamma} = 0 \,, \\ &\partial\tilde{\rho} + \frac{2\bar{\partial}\gamma}{\sin 2\gamma} \rho = 0 \,, \qquad \bar{\partial}\rho + \frac{2\partial\gamma}{\sin 2\gamma} \tilde{\rho} = 0 \,, \end{aligned} \tag{7.1.11}$$

where ρ and $\tilde{\rho}$ are defined by

$$\rho \equiv \frac{1}{2} N \cdot \partial^2 Y \,, \quad \tilde{\rho} \equiv \frac{1}{2} N \cdot \bar{\partial}^2 Y \,. \tag{7.1.12}$$

Just as in the case of the sigma model formulation, the integrability of the system allows one to introduce a spectral parameter ζ, related to x by

$$\zeta = \frac{1-x}{1+x} \,, \tag{7.1.13}$$

without spoiling the flatness conditions. The Lax equation so obtained is given by

$$[\partial + B_z(\zeta), \bar{\partial} + B_{\bar{z}}(\zeta)] = 0 \,, \tag{7.1.14}$$

where

$$\begin{aligned}
&B_z(\zeta) \equiv \frac{\Phi_z}{\zeta} + A_z \,, \quad B_{\bar{z}}(\zeta) \equiv \zeta \Phi_{\bar{z}} + A_{\bar{z}} \,, \\
&\Phi_z \equiv \begin{pmatrix} 0 & -\frac{\sqrt{T}}{2} e^{-i\gamma} \\ -\frac{\sqrt{T}}{2} e^{i\gamma} & 0 \end{pmatrix} \,, \quad \Phi_{\bar{z}} \equiv \begin{pmatrix} 0 & \frac{\sqrt{\bar{T}}}{2} e^{i\gamma} \\ \frac{\sqrt{\bar{T}}}{2} e^{-i\gamma} & 0 \end{pmatrix} \,, \\
&A_z \equiv \begin{pmatrix} -\frac{i\partial\gamma}{2} & \frac{\rho e^{i\gamma}}{\sqrt{T}\sin 2\gamma} \\ \frac{\rho e^{-i\gamma}}{\sqrt{T}\sin 2\gamma} & \frac{i\partial\gamma}{2} \end{pmatrix} \,, \quad A_{\bar{z}} \equiv \begin{pmatrix} \frac{i\bar{\partial}\gamma}{2} & \frac{\tilde{\rho} e^{-i\gamma}}{\sqrt{\bar{T}}\sin 2\gamma} \\ \frac{\tilde{\rho} e^{i\gamma}}{\sqrt{\bar{T}}\sin 2\gamma} & -\frac{i\bar{\partial}\gamma}{2} \end{pmatrix} \,.
\end{aligned} \tag{7.1.15}$$

One can consider the auxiliary linear problem also for the Pohlmeyer connection (7.1.14),

$$(\partial + B_z(\zeta))\,\hat{\psi} = 0 \,, \quad \left(\bar{\partial} + B_{\bar{z}}(\zeta)\right)\hat{\psi} = 0 \,. \tag{7.1.16}$$

As shown in Appendix C.3.2, the Pohlmeyer connection (7.1.14) is related to the connections in the sigma model formulation, (7.1.2) and (7.1.3), by the gauge transformation. Thus the solutions to the ALP are also related by the gauge transformation as[2]

$$\psi = \mathcal{G}^{-1}\hat{\psi} \,, \quad \tilde{\psi} = \tilde{\mathcal{G}}^{-1}\hat{\psi} \,, \tag{7.1.17}$$

where ψ and $\tilde{\psi}$ are the solutions to the right ALP and the left ALP respectively. Here and below, we often call the choice of the gauge which gives the Pohlmeyer connection the *Pohlmeyer gauge*.

7.1.3 One-cut solutions in S^3

We now describe a particular class of solutions to the equations of motion and the Virasoro constraints, which can be constructed by the so-called *finite gap integration method*[3] [41–43].

[2]The explicit forms of $\mathcal{G}$ and $\tilde{\mathcal{G}}$ will be given in Appendix C.3.2.

[3]For a comprehensive review, see [41].

The finite gap method is a powerful framework which allows us to construct a large class of solutions describing two-point functions. In addition, as we shall emphasize in section 7.1.6, they also characterize the local behaviors of the saddle point solution for the three-point function in the vicinity of the vertex insertion point. Among various solutions constructible by the finite gap method, the class of our interest in this chapter is the simplest one; the one-cut solutions, which are characterized by the associated spectral curve having one square-root branch cut of finite size.

Before writing down the explicit form of the one-cut solutions, let us first sketch the general procedures of the finite-gap integration method. As the first step, the solutions to the left and the right ALP, called the Baker-Akhiezer functions, are constructed by treating the problems as Riemann-Hilbert problems on a finite genus Riemann surface. Namely, by proving that the function satisfying all the required analytic properties is unique, one constructs such a function in terms of the Riemann theta functions and the exponential functions. Then, as the second step, one develops the "reconstruction" formula[4] , which constructs the solutions to the original equations of motion from the knowledge of the Baker-Akhiezer functions. Important features of the finite gap solutions are

1. the spectral curve has only a finite number of branch points (cusp-like points),
2. the monodromy matrix is proportional to the identity matrix at all the node-like points[5].

These features will play an important role when we discuss the difference between the finite-gap solutions, which describe two-point functions, and more general solutions describing three-point functions in subsection 7.1.6.

Let us now see explicitly how the aforementioned procedures are applied to the case of the one-cut solutions.

Baker-Akhiezer vector

Consider first the right ALP given in (7.1.2) and let $\psi_{\pm}(x, z, \bar{z})$ be the Baker-Akhiezer vector which are at the same time the eigenvectors of the monodromy matrix $\Omega(x)$ corresponding to the eigenvalues $e^{\pm ip(x)}$ respectively. According to the general theory of finite gap integration,

[4]Although it is usually referred to as the "reconstruction" formula, in practice it is used as a solution-generating formula.

[5]For a discussion on the behavior of the monodromy matrix at cusp-like points and node-like points, see section 3.2.2.

$\psi_\pm$ corresponding to the one-cut solution are given by simple exponential functions as

$$\psi_+(x;\tau,\sigma) = \begin{pmatrix} c_1^+ \exp\left(\frac{i\sigma}{2\pi}\int_{\infty^+}^x dp + \frac{\tau}{2\pi}\int_{\infty^+}^x dq\right) \\ c_2^+ \exp\left(\frac{i\sigma}{2\pi}\int_{\infty^-}^x dp + \frac{\tau}{2\pi}\int_{\infty^-}^x dq\right) \end{pmatrix}, \tag{7.1.18}$$

$$\psi_-(x;\tau,\sigma) = \psi_+(\hat{\sigma}x;\tau,\sigma)\,. \tag{7.1.19}$$

where c_i^+ are constants, $\hat{\sigma}x$ denotes the point x on the opposite sheet, and $\infty^+(\infty^-)$ is the point at infinity on the first (resp. second) sheet. The quantity dp is the differential of the quasi-momentum $p(x)$, while dq is the differential of the quasi-energy $q(x)$. Just like $p(x)$, the quasi-energy $q(x)$ is defined by the pole behavior at $x = \pm 1^+$ of the form

$$q(x) \sim \frac{-2\pi\kappa}{x-1} + O((x-1)^0)\,, \qquad (x \to 1^+)\,, \tag{7.1.20}$$

$$q(x) \sim \frac{+2\pi\kappa}{x+1} + O((x+1)^0)\,, \qquad (x \to -1^+)\,. \tag{7.1.21}$$

The structure and the signs of the residue at $x = \pm 1$ for $q(x)$ are determined so that the holomorphicity of the solution (7.1.18) at $x \simeq \pm 1$ is as dictated by the ALP. For example at $x = 1$ the holomorphic part of the ALP is dominating and hence the Baker-Akhiezer vector should be holomorphic. This is in fact realized since $p(x) = q(x)$ near $x = 1$ and hence the exponent of $\psi_\pm$ is a function of the combination $z = \tau + i\sigma$. In the same way, at $x = -1$ the exponent of $\psi_\pm$ becomes anti-holomorphic as desired.

Now for the left ALP, the Baker-Akhiezer eigenvectors, denoted by $\tilde{\psi}_\pm(x, z, \bar{z})$, are given by

$$\tilde{\psi}_+(x;\tau,\sigma) = \begin{pmatrix} c_1^- \exp\left(\frac{i\sigma}{2\pi}\int_{0^+}^x dp + \frac{\tau}{2\pi}\int_{0^+}^x dq\right) \\ c_2^- \exp\left(\frac{i\sigma}{2\pi}\int_{0^-}^x dp + \frac{\tau}{2\pi}\int_{0^-}^x dq\right) \end{pmatrix}, \tag{7.1.22}$$

$$\tilde{\psi}_-(x;\tau,\sigma) = \tilde{\psi}_+(\hat{\sigma}x;\tau,\sigma)\,, \tag{7.1.23}$$

where the notations are similar and should be self-explanatory.

We will be interested in the case where the branch cut runs between u and its complex conjugate $\bar{u}$ on the spectral curve. Such a cut is described by a factor of the form

$$y(x) \equiv \sqrt{(x-u)(x-\bar{u})}\,. \tag{7.1.24}$$

We define the branch of $y(x)$ to be such that the sign of $y(x)$ is $+1$ at $x = 1^+$. Then $p(x)$

and $q(x)$ satisfying the prescribed analyticity properties are fixed to be

$$p(x) = -2\pi\kappa y(x)\left(\frac{1}{|1-u|}\frac{1}{x-1} + \epsilon\frac{1}{|1+u|}\frac{1}{x+1}\right), \tag{7.1.25}$$

$$q(x) = -2\pi\kappa y(x)\left(\frac{1}{|1-u|}\frac{1}{x-1} - \epsilon\frac{1}{|1+u|}\frac{1}{x+1}\right), \tag{7.1.26}$$

$$\epsilon = \begin{cases} +1 & \text{for} \quad |\mathrm{Re}\, u| > 1 \\ -1 & \text{for} \quad |\mathrm{Re}\, u| < 1 \end{cases}. \tag{7.1.27}$$

Here we fixed $p(x)$ and $q(x)$ such that they vanish at the branch points although the analyticity properties only determine the differential dp and dq. This choice is suitable for the purpose of this chapter since the solutions to the ALP in the Pohlmeyer gauge. The forms of $p(x)$ and $q(x)$ depend on whether the cut is placed to the right or to the left of $x = 1$. Substituting these forms into the formulas for $\psi_\pm$ and $\tilde{\psi}_\pm$ we get the one-cut solutions for the ALP.

Reconstruction formula

Let us now describe the second step, the reconstruction of the solutions of the equations of motion from the Baker-Akhiezer vectors. Although this has been discussed in the literature [41–43], we present below a more transparent formula. Let us form a 2×2 matrix Ψ in terms of the two independent Baker-Akhiezer column vectors $\psi_\pm$ satisfying the right ALP as $\Psi = (\psi_+\, \psi_-)$ and consider the quantity

$$\tilde{\Psi} \equiv \mathbb{Y}\Psi\,. \tag{7.1.28}$$

Then, by using the definitions $l_z = \partial\mathbb{Y}\mathbb{Y}^{-1}$ and $j_z = \mathbb{Y}^{-1}\partial\mathbb{Y}$, we can easily show that

$$\left(\partial + \frac{x l_z}{1-x}\right)\tilde{\Psi} = \mathbb{Y}\left(\partial + \frac{j_z}{1-x}\right)\Psi = 0\,, \tag{7.1.29}$$

$$\left(\bar{\partial} - \frac{x l_{\bar{z}}}{1+x}\right)\tilde{\Psi} = \mathbb{Y}\left(\partial + \frac{j_{\bar{z}}}{1+x}\right)\Psi = 0\,. \tag{7.1.30}$$

If we express $\tilde{\Psi}$ in terms of two column vectors $\tilde{\psi}_\pm$ as $\tilde{\Psi} = (\tilde{\psi}_+\, \tilde{\psi}_-)$, the above equations show that $\tilde{\psi}_\pm$ are actually two independent solutions to the left ALP. This means that there exist solutions $\psi_\pm$ and $\tilde{\psi}_\pm$ to the right and the left ALP respectively so that $\mathbb{Y}$ can be expressed as

$$\mathbb{Y} = \tilde{\Psi}\Psi^{-1}\,. \tag{7.1.31}$$

This general relation by itself, however, is not useful since even if we provide a solution Ψ explicitly, finding $\tilde{\Psi}$ which satisfies (7.1.31) tantamounts to finding $\mathbb{Y}$ itself. Now the formula

(7.1.31) turns into a genuine reconstruction formula when we consider the special values of the spectral parameter x. If we set $x = 0$, it is evident from the form of ALP redisplayed above in (7.1.29) and (7.1.30) that the left ALP equations for $\tilde{\Psi}$ reduce to $\partial\tilde{\Psi} = \bar{\partial}\tilde{\Psi} = 0$, and hence $\tilde{\Psi}(x = 0)$ becomes a constant matrix. Therefore the solution $\mathbb{Y}$ is reconstructed from the right ALP solution Ψ as $\mathbb{Y}(z, \bar{z}) = \tilde{\Psi}(x = 0)\Psi^{-1}(z, \bar{z}; x = 0)$, where the constant matrix $\tilde{\Psi}(x = 0)$ represents the freedom of making a global transformation from left. Similarly, by setting $x = \infty$, we can make the right ALP equations trivial, namely $\partial\Psi = \bar{\partial}\Psi = 0$. Then $\Psi(x = \infty)$ becomes a constant matrix and $\mathbb{Y}$ can be reconstructed from the left ALP solution $\tilde{\Psi}$ as $\mathbb{Y}(z, \bar{z}) = \tilde{\Psi}(z, \bar{z}; x = \infty)\Psi^{-1}(x = \infty)$. Summarizing, we have two types of simple reconstruction formulas

$$\mathbb{Y}(z, \bar{z}) = \tilde{\Psi}(0)\Psi^{-1}(z, \bar{z}; 0)\,, \tag{7.1.32}$$

$$\mathbb{Y}(z, \bar{z}) = \tilde{\Psi}(z, \bar{z}; \infty)\Psi^{-1}(\infty)\,. \tag{7.1.33}$$

By using the reconstruction formula given above, one can write down the general basic one-cut solution explicitly. It can be written in the form [40, 41]

$$\mathbb{Y} = \begin{pmatrix} \cos\frac{\theta_0}{2} e^{\nu_1\tau + im_1\sigma} & \sin\frac{\theta_0}{2} e^{\nu_2\tau + im_2\sigma} \\ -\sin\frac{\theta_0}{2} e^{-\nu_2\tau - im_2\sigma} & \cos\frac{\theta_0}{2} e^{-\nu_1\tau - im_1\sigma} \end{pmatrix}, \tag{7.1.34}$$

where the parameters ν_i, m_i and θ_0 must satisfy the following conditions expressing the equations of motion and the Virasoro conditions:

$$\nu_1^2 - m_1^2 = \nu_2^2 - m_2^2\,, \tag{7.1.35}$$

$$4\kappa^2 = (\nu_1^2 + m_1^2)\cos^2\frac{\theta_0}{2} + (\nu_2^2 + m_2^2)\sin^2\frac{\theta_0}{2}\,, \tag{7.1.36}$$

$$\nu_1 m_1 \cos^2\frac{\theta_0}{2} + \nu_2 m_2 \sin^2\frac{\theta_0}{2} = 0\,. \tag{7.1.37}$$

Applying the reconstruction formula (7.1.32) with the constant matrix $\tilde{\Psi}(0)$ taken to be the identity matrix and using the form of ψ_+ given in (7.1.18), we easily find that the parameters m_i and ν_i can be expressed in terms of $p(x)$ and $q(x)$ as

$$m_1 = \frac{1}{2\pi}\int_{0^+}^{\infty^+} dp\,, \qquad \nu_1 = \frac{1}{2\pi}\int_{0^+}^{\infty^+} dq\,, \tag{7.1.38}$$

$$m_2 = \frac{1}{2\pi}\int_{0^+}^{\infty^-} dp\,, \qquad \nu_2 = \frac{1}{2\pi}\int_{0^+}^{\infty^-} dq\,. \tag{7.1.39}$$

Left and right charges

The right and the left Nöether charges R and L can be computed directly from the solution (7.1.34) and are given in terms of the parameters ν_i, m_i and θ_0 in a universal manner as

$$\frac{R}{\sqrt{\lambda}} = \frac{1}{2}\left(-\nu_1 \cos^2\frac{\theta_0}{2} + \nu_2 \sin^2\frac{\theta_0}{2}\right), \tag{7.1.40}$$

$$\frac{L}{\sqrt{\lambda}} = \frac{1}{2}\left(-\nu_1 \cos^2\frac{\theta_0}{2} - \nu_2 \sin^2\frac{\theta_0}{2}\right). \tag{7.1.41}$$

Explicit expressions of R and L in terms of the position of the cut are given in Appendix C.1.1. As a result, we find that the charges R and L are positive irrespective of the position of the cut. This means that they should be regarded not as the charges themselves but as their *absolute magnitudes*. On the other hand, the relative magnitude of R and L depends on the position of the cut as

$$R < L \qquad \text{for} \quad |\mathrm{Re}\, u| > 1\,, \tag{7.1.42}$$

$$R > L \qquad \text{for} \quad |\mathrm{Re}\, u| < 1\,. \tag{7.1.43}$$

In section 7.3.4, we will see that the difference in the relative magnitude corresponds to the difference of the class of vertex operators for which the solution is the saddle point of the two-point function.

7.1.4 Action-angle variables and infinite-gap solutions

Let us now discuss the action-angle variables which we will utilize later in section 7.3 to compute the contribution from the wave functions. The action-angle variables for the string on S^3-subspace was first constructed in [41, 43] by employing the so-called Sklyanin's separation of variables [94]. The discussion below will closely follow such works. However, there is an important difference. While the works [41, 43] focused exclusively on the solutions constructible by the finite-gap method, which we reviewed in the previous subsection, we shall deal with an enlarged category of solutions which have an infinite number of cusp-like points but no node-like points. We will refer to such solutions as "infinite-gap" solutions. We exclude the presence of node-like points in the above definition because such a point can be universally described by shrinkage of a branch cut between two cusp-like points. The framework of infinite gap solutions is extremely important and useful in controlling the complete degrees of freedom of the string. Of course all the other solutions, including the finite gap solutions discussed in the previous subsection, can be obtained by certain degeneration limits[6] of such infinite gap solutions.

[6]Details of the limiting procedure will be discussed in section 7.1.5.

Now let us describe the Sklyanin's method, as applied to a string in S^3. It is a powerful method for constructing canonically conjugate variables and is known to be applicable to a wide variety of integrable systems possessing Lax representation. The main object of concern is again the Baker-Akhiezer vector, which is the eigenvector ψ of the monodromy matrix Ω and satisfies the eigenvalue equation of the form

$$\Omega(x;\tau,\sigma)\psi(x;\tau,\sigma) = e^{i\hat{p}(x)}\psi(x;\tau,\sigma)\,. \tag{7.1.44}$$

Actually, it is of crucial importance to consider the *normalized Baker-Akhiezer vector* $h(x;\tau)$, defined to be proportional to $\psi(x;\tau,\sigma=0)$ and normalized by the condition

$$n\cdot h = n_1 h_1 + n_2 h_2 = 1\,, \tag{7.1.45}$$

$$h = \begin{pmatrix} h_1 \\ h_2 \end{pmatrix}\,. \tag{7.1.46}$$

The constant vector $n = (n_1\,, n_2)^t$ is called the *normalization vector* and will be determined later in section 7.3 from the consideration of global symmetry property. At present, however, it can be chosen arbitrarily. It is known that for a finite gap solution associated to a genus g algebraic curve the normalized Baker-Akhiezer vector has $g+1$ poles as a function of x. By contrast, for an infinite gap solution of our interest it has infinite number of poles. We will denote the positions of these poles on the spectral curve by $\{\gamma_1, \gamma_2, \cdots\}$. Since the monodromy matrix Ω is constructed out of the string variables, through the relation (7.1.44) the positions of the poles γ_i on the spectral curve as well as the quasi-momentum at these poles $p(\gamma_i)$ become dynamical variables. As described in [41, 43], it turns out that the variables $(z(\gamma_i)\,, -ip(\gamma_i))$, where z is the Zhukovsky variable given in (3.2.55) and p is the quasi-momentum, form canonically conjugate pairs satisfying the following Poisson bracket relations

$$\{z(\gamma_i)\,, -ip(\gamma_j)\} = \delta_{ij}\,, \tag{7.1.47}$$

$$\{z(\gamma_i)\,, z(\gamma_j)\} = \{p(\gamma_i)\,, p(\gamma_j)\} = 0\,. \tag{7.1.48}$$

This shows that the filling fractions S_i defined previously provide the action variables of the system. Since the derivation of the Poisson bracket (7.1.48) is technically complicated, we will not write it down in this thesis. Instead, we describe in detail the construction of the action-angle variables in a related simpler system, the Landau-Lifshitz model, in Appendix B, to illustrate the basic logic.

To construct the angle variables ϕ_i conjugate to S_i, we need to find the generating function $F(S_i\,, z(\gamma_i))$ which provides the canonical transformation from the pair $(z(\gamma_i)\,, -ip(\gamma_i))$ to

(ϕ_i, S_i). Such a function is defined by the following properties:

$$\frac{\partial F}{\partial z(\gamma_i)} = -ip(\gamma_i)\,, \tag{7.1.49}$$

$$\frac{\partial F}{\partial S_i} = \phi_i\,. \tag{7.1.50}$$

In the present context, the first equation should be viewed as the definition of F, while the second equation should be regarded as the definition of the angle variables ϕ_i. Therefore, to determine F, we need to integrate the first equation with S_i's fixed. Since the filling fractions are given by the integrals of pdz along various cycles on the spectral curve, fixing all the filling fractions is equivalent to fixing the functional form of $p(x)$. Therefore, the integration can be performed as

$$F(S_i\,, z(\gamma_i)) = -i\sum_i \int_{z(x_0)}^{z(\gamma_i)} p(x')dz'\,. \tag{7.1.51}$$

The initial point of the integration x_0 on the spectral curve can be chosen arbitrarily. A change of x_0 can be absorbed by the change of overall normalization of the wave function. Similarly, a possible integration constant in F, which may depend only on S_i, can be ignored as it can also be absorbed in the normalization of the wave function.

Next we compute $\phi_i = \partial F/\partial S_i$. This requires changing the value of S_i with all the other filling fractions fixed. This is equivalent to adding to pdz a one-form whose period integral along a-cycles is nonvanishing only for a_i. Such a one-form should be proportional to a normalized holomorphic differential ω_i, which satisfies the following properties:

$$\oint_{a_j} \omega_i = \delta_{ij}\,. \tag{7.1.52}$$

Using such ω_i, the partial derivative $\partial F/\partial S_i$ can be expressed as[7]

$$\phi_i = \frac{\partial F}{\partial S_i} = 2\pi\sum_j \int_{x_0}^{\gamma_j} \omega_i\,. \tag{7.1.53}$$

This is an appropriate generalization of the so-called *Abel map*, which normally maps an algebraic curve to its Jacobian variety, for non-algebraic curves[8].

We have now obtained an infinite set of action-angle variables, which satisfy the following canonical form of Poisson bracket relations:

$$\{\phi_i\,, S_j\} = \delta_{ij}\,, \qquad \{\phi_i\,, \phi_j\} = \{S_i\,, S_j\} = 0\,. \tag{7.1.54}$$

[7]Here and hereafter, we regard ω_i as a differential in x.

[8]When restricted to finite gap solutions, this expression exactly reproduces the definition of the Abel map.

However, there is an important caveat: Since the above construction is based purely on the right current j, which is invariant under the left global transformation $\mathbb{Y} \to V_L \mathbb{Y}$, the angle variable conjugate to the right global charge S_0 cannot be obtained by this method[9]. To obtain such a variable, we need to make use of the left current l. In an entirely similar manner, we can construct from the left current a set of angle variables $\tilde{\phi}_i$, which satisfy

$$\{\tilde{\phi}_i \, , S_j\} = \delta_{ij} \, , \qquad \{\tilde{\phi}_i \, , \tilde{\phi}_j\} = \{S_i \, , S_j\} = 0 \, . \tag{7.1.55}$$

The set $\{\tilde{\phi}_i\}$ contains the desired angle variable $\tilde{\phi}_0$ conjugate to S_0. However, it does not contain $\tilde{\phi}_\infty$, which is conjugate to S_∞. Therefore, to construct a complete set of angle variables, we must utilize the two individually incomplete sets, $(\phi_{i\neq 0,\infty} \, , \phi_\infty)$ and $(\tilde{\phi}_0 \, , \tilde{\phi}_{i\neq 0\, ,\infty})$. A naïve guess would be to use $(\phi_{i\neq 0\, ,\infty} \, , \phi_\infty)$ plus $\tilde{\phi}_0$. This, however, is not guaranteed to be correct since ϕ_i and $\tilde{\phi}_0$ do not commute in general. Nevertheless, we can use $(\tilde{\phi}_0 \, , \phi_{i\neq 0,\infty} \, , \phi_\infty)$ as if they constituted a complete set of angle variables, for the following reason. Suppose we find the "correct" angle variable ϕ_0 satisfying the following properties:

$$\{\phi_0 \, , S_0\} = 1 \, , \qquad \{\phi_0 \, , S_i\} = \{\phi_0 \, , \phi_i\} = 0 \qquad (i \neq 0) \, . \tag{7.1.56}$$

Then, from the Poisson bracket relations, we immediately see that the difference $\delta\phi_0 = \phi_0 - \tilde{\phi}_0$ commutes with all the action variables, namely $\{\delta\phi_0 \, , S_i\} = 0$ for all i. This means that it commutes with the worldsheet Hamiltonian, which is made up of the action variables S_i, and hence is conserved. Therefore $\delta\phi_0$ merely causes a constant shift of the angle variable and it can be absorbed in the normalization of the wave function. Thus, in practice, we can use $(\tilde{\phi}_0 \, , \phi_{i\neq 0\, ,\infty} \, , \phi_\infty)$ as a set of angle variables.

7.1.5 From infinite gap to finite gap

Let us next discuss the relation between the materials discussed in the two preceding sections, the finite gap solutions and the infinite gap solutions, and explain how the method of construction of the action-angle variables developed above for infinite gap solutions can be applied to the case of the familiar finite gap solutions, which describe two-point functions of various string states. We shall see below that this procedure requires some careful considerations.

As is well-known, for a finite gap solution of genus g, there are $g+2$ non-vanishing filling fractions $(S_0 \, , S_\infty ; S_1 \, , \cdots , S_g)$ and the associated normalized Baker-Akhiezer vector has $g+1$ dynamical poles. To obtain such a solution from an infinite gap solution, we must first set an infinite number of filling fractions to zero, except for $(S_0 \, , S_\infty ; S_1 \, , \cdots , S_g)$, by

[9] In other words, the motion of such an angle variable is completely decoupled from the rest and cannot be seen from j.

shrinking the corresponding cuts into node-like points. Through this degeneration process, the infinitely many poles of the Baker-Akhiezer vectors must somehow "disappear", leaving $g+1$ dynamical poles of the finite gap solutions. To understand what really happens, it is helpful to study similar degeneration limit for known finite gap solutions [41]. By closely analyzing the motion of the poles in such a degeneration limit, we find that actually the unwanted poles do not disappear. Instead, they cease to be dynamical. These nondynamical poles cannot be seen if we use a solution with lower genus from the beginning. They can be seen only through the degeneration limit from a higher genus solution. This observation strongly suggests that, to obtain a complete set of action-angle variables, we should start from an infinite gap solution, construct the angle variables from infinitely many poles and then consider the limit of those angle variables. Carrying out this procedure, we can trace all the poles including non-dynamical ones and obtain the following expression for the angle variables of a finite gap solution with genus g:

$$\phi_i = 2\pi \sum_{j=1}^{g+1} \int_{x_0}^{\gamma_j} \omega_i + 2\pi \sum_{J} \int_{x_0}^{\gamma_J} \omega_i \,. \tag{7.1.57}$$

Here, γ_j's denote the dynamical poles, while γ_J's signify the non-dynamical ones.

Let us discuss the nature of the contributions from the non-dynamical poles. A detailed argument on the motion of the poles given in Appendix E of [42] shows that non-dynamical poles are trapped either at node-like points or at cusp-like points. Since such points are discretely placed on the spectral curve, the positions of the non-dynamical poles γ_J do not change under any continuous deformations of the solution which keeps the spectral curve intact. In particular, they do not change under the (continuous) global symmetry transformations. As we shall discuss later, the only necessary information for the evaluation of the correlation functions is the shift of angle variables under such global transformations. Thus, in practice, the second term in (7.1.57) gives the same constant contribution, which can be absorbed into the normalization of the wave function. Consequently, the angle variables for the finite gap solution can be effectively defined without the second term[10] as

$$\phi_i = 2\pi \sum_{j=1}^{g+1} \int_{x_0}^{\gamma_j} \omega_i \,. \tag{7.1.58}$$

This expression is quite convenient in practice since we do not have to consider the degeneration limits from the infinite gap solutions. Thus we will use (7.1.58) instead of (7.1.57) as the definition of angle variables for finite gap solutions when we evaluate the correlation functions later in section 7.3.

[10]The expression (7.1.58) coincides with the one derived in [41, 43] for finite gap solutions. There it was derived within the finite dimensional subspace of the total phase space, appropriate for finite gap solutions with fixed genus. Our discussion in this section corroborates the result of [41, 43] from a more general point of view.

7.1.6 Structure of three-pronged solutions

The method of construction of the angle variables given above is for finite gap solutions, which serve as saddle point configurations for two-point functions. Since we are interested in computing three-point functions as well, we must discuss how the method can be generalized to such cases.

Before giving the simple procedure, which turns out to require only the knowledge of the local behavior of the saddle point solution in the vicinity of each vertex insertion point, it is instructive to first clarify the difference of the analytic structures between two-pronged and three-pronged solutions[11] in the framework of the finite gap method.

Although a solution with three prongs is much more difficult to construct compared to the corresponding two-pronged solution, the behavior around each prong should be the same if it is generated by the same vertex operator. This implies that the spectral curve constructed from the local monodromy matrix should be the same as that of the two-point solution. Therefore the knowledge of the spectral curve alone cannot distinguish between two-point and three-point solutions.

What can distinguish between the two is the number of dynamical poles of the normalized Baker-Akhiezer vector. In the case of a finite gap solution of genus g relevant for a two-point function, there are $g+2$ non-vanishing filling fractions, which are dictated by the spectral curve, and $g+1$ dynamical poles of the normalized Baker-Akhiezer vector. The reconstruction formula then tells us that these two sets of data determine the (two-point) solution uniquely, up to a global symmetry transformation. What this implies is that for more general finite gap solutions, relevant for three-point functions etc., the number of dynamical poles can be larger than $g+1$, while the number of branch cuts of finite length on the spectral curve remains to be $g+1$. This possibility has been overlooked until quite recently and is first utilized in [109] to reconstruct the solution which describes a correlation function of a circular Wilson loop and a half-BPS operator from the algebraic curve perspective[12]. The easiest way to obtain solutions with more than $g+1$ dynamical poles is to take the degeneration limit of the infinite gap solutions. Although only $g+1$ poles remained dynamical in the special degeneration limit considered in section 7.1.5, more general limits can be considered in which more than $g+1$ dynamical poles survive. An example of such a procedure will be explained later in this subsection. In principle, it is even possible for the Baker-Akhiezer vector to have an infinite number of poles when the spectral curve has only a finite number

[11] The discussion to follow is applicable to higher-prong solutions as well.

[12] In [109], the authors reconstructed the solution by requiring the existence of two distinct poles in the Baker-Akhiezer vector. Since the spectral curve of this solution has no branch cuts with finite length, this certainly goes beyond the ordinary finite gap construction.

of branch cuts. This phenomenon is demonstrated for a string in flat spacetime explicitly in Appendix C.4.

An important feature of the solution obtained by such nontrivial degeneration is that its monodromy matrix is not proportional to the identity matrix but takes the form of the Jordan block at node-like points obtained by the degeneration. The reason is quite simple. As we have seen in section 3.2.2, the monodromy matrix is always of the Jordan-block form at the branch points. If we take nontrivial degeneration limit, such a property is retained even after the branch points coalesces into a node-like point[13]. As we will later see in section 7.4.1, the monodromy matrix for the three-point function take the form of the Jordan block at *all the node-like points*. This means that one must necessarily start from an infinite gap solution to obtain the solution for the three-point functions.

Despite the existence of important structural differences between two- and multi-pronged solutions as analyzed above, we now emphasize that as far as the evaluation of the angle variables needed to compute the contribution of the wave functions is concerned, only the local asymptotic behavior of the solution near the vertex insertion point suffices. This should indeed be the case because the vertex operator is defined locally and it produces the local source term for the equations of motion (6.1.3). Therefore possible local behavior around such a point is the same for two and higher-point functions[14]. More explicitly, the crucial information about the angle variables of the three-point solutions needed for the evaluation of the wave functions can be extracted from the behavior of the angle variables for two-point functions under suitable global symmetry transformations.

An example of nontrivial degeneration

To understand what really happens in the aforementioned degeneration processes discussed above, we shall now discuss the degeneration from $g = 1$ (two-cut) to $g = 0$ (one-cut). The Baker-Akhiezer vector for general finite-gap solutions are given by the following expressions

[13] We can check this statement by analyzing the explicit degeneration process discussed later in this subsection although we will not demonstrate it in this thesis.

[14] Indeed we can show, by using the explicit examples discussed below, that the aforementioned nontrivial degeneration procedure does not modify the asymptotic behavior in the vicinity of the vertex operator.

containing ratios of Riemann theta functions $\Theta(\boldsymbol{z})$ in addition to the exponential part:

$$\psi_1 = h_+(x)\frac{\Theta(\mathcal{A}(x)+k\sigma-i\omega\tau-\zeta_{\gamma_-(0)})\Theta(\mathcal{A}(\infty^+)-\zeta_{\gamma_-(0)})}{\Theta(\mathcal{A}(x)-\zeta_{\gamma_-(0)})\Theta(\mathcal{A}(\infty^+)+k\sigma-i\omega\tau-\zeta_{\gamma_-(0)})}\exp\left(\frac{i\sigma}{2\pi}\int_{\infty^+}^{x}dp+\frac{\tau}{2\pi}\int_{\infty^+}^{x}dq\right), \tag{7.1.59}$$

$$\psi_2 = h_-(x)\frac{\Theta(\mathcal{A}(x)+k\sigma-i\omega\tau-\zeta_{\gamma_+(0)})\Theta(\mathcal{A}(\infty^-)-\zeta_{\gamma_+(0)})}{\Theta(\mathcal{A}(x)-\zeta_{\gamma_+(0)})\Theta(\mathcal{A}(\infty^-)+k\sigma-i\omega\tau-\zeta_{\gamma_+(0)})}\exp\left(\frac{i\sigma}{2\pi}\int_{\infty^-}^{x}dp+\frac{\tau}{2\pi}\int_{\infty^-}^{x}dq\right). \tag{7.1.60}$$

As it is not our purpose here to review the details of the finite gap construction, below we will only explain the minimum of the ingredients and refer the reader to a review article such as [41].

For a $g=1$ two-cut solution, the Riemann theta function $\Theta(\boldsymbol{z})$ reduces to the elliptic theta function $\theta(z)$ defined by

$$\theta(z)\equiv\sum_{m\in\mathbb{Z}}\exp\left(imz+\pi i\Pi m^2\right), \tag{7.1.61}$$

where Π is the period given by the integral of the holomorphic differential w over the b-cycle of the torus

$$\Pi=\oint_b w\,. \tag{7.1.62}$$

As usual, w is normalized by the integral over the a-cycle as $\oint_a w=1$. $\mathcal{A}(x)$ appearing in the argument of the Θ-functions is the Abel map defined by

$$\mathcal{A}(x)=2\pi\int_{\infty^+}^{x}w\,. \tag{7.1.63}$$

$h_\pm(x)$ are normalization constants and k and ω are the "momentum" and the "energy" defined by the integrals

$$k\equiv\frac{1}{2\pi}\oint_b dp\,,\qquad \omega\equiv\frac{1}{2\pi}\oint_b dq\,. \tag{7.1.64}$$

A quantity of importance is the constant $\zeta_{\gamma_\pm(0)}$ defined by

$$\zeta_{\gamma_\pm(0)}\equiv\mathcal{A}(\gamma_\pm(0))+\mathcal{K}\,, \tag{7.1.65}$$

In this formula, $\mathcal{K}$ is the "vector of Riemann constants", which for a torus is simply a number proportional to the period Π as[15]

$$\mathcal{K}=\pi\Pi\,. \tag{7.1.66}$$

[15]For its definition for a general genus g surface, see for example [110].

Finally $\gamma_\pm(0)$ are certain points[16] on the Riemann surface, which determine the initial conditions for the solution.

Let us now study what happens when we pinch the a-cycle. In order to keep the normalization condition $\oint_a w = 1$ intact, w must behave near the position of the infinitesimal cut x_c as

$$w \sim \begin{cases} \frac{1}{2\pi i}\frac{1}{x-x_c} & \text{for } x \text{ on the first sheet} \\ -\frac{1}{2\pi i}\frac{1}{x-x_c} & \text{for } x \text{ on the second sheet} \end{cases} . \tag{7.1.67}$$

This means that the imaginary part of the period Π defined by the integral over the b-cycle approaches positive infinity in the manner

$$\Pi = \oint_b w \sim \frac{1}{2\pi i}\int_{x_c-\epsilon}^{x_c+\epsilon}\frac{dx}{x-x_c} \sim -\frac{i}{\pi}\ln\epsilon \to +i\infty\,. \tag{7.1.68}$$

Now writing the θ-function as

$$\theta(z) = \sum_{m\in\mathbb{Z}} \exp\left(imz + \pi i(\mathrm{Re}\,\Pi)m^2\right)\cdot\exp\left(-\pi \mathrm{Im}\,\Pi m^2\right)\,, \tag{7.1.69}$$

we see that the last factor vanishes as $\mathrm{Im}\,\Pi \to \infty$, except for $m = 0$. Therefore in this limit we get $\theta(z) \to 1$ and one gets the usual genus 0 solution with only the exponential part.

Now if we identify $z = k\sigma - i\omega\tau$ in the formulas for ψ_i given in (7.1.59) and (7.1.60), the arguments of the θ-functions containing z are actually of the form $z - a$, with a constant shift a given by $a = \zeta_{\gamma^\pm(0)} + \cdots$. What is important is that $\zeta_{\gamma^\pm(0)}$ diverges as we pinch the a-cycle. First, obviously $\mathrm{Im}\,\mathcal{K}$ diverges as $\pi\mathrm{Im}\,\Pi$. Second, if $\gamma_\pm(0)$ is at the position of the shrunk cut x_c, $\mathrm{Im}\,\mathcal{A}(\gamma_\pm(0))$ diverges just like $\pi\mathrm{Im}\,\Pi$:

$$\mathcal{A}(\gamma_\pm(0)) = 2\pi\int_{\infty^+}^{x_c+\epsilon} dw \sim 2\pi\frac{1}{2\pi i}\ln\epsilon \sim i\pi\mathrm{Im}\,\Pi \to i\infty\,. \tag{7.1.70}$$

Since $\mathcal{A}(\gamma_\pm(0))$ is finite otherwise, we must distinguish two cases: case (a) $\mathrm{Im}\,\zeta_{\gamma^\pm(0)} \sim 2\pi\mathrm{Im}\,\Pi$ for $\gamma_{\pm(0)} = x_c$ and case (b) $\mathrm{Im}\,\zeta_{\gamma^\pm(0)} \sim \pi\mathrm{Im}\,\Pi$ for $\gamma_{\pm(0)} \neq x_c$. Therefore let us write $a = l\mathrm{Im}\,\pi\Pi + c$, where $l = 2$ or $l = 1$ and c is a finite constant. Then the θ-function with this shift can be written as

$$\theta(z-a) = \sum_{m\in\mathbb{Z}} \exp\left(im(z - \pi\mathrm{Re}\,\Pi - c) + \pi i(\mathrm{Re}\,\Pi)m^2\right)\cdot\exp\left(-\pi\mathrm{Im}\,\Pi(m^2 - lm)\right)\,. \tag{7.1.71}$$

First consider the case (a). It is easy to see that terms with negative m all vanish in the limit $\mathrm{Im}\,\Pi \to \infty$. On the other hand, the terms with $m = 0$ and $m = 2$ are finite and those

[16] Precisely speaking, $\gamma_\pm(0)$ are certain divisors $\gamma_\pm(t)$ depending on the infinite set of higher times $t = (t_0, t_1, t_2, \ldots)$ evaluated at $t = 0$. For a detailed definition, see [41].

with $m \geq 3$ vanish in the degeneration limit while the single term with $m = 1$ diverges. In other words,

$$\theta(z-a) \to \hat{C} e^{iz}\,, \qquad \hat{C} \to \infty\,. \tag{7.1.72}$$

As the θ-functions occur in pairs in the numerator and the denominator in ψ_i, their ratio goes to a z-independent finite constant in the degeneration limit and we get back the usual $g = 0$ one-cut solution. In fact, by repeating this type of process, one can produce a finite gap solution describing a two-point function from an infinite gap solution.

Now the truly nontrivial case is the case (b). For $l = 1$, two terms in the series survive in the limit $\mathrm{Im}\,\Pi \to \infty$, namely $m = 0$ and $m = 1$. Therefore we obtain a non-trivial function of the form

$$\theta(z-a) \to 1 + C e^{iz} = 1 + C e^{ik\sigma + \omega\tau}\,, \tag{7.1.73}$$

where C is a constant. In particular, this function can vanish at certain points, the number of which depend on the magnitude of k. Such a θ-function in the denominator of the expressions for ψ_i gives rise to additional simple poles on the worldsheet. Such additional poles are necessary to construct the solution with several prongs, including the ones which correspond to the three-point functions. However, precisely speaking, the singularities constructed above do not carry any charges because the solution is obtained without changing the form of $p(x)$. Therefore, we expect that the monodromy around them is trivial. Thus, as far as we consider the degeneration process in which only a *finite* number of cuts shrinks, one cannot obtain the solution for the three-point function, which has nontrivial monodromy around the third puncture. The situation will change if we consider the limit where an *infinite* number of cuts degenerate. In such a limit, we expect an infinite number of monodromy-free singularities pile up and can produce nontrivial monodromy. Although it is technically difficult to justify this statement, we can at least say that a similar phenomenon happens in the case of the string in the flat space, which is discussed in Appendix C.4. This provides a further reason why the solutions with *infinite* cuts and their degeneration are of extreme importance when we consider three-point functions.

Before closing this section, let us make one additional remark. The above analysis shows that the existence of additional singularities are quite common if we consider infinite gap solutions and their degeneration. This implies that the solution for the three-point function may also have such (monodromy-free) singularities in addition to the ones which correspond to the vertex operators. At the end of section 7.6.5, we discuss that the existence of such additional singularities can modify the contours of the integrals which express the three-point functions and may play an important role in the interpretation of our final result.

7.1.7 Preliminary remarks on three-point functions

Let us now discuss the general properties of the three-point functions and clarify the notations and the assumptions used in the subsequent analysis.

In the case of three-point functions, the saddle-point configuration is given by a spherical worldsheet with three vertex operators. The points at which the vertex operators are inserted, z_1, z_2 and z_3, are also referred to as punctures. Since the contribution from the action and the contribution from the vertex operators are separately divergent, we regularize them by cutting out a small disk of radius ϵ_i at each puncture and then evaluate the following two contributions (see Figure 7.1.1):

1. The action outside the disks.

2. The wave functions defined on the boundaries of the disks.

As we can perform the computation of the $EAdS_3$ part and the S^3 part separately, the three-point functions computed in this way have the following structure:

$$\langle \mathcal{V}_1 \mathcal{V}_1 \mathcal{V}_3 \rangle \sim \exp\left(F_{S^3} + F_{EAdS_3}\right) , \tag{7.1.74}$$

where

$$F_{S^3} = \mathcal{F}_{\text{action}} + \mathcal{F}_{\text{vertex}} , \tag{7.1.75}$$

$$F_{EAdS_3} = \hat{\mathcal{F}}_{\text{action}} + \hat{\mathcal{F}}_{\text{vertex}} . \tag{7.1.76}$$

Here $\mathcal{F}_{\text{action}}$ and $\hat{\mathcal{F}}_{\text{action}}$ denote the regularized contributions from the action whereas $\mathcal{F}_{\text{vertex}}$ and $\hat{\mathcal{F}}_{\text{vertex}}$ denote the regularized contributions from the vertex operators, which are replaced with the wave functions. An assumption we make in the subsequent analysis is that the saddle-point configuration has singularities only at the insertion points of the vertex operators and the rest of the worldsheet is completely smooth. Since a generic classical string solution may have additional singularities as discussed in the previous section, this is indeed an important assumption.

Since there are three punctures on the worldsheet, one can define the monodromy matrix Ω_i for each puncture. The eigenvectors and the eigenvalues of Ω_i are denoted by $i_\pm$ and $e^{\pm i p_i(x)}$ respectively and satisfy the following relation:

$$\Omega_i i_\pm = e^{\pm p_i(x)} i_\pm . \tag{7.1.77}$$

Of crucial importance in the computation of three-point functions are the SL(2,C) invariant product,

$$\langle \psi, \chi \rangle \equiv \det\left(\psi, \chi\right) , \tag{7.1.78}$$

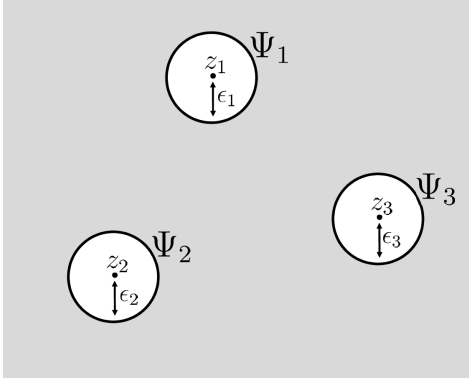

Figure 7.1.1: Regularization of the action and the vertex operators. We cut out a small disk of radius ϵ_i around the puncture z_i. The wave function is evaluated on the small circle whereas the action is evaluated only in the shaded region outside the disks.

of the eigenvectors, $\langle i_\pm, j_\pm \rangle$. In the rest of this chapter, we refer to this skew-product as *Wronskian*. Since the Wronskians are invariant under the gauge transformation, we can use the results in various gauges interchangeably:

$$\langle i_\pm, j_\pm \rangle = \langle \tilde{i}_\pm, \tilde{j}_\pm \rangle = \langle \hat{i}_\pm, \hat{j}_\pm \rangle \,, \tag{7.1.79}$$

where $i_\pm$, $\tilde{i}_\pm$ and $\hat{i}_\pm$ are the eigenvectors in the right connection, the left connection and the Pohlmeyer connection respectively.

For later convenience, let us now fix the normalization of the eigenvectors $i_\pm$. Part of the normalization is determined by the condition for the Wronskian,

$$\langle i_+, i_- \rangle = 1 \,. \tag{7.1.80}$$

However, this cannot fix the normalization completely since we can rescale $i_\pm$ without violating the condition (7.1.80) as $i_+ \to a i_+$ and $i_- \to a^{-1} i_-$. To determine the normalization completely, we will fix the asymptotic behavior of $i_\pm$ around the puncture z_i. For this purpose, it is convenient to use the ALP in the Pohlmeyer gauge, which is invariant under the global transformation. Although the explicit form of the solution for the three-point function is not known, it should be approximated by the solution for the two-point function in the vicinity of the punctures. Therefore, we determine the normalization of each eigenvectors using the explicit form of the eigenvectors for the two-point function as

$$\hat{i}_\pm(x; \tau^{(i)}, \sigma^{(i)}) \to \hat{i}^{\rm 2pnt}_\pm(x; \tau = \tau^{(i)}, \sigma = \sigma^{(i)}) \,, \tag{7.1.81}$$

where $(\tau^{(i)}, \sigma^{(i)})$ is a local coordinate around z_i, defined by

$$\tau^{(i)} + i\sigma^{(i)} = \ln \left(\frac{z - z_i}{\epsilon_i} \right) \,. \tag{7.1.82}$$

The eigenvectors for the two-point function $\hat{i}_{\pm}^{\text{2pnt}}$ are computed using the results in Appendix C.1 as

$$\hat{i}_{+}^{\text{2pnt}}(x;\tau,\sigma) = \begin{pmatrix} \frac{e^{\pi i/8}}{\sqrt{2}} \left(\frac{x-\bar{u}_i}{x-u_i}\right)^{1/4} \left(\frac{\bar{u}_i^2-1}{u_i^2-1}\right)^{1/8} \\ \frac{e^{\pi i/8}}{\sqrt{2}} \left(\frac{x-u_i}{x-\bar{u}_i}\right)^{1/4} \left(\frac{u_i^2-1}{\bar{u}_i^2-1}\right)^{1/8} \end{pmatrix} \exp\left(\frac{q_i(x)\tau + ip_i(x)\sigma}{2\pi}\right), \tag{7.1.83}$$

$$\hat{i}_{-}^{\text{2pnt}}(x;\tau,\sigma) = \begin{pmatrix} \frac{e^{-\pi i/8}}{\sqrt{2}} \left(\frac{x-\bar{u}_i}{x-u_i}\right)^{1/4} \left(\frac{\bar{u}_i^2-1}{u_i^2-1}\right)^{1/8} \\ -\frac{e^{-\pi i/8}}{\sqrt{2}} \left(\frac{x-u_i}{x-\bar{u}_i}\right)^{1/4} \left(\frac{u_i^2-1}{\bar{u}_i^2-1}\right)^{1/8} \end{pmatrix} \exp\left(-\frac{(q_i(x)\tau + ip_i(x)\sigma)}{2\pi}\right), \tag{7.1.84}$$

where u_i and $\bar{u}_i$ are the positions of the branch points of the quasi-momentum for the i-th puncture $p_i(x)$. The conditions, (7.1.81), (7.1.83) and (7.1.84), determine the normalization of $i_{\pm}$ completely. Importantly, the eigenvectors thus normalized transform in the following way when they cross the branch cut[17]:

$$\hat{i}_{+}(x)\Big|_{\text{on 2nd sheet}} = \hat{i}_{-}(x)\Big|_{\text{on 1st sheet}}, \quad \hat{i}_{-}(x)\Big|_{\text{on 2nd sheet}} = -\hat{i}_{+}(x)\Big|_{\text{on 1st sheet}}. \tag{7.1.85}$$

This relation will be used in section 7.4.5 to determine the normalization of the Wronskians.

7.2 The action in terms of Wronskians

Let us now start our study of the three-point functions. In this section, we focus on the contribution of the action for the S^3 part, namely $\mathcal{F}_{\text{action}}$. First, in subsection 7.2.1, we rewrite the action as a boundary contour integral using the Stokes theorem and then apply the generalized Riemann bilinear identity derived in [16] to bring it to a more convenient form. Next we turn in subsection 7.2.2 to the analysis of the WKB expansion of the auxiliary linear problem. We then find that the same contour integrals we used to rewrite the action appear also in the WKB expansion of the Wronskians of the solutions to the ALP. Using this relation, we re-express the action in terms of the Wronskians in subsection 7.2.3. The resultant expression will be used for the explicit evaluation of the contribution of the action in section 7.5.

[17]Note that the extra minus sign is necessary in the second equation of (7.1.85) in order to retain the condition (7.1.80).

7.2.1 Contour integral representation of the action

For the three-point function of our interest, the (regularized) action for the S^3 part of the string is given by

$$S_{S^3} = \frac{\sqrt{\lambda}}{\pi} \int_{\Sigma\backslash\{\epsilon_i\}} d^2z \partial Y_I \bar{\partial} Y_I \,, \tag{7.2.1}$$

where the symbol $\Sigma\backslash\{\epsilon_i\}$ denotes the worldsheet for the three-point function, which is a two-sphere with a small disk of radius ϵ_i cut out at each puncture z_i. In [105] and [111], such worldsheet cut-offs are related to the spacetime cut-off in AdS in order to obtain the spacetime dependence of the correlation functions without introducing the vertex operators. In contrast, as we shall separately take into account the contribution of the vertex operators, ϵ_i's can be taken to be arbitrary in our approach, as long as they are sufficiently small and the same for the S^3 part and the $EAdS_3$ part.

As the action is invariant under the global symmetry transformations, it is natural to express (7.2.1) in terms of the quantities used in the Pohlmeyer reduction. From (7.1.5), we can indeed write

$$S_{S^3} = \frac{\sqrt{\lambda}}{\pi} \int_{\Sigma\backslash\{\epsilon_i\}} d^2z \sqrt{T\bar{T}} \cos 2\gamma \,. \tag{7.2.2}$$

We further rewrite (7.2.2) by introducing the following one-forms:

$$\varpi \equiv \sqrt{T} dz \,, \tag{7.2.3}$$

$$\eta \equiv -\sqrt{\bar{T}} \cos 2\gamma d\bar{z} + \frac{2}{\sqrt{T}} \left(-(\partial\gamma)^2 + \frac{\rho^2}{T} \right) dz \,. \tag{7.2.4}$$

The second term on the right hand side of (7.2.4) is added to make η closed, as one can verify using the relation (7.1.11). With these one-forms, we can re-express the action (7.2.2) as a wedge product of the form

$$S_{S^3} = \frac{i\sqrt{\lambda}}{2\pi} \int_{\Sigma\backslash\{\epsilon_i\}} \varpi \wedge \eta \,, \tag{7.2.5}$$

where an extra prefactor $i/2$ comes from the definition of the volume form, $dz \wedge d\bar{z} = -2i\, d^2z$. Then denoting the integral of $\varpi(z)$ as

$$\Pi(z) = \int_{z_0}^{z} \varpi(z') dz' \,, \tag{7.2.6}$$

the action can be rewritten, using the Stokes theorem, as a contour integral along a boundary $\partial\tilde{\Sigma}$ of a certain region $\tilde{\Sigma}$ (see Figure 7.2.1):

$$S_{S^3} = \frac{i\sqrt{\lambda}}{4\pi} \int_{\tilde{\Sigma}} \varpi \wedge \eta = \frac{i\sqrt{\lambda}}{4\pi} \int_{\tilde{\Sigma}} d\left(\Pi\eta\right) = \frac{i\sqrt{\lambda}}{4\pi} \int_{\partial\tilde{\Sigma}} \Pi\eta \,. \tag{7.2.7}$$

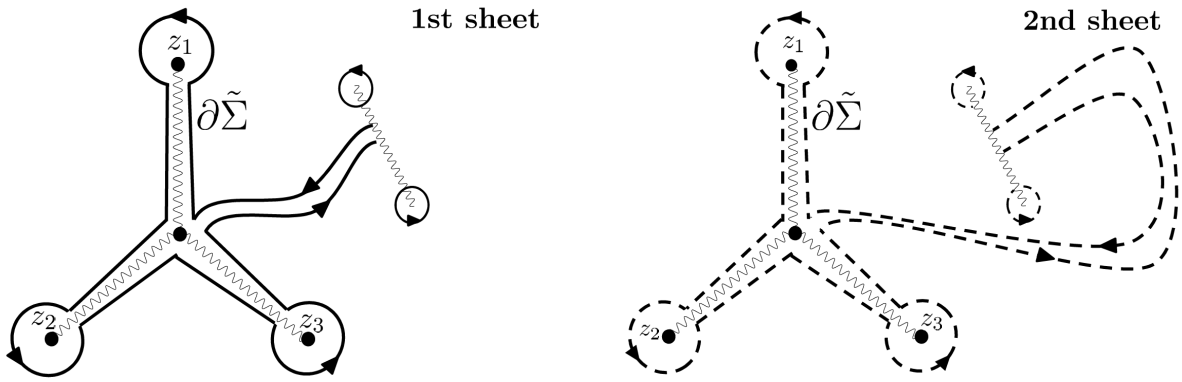

Figure 7.2.1: The boundary $\partial\tilde{\Sigma}$ of the double-cover of the worldsheet $\tilde{\Sigma}$. There are three logarithmic branch cuts attached to the punctures and one square-root branch cut. $\partial\tilde{\Sigma}$ is determined such that the function Π is single-valued on $\tilde{\Sigma}$.

To determine the proper region of integration $\tilde{\Sigma}$, we need to know the analytic structure of $\Pi(z)$, which in turn is dictated by that of $T(z)$. As shown in (3.2.27) in section 3.2.2, the asymptotic behavior of $T(z)$ at each puncture z_i is determined by the spacetime conformal dimension. In the case of three-point functions, this information is sufficiently restrictive to determine $T(z)$ exactly to be of the form

$$T(z) = \left(\frac{\kappa_1^2 z_{12} z_{13}}{z - z_1} + \frac{\kappa_2^2 z_{21} z_{23}}{z - z_2} + \frac{\kappa_3^2 z_{31} z_{32}}{z - z_3} \right) \frac{1}{(z - z_1)(z - z_2)(z - z_3)} , \tag{7.2.8}$$

$$z_{ij} \equiv z_i - z_j \, .$$

From this, one can show that $\Pi(z)$ has three logarithmic branch cuts running from the punctures z_i, and one square-root branch cut connecting two zeros of $T(z)$, to be denoted by t_1 and t_2. Therefore, we should take $\tilde{\Sigma}$ to be the double cover ($y^2 = T(z)$) of the worldsheet Σ with an appropriate boundary $\partial\tilde{\Sigma}$, so that $\Pi(z)$ is single-valued on the whole integration region. In what follows, we will consider the case where the branch cut is located between z_1 and z_3 as depicted in Figure 7.2.1. In such a case, the branch of the square-root of $T(z)$ can be chosen so that it behaves near the punctures on the first sheet as

$$\begin{aligned} \sqrt{T(z)} &\sim \frac{\kappa_i}{z - z_i} \qquad \text{as } z \to z_i \quad (i = 1, 3) \, , \\ &\sim \frac{-\kappa_2}{z - z_2} \qquad \text{as } z \to z_2 \, . \end{aligned} \tag{7.2.9}$$

Although the discussion to follow is tailored for this particular case, the final result for the three-point function, to be obtained in section 7.5, will turn out to be completely symmetric under the permutation of the punctures.

At this point, we shall apply the generalized Riemann bilinear identity (gRBI), derived in [16], to the integral (7.2.7). The gRBI can be derived straightforwardly by evaluating

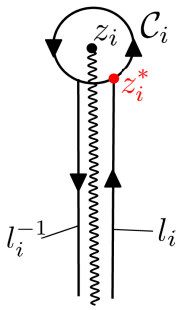

Figure 7.2.2: The portions of the contour we used to explain the generalized Riemann bilinear identity.

the rightmost side (7.2.7). However, as the derivation explained in detail in [16] is lengthy, here we just explain the idea of the derivation. First, notice that the integration contour $\partial\tilde{\Sigma}$ contains a line which approaches the puncture z_i (l_i in Figure 7.2.2) and a line which moves away from the puncture z_i (l_i^{-1} in Figure 7.2.2). Along these lines, which have mutually opposite directions, the one-form η takes exactly the same value while the function Π has different values. The difference of these values is given by the integral of ϖ along the small circle $\mathcal{C}_i$ which encircles the puncture z_i. Therefore the sum of the integrals along these two lines can be computed as

$$\int_{l_i+l_i^{-1}} \Pi\eta = \oint_{\mathcal{C}_i} \varpi \int_{l_i} \eta\,. \tag{7.2.10}$$

Performing a similar analysis for other portions of the contour, we arrive at the following formula:

$$\int_{\tilde{\Sigma}} \varpi \wedge \eta = \mathsf{Local} + \mathsf{Double} + \mathsf{Global} + \mathsf{Extra}\,, \tag{7.2.11}$$

where the definition of each term will be given successively below[18]. The first term, Local, denotes the contribution from the product of contour integrals, each of which is just around the puncture and hence called "local". It is of the form

$$\mathsf{Local} = \sum_i \oint_{\mathcal{C}_i} \varpi \oint_{\mathcal{C}_i} \eta + \sum_{i<j} \left(\oint_{\mathcal{C}_i} \varpi \oint_{\mathcal{C}_j} \eta - (\varpi \leftrightarrow \eta) \right)\,, \tag{7.2.12}$$

where $\mathcal{C}_i$ is a contour encircling the puncture z_i counterclockwise. Here and hereafter, the symbol $(\varpi \leftrightarrow \eta)$ stands for the contribution obtained by exchanging ϖ and η in the preceding

[18]In [105] and [111], the ordinary Riemann bilinear identity was applied to derive an expression similar to (7.2.11) but without the terms Local and Double . In their cases, Local and Double vanish and the use of the ordinary Riemann bilinear identity is justified. On the other hand, these two terms do not vanish in our case and we must use the generalized Riemann bilinear identity.

term. The second term, Double, denotes the double integrals around the punctures given by

$$\mathsf{Double} = -2\sum_i \oint_{\mathcal{C}_i} \eta \int_{z_i^*}^{z} \varpi \,. \tag{7.2.13}$$

The third term, Global, denotes the contribution from the product of contour integrals, one of which is along a contour connecting two different punctures. It is given by

$$\mathsf{Global} = \left(\oint_{\mathcal{C}_1+\mathcal{C}_{\bar{2}}-\mathcal{C}_3} \varpi \int_{\ell_{21}} \eta + \oint_{\mathcal{C}_{\bar{2}}+\mathcal{C}_3-\mathcal{C}_1} \varpi \int_{\ell_{23}} \eta + \oint_{\mathcal{C}_3+\mathcal{C}_1-\mathcal{C}_{\bar{2}}} \varpi \int_{\ell_{\bar{3}1}} \eta \right) - (\varpi \leftrightarrow \eta) \,. \tag{7.2.14}$$

More precisely, ℓ_{ij} denotes the contour connecting z_i^* and z_j^*, where z_i^* is the point near the puncture z_i satisfying $z_i^* - z_i = \epsilon_i$. The barred indices indicate the points on the second sheet of the double cover $y^2 = T(z)$. For instance, $\mathcal{C}_{\bar{i}}$ is a contour encircling the point $z_{\bar{i}}$, which is on the second sheet right below z_i. Finally, the term Extra denotes additional terms which come from the integrals around the zeros of $\sqrt{T}$, to be denoted by t_k, at which η becomes singular, and is given by

$$\mathsf{Extra} = \sum_k \oint_{\mathcal{D}_k} \Pi\eta \,. \tag{7.2.15}$$

Here $\mathcal{D}_k$ is the contour which encircles t_k twice as depicted in Figure 7.2.3.

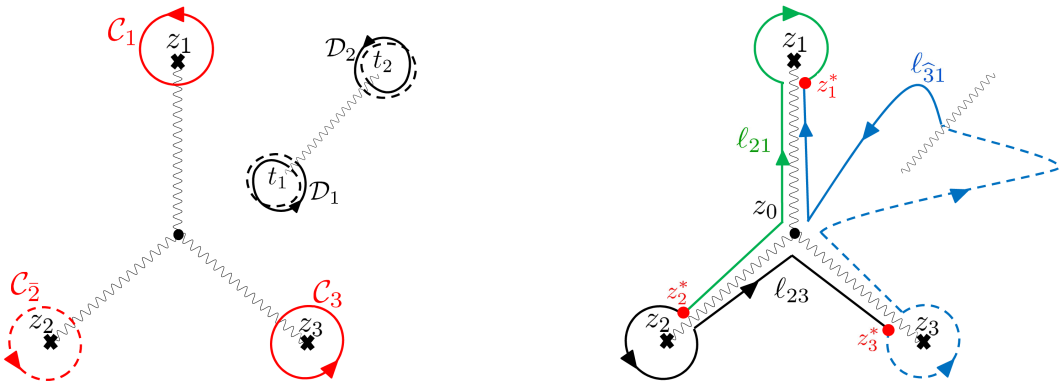

Figure 7.2.3: Definitions of the contours used to rewrite the action: The contours which enclose the punctures ($\mathcal{C}_i$) are shown in the left figure and the ones which connect two punctures (ℓ_{ij}) are shown in the right figure. In both figures, the portions of the contours on the second sheet are drawn as dashed lines. Also depicted in the right figure are the starting points and the end points of the contours, z_i^*'s.

Among these four terms, Local and Double are expressed solely in terms of the integrals around the punctures and are easy to compute. The explicit results, computed in Appendix

C.1.3 are[19]

$$\oint_{\mathcal{C}_i} \varpi = 2\pi i \kappa_i \,, \quad \oint_{\mathcal{C}_i} \eta = 2\pi i \kappa_i \Lambda_i \,, \tag{7.2.16}$$

$$\oint_{\mathcal{C}_i} \eta \int_{z_i^*}^{z} \varpi = -2\pi \kappa_i^2 \Lambda_i \,, \qquad \text{for } i = 1, \bar{2}, 3 \,. \tag{7.2.17}$$

Here Λ_i's are given in terms of γ_i and ρ_i, defined in (C.1.21) and (C.1.22) respectively, as

$$\Lambda_i = \cos 2\gamma_i + \frac{2\rho_i^2}{\kappa_i^4} \,. \tag{7.2.18}$$

It is important to note that Local and Double are real since κ_i and g_i are all real. Therefore they contribute exclusively to the imaginary part of the action (7.2.7) and hence only yield an overall phase of the three-point functions. We shall neglect such quantities in the discussions below.

Among the remaining two types of terms, Extra can be explicitly evaluated as follows. Since the worldsheet is assumed to be smooth except at the punctures, the quantity $\sqrt{T\bar{T}}\cos 2\gamma$, which is the integrand of the action integral given in (7.2.2), should not vanish even at the zeros of $T(z)$. This in turn implies that γ is logarithmically divergent at such points in the manner

$$\gamma \sim \pm \frac{i}{2} \ln |z - t_k| \quad \text{as } z \to t_k \,. \tag{7.2.19}$$

Then, by approximating $T(z)$ as $T(z) \sim c(z - t_k)$ around t_k, we can write down the leading singular behavior of η around t_k as

$$\eta \sim -\frac{2}{\sqrt{T}} (\partial\gamma)^2 d\bar{z} \sim \frac{d\bar{z}}{8\sqrt{c}(z - t_k)^{5/2}} \,. \tag{7.2.20}$$

Thus the integral along $\mathcal{D}_k$ can be computed as

$$\oint_{\mathcal{D}_k} \Pi\eta = \oint_{\mathcal{D}_k} \frac{2\sqrt{c}(z - t_k)^{3/2}}{3} \frac{d\bar{z}}{8\sqrt{c}(z - t_k)^{5/2}} = -\frac{\pi i}{6} \,. \tag{7.2.21}$$

Since there exist two zeros, Extra is twice this integral and hence is given by

$$\mathsf{Extra} = -\frac{\pi i}{3} \,. \tag{7.2.22}$$

For later convenience, we shall derive another expression for the action using a different set of one-forms given by

$$\bar{\varpi} = \sqrt{\bar{T}} d\bar{z} \,, \tag{7.2.23}$$

$$\tilde{\eta} = -\sqrt{T}\cos 2\gamma dz + \frac{2}{\sqrt{T}} \left(-(\bar{\partial}\gamma)^2 + \frac{\rho^2}{\bar{T}} \right) d\bar{z} \,, \tag{7.2.24}$$

[19]The one-forms ϖ and η flip the sign under the exchange of two sheets. Therefore (7.2.16) is odd whereas (7.2.17) is even under such sheet-exchange. In (7.2.17), κ_i for $i = \bar{2}$ is set to be equal to κ_2.

and then consider the average of the two expressions. Using the forms above, the action can be written as

$$S_{S^3} = -\frac{i\sqrt{\lambda}}{4\pi}\int_{\tilde{\Sigma}} \bar{\varpi}\wedge\tilde{\eta}\,. \tag{7.2.25}$$

As compared to (7.2.7), the expression (7.2.25) has an extra minus sign, which is due to the property $dz\wedge d\bar{z} = -d\bar{z}\wedge dz$. Applying the generalized Riemann bilinear identity to (7.2.25), we get

$$-\int_{\tilde{\Sigma}} \bar{\varpi}\wedge\tilde{\eta} = -\left(\overline{\mathsf{Local}} + \overline{\mathsf{Double}} + \overline{\mathsf{Global}} + \overline{\mathsf{Extra}}\right)\,, \tag{7.2.26}$$

where $\overline{\mathsf{Local}}$, $\overline{\mathsf{Double}}$ and $\overline{\mathsf{Global}}$ are given respectively by (7.2.12), (7.2.13) and (7.2.14) with ϖ and η replaced by $\bar{\varpi}$ and $\tilde{\eta}$. The integrals of $\bar{\varpi}$ and $\tilde{\eta}$ around the punctures are given by[20]

$$\oint_{\mathcal{C}_i}\bar{\varpi} = -2\pi i\kappa_i\,,\qquad \oint_{\mathcal{C}_i}\tilde{\eta} = -2\pi i\kappa_i\bar{\Lambda}_i\,, \tag{7.2.27}$$

$$\oint_{\mathcal{C}_i}\tilde{\eta}\int_{z_i^*}^{z}\bar{\varpi} = -2\pi\kappa_i^2\bar{\Lambda}_i\,,\qquad \text{for } i=1,\widehat{2},3 \tag{7.2.28}$$

where $\bar{\Lambda}_i$'s are given in terms of γ_i and $\tilde{\rho}_i$, defined in Appendix C.1.2, as

$$\bar{\Lambda}_i = \cos 2\gamma_i + \frac{2\tilde{\rho}_i^{\,2}}{\kappa_i^4}\,. \tag{7.2.29}$$

Again $\overline{\mathsf{Local}}$ and $\overline{\mathsf{Double}}$ are real and they contribute only to the overall phase. On the other hand, $\overline{\mathsf{Extra}}$ can be evaluated just like Extra and yields $+\pi i/3$. Thus, by averaging over the two expressions (7.2.11) and (7.2.26) and neglecting terms which contribute exclusively to the overall phase, we arrive at the following more symmetric expression:

$$\frac{1}{2}\left(\int_{\tilde{\Sigma}}\varpi\wedge\eta - \int_{\tilde{\Sigma}}\bar{\varpi}\wedge\tilde{\eta}\right) = -\frac{\pi i}{3} + \frac{1}{2}\left(\mathsf{Global} - \overline{\mathsf{Global}}\right)\,. \tag{7.2.30}$$

The quantity (7.2.30) consists of various integrals along the contours $\mathcal{C}_i$ and ℓ_{ij}. Among them, the ones along $\mathcal{C}_i$ can be easily computed using (7.2.16) and (7.2.27). The integral of ϖ along ℓ_{ij} can also be computed in principle as we know the explicit form of ϖ. Thus the major nontrivial task is the evaluation of $\int_{\ell_{ij}}\eta$ and $\int_{\ell_{ij}}\tilde{\eta}$. In the rest of this section, we will see how these integrals are related to the Wronskians of the form $\langle i_\pm\,, j_\pm\rangle$, where $i_\pm$ are the Baker-Akhiezer eigenvectors at z_i of the ALP, corresponding to the eigenvalues $e^{\pm ip_i(x)}$.

[20] (7.2.27) is odd and (7.2.28) is even under the exchange of the first and the second sheets, as in the case of the integrals of ϖ and η given in (7.2.16) and (7.2.17).

7.2.2 WKB expansions of the auxiliary linear problem

We now perform the WKB expansion of the auxiliary linear problem and observe that the contour integrals of our interest, $\int_{\ell_{ij}} \eta$ and $\int_{\ell_{ij}} \tilde{\eta}$, appear in the expansion of the Wronskians between the eigenvectors of the monodromy matrices.

Let us first consider the WKB expansion of the solutions to the ALP. For this purpose, it is convenient to use the ALP of the Pohlmeyer reduction (7.1.16). The use of (7.1.16) has two main virtues. First, as Φ's are given explicitly in terms of $T(z)$ and $\bar{T}(\bar{z})$, it is easier to perform the expansion around $\zeta = 0$ or around $\zeta = \infty$. Second, since the connection (7.1.14) is expressed solely in terms of the quantities invariant under the global symmetry transformation, we can directly explore the dynamical aspect of the problem setting aside all the kinematical information.

We shall first perform the expansion around $\zeta = 0$. To facilitate this task, it is convenient to perform a further gauge transformation and convert (7.1.16) to the "diagonal gauge", where the ALP take the form

$$\left(\partial + \frac{1}{\zeta}\Phi^d_z + A^d_z\right)\hat{\psi}^d = 0\,, \quad \left(\bar{\partial} + \zeta\Phi^d_{\bar{z}} + A^d_{\bar{z}}\right)\hat{\psi}^d = 0\,. \tag{7.2.31}$$

In the above, $\hat{\psi}^d$ in the diagonal gauge is defined by

$$\hat{\psi}^d \equiv \frac{1}{\sqrt{2}}\begin{pmatrix} e^{i\gamma/2} & -e^{-i\gamma/2} \\ e^{i\gamma/2} & e^{-i\gamma/2} \end{pmatrix}\hat{\psi}\,, \tag{7.2.32}$$

and Φ^d's and A^d's are given by

$$\begin{aligned} \Phi^d_z &= \frac{\sqrt{T}}{2}\begin{pmatrix} 1 & 0 \\ 0 & -1 \end{pmatrix}, & \Phi^d_{\bar{z}} &= \frac{\sqrt{\bar{T}}}{2}\begin{pmatrix} -\cos 2\gamma & i\sin 2\gamma \\ -i\sin 2\gamma & \cos 2\gamma \end{pmatrix}, \\ A^d_z &= \begin{pmatrix} -\frac{\rho}{\sqrt{T}}\cot 2\gamma & \frac{i\rho}{\sqrt{T}} - i\partial\gamma \\ -\frac{i\rho}{\sqrt{T}} - i\partial\gamma & \frac{\rho}{\sqrt{T}}\cot 2\gamma \end{pmatrix}, & A^d_{\bar{z}} &= \frac{-\tilde{\rho}}{\sqrt{\bar{T}}\sin 2\gamma}\begin{pmatrix} 1 & 0 \\ 0 & -1 \end{pmatrix}. \end{aligned} \tag{7.2.33}$$

Note that the leading terms in the ALP equations as $\zeta \to 0$, namely Φ^d_z for the first equation and $A^d_{\bar{z}}$ for the second, have been diagonalized. Because of this feature, the leading exponential behavior of the two linearly independent solutions around $\zeta \sim 0$ can be readily determined as

$$\hat{\psi}^d_1 \sim \begin{pmatrix} 0 \\ 1 \end{pmatrix}\exp\left[\frac{1}{2\zeta}\int_{z_0}^{z}\varpi\right], \quad \hat{\psi}^d_2 \sim \begin{pmatrix} 1 \\ 0 \end{pmatrix}\exp\left[\frac{-1}{2\zeta}\int_{z_0}^{z}\varpi\right], \tag{7.2.34}$$

By performing the WKB expansion around $\zeta \sim 0$ systematically, one can also determine the subleading terms of (7.2.34) in ζ, as shown in Appendix C.5.1.

The quantities of prime interest in the subsequent discussions are the Wronskians of the eigenvectors of the monodromy matrices. To perform the WKB expansion of such Wronskians, we need to have a good control over the asymptotics of the Wronskians $\langle i_\pm\,,j_\pm\rangle$ around $\zeta=0$. For this purpose, both of the eigenvectors in the Wronskian need to be small solutions since big solutions can contain a multiple of small solutions and hence are ambiguous [112, 113]. When ζ is sufficiently close to zero, one can show that the plus solutions i_+ are the small solutions if $\mathrm{Re}\,\zeta$ is positive whereas it is the minus solutions i_- which are small if $\mathrm{Re}\,\zeta$ is negative. Thus, the Wronskians that can be expanded consistently around $\zeta=0$ are $\langle i_+\,,j_+\rangle$'s for $\mathrm{Re}\,\zeta>0$ and $\langle i_-\,,j_-\rangle$'s for $\mathrm{Re}\,\zeta<0$. The detailed form of the expansion can be determined by employing the Born series expansion explained in Appendix C.5.2 and the results are given in the following simple form:

For $\mathrm{Re}\,\zeta>0$,

$$\langle 2_+\,,1_+\rangle=\exp\left(-S_{2\to1}\right)\,,\quad \langle 2_+\,,3_+\rangle=\exp\left(-S_{2\to3}\right)\,,\quad \langle 3_+\,,1_+\rangle=\exp\left(-S_{\hat{3}\to1}\right)\,, \tag{7.2.35}$$

For $\mathrm{Re}\,\zeta<0$,

$$\langle 2_-\,,1_-\rangle=\exp\left(S_{2\to1}\right)\,,\quad \langle 2_-\,,3_-\rangle=\exp\left(S_{2\to3}\right)\,,\quad \langle 1_-\,,3_-\rangle=\exp\left(S_{\hat{3}\to1}\right)\,. \tag{7.2.36}$$

In these expressions, $S_{i\to j}$ stands for the quantity

$$S_{i\to j}=\frac{1}{2\zeta}\int_{\ell_{ij}}\varpi+\int_{\ell_{ij}}\alpha+\frac{\zeta}{2}\int_{\ell_{ij}}\eta+\cdots\,, \tag{7.2.37}$$

where the one-form α is given in (C.5.41) in Appendix C.5.2. A remarkable feature of (7.2.37) is that the integral of our interest $\int_{\ell_{ij}}\eta$ makes its appearance in the exponent $S_{i\to j}$.

Now to make use of the averaging procedure described in the previous subsection, we need the other type of integrals $\int_{\ell_{ij}}\tilde{\eta}$ which appear in $\overline{\mathsf{Global}}$. To obtain them, we need to expand the Wronskians this time around $\zeta=\infty$. Since the discussion is similar to the expansion around $\zeta=0$, we will not elaborate on the details and simply give the results:

For $\mathrm{Re}\,\zeta>0$,

$$\langle 2_+\,,1_+\rangle=\exp\left(-\tilde{S}_{2\to1}\right)\,,\quad \langle 2_+\,,3_+\rangle=\exp\left(-\tilde{S}_{2\to3}\right)\,,\quad \langle 3_+\,,1_+\rangle=\exp\left(-\tilde{S}_{\hat{3}\to1}\right)\,, \tag{7.2.38}$$

For $\mathrm{Re}\,\zeta<0$,

$$\langle 2_-\,,1_-\rangle=\exp\left(\tilde{S}_{2\to1}\right)\,,\quad \langle 2_-\,,3_-\rangle=\exp\left(\tilde{S}_{2\to3}\right)\,,\quad \langle 1_-\,,3_-\rangle=\exp\left(\tilde{S}_{\hat{3}\to1}\right)\,, \tag{7.2.39}$$

Here $\tilde{S}_{i\to j}$ is defined by

$$\tilde{S}_{i\to j} = \frac{\zeta}{2}\int_{\ell_{ij}} \bar{\varpi} + \int_{\ell_{ij}} \tilde{\alpha} + \frac{1}{2\zeta}\int_{\ell_{ij}} \tilde{\eta} + \cdots , \tag{7.2.40}$$

where $\tilde{\alpha}$ is a one-form given in (C.5.42) in Appendix C.5.2. Making use of these two types of expansions, we will be able to rewrite the action in terms of the Wronskians, as described in the next subsection.

7.2.3 The expression of the action in terms of the Wronskians

We are now ready to derive an explicit expression of the action in terms of the Wronskians. As shown in the previous subsection, the integrals we used to rewrite the action, namely $\oint_{\ell_{ij}} \eta$ and $\oint_{\ell_{ij}} \tilde{\eta}$, can be extracted from the Wronskians. For instance, consider the integral $\oint_{\ell_{21}} \eta$, which appears in $\langle 2_-, 1_-\rangle$. Differentiating $\ln\langle 2_-, 1_-\rangle$ with respect to ζ using (7.2.36) and (7.2.37), we get

$$\partial_\zeta \ln\langle 2_-, 1_-\rangle = -\frac{1}{\zeta^2}\int_{\ell_{21}} \varpi + \frac{1}{2}\int_{\ell_{21}} \eta + O(\zeta)\,. \tag{7.2.41}$$

Therefore we can get the integral $\oint_{\ell_{21}} \eta$ by subtracting the first divergent term and then taking the limit $\zeta \to 0$. Similarly $\oint_{\ell_{21}} \tilde{\eta}$ can be obtained from $\langle 2_-, 1_-\rangle$ in the $\zeta \to \infty$ limit. Such procedures can be compactly implemented if we use the variable x instead of ζ, which are related as in (7.1.13). Then, we can write

$$\oint_{\ell_{21}} \eta = -4{:}\partial_x \ln\langle 2_-\,, 1_-\rangle{:}_+\,, \qquad \oint_{\ell_{21}} \tilde{\eta} = -4{:}\partial_x \ln\langle 2_-\,, 1_-\rangle{:}_-\,, \tag{7.2.42}$$

where the "normal ordering" symbol ${:}A(x){:}_\pm$ is defined by

$${:}A(x){:}_\pm \equiv \lim_{x\to\pm 1}\left[A(x) - (\text{double pole at } x = \pm 1)\right]\,. \tag{7.2.43}$$

This precisely subtracts the divergent term mentioned above. Substituting such expressions to the definitions of Global and $\overline{\mathsf{Global}}$, we can express them in terms of the Wronskians. Then, using (7.2.30), we arrive at the following expression for the contribution from the S^3 part of the action $\mathcal{F}_{\text{action}}$:

$$\mathcal{F}_{\text{action}} = -S_{S^3} = \frac{\sqrt{\lambda}}{6} + \mathcal{A}_\varpi + \mathcal{A}_\eta\,. \tag{7.2.44}$$

The first term in (7.2.44) expresses the contributions of Extra and $\overline{\text{Extra}}$. The second term $\mathcal{A}_\varpi$ denotes the contribution of $\int_{\ell_{ij}} \varpi$ and $\int_{\ell_{ij}} \bar{\varpi}$ in Global and $\overline{\text{Global}}$ and is given by

$$\begin{aligned}
&\mathcal{A}_\varpi = \\
&\frac{\sqrt{\lambda}}{4}\Bigg((\kappa_1\Lambda_1 + \kappa_2\Lambda_2 - \kappa_3\Lambda_3) \int_{\ell_{21}} \varpi + (\kappa_1\Lambda_1 - \kappa_2\Lambda_2 + \kappa_3\Lambda_3) \int_{\ell_{\hat{3}1}} \varpi \\
&+ (-\kappa_1\Lambda_1 + \kappa_2\Lambda_2 + \kappa_3\Lambda_3) \int_{\ell_{23}} \varpi \Bigg) + \left(\Lambda_i \to \bar{\Lambda}_i\,,\ \varpi \to \bar{\varpi}\right)\,, \qquad (7.2.45)
\end{aligned}$$

where Λ_i and $\bar{\Lambda}_i$ are as given in (7.2.18) and (7.2.29) and $\left(\Lambda_i \to \bar{\Lambda}_i\,,\ \varpi \to \bar{\varpi}\right)$ in the last line denotes the terms obtained by replacing Λ_i and ϖ in the second line with $\bar{\Lambda}_i$ and $\bar{\varpi}$ respectively. The third term $\mathcal{A}_\eta$ is the contribution of $\int_{\ell_{ij}} \eta$ and $\int_{\ell_{ij}} \tilde{\eta}$, which is expressed in terms of the Wronskians in the following way:

$$\begin{aligned}
\mathcal{A}_\eta = \sqrt{\lambda}\big[&(\kappa_1 + \kappa_2 - \kappa_3)\left(:\partial_x \ln\langle 2_-\,, 1_-\rangle:_+ - :\partial_x \ln\langle 2_+\,, 1_+\rangle:_-\right) \\
&+ (\kappa_1 - \kappa_2 + \kappa_3)\left(:\partial_x \ln\langle 3_-\,, 1_-\rangle:_+ - :\partial_x \ln\langle 3_+\,, 1_+\rangle:_-\right) \\
&+ (-\kappa_1 + \kappa_2 + \kappa_3)\left(:\partial_x \ln\langle 2_-\,, 3_-\rangle:_+ - :\partial_x \ln\langle 2_-\,, 3_-\rangle:_-\right)\big]\,. \qquad (7.2.46)
\end{aligned}$$

The general formula (7.2.44) will later be used in section 7.5 to compute the three-point functions.

7.3 Vertex operators in terms of Wronskians

Having found the structure of the contribution of the action part, we shall now study that of the vertex operators.

7.3.1 Basic idea and framework

Before plunging into the details of the analysis, let us describe in this subsection the basic idea and the framework.

The precise form of the conformally invariant vertex operator corresponding to a string solution in a curved spacetime, such as $E!AdS_5 \times S^3$ of our interest, is in general not known. In particular, for a non-BPS solution with non-trivial σ-dependence the corresponding vertex operator would contain infinite number of derivatives and is hard to construct. To overcome this difficulty, we will employ the state-operator correspondence and construct the corresponding wave function in terms of the action-angle variables[21].

[21] This idea was successfully applied to the case of the GKP string in AdS_3 in [17].

Let us briefly overview the essential ingredients of the method[22]. The state-operator correspondence, in the semi-classical approximation, is expressed by the following equation:

$$\mathcal{V}[q_*(z=0)]e^{-S_{q_*}(\tau<0)} = \Psi[q_*]\big|_{\tau=0}\,. \tag{7.3.1}$$

Here q_* signifies the saddle point configuration, $\mathcal{V}[q_*(z=0)]$ is the value of the vertex operator inserted at the origin of the worldsheet $z = e^{\tau+i\sigma} = 0$, corresponding to the cylinder time $\tau = -\infty$, the factor $\exp[-S_{q_*}(\tau < 0)]$ is the amplitude to develop into the state on a unit circle and the $\Psi[q_*]\big|_{\tau=0}$ is the semi-classical wave function describing the state on that circle. The relation (7.3.1) is nothing but the semi-classical approximation of the usual state-operator correspondence. If we employ the action-angle variables basis (S_i, ϕ_i), constructed in section 7.1.4, and use $\{\phi_i\}$ as q, then the wave function evaluated at the cylinder time τ can be expressed simply as

$$\Psi[\phi] = \exp\left(i\sum_i S_i\phi_i - \mathcal{E}(\{S_i\})\tau\right)\,, \tag{7.3.2}$$

where the action variables S_i and the worldsheet energy $\mathcal{E}(\{S_i\})$ are constant.

Now the serious problem is that we do not know the exact saddle point solution for the three-point function. The only information we know is that in the vicinity of each vertex insertion point z_i, the exact three-point solution, to be represented by a 2×2 matrix $\mathbb{Y}$ given by

$$\mathbb{Y} = \begin{pmatrix} Z & X \\ -\bar{X} & \bar{Z} \end{pmatrix}\,, \qquad Z = Y_1 + iY_2\,, \qquad X = Y_3 + iY_4\,, \tag{7.3.3}$$

which must be almost identical to the two-point solution produced by the same vertex operator. Let us denote such a solution by $\mathbb{Y}^{\rm ref}$ and call it a reference solution[23]. As we have to normalize the three-point function precisely by such a two-point function for each leg, what is important is the difference between $\mathbb{Y}$ and $\mathbb{Y}^{\rm ref}$. Note that even if they are produced by the same vertex operator, they are different because $\mathbb{Y}$ is influenced by the presence of other vertex operators in the three-point function.

Here and in what follows, the global isometry group $G = \mathrm{SU}(2)_L \times \mathrm{SU}(2)_R$ and its complexification $G^c = \mathrm{SL}(2,\mathrm{C})_L \times \mathrm{SL}(2,\mathrm{C})_R$ play the central roles. Being the symmetry groups of the equations of motion (and the Virasoro conditions), two solutions of the equations of motion are connected by the action of G and/or G^c. The difference between their actions are that (when expressed in terms of the Minkowski worldsheet variables) while G connects a real solution to a real solution, G^c transforms a real solution to a complex solution. Since

[22]For a detail, see also section 3 of [17].

[23]A more precise definition of the reference solution will be given later in section 7.3.3.

the three-point interaction is inherently a tunneling process, the saddle point solution for such a process must be complex. Therefore near z_i the two solutions $\mathbb{Y}$ and $\mathbb{Y}^{\rm ref}$ must be connected by an element of G^c in the manner

$$\mathbb{Y} = \tilde{V}\mathbb{Y}^{\rm ref}V\,, \qquad \tilde{V} \in {\rm SL}(2,{\rm C})_L, V \in {\rm SL}(2,{\rm C})_R \tag{7.3.4}$$

This means that the angle variables associated to $\mathbb{Y}$, as defined relative to the ones associated to $\mathbb{Y}^{\rm ref}$, should be computable from the knowledge of the transformation matrices $\tilde{V}$ and V. As will be discussed in Appendix C.6, it turns out that most of the angle variables are invariant under the global transformations except those which are conjugate to the global charges, ϕ_R and ϕ_L. In terms of the solutions to the right and left ALP, $\psi(x)$ and $\tilde{\psi}(x)$, their shifts can be computed using a useful formula derived in Appendix C.6 as

$$\Delta\phi_R = -i\ln\left(\frac{(n\cdot\psi_+(\infty))(n\cdot\psi_-^{\rm ref}(\infty))}{(n\cdot\psi_+^{\rm ref}(\infty))(n\cdot\psi_-(\infty))}\right)\,, \tag{7.3.5}$$

$$\Delta\phi_L = -i\ln\left(\frac{(\tilde{n}\cdot\tilde{\psi}_+(0))(\tilde{n}\cdot\tilde{\psi}_-^{\rm ref}(0))}{(\tilde{n}\cdot\tilde{\psi}_+^{\rm ref}(0))(\tilde{n}\cdot\tilde{\psi}_-(0))}\right)\,, \tag{7.3.6}$$

where n and $\tilde{n}$ are the normalization vectors for the right and the left sector and $\psi_\pm(x)$ and $\psi_\pm^{\rm ref}(x)$ are the Baker-Akhiezer eigenvectors corresponding to the solutions $\mathbb{Y}$ and $\mathbb{Y}^{\rm ref}$ respectively and are related by

$$\psi_\pm = V^{-1}\psi_\pm^{\rm ref}\,, \qquad \tilde{\psi}_\pm = \tilde{V}\tilde{\psi}_\pm^{\rm ref}\,. \tag{7.3.7}$$

How V and $\tilde{V}$ can be obtained will be described in detail in subsection 7.3.3.

The remaining problem is to fix the normalization vectors n and $\tilde{n}$, relevant for the left and the right sectors. In the case of the string which is entirely in $EAdS_3$ [17], we can fix them by the following argument. Consider for simplicity the wave function corresponding to a conformal primary operator of the gauge theory sitting at the origin of the boundary of AdS_5. Such an operator is characterized by the invariance under the special conformal transformation. Therefore the corresponding wave function and the angle variables comprising it should also be invariant. Explicitly it requires that $n\cdot\psi$ and $\tilde{n}\cdot\tilde{\psi}$ must be preserved under the special conformal transformation and this determines n and $\tilde{n}$.

The essence of the argument we shall employ for the case of a string in S^3 studied in the present chapter is the same. Namely, we characterize the string state by certain highest weight condition and determine the normalization vector. However because the structures of the gauge theory operators and the corresponding string solutions are more complicated, we need to generalize and refine the argument. As a result of this improvement, not only has the determination of the normalization vectors become more systematic but also their physical meaning has been identified more clearly. Moreover, the entire procedure of the constructions

of the wave functions for the S^3 part and the $EAdS_3$ part has become completely parallel and transparent. Below we shall begin the analysis first from the gauge theory side.

7.3.2 Characterization of the gauge theory operators by symmetry properties

As sketched above, in order to construct the wave functions expressing the effect of the insertion of the vertex operators, we must study how to characterize the global symmetry properties of the vertex operators and the classical configurations that they produce in their vicinity.

For this purpose, it is convenient to first look at the symmetry properties of the corresponding gauge theory operators. Recall that the operators in the "SU(2) sector" are composed of the complex scalar fields $Z \equiv \Phi_1 + i\Phi_2$, $X \equiv \Phi_3 + i\Phi_4$ and their complex conjugates $\bar{Z}$ and $\bar{X}$, where Φ_I $(I = 1, 2, 3, 4)$ are four of the six real hermitian fields in the adjoint representation of the gauge group. Under the global symmetry group $\mathrm{SO}(4) = \mathrm{SU}(2)_R \times \mathrm{SU}(2)_L$, these fields transform in the doublet representations of $\mathrm{SU}(2)_R$ and $\mathrm{SU}(2)_L$ with the right and the left charges $\mathcal{R}$ and $\mathcal{L}$ given as follows:

	$\mathcal{R}$	$\mathcal{L}$
Z	$+1/2$	$+1/2$
$\bar{Z}$	$-1/2$	$-1/2$
X	$-1/2$	$+1/2$
$\bar{X}$	$+1/2$	$-1/2$

(7.3.8)

These transformation properties are succinctly represented by the 2×2 matrix

$$\Phi = \begin{pmatrix} Z & X \\ -\bar{X} & \bar{Z} \end{pmatrix}, \tag{7.3.9}$$

which gets transformed as $U_L \Phi U_R$, where $U_L \in \mathrm{SU}(2)_L, U_R \in \mathrm{SU}(2)_R$. In spite of this SO(4) symmetry, in the existing literature[24] the operators $\mathcal{O}_i$ are taken to be composed of a special pair of fields[25] as indicated in (4.1.2) in section 4.1. For example, $\mathcal{O}_1$ is of the form $\mathrm{tr}\,(ZZ\cdots XZZX\cdots Z)$. In the spin-chain interpretation, Z and X represent the up and the down spin respectively so that $\mathcal{O}_1$ is a state built upon the all-spin-up vacuum state $\mathrm{tr}\, Z^\ell$ on ℓ sites by flipping some of the up-spins into the down-spins which represent excitations. Therefore at each site there is an SU(2) group acting on a spin, and according to (7.3.8), it is identified with $\mathrm{SU}(2)_{\mathrm{R}}$ for this case. For the entire operator $\mathcal{O}_1$, what is relevant is the total $\mathrm{SU}(2)_{\mathrm{R}}$, the generator of which will be denoted by S^i_R.

[24] See, for example, [80].

[25] The reason for this choice is that it is the simplest one that can produce non-extremal three-point functions.

Let us now characterize the spin-chain states corresponding to the operators of the type $\mathcal{O}_1$ from the point of view of this total $\mathrm{SU}(2)_R$. First, since the constituents Z and X carry definite spin quantum numbers, every state of type $\mathcal{O}_1$ carries a definite right and left global charges. Second, every such state is actually a highest weight state annihilated by the operator $S_R^+ = S_R^1 + iS_R^2$. For the vacuum state $|Z^\ell\rangle = |\uparrow^\ell\rangle$ it is obvious. As for the excited states, they can be written as the Bethe states $\prod_{i=1} B(u_i)|\uparrow^\ell\rangle$, where $B(u_i)$ is the familiar magnon creation operator carrying the rapidity u_i. As we mentioned in section 3.1.3, such a state is a highest-weight state of the total $\mathrm{SU}(2)_R$ and hence annihilated by the same S_R^+, provided that the Bethe state is on-shell. Thus all the operators of type $\mathcal{O}_1$ can be characterized as the highest weight state of the total $\mathrm{SU}(2)_{\mathrm{R}}$.

Now in order to deal with other operators built upon a "vacuum state" different from $\mathrm{tr}\, Z^\ell$, let us introduce the general linear combinations of Φ_I as $\vec{P}\cdot\vec{\Phi} = \sum_{I=1}^4 P_I\Phi_I$. To discuss the transformation property under $\mathrm{SU}(2)_R \times \mathrm{SU}(2)_L$, it is more convenient to deal with the matrix

$$\mathbb{P} \equiv \begin{pmatrix} P_1 + iP_2 & P_3 + iP_4 \\ -(P_3 - iP_4) & P_1 - iP_2 \end{pmatrix} = P_I\Sigma_I\,, \tag{7.3.10}$$

$$\Sigma_I \equiv (1, i\sigma_3, i\sigma_2, i\sigma_1)\,. \tag{7.3.11}$$

Then, we have the representation

$$\vec{P}\cdot\vec{\Phi} = \frac{1}{2}\mathrm{tr}\,\left(\sigma_2\mathbb{P}^t\sigma_2\Phi\right)\,. \tag{7.3.12}$$

In this notation, $\mathbb{P}$ corresponding to $Z, \bar{Z}, X, \bar{X}$ take the form $\mathbb{P}_Z = 1-\sigma_3, \mathbb{P}_{\bar{Z}} = 1+\sigma_3, \mathbb{P}_X = -(\sigma_1 - i\sigma_2), \mathbb{P}_{\bar{X}} = \sigma_1 + i\sigma_2$.

As we argued above, all the on-shell states built upon a common vacuum are annihilated by the same element of the global symmetry algebra, such as S_R^+. In other words as long as the global transformation property is concerned, the vacuum state can be considered as the representative of all the states built upon it. As it will be slightly more convenient, instead of the annihilation operator, we will use the "raising operator" $K = \exp(\alpha\hat{a})$, where α is any constant and $\hat{a}$ is the element of the algebra which annihilates the corresponding vacuum state. The vacuum is then characterized by the form of K that leaves its building block *invariant*.

Let us explain this idea concretely for the simplest vacuum state $\mathrm{tr}\, Z^\ell$. In the general notation (7.3.12), we can express Z as $Z = \frac{1}{2}\mathrm{tr}\,(\sigma_2\mathbb{P}_Z^t\sigma_2\Phi)$ with $\mathbb{P}_Z = 1 - \sigma_3$. Now let us look for the raising operators K_Z and $\tilde{K}_Z$ for $\mathrm{SU}(2)_R$ and $\mathrm{SU}(2)_L$ respectively, which leave Z invariant. Since Φ transforms into $\tilde{K}_Z\Phi K_Z$, the invariance condition reads

$$\frac{1}{2}\mathrm{tr}\,\left(\sigma_2\mathbb{P}_Z^t\sigma_2\tilde{K}_Z\Phi K_Z\right) = \frac{1}{2}\mathrm{tr}\,\left(\sigma_2\mathbb{P}_Z^t\sigma_2\Phi\right)\,. \tag{7.3.13}$$

This is equivalent to the condition

$$\mathbb{P}_Z = \tilde{K}_Z^{-1} \mathbb{P}_Z K_Z^{-1} \,. \tag{7.3.14}$$

It is easy to find the solutions, which read

$$K_Z = \begin{pmatrix} 1 & \beta \\ 0 & 1 \end{pmatrix} = e^{\frac{1}{2}\beta\sigma_+} \,, \qquad \tilde{K}_Z = \begin{pmatrix} 1 & 0 \\ \tilde{\beta} & 1 \end{pmatrix} = e^{\frac{1}{2}\tilde{\beta}\sigma_-} \,, \tag{7.3.15}$$

where β and $\tilde{\beta}$ are arbitrary constants.

Next we consider a general case where the vacuum state is given by $\mathrm{tr}\,(\vec{P}\cdot\vec{\Phi})^l$, with arbitrary $\vec{P}$. We can characterize this family of states again by the raising operators K and $\tilde{K}$ which leave $\vec{P}\cdot\vec{\Phi}$ invariant. Just as in (7.3.14), this condition is expressed as

$$\mathbb{P} = \tilde{K}^{-1} \mathbb{P} K^{-1} \,. \tag{7.3.16}$$

where $\mathbb{P}$ corresponds to $\vec{P}$. Since $\vec{P}\cdot\vec{\Phi}$ can be obtained from Z by an $\mathrm{SU}(2)_L \times \mathrm{SU}(2)_R$ transformation, $\mathbb{P}$ can be obtained from $\mathbb{P}_Z$ by a corresponding transformation of the form

$$\mathbb{P} = U_L \mathbb{P}_Z U_R \,. \tag{7.3.17}$$

Then combined with (7.3.16) we readily obtain the relation $\mathbb{P}_Z = (U_L^{-1}\tilde{K}^{-1}U_L)\mathbb{P}_Z(U_R K^{-1} U_R^{-1})$. Comparing this with (7.3.14) we can express the raising operators K and $\tilde{K}$ in terms of the ones for the operator Z given in (7.3.15) in the form

$$K = U_R^{-1} K_Z U_R \,, \qquad \tilde{K} = U_L \tilde{K}_Z U_L^{-1} \,. \tag{7.3.18}$$

Now these raising operators can in turn be characterized by the two-component vectors $\mathfrak{p}$ and $\tilde{\mathfrak{p}}$, which are left invariant under the following action of K and $\tilde{K}$ respectively:

$$K^t \mathfrak{p} = \mathfrak{p} \,, \qquad \tilde{K}^t \tilde{\mathfrak{p}} = \tilde{\mathfrak{p}} \,. \tag{7.3.19}$$

Since the overall factor for these vectors are inessential, we can freely normalize them to have unit length as $\mathfrak{p}^\dagger \cdot \mathfrak{p} = \tilde{\mathfrak{p}}^\dagger \cdot \tilde{\mathfrak{p}} = 1$. We shall refer to them as *polarization spinors*, as they characterize, so to speak, the "direction of polarization" of the highest weight operator $\vec{P}\cdot\vec{\Phi}$. It should be noted that from the knowledge of $\mathfrak{p}$ and $\tilde{\mathfrak{p}}$, one can reconstruct $\mathbb{P}$ which is invariant under the raising operators, as in (7.3.16). In fact, if we set

$$\mathbb{P} = -2i\sigma_2 \tilde{\mathfrak{p}} \mathfrak{p}^t \,, \tag{7.3.20}$$

one can easily check that this $\mathbb{P}$ satisfies (7.3.16), with the use of the defining equations (7.3.19) and a simple formula $\sigma_2 U^{-1} \sigma_2 = U^t$ valid for any invertible 2×2 matrix U satisfying $\det U = 1$.

Let us illustrate these concepts by computing the polarization spinors for the operators Z and $\bar{Z}$ respectively. For the operator Z we already computed the right and the left raising operators in (7.3.15). Then it is easy to see that the corresponding polarization spinors $\mathfrak{p}_Z$ and $\tilde{\mathfrak{p}}_Z$ satisfying $K_Z^t \mathfrak{p}_Z = \mathfrak{p}_Z$ and $\tilde{K}_Z^t \tilde{\mathfrak{p}}_Z = \tilde{\mathfrak{p}}_Z$ are given by

$$\mathfrak{p}_Z = \begin{pmatrix} 0 \\ 1 \end{pmatrix}, \qquad \tilde{\mathfrak{p}}_Z = \begin{pmatrix} 1 \\ 0 \end{pmatrix}. \tag{7.3.21}$$

As a check, from the formula (7.3.20), we immediately get $\mathbb{P}_Z = \begin{pmatrix} 0 & 0 \\ 0 & 2 \end{pmatrix}$, which is the desired form. As for the operator $\bar{Z}$, repeating the similar analysis, the raising operators leaving $\mathbb{P}_{\bar{Z}} = 1 + \sigma_3$ invariant can be readily obtained to be

$$K_{\bar{Z}} = \begin{pmatrix} 1 & 0 \\ \alpha & 1 \end{pmatrix}, \qquad \tilde{K}_{\bar{Z}} = \begin{pmatrix} 1 & \tilde{\alpha} \\ 0 & 1 \end{pmatrix}, \tag{7.3.22}$$

with α and $\tilde{\alpha}$ being arbitrary constants. The corresponding polarization spinors can be taken to be

$$\mathfrak{p}_{\bar{Z}} = \begin{pmatrix} 1 \\ 0 \end{pmatrix}, \qquad \tilde{\mathfrak{p}}_{\bar{Z}} = \begin{pmatrix} 0 \\ 1 \end{pmatrix}. \tag{7.3.23}$$

Finally consider the normalization spinors for a general operator $\vec{P} \cdot \vec{\Phi}$ which is related to $Z = \vec{P}_Z \cdot \vec{\Phi}$ through the relation of the form (7.3.17). Since the raising operators for such an operator are obtained from those for Z in the manner (7.3.18), the polarization vectors $\mathfrak{p}$ and $\tilde{\mathfrak{p}}$ are expressed in terms of $\mathfrak{p}_Z$ and $\tilde{\mathfrak{p}}_Z$ as

$$\mathfrak{p} = U_R^t \mathfrak{p}_Z \,, \qquad \tilde{\mathfrak{p}} = (U_L^t)^{-1} \tilde{\mathfrak{p}}_Z \,. \tag{7.3.24}$$

As an application of this formula, let us re-derive $\mathfrak{p}_{\bar{Z}}$ and $\tilde{\mathfrak{p}}_{\bar{Z}}$ from this perspective. Since $\mathbb{P}_{\bar{Z}} = 1 + \sigma_3$ and $\mathbb{P}_Z = 1 - \sigma_3$, it is easy to see that they are related by an $\mathrm{SU}(2)_L \times \mathrm{SU}(2)_R$ transformation of the form

$$\mathbb{P}_{\bar{Z}} = U_L \mathbb{P}_Z U_R \,, \qquad U_L = i\sigma_2 \,, \quad U_R = -i\sigma_2 \,. \tag{7.3.25}$$

In fact this transformation realizes the mapping $(Z, X) \to (\bar{Z}, -\bar{X})$. Substituting the forms of U_L and U_R into the above formula (7.3.24), we obtain $U_R^t \mathfrak{p}_Z = (1, 0)^t$ and $(U_L^t)^{-1} \tilde{\mathfrak{p}}_Z = -(0, 1)^t \propto (0, 1)^t$, which agree with (7.3.23).

The importance of the above analysis is that, as we shall describe below, precisely the same characterization scheme must be valid for the vertex operators in string theory which correspond to the gauge theory composite operators. Moreover, it will be shown that the polarization spinors introduced purely from the group theoretic point of view above will be identified with the *normalization vectors* that appeared in (7.1.45), which play pivotal roles in the construction of the angle variables and hence the construction of the wave functions describing the contribution of the vertex operators.

7.3.3 Wave functions for the S^3 part

Symmetry structure of the vertex operators and the classical solutions

We now begin the explicit construction of the wave functions contributing to the three-point functions in string theory. As we see below, the contribution from the wave functions separates into the kinematical and the dynamical factors. Although the dynamics is quite different between the gauge theory and the corresponding string theory, the kinematical symmetry properties correspond quite directly between the gauge theory operators and the vertex operators of string theory. Therefore in this subsection we will describe how we can implement the scheme of the symmetry characterization of the operators developed in the preceding subsection for the gauge theory operators to the vertex operators and the classical solutions produced by them. Since the analysis concerning the each factor of the symmetry group $\mathrm{SU}(2)_R \times \mathrm{SU}(2)_L$ is completely similar and can be performed independently, after some general discussions we will almost exclusively focus on the $\mathrm{SU}(2)_R$ part of the symmetry transformations and various corresponding quantities for clarity of presentations.

In the saddle point approximation scheme we are employing, we cannot directly deal with the vertex operator: What we can deal with are the classical solutions produced by the vertex operators carrying large charges. Therefore we need to extract the information of the quantum vertex operators indirectly through such classical solutions.

For definiteness, we first focus on a solution with diagonal $\mathrm{SU}(2)_R \times \mathrm{SU}(2)_L$ charges describing a two-point function of an operator built on the $\mathrm{tr}\,(Z^l)$-vacuum ($\mathcal{O}_1$ and $\mathcal{O}_3$ in section 4.1) and its conjugate[26]. In what follows, we shall denote such a solution by $\mathbb{Y}^{\mathrm{diag}}$. Then we can associate a pair of polarization spinors $\mathfrak{p}_Z$ and $\tilde{\mathfrak{p}}_Z$ and the raising operators (7.3.15) to the vertex operator that produces the solution. For convenience, we display them again with appropriate renaming:

$$\mathfrak{p}^{\mathrm{diag}} = \begin{pmatrix} 0 \\ 1 \end{pmatrix}, \qquad \tilde{\mathfrak{p}}^{\mathrm{diag}} = \begin{pmatrix} 1 \\ 0 \end{pmatrix}, \tag{7.3.26}$$

$$K^{\mathrm{diag}}(\beta) = \begin{pmatrix} 1 & \beta \\ 0 & 1 \end{pmatrix}, \qquad \tilde{K}^{\mathrm{diag}}(\tilde{\beta}) = \begin{pmatrix} 1 & 0 \\ \tilde{\beta} & 1 \end{pmatrix}. \tag{7.3.27}$$

All the solutions describing a two-point function of mutually conjugate operators, $\langle \mathcal{O}\overline{\mathcal{O}} \rangle$, can be obtained from this basic solution $\mathbb{Y}^{\mathrm{diag}}$ by an $\mathrm{SU}(2)_R \times \mathrm{SU}(2)_L$ transformation[27]. Since a normalized three-point function in the gauge theory can be obtained by dividing an

[26] Here the "conjugation" means the usual complex conjugation of the fields, $Z \to \bar{Z}$ and $X \to \bar{X}$.

[27] This class of solutions include the one-cut solutions (7.1.34) in section 7.1.3.

unnormalized one by $\langle \mathcal{O}\overline{\mathcal{O}}\rangle$-type two-point functions as

$$\frac{\langle \mathcal{O}_i \mathcal{O}_j \mathcal{O}_k\rangle}{\sqrt{\langle \mathcal{O}_i \overline{\mathcal{O}}_i\rangle\langle \mathcal{O}_j \overline{\mathcal{O}}_j\rangle\langle \mathcal{O}_k \overline{\mathcal{O}}_k\rangle}}\,, \tag{7.3.28}$$

the aforementioned solutions, to be called *reference solutions*, play an important role to obtain a correctly normalized wave function. Below, we will denote them by $\mathbb{Y}^{\rm ref}$. A distinctive feature of such solutions is that they are real-valued when expressed in terms of the Minkowski worldsheet variables. This qualification will be extremely important since the equation of motion is actually invariant under a larger group $\mathrm{SL}(2,\mathrm{C})_R \times \mathrm{SL}(2,\mathrm{C})_L$ and its action can produce "complex" solutions which signify tunneling. Such a tunneling process is necessary for the three-point interactions to take place, as we shall see.

From now on till the end of this subsection, we shall suppress all the left transformations and display only the right transformations. The results for the left transformations will be summarized later in this subsection.

Now consider a three-point function produced by vertex operators, corresponding to the gauge theory operators, inserted at z_i on the worldsheet. We will take the operators to be those obtained by SO(4) rotations of the operators built on the $\mathrm{tr}\,(Z^l)$-vacuum. This suffices for the present purpose since such three-point functions include[28] the ones discussed in section 4.1.

Although the saddle point solution for such a three-point function is so far not available explicitly, let us denote the solution in the vicinity of z_i by $\mathbb{Y}$. Asymptotically as $z \to z_i$ such a configuration must be well-approximated by a two-point reference solution $\mathbb{Y}^{\rm ref}$, which is produced by the *same* vertex operator. Even if they are produced by the same vertex operator, $\mathbb{Y}$ and $\mathbb{Y}^{\rm ref}$ are different since $\mathbb{Y}$ is influenced non-trivially and dynamically by the other two vertex operators present. We write the transformation between them at $z \simeq z_i$ as[29]

$$\mathbb{Y}(z \simeq z_i) = \mathbb{Y}^{\rm ref} V \qquad (z \to z_i)\,, \qquad V \in \mathrm{SL}(2,\mathrm{C})_R\,. \tag{7.3.29}$$

This relative difference is the quantity of interest since we need to normalize the three-point function by the two-point functions. In general V belongs to $\mathrm{SL}(2,\mathrm{C})_R \supset \mathrm{SU}(2)_R$, since the three-point interaction is necessarily a tunneling process. In contrast the reference solution $\mathbb{Y}^{\rm ref}$ can be obtained from $\mathbb{Y}^{\rm diag}$ by a transformation belonging to $\mathrm{SU}(2)_R$ in the form

$$\mathbb{Y}^{\rm ref} = \mathbb{Y}^{\rm diag} U^{\rm ref}\,, \qquad U^{\rm ref} \in \mathrm{SU}(2)_R\,. \tag{7.3.30}$$

[28] Note that $\mathcal{O}_1$ and $\mathcal{O}_3$ in section 4.1 are built on the $\mathrm{tr}\,(Z^l)$-vacuum while $\mathcal{O}_2$ can be obtained from the operator built on $\mathrm{tr}\,(Z^l)$ by an SO(4) rotation (7.3.25), which effects $(Z, X) \to (\bar{Z}, -\bar{X})$.

[29] Note that $\mathbb{Y}^{\rm ref}$ is the solution for the two-point function, expressed globally in terms of the cylinder coordinate. Thus we need to express $\mathbb{Y}$ in terms of the local coordinate $\left(\tau^{(i)}, \sigma^{(i)}\right)$ given in (7.1.82) to compare two solutions.

The relation among $\mathbb{Y}$, $\mathbb{Y}^{\rm ref}$ and $\mathbb{Y}^{\rm diag}$ is summarized pictorially in Figure 7.3.1.

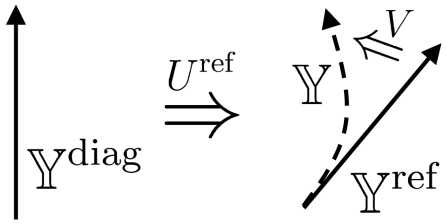

Figure 7.3.1: Schematic relation among $\mathbb{Y}$, $\mathbb{Y}^{\rm ref}$ and $\mathbb{Y}^{\rm diag}$. $\mathbb{Y}^{\rm ref}$ is obtained from $\mathbb{Y}^{\rm diag}$ by the *real* global transformation while $\mathbb{Y}$ is obtained from $\mathbb{Y}^{\rm ref}$ by the *complexified* global transformation.

Now just as we did already for the solution $\mathbb{Y}^{\rm diag}$, we can associate to the solution $\mathbb{Y}^{\rm ref}$ the polarization spinor $\mathfrak{p}^{\rm ref}$ and the raising transformation $K^{\rm ref}$ which leaves it invariant. Then from the general formula (7.3.24) and (7.3.18) we can express them in terms of the quantities associated to the diagonal solution as

$$\mathfrak{p}^{\rm ref} = (U^{\rm ref})^t \mathfrak{p}^{\rm diag}\,, \tag{7.3.31}$$

$$K^{\rm ref}(\beta) = (U^{\rm ref})^{-1} K^{\rm diag}(\beta) U^{\rm ref}\,. \tag{7.3.32}$$

By the same token we can associate the polarization spinor $\mathfrak{p}$ and the raising transformation K to the local solution $\mathbb{Y}$. However since $\mathbb{Y}$ is produced by the same vertex operator as $\mathbb{Y}^{\rm ref}$, we must have $\mathfrak{p} = \mathfrak{p}^{\rm ref}$. On the other hand, K is given by $K(\beta) = V^{-1} K^{\rm ref}(\beta) V$, as in (7.3.32), since $\mathbb{Y}$ is obtained by performing the transformation V to $\mathbb{Y}^{\rm ref}$. Since $K(\beta)$ must leave $\mathfrak{p}$, which is equal to $\mathfrak{p}^{\rm ref}$, invariant, the following identity must hold for some β':

$$V^{-1} K^{\rm ref}(\beta) V = K^{\rm ref}(\beta')\,. \tag{7.3.33}$$

Substituting the relation (7.3.32), we get

$$\begin{aligned} &(V')^{-1}\, K^{\rm diag}(\beta) V' = K^{\rm diag}(\beta')\,, \\ &V' \equiv U^{\rm ref} V (U^{\rm ref})^{-1}\,. \end{aligned} \tag{7.3.34}$$

This means that the operator V' transforms a raising operator into a raising operator for the diagonal solution. Using the explicit form of $K^{\rm diag}$ (7.3.27), it is not difficult to show that the general form of such an operator is $\begin{pmatrix} a & b \\ 0 & a^{-1} \end{pmatrix}$. Note that this contains a scale transformation which is in $\mathrm{SL}(2,\mathrm{C})_R$ but not in $\mathrm{SU}(2)_R$. From this result we can solve for

V and its inverse and obtain the following useful representations

$$V = (U^{\text{ref}})^{-1} \begin{pmatrix} a & b \\ 0 & a^{-1} \end{pmatrix} U^{\text{ref}}\,, \tag{7.3.35}$$

$$V^{-1} = (U^{\text{ref}})^{-1} \begin{pmatrix} a^{-1} & -b \\ 0 & a \end{pmatrix} U^{\text{ref}}\,. \tag{7.3.36}$$

At this stage we need not know the actual values of a and b in these formulas. b will turn out to be irrelevant and a will be expressed in terms of certain Wronskians.

Construction of the wave function for the right sector

We are now ready for the construction of the wave function for the right sector using the formula for the shift of the angle variable ϕ_R given in (7.3.5).

First we need to fix the normalization vector n appearing in that formula. As we shall show, the answer is that it coincides precisely with the polarization spinor n introduced from the group theoretical point of view in (7.3.19) in subsection 7.3.2. Recall that the zeros of $n \cdot \psi(x)$, where ψ is the Baker-Akhiezer vector and n is the normalization vector, determines the angle variables. When one makes a global $\mathrm{SL}(2,\mathrm{C})_R$ transformation V_R on the string solution $\mathbb{Y}$ like $\mathbb{Y} \to \mathbb{Y}V_R$, the Baker-Akhiezer vector transforms like $\psi \to V_R^{-1}\psi$. In particular, take V_R to be the raising operator K under which the vertex operator producing the solution $\mathbb{Y}$ is invariant. Then the wave function corresponding to the vertex operator and hence the angle variables comprising it must also be invariant. This means that the zeros of $n\cdot(K^{-1}\psi) = (K^t n)\cdot\psi$ must coincide with the zeros of $n\cdot\psi$ and hence we must have $K^t n \propto n$. However since K is similar to K^{diag}, it is clear that the constant of proportionality can only be unity and n must satisfy $K^t n = n$. This, however, is nothing but the definition of the polarization spinor given in (7.3.19). In other words, the proper choice of the normalization vector for constructing the wave function is precisely the polarization spinor associated to the vertex operator to which the wave function corresponds. Therefore, we arrive at the following crucial relation,

$$\text{Normalization vector } (n) \quad = \quad \text{Polarization spinor } (\mathfrak{p})\,. \tag{7.3.37}$$

Thus, we will henceforth denote the polarization spinors also by n. Note that various formulas derived so far for the polarization spinors are valid also for the normalization vectors.

Having found the proper choice of the normalization vector in the formula (7.3.5) for the shift of the angle variable ϕ_R, what remains to be understood is how to evaluate the inner products $n\cdot\psi_\pm(\infty)$ and $n\cdot\psi_\pm^{\text{ref}}(\infty)$. Corresponding to the relation (7.3.29), in the vicinity of

z_i, $\psi_\pm$ and $\psi_\pm^{\rm ref}$ are related by the constant transformation V as $\psi_\pm(z \simeq z_i) = V^{-1}\psi_\pm^{\rm ref}(z \simeq z_i)$. Now recall the form of the ALP for the right sector given in (7.1.2). We see that for $x = \infty$ the coefficients of the connections j_z and $j_{\bar z}$ vanish and hence the solutions $\psi_\pm(x = \infty)$ and $\psi_\pm^{\rm ref}(x = \infty)$ themselves become constant. Combining these pieces of information, we obtain the relation

$$\psi_\pm(\infty) = V^{-1}\psi_\pm^{\rm ref}(\infty)\,. \tag{7.3.38}$$

The right hand side can be evaluated using the representation (7.3.36) as

$$\psi_\pm(\infty) = (U^{\rm ref})^{-1}\begin{pmatrix} a^{-1} & -b \\ 0 & a \end{pmatrix} U^{\rm ref}\psi_\pm^{\rm ref}(\infty) = (U^{\rm ref})^{-1}\begin{pmatrix} a^{-1} & -b \\ 0 & a \end{pmatrix}\psi_\pm^{\rm diag}(\infty)\,, \tag{7.3.39}$$

where $\psi_\pm^{\rm diag}(x)$ is the Baker-Akhiezer vector for $\mathbb{Y}^{\rm diag}$, which is related to $\psi_\pm^{\rm ref}(x)$ by

$$\psi_\pm^{\rm ref}(x) = \left(U^{\rm ref}\right)^{-1}\psi_\pm^{\rm diag}(x)\,. \tag{7.3.40}$$

We now need to know $\psi_\pm^{\rm diag}(\infty)$, which are the eigenstates of the monodromy matrix near $x = \infty$ corresponding to the eigenvalues $e^{\pm ip(x)}$. For a charge-diagonal solution $\mathbb{Y}^{\rm diag}$, the monodromy matrix near $x = \infty$ is diagonal and hence is either of the form (a) $\mathrm{diag}\,(e^{ip(x)}, e^{-ip(x)})$ or (b) $\mathrm{diag}\,(e^{-ip(x)}, e^{ip(x)})$, depending on the solution. For the case (a) the eigenvectors are $\psi_+^{\rm diag}(\infty) = (1, 0)^t, \psi_-^{\rm diag}(\infty) = (0, 1)^t$, while for the case (b) their forms are swapped. Since $\mathbb{Y}^{\rm diag}$ is produced by the vertex operator with the definite polarization spinor specified in (7.3.26), there should be a definite answer. To determine the proper choice of (a) or (b), we need to construct the wave function for each choice and see if it has the same transformation property as the corresponding operator in the gauge theory. As it will be checked later in this subsection, it turned out that the case (b) is the correct choice. Therefore we will take

$$\psi_+^{\rm diag}(\infty) = \begin{pmatrix} 0 \\ 1 \end{pmatrix}\,, \qquad \psi_-^{\rm diag}(\infty) = \begin{pmatrix} 1 \\ 0 \end{pmatrix}\,. \tag{7.3.41}$$

Substituting them into (7.3.39), we obtain the important relations

$$\psi_+(\infty) = (U^{\rm ref})^{-1}\left(a\psi_+^{\rm diag}(\infty) - b\psi_-^{\rm diag}(\infty)\right) = a\psi_+^{\rm ref}(\infty) - b\psi_-^{\rm ref}(\infty)\,, \tag{7.3.42}$$

$$\psi_-(\infty) = (U^{\rm ref})^{-1}a^{-1}\psi_-^{\rm diag}(\infty) = a^{-1}\psi_-^{\rm ref}(\infty)\,. \tag{7.3.43}$$

As for the polarization spinor, observe that by inspection the following relation holds:

$$n^{\rm diag} = (-i\sigma_2)\psi_-^{\rm diag}(\infty)\,. \tag{7.3.44}$$

This relation is actually universally satisfied for any reference solutions. To see this, let us act $(U^{\rm ref})^t$ from left. Then the relation becomes

$$\begin{aligned}\big(\,(U^{\rm ref})^t n^{\rm diag} = \big)\; n^{\rm ref} &= (U^{\rm ref})^t(-i\sigma_2)\psi_-^{\rm diag}(\infty)\\ &= (-i\sigma_2)(U^{\rm ref})^{-1}\psi_-^{\rm diag}(\infty)\\ &= -i\sigma_2\psi_-^{\rm ref}(\infty)\,,\end{aligned} \tag{7.3.45}$$

where we used the identity $\sigma_2(U^{\rm ref})^t\sigma_2 = (U^{\rm ref})^{-1}$. On the other hand, for the solution $\mathbb{Y}$, which describes the three-point function, the relation is slightly modified. In fact, using the formula (7.3.43) we get the relation

$$n = -ia\sigma_2\psi_-(\infty)\,. \tag{7.3.46}$$

Compared to (7.3.45), (7.3.46) contains an additional prefactor a. This factor will be extremely important as we shall see below.

Let us now recall the formula (7.3.5) for the shift of the angle variable ϕ_R. Displaying it again for convenience, it is of the form

$$\Delta\phi_R = -i\ln\left(\frac{(n\cdot\psi_+(\infty))(n\cdot\psi_-^{\rm ref}(\infty))}{(n\cdot\psi_+^{\rm ref}(\infty))(n\cdot\psi_-(\infty))}\right)\,. \tag{7.3.47}$$

From (7.3.42) and (7.3.45), we can write $n\cdot\psi_+(\infty) = an\cdot\psi_+^{\rm ref}(\infty)$. As for $n\cdot\psi_-(\infty)$, use of (7.3.43) gives $n\cdot\psi_-(\infty) = a^{-1}n\cdot\psi_-^{\rm ref}(\infty)$. Now due to the relation (7.3.45), the quantity $n\cdot\psi_-(\infty) = n^{\rm ref}\cdot\psi_-(\infty)$, which appears both in the numerator and the denominator of the formula (7.3.47), vanishes. Therefore we must first regularize n slightly to make the quantity $n\cdot\psi_-(\infty)$ finite, cancel them in the formula and then remove the regularization. As for the same quantity appearing in $n\cdot\psi_+(\infty)$, we can safely set it to zero from the beginning since $n\cdot\psi_+^{\rm ref}(\infty)$ is non-vanishing. In this way we find that $n\cdot\psi_\pm^{\rm ref}(\infty)$'s all cancel out and we are left with an extremely simple formula for $\Delta\phi_R$ given by

$$\Delta\phi_R = -i\ln a^2\,. \tag{7.3.48}$$

Note that the shift depends only on the quantity a, which parametrizes the scale transformation not belonging to $\mathrm{SU}(2)_R$, showing the tunneling nature of the effect.

Let us now write the formula (7.3.46) for the operator at z_i with a subscript i as $n_i = -ia_i\sigma_2 i_-(\infty)$. Then, from the definition of the Wronskian we obtain $\langle n_i, n_j\rangle = a_i a_j\langle i_-, j_-\rangle\big|_\infty$. Writing out all the relations of this form and forming appropriate ratios, we can easily extract out each a_i^2. The result can be written in a universal form as

$$a_i^2 = \frac{\langle j_-, k_-\rangle}{\langle i_-, j_-\rangle\langle k_-, i_-\rangle}\bigg|_\infty \frac{\langle n_i, n_j\rangle\langle n_k, n_i\rangle}{\langle n_j, n_k\rangle}\,. \tag{7.3.49}$$

Then substituting this expression into the formula (7.3.48) we obtain the shift of the angle variable ϕ_R at the position z_i as

$$e^{i\Delta\phi_{R,i}} = \frac{\langle j_-, k_-\rangle}{\langle i_-, j_-\rangle\langle k_-, i_-\rangle}\bigg|_\infty \frac{\langle n_i, n_j\rangle\langle n_k, n_i\rangle}{\langle n_j, n_k\rangle}\,. \tag{7.3.50}$$

This formula is remarkable in that it cleanly separates the kinematical part composed of $\langle n_i, n_j\rangle$ and the dynamical part described by $\langle i_-, j_-\rangle\big|_\infty$.

As the last step of the construction of the wave function, we need to pay attention to the convention of [41] that we are adopting. In that work, the Poisson bracket is defined to be $\{p, q\} = 1$ for the usual momentum p and the coordinate q. In this convention the Poisson bracket of the action angle variables was worked out to be given by $\{\phi, S\} = 1$. In other words the action variable S corresponds to q and the angle variable ϕ corresponds to p. Therefore upon quantization in the angle variable representation, we must set $S = i\partial/\partial\phi$. This means that the wave function that carries charge S is given by $e^{-iS\phi}$, *not* by $e^{iS\phi}$.

Recalling the relation (3.2.56) between the action variable S_∞ and the right charge R, namely $S_\infty = -R$, and employing the formula (7.3.50), the contribution to the wave function from the right sector is obtained as

$$\Psi_R^{S^3} = \exp\left(-i\sum_{i=1}^{3}(-R_i)\,\Delta\phi_{R,i}\right) = \prod_{\{i,j,k\}}\left(\frac{\langle n_i, n_j\rangle}{\langle i_-, j_-\rangle\big|_\infty}\right)^{R_i+R_j-R_k}\,, \tag{7.3.51}$$

where $\{i, j, k\}$ denotes the cyclic permutations of $\{1, 2, 3\}$.

At this stage, let us confirm that the wave function so constructed indeed carries the correct charge. To see this, it suffices to consider the U(1) transformation which corresponds to the diagonal right-charge rotations. Let us examine the case of the charge-diagonal operator built upon the Z-type vacuum, such as $\mathcal{O}_1$ or $\mathcal{O}_3$ in section 4.1. In such a case the reference state is the charge-diagonal state itself, hence $U^{\rm ref} = 1$. Then if we set $a = e^{i\theta/2}, b = 0$ in the formula (7.3.35), the $\mathrm{SU}(2)_R$ transformation matrix V becomes diag $(e^{i\theta/2}, e^{-i\theta/2})$, which is a U(1) transformation under which Z and $\bar{Z}$, carrying the right charge $1/2$ and $-1/2$ respectively, transform as $Z \to e^{i\theta/2}Z$ and $\bar{Z} \to e^{-i\theta/2}$. Now according to (7.3.48), under such a transformation the wave function acquires the phase $e^{-i(-R)\ln a^2} = e^{iR\theta}$. This shows that the wave function has the same (positive) charge R as the operator of the form tr (Z^{2R}). This proves that the choice of $\psi_\pm^{\rm diag}(\infty)$ we made in (7.3.41) is the correct one. If we had made the other choice, the wave function would have acquired the phase $e^{-iR\theta}$, which contradicts the fact that the corresponding operator in the gauge theory is built on the tr (Z^ℓ)-vacuum and hence has the positive right charge. Similar argument can be made for the left sector and again one can check that the wave function (7.3.51) carries the correct charges.

Contribution of the left sector and complete wave function for the S^3 part

We now briefly describe the analysis for the left sector, to complete the construction of the wave function for the S^3 part.

The procedure is exactly the same as for the right sector but there are a couple of notable differences. First, the transformation matrices act from the left and consequently in various formulas the matrices are replaced by their inverses. In particular, the formulas corresponding to (7.3.35) and (7.3.38) for the transformation $\tilde{V}$ that connects three-point solution and the reference solution in the manner $\mathbb{Y} = \tilde{V}\mathbb{Y}^{\text{ref}}$ take the form

$$\tilde{V} = \tilde{U}^{\text{ref}} \begin{pmatrix} a & 0 \\ b & a^{-1} \end{pmatrix} (\tilde{U}^{\text{ref}})^{-1} , \tag{7.3.52}$$

$$\tilde{\psi}_{\pm}(0) = \tilde{V}\tilde{\psi}^{\text{ref}}_{\pm}(0) , \tag{7.3.53}$$

where $\tilde{U}^{\text{ref}} \in \text{SU}(2)_L$ is the matrix effecting the connection $\mathbb{Y}^{\text{ref}} = \tilde{U}^{\text{ref}}\mathbb{Y}^{\text{diag}}$. Second, the raising matrix for the diagonal solution is now lower triangular, namely

$$\tilde{K}^{\text{diag}}(\beta) = \begin{pmatrix} 1 & 0 \\ \beta & 1 \end{pmatrix} . \tag{7.3.54}$$

Thirdly, the polarization spinor for Z is $\tilde{n}^{\text{diag}} = (1, 0)^t$, as discussed in (7.3.23). Lastly, because of the form of the ALP for the left sector, the Baker-Akhiezer vector becomes coordinate-independent at $x = 0$ instead of at $x = \infty$.

Let us now list the basic results for the left sector, omitting the intermediate details. Just as for the right sector, the formulas below are valid for any type of operator.

$$\psi^{\text{diag}}_{+} = \begin{pmatrix} 0 \\ 1 \end{pmatrix} , \qquad \psi^{\text{diag}}_{-} = \begin{pmatrix} 1 \\ 0 \end{pmatrix} , \tag{7.3.55}$$

$$\tilde{\psi}_{+}(0) = a^{-1}\tilde{\psi}^{\text{ref}}_{+}(0) + b\tilde{\psi}^{\text{ref}}_{-}(0) , \qquad \tilde{\psi}_{-}(0) = a\tilde{\psi}^{\text{ref}}_{-}(0) , \tag{7.3.56}$$

$$\tilde{n} = ai\sigma_2\tilde{\psi}_{+}(0) , \qquad \Delta\phi_L = -i \ln a^{-2} . \tag{7.3.57}$$

Using these formulas, we obtain the contribution to the wave function from the left sector as

$$\Psi^{S^3}_{L} = \exp\left(-i\sum_{i=1}^{3} L_i \Delta\phi_{L,i}\right) = \prod_{\{i,j,k\}} \left(\frac{\langle \tilde{n}_i, \tilde{n}_j\rangle}{\langle i_+, j_+\rangle\big|_0}\right)^{L_i+L_j-L_k} , \tag{7.3.58}$$

where we used the gauge invariance of the Wronskians and replaced $\langle \tilde{i}_+, \tilde{j}_+\rangle$ with $\langle i_+, j_+\rangle$. Together with $\Psi^{S^3}_{R}$ obtained in (7.3.51) we now have the complete wave function for the S^3

part. It is of the structure

$$e^{\mathcal{F}_{\text{vertex}}} = \Psi_L^{S^3}\Psi_R^{S^3}e^{\mathcal{V}_{\text{energy}}}\,,$$
$$\mathcal{F}_{\text{vertex}} = \mathcal{V}_{\text{kin}} + \mathcal{V}_{\text{dyn}} + \mathcal{V}_{\text{energy}}\,. \tag{7.3.59}$$

Let us explain each term in (7.3.59) in order. The first term $\mathcal{V}_{\text{kin}}$ stands for the kinematical part composed of the Wronskians $\langle n_i, n_j\rangle$ and $\langle \tilde{n}_i, \tilde{n}_j\rangle$,

$$\begin{aligned}\mathcal{V}_{\text{kin}} =& \\ &(R_1+R_2-R_3)\ln\langle n_1,n_2\rangle + (R_2+R_3-R_1)\ln\langle n_2,n_3\rangle + (R_3+R_1-R_2)\ln\langle n_3,n_1\rangle \\ &+ (L_1+L_2-L_3)\ln\langle \tilde{n}_1,\tilde{n}_2\rangle + (L_2+L_3-L_1)\ln\langle \tilde{n}_2,\tilde{n}_3\rangle + (L_3+L_1-L_2)\ln\langle \tilde{n}_3,\tilde{n}_1\rangle\,.\end{aligned} \tag{7.3.60}$$

The second term $\mathcal{V}_{\text{dyn}}$ refers to the dynamical part consisting of the Wronskians $\langle i_-, j_-\rangle\big|_\infty$ and $\langle \tilde{i}_+, \tilde{j}_+\rangle\big|_0$,

$$\begin{aligned}\mathcal{V}_{\text{dyn}} =& \\ &-(R_1+R_2-R_3)\ln\langle 1_-,2_-\rangle\big|_\infty - (R_2+R_3-R_1)\ln\langle 2_-,3_-\rangle\big|_\infty - (R_3+R_1-R_2)\ln\langle 3_-,1_-\rangle\big|_\infty \\ &-(L_1+L_2-L_3)\ln\langle 1_+,2_+\rangle\big|_0 - (L_2+L_3-L_1)\ln\langle 2_+,3_+\rangle\big|_0 - (L_3+L_1-L_2)\ln\langle 3_+,1_+\rangle\big|_0\,.\end{aligned} \tag{7.3.61}$$

The last term $\mathcal{V}_{\text{energy}}$ denotes the contribution involving the worldsheet energy shown in the last term of (7.3.2). Such a term is necessary to account for the time evolution of the wave functions since we evaluate the wave function at $\tau^{(i)} = 0$, which corresponds to $\ln|z-z_i| = \ln\epsilon_i$, whereas the state-operator mapping is performed on the unit circle, $\ln|z-z_i| = 0$. As the energy of the each external state is given[30] by $2\sqrt{\lambda}\kappa_i^2$, $\mathcal{V}_{\text{energy}}$ can be evaluated explicitly as

$$\mathcal{V}_{\text{energy}} = 2\sqrt{\lambda}\sum_{i=1}^{3}\kappa_i^2\ln\epsilon_i\,. \tag{7.3.62}$$

Before ending this subsection, let us make two comments. First, it is not guaranteed at this stage that the wave function thus constructed produces a correctly normalized two-point function. In addition, as discussed in [17], there may be additional contributions which come from the canonical change of variables, $\{\mathbb{Y}, \partial_\tau\mathbb{Y}\} \to \{\phi_i, S_i\}$. However, in section 7.6.3, it will be checked that our result for the three-point function correctly reproduces the normalized two-point function in an appropriate limit. Therefore we can a posteriori confirm that the

[30]The energy can be computed from the behavior of the stress-energy tensor around the puncture (3.2.27).

wave function is completely normalized and the additional contributions are absent. Second, one recognizes that the power of $\langle n_i, n_j \rangle$, namely $R_i + R_j - R_k$, is the familiar combination, made out of conformal weights and spins, for the coordinate differences in the three-point functions of a conformal field theory, *except for the overall sign*. In the next subsection, we will elaborate on this structure of the power from the point of view of the dual gauge theory. Also in section 7.5.2, where we construct the wave function for the $EAdS_3$ part, the above difference in the overall sign will be explained.

7.3.4 Detailed relation with the operators in the gauge theory

The wave function constructed above is expressed in terms of the polarization spinors, which depend only on the type of the vacuum on which the corresponding gauge theory operator is built, the eigenvectors of the ALP in the vicinity of the insertion point z_i, and the charges carried by the vertex operators. A natural question is how we can distinguish the type of vertex operators involved from these data. Operators of $\mathcal{O}_1$ and $\mathcal{O}_2$ in section 4.1 can be distinguished by the structure of their polarization spinors because the vacuum on which they are built are different. On the other hand, operators of $\mathcal{O}_1$ and $\mathcal{O}_3$, which are built on the same type of the vacuum, are characterized by the same polarization spinors and hence it appears that one cannot distinguish them from the formula for the wave function. Since these operators differ only in the types of excitations, X or $\bar{X}$, the question is how this is reflected. The answer is in the relation between the absolute magnitude of the charges $\mathcal{R}$ and $\mathcal{L}$, which are given by R and L respectively. Because the charges carried by the operator X are $(\mathcal{R}, \mathcal{L}) = (-1/2, 1/2)$, the magnitude of the total charges of the type $\mathcal{O}_1$ operator built upon Z-vacuum with X as excitations must satisfy the inequality $R < L$. Similarly, the magnitudes of the total charges for the operator of type $\mathcal{O}_2$ also obey $R < L$. On the other hand, for the operator of type $\mathcal{O}_3$, we have $R > L$.

Such distinction is reflected not only on the charges but also on the dynamical property of the eigenstates $i_\pm$ appearing in the wave function formula. As discussed in (7.1.42) and (7.1.43), the relative magnitude of R and L for a one-cut solution is determined by the position of the cut in the quasi-momentum $p(x)$: When the real part of the position of the branch cut is in the interval $[-1, 1]$ in the spectral parameter space such a solution has $R > L$ and hence corresponds to the operator of type $\mathcal{O}_3$. Contrarily the operator of type $\mathcal{O}_1$ having $R < L$ corresponds to a solution with the cut outside the above interval. Conceptually this is quite intriguing. From the spin-chain perspective, since $\mathcal{O}_1$ and $\mathcal{O}_3$ form distinct types of spin chains not related by the $\mathrm{SU}(2)_R \times \mathrm{SU}(2)_L$ symmetry, it is difficult to describe them at the same time. On the other hand, in string theory the solutions corresponding to these distinct spin chains are described in a more unified way. It would be interesting to realize

such a unified treatment on the gauge theory side as well.

Let us next examine the role and the meaning of the kinematical factor $\mathcal{V}_{\rm kin}$ from the point of view of the dual gauge theory. In this regard, note that the quantity $\langle n_i, n_j\rangle$, being a skew product, vanishes when n_i and n_j coincide. This in fact happens for the case of the operators $\mathcal{O}_1$ and $\mathcal{O}_3$ discussed in section 4.1, which are built upon the same Z-vacuum and hence carry the same polarization spinors. In such cases, the three-point function vanishes unless the conservation laws, $R_1 + R_3 - R_2 = 0$ and $L_1 + L_3 - L_2 = 0$, are satisfied. On the gauge-theory side, the charges of the composite operator can be easily computed from the charges of the constituents (4.1.2). Then the conservation laws can be explicitly written down in terms of the length of the operator ℓ_i and the number of magnons M_i as[31]

$$\begin{aligned} R_1 + R_3 - R_2 &= M_3 + M_2 - M_1 = 0\,, \\ L_1 + L_3 - L_2 &= \frac{1}{2}(\ell_1 + \ell_3 - \ell_2) - M_3 = 0\,. \end{aligned} \tag{7.3.63}$$

This condition is precisely the same as the one we derived in section 4.1 from the Wick-contraction rule in the gauge theory.

Up to this point we have obtained the general formulas for the contribution of the action part and the wave function part, both of which are expressed in terms of the Wronskians of the form $\langle i_\pm, j_\pm\rangle$. In the next section we will evaluate these quantities to substantiate the general formulas.

7.4 Evaluation of the Wronskians

In the previous two sections, we have shown that both the contribution of the action and that of the vertex operators are expressible in terms of the Wronskians $\langle i_\pm, j_\pm\rangle$ between the eigenvectors of the monodromy matrices. The goal of this section is to evaluate those Wronskians. First, in section 7.4.1, we show that certain products of Wronskians are expressed in terms of the quasi-momenta. Next, in sections 7.4.2 and 7.4.3, we determine the analytic properties (*i.e.* poles and zeros) of each Wronskian as a function of the spectral parameter x. With such a knowledge, we apply, in section 7.4.4, a generalized version of the Wiener-Hopf decomposition formula to the products of the Wronskians and determine the individual factor. Finally, in section 7.4.5, we compute the singular part and the constant part of the Wronskian, which cannot be determined by the Wiener-Hopf method.

[31] Recall that R and L are *absolute magnitudes* of the charges.

7.4.1 Products of Wronskians in terms of quasi-momenta

To obtain the information of the Wronskian $\langle i_\pm, j_\pm \rangle$ between the eigenvectors of the ALP at different points, we need some condition which governs the global property of such Wronskians. As we shall see, such a condition is provided by the global consistency condition for the product of the local monodromy matrices Ω_i associated with the vertex insertion points z_i. Since the total monodromy must be trivial upon going around the entire worldsheet, we must have

$$\Omega_1 \Omega_2 \Omega_3 = 1 \,. \tag{7.4.1}$$

Although this appears to be a rather weak condition, it is sufficiently powerful to determine the forms of certain products of the Wronskians in terms of the quasi-momenta $p_i(x)$, as discussed in [16, 105]. Let us quickly reproduce those expressions. Take the basis in which Ω_1 is diagonal, namely

$$\Omega_1 = \begin{pmatrix} e^{ip_1} & 0 \\ 0 & e^{-ip_1} \end{pmatrix} . \tag{7.4.2}$$

Since the set of eigenvectors $j_\pm$ at z_j form a complete basis, one can expand the eigenvectors $i_\pm$ at z_i in terms of them in the following way:

$$i_\pm = \langle i_\pm \,, j_- \rangle j_+ - \langle i_\pm \,, j_+ \rangle j_- \,. \tag{7.4.3}$$

Making use of this formula, Ω_2 can be expressed in the Ω_1-diagonal basis as

$$\Omega_2 = M_{12} \begin{pmatrix} e^{ip_2} & 0 \\ 0 & e^{-ip_2} \end{pmatrix} M_{21} \,, \tag{7.4.4}$$

where the matrix M_{ij}, effecting the change of basis, is given by

$$M_{ij} = \begin{pmatrix} -\langle i_- \,, j_+ \rangle & -\langle i_- \,, j_- \rangle \\ \langle i_+ \,, j_+ \rangle & \langle i_+ \,, j_- \rangle \end{pmatrix} . \tag{7.4.5}$$

Now owing to the constraint (7.4.1), Ω_1 and Ω_2 must satisfy the following relation:

$$\mathrm{tr}\ (\Omega_1 \Omega_2) = \mathrm{tr}\, \Omega_3^{-1} = 2 \cos p_3 \,. \tag{7.4.6}$$

Substituting the equations (7.4.2) and (7.4.4) into (7.4.6), we obtain an equation for $\langle 1_\pm \,, 2_\pm \rangle$ of the form

$$\cos\left(p_1 - p_2\right) \langle 1_+ \,, 2_+ \rangle \langle 1_- \,, 2_- \rangle - \cos\left(p_1 + p_2\right) \langle 1_+ \,, 2_- \rangle \langle 1_- \,, 2_+ \rangle = \cos p_3 \,. \tag{7.4.7}$$

This equation, together with the Schouten identity[32] for $1_\pm$ and $2_\pm$ given by

$$\langle 1_+\,,2_+\rangle\langle 1_-\,,2_-\rangle - \langle 1_+\,,2_-\rangle\langle 1_-\,,2_+\rangle = \langle 1_+\,,1_-\rangle\langle 2_+\,,2_-\rangle = 1\,, \tag{7.4.8}$$

completely determines the products of Wronskians, $\langle 1_+\,,2_+\rangle\langle 1_-\,,2_-\rangle$ and $\langle 1_+\,,2_-\rangle\langle 1_-\,,2_+\rangle$. In a similar manner, products of certain other Wronskians can also be obtained, which are summarized as the following set of equations:

$$\langle 1_+\,,2_+\rangle\langle 1_-\,,2_-\rangle = \frac{\sin\frac{p_1+p_2+p_3}{2}\sin\frac{p_1+p_2-p_3}{2}}{\sin p_1 \sin p_2}\,, \tag{7.4.9}$$

$$\langle 2_+\,,3_+\rangle\langle 2_-\,,3_-\rangle = \frac{\sin\frac{p_1+p_2+p_3}{2}\sin\frac{-p_1+p_2+p_3}{2}}{\sin p_2 \sin p_3}\,, \tag{7.4.10}$$

$$\langle 3_+\,,1_+\rangle\langle 3_-\,,1_-\rangle = \frac{\sin\frac{p_1+p_2+p_3}{2}\sin\frac{p_1-p_2+p_3}{2}}{\sin p_3 \sin p_1}\,, \tag{7.4.11}$$

$$\langle 1_+\,,2_-\rangle\langle 1_-\,,2_+\rangle = \frac{\sin\frac{p_1-p_2+p_3}{2}\sin\frac{p_1-p_2-p_3}{2}}{\sin p_1 \sin p_2}\,, \tag{7.4.12}$$

$$\langle 2_+\,,3_-\rangle\langle 2_-\,,3_+\rangle = \frac{\sin\frac{p_1+p_2-p_3}{2}\sin\frac{-p_1+p_2-p_3}{2}}{\sin p_2 \sin p_3}\,, \tag{7.4.13}$$

$$\langle 3_+\,,1_-\rangle\langle 3_-\,,1_+\rangle = \frac{\sin\frac{-p_1+p_2+p_3}{2}\sin\frac{-p_1-p_2+p_3}{2}}{\sin p_3 \sin p_1}\,. \tag{7.4.14}$$

What we need for the computation of the three-point functions, however, are the individual Wronskians and not just the products given in (7.4.9)–(7.4.14). Such a knowledge will be extracted based on the analytic properties of the Wronskians regarded as functions of the complex spectral parameter x. We will analyze such properties in the next two subsections.

7.4.2 Analytic properties of the Wronskians I: Poles

An individual Wronskian, viewed as a function of x, is almost uniquely determined[33] by its analytic properties, namely the positions of the poles and the zeros. From the expressions exhibited in (7.4.9)–(7.4.14), we know that the products of Wronskians have poles at $\sin p_i = 0$ and zeros at $\sin\left((\pm p_1 \pm p_2 \pm p_3)/2\right) = 0$. Therefore the question is which factor of the product is responsible for such a pole and/or a zero. In this subsection, we will describe how to analyze the structure of the poles.

[32] The general form of the Schouten identity is given by $\langle i\,,j\rangle\langle k\,,l\rangle + \langle i\,,k\rangle\langle j\,,l\rangle + \langle i\,,l\rangle\langle j\,,k\rangle = 0$. It can be proven directly from the definition of the Wronskians.

[33] As we will discuss later, the Wronskian also contains essential singularities at $x = \pm 1$. In addition, an overall proportionality constant cannot be determined by the positions of zeros and poles. These ambiguities will be fixed in section 7.4.5.

To illustrate the basic idea, we will consider the Wronskians $\langle 1_+\,, 2_+\rangle$ and $\langle 1_-\,, 2_-\rangle$ as examples, for which the product is given by

$$\langle 1_+\,, 2_+\rangle\langle 1_-\,, 2_-\rangle = \frac{\sin\frac{p_1+p_2+p_3}{2}\sin\frac{p_1+p_2-p_3}{2}}{\sin p_1 \sin p_2}\,.$$

Let us focus on the pole associated with $\sin p_1 = 0$ and denote the position of the pole by $x_{\rm pole}$. There are two types of points at which $\sin p_1$ vanishes, the branch points and the "singular points". First consider the case where $x_{\rm pole}$ is a singular point, at which the two eigenvalues of the monodromy matrix Ω_1 degenerate to either $+1$ or -1. This, however, does not mean that Ω_1 is proportional to the unit matrix for the following reason: If $\Omega_1 \propto 1$, the monodromy condition $\Omega_1\Omega_2\Omega_3 = 1$ forces p_2 to be equal to $+p_3$ or $-p_3$ modulo π. However, since p_1, p_2 and p_3 can be chosen completely independently, there is no reason for such special relation to hold. Thus, the only remaining possibility is that the monodromy matrix Ω_1 takes the form of a Jordan-block at $x = x_{\rm pole}$, namely,

$$\Omega_1(x_{\rm pole}) \sim \pm \begin{pmatrix} 1 & c \\ 0 & 1 \end{pmatrix}\,. \tag{7.4.15}$$

In this case, the eigenvectors 1_+ and 1_- degenerate at $x = x_{\rm pole}$ and we have one eigenvector.

To see what happens at $x = x_{\rm pole}$ more explicitly, let us study the asymptotic behavior of $1_\pm$ near z_1. In the vicinity of each puncture, the saddle point solution for the three-point function can be well-approximated by an appropriate solution for a two-point function. Consequently, the eigenvectors for the three-point function $1_\pm$ can also be approximated near z_1 by the eigenvectors for the two-point function $1_\pm^{\rm 2pt}$. As shown in (7.1.81), this structure can be seen most transparently in the Pohlmeyer gauge. Working out the subleading corrections, we obtain the following expansion for the eigenfunctions $\hat{1}_\pm$:

$$\hat{1}_+ = \hat{1}_+^{\rm 2pt}\left(1 + c_1(\sigma, x)e^{a_1\tau^{(1)}} + c_2(\sigma^{(1)}, x)e^{a_2\tau^{(1)}} + \cdots\right)\,, \tag{7.4.16}$$

$$\hat{1}_- = \hat{1}_-^{\rm 2pt}\left(1 + \tilde{c}_1(\sigma^{(1)}, x)e^{\tilde{a}_1\tau^{(1)}} + \tilde{c}_2(\sigma^{(1)}, x)e^{\tilde{a}_2\tau^{(1)}} + \cdots\right)\,. \tag{7.4.17}$$

Here $\tau^{(1)}$ and $\sigma^{(1)}$ are the local coordinates near z_1 given in (7.1.82) and c_k and $\tilde{c}_k$ are 2×2 matrices dependent only on $\sigma^{(1)}$ and x. The constants a_k in the exponents are such that successive terms are becoming smaller by exponential factors as $\tau \to -\infty$. An important observation is that since $\hat{1}_\pm^{\rm 2pt}$ are eigenfunctions corresponding to a two-point function, they are insensitive to the global monodromy constraint (7.4.1) on the three-point function and hence non-singular at $x = x_{\rm pole}$. An apparent puzzle now is how exponentially small corrections can produce the degeneracy of $\hat{1}_\pm$.

The answer is the following. Since one of the eigenvectors $\hat{1}_\pm^{\rm 2pt}$ is exponentially increasing (*i.e.* big) and the other is decreasing (*i.e.* small) as $\tau \to -\infty$, let us consider the case where

$\hat{1}_+^{\rm 2pt}$ is big and $\hat{1}_-^{\rm 2pt}$ is small. Now for $\hat{1}_\pm$ to become degenerate at $x = x_{\rm pole}$, logically there are three possibilities

$$(a) \qquad \hat{1}_+ = \alpha \hat{1}_- \,, \qquad \alpha = \text{finite}\,, \tag{7.4.18}$$

$$(b) \qquad \hat{1}_+ = \beta \hat{1}_- \,, \qquad \beta \to \infty\,, \tag{7.4.19}$$

$$(c) \qquad \hat{1}_- = \beta \hat{1}_+ \,, \qquad \beta \to \infty\,. \tag{7.4.20}$$

First, since $\hat{1}_+^{\rm 2pt}$, which is the leading term for 1_+, is much larger than $\hat{1}_-^{\rm 2pt}$, which is the leading term for 1_-, by assumption, the case (a) cannot occur. Now consider the case where x is slightly different from $x_{\rm pole}$. Then β is large but finite and the relations (b) or (c) must be realized approximately. But it is obvious that (b) is the only consistent relation since exponentially small eigenvector can appear in the expansion of the big eigenvector but not the other way around. Therefore we must have the situation

$$\hat{1}_+ = \hat{1}_+^{\rm 2pt} + \cdots + \beta \hat{1}_- + \cdots\,, \tag{7.4.21}$$

As $x \to x_{\rm pole}$, β diverges and (7.4.21) goes over to the relation (b). The situation is the same if $\hat{1}_-$ is the big eigenvector: Always the big eigenvector diverges at the degeneration point, while the small solution remains finite.

Similar argument can be applied to the other Wronskians, making use of the general asymptotic behavior of the eigenvectors in the Pohlmeyer gauge, which is of the form

$$\hat{i}_\pm \sim e^{\pm q(x)\tau^{(i)}} \quad (z \sim z_i)\,. \tag{7.4.22}$$

It is clear from this expression that which one of the $\hat{i}_\pm$ diverges as $z \to z_i$ is governed by the sign of the real part of the quasi-energy $q(x)$. Since the divergence of the eigenvector produces a pole on the Wronskian containing it, we can determine which Wronskian of the product is responsible for the pole with the following general rule: At $\sin p_i = 0$, the Wronskians behave as

$$\mathrm{Re}\, q(x) > 0 \Rightarrow \langle i_+\,, \bullet \rangle = \text{finite}\,, \quad \langle i_-\,, \bullet \rangle = \infty\,, \tag{7.4.23}$$

$$\mathrm{Re}\, q(x) < 0 \Rightarrow \langle i_+\,, \bullet \rangle = \infty\,, \quad \langle i_-\,, \bullet \rangle = \text{finite}\,. \tag{7.4.24}$$

Hence, for $\mathrm{Re}\, q(x) > 0$ the pole occurs in $\langle i_-\,, \bullet \rangle$, while for $\mathrm{Re}\, q(x) < 0$ it occurs in $\langle i_+\,, \bullet \rangle$.

7.4.3 Analytic properties of the Wronskians II: Zeros

Having determined the pole structure, let us next discuss the zeros of the Wronskians. The determination of the zeros is substantially more difficult since, in contrast to the poles which

are local phenomena, the zeros are determined by the global properties on the Riemann surface. As shown in the works [16, 105, 111–113], the notion of the WKB curve is one of the main tools to explore such global properties. However, as its name indicates, the WKB curve is useful only when the leading term in the WKB expansion is sufficiently accurate. For this reason, it is not powerful enough to fully determine the zeros of the Wronskians in the whole region of the spectral parameter space. In this subsection we shall introduce an appropriate generalization of the WKB curve, to be called the *exact WKB curve*, to overcome this difficulty.

WKB approximation and WKB curves

In order to motivate the generalized version, we shall first briefly review the ordinary WKB curves defined in [112].

When the expansion parameter ζ is sufficiently small, the leading term of the WKB expansion for the solutions to ALP (7.2.31) around z_i is given by

$$\hat{\psi} \sim \exp\left(\pm\frac{1}{\zeta}\int_{z_i^*}^{z}\sqrt{T}dz\right). \tag{7.4.25}$$

Of the two independent solutions given above, one is the *small solution*, which decreases exponentially as it approaches z_i and the other is the *big solution*, which increases exponentially in the same limit. In order to make the variation of the magnitude of the solution more precise, one defines the WKB curves as the curves along which the phase of the leading term (7.4.25) in the WKB expansion is constant. More explicitly, they are characterized by the equation

$$\mathrm{Im}\left(\frac{\sqrt{T}}{\zeta}dz\right) = 0\,. \tag{7.4.26}$$

By analyzing the structure of (7.4.26), one finds the following three characteristic properties of the WKB curves. (i) At generic points on the worldsheet, the WKB curves are non-intersecting. (ii) At a puncture, the WKB curves radiate in all directions from the puncture. (iii) At a zero of $T(z)$, there are three special WKB curves which radiate from the zero and separate three different regions of the WKB curves. For details, see Figure 7.4.1.

Along the WKB curve, the magnitude of the leading term in the WKB expansion (7.4.25) increases or decreases monotonically, until they reach a zero or a pole of $T(z)$. Thus, if two punctures z_i and z_j are connected by a WKB curve and the spectral parameter ζ is sufficiently small, the small solution s_i defined around z_i will grow exponentially as it approaches the other puncture z_j. In other words, the small solution s_i behaves like the big solution around

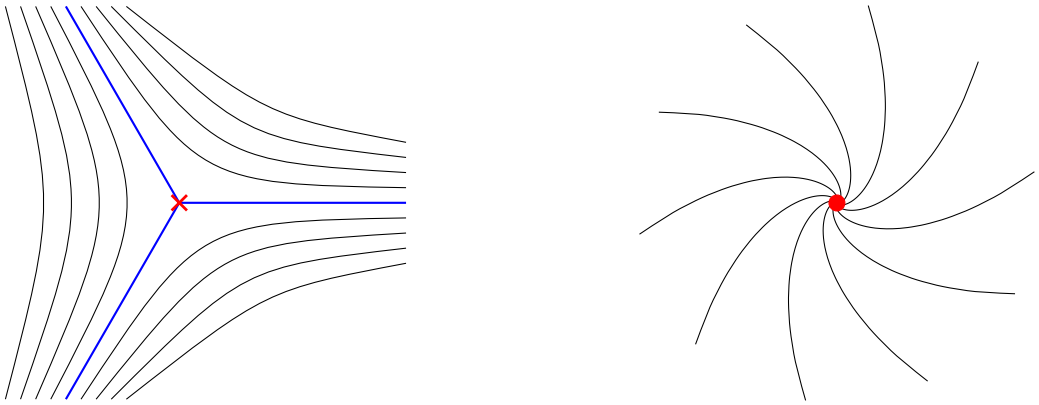

Zero Pole

Figure 7.4.1: Structures of the WKB curves around zeros and poles. The exact WKB curves, to be introduced later, also have similar structures.

z_j. Therefore s_i will be linearly independent of s_j and hence the Wronskian between these two small solutions $\langle s_i\,, s_j\rangle$ must be non-vanishing.

With this logic, we conclude that the Wronskians $\langle i_\pm\,, j_\pm\rangle$ are non-vanishing if the following three conditions are satisfied: (a) Two punctures z_i and z_j are connected by a WKB curve. (b) Two eigenvectors $i_\pm$ and $j_\pm$ are both small solutions. (c) The leading WKB solutions (7.4.25) are sufficiently accurate.

Exact WKB curves

Evidently, the analysis above is valid only in a restricted region of the spectral parameter plane where the approximation by the leading term of the WKB expansion is reliable. Actually, even if we improve the approximation by going to the next order approximation, we still cannot cover the entire spectral parameter plane because such an expansion is only an asymptotic series. It is indeed possible that as we change x the small and the big solutions interchange their roles. Such a phenomenon is clearly non-perturbative and cannot be captured by the usual expansion. So to understand the structure of the zeros on the whole spectral parameter plane, it is necessary to generalize the notion of WKB curves in a non-perturbative fashion.

In order to seek such an improvement, we need to look closely at the general structure of the conventional WKB expansion. Let us denote the components of the solution $\hat{\psi}^d$ to the

ALP in the diagonal gauge (7.2.31) as

$$\hat{\psi}^d = \begin{pmatrix} \psi^{(1)} \\ \psi^{(2)} \end{pmatrix} . \tag{7.4.27}$$

By substituting (7.4.27) into the ALP (7.2.31), we obtain the equations for the components $\psi^{(1)}$ and $\psi^{(2)}$. Then, upon eliminating $\psi^{(2)}$ in favor of $\psi^{(1)}$, we get a second-order differential equation for $\psi^{(1)}$. To solve this equation, we expand $\psi^{(1)}$ in powers of ζ in the form

$$\psi^{(1)} = \sqrt{\frac{\rho}{T} - \frac{\partial\gamma}{\sqrt{T}}} \exp\left[\int_{z_0}^{z} \left(\frac{W_{-1}}{\zeta} + W_0 + \zeta W_1 + \cdots\right)\right] . \tag{7.4.28}$$

One can then determine the one-forms W_n order by order recursively. This procedure is described in Appendix C.5.1. As a result of such a computation, we find that the WKB expansions for two linearly independent solutions to the ALP can be expressed in the following form:

$$\begin{pmatrix} f_{\pm}^{(1)} \\ f_{\pm}^{(2)} \end{pmatrix} \exp\left(\pm \int_{z_0}^{z} W_{\text{WKB}}(z, \bar{z}; \zeta)\right) . \tag{7.4.29}$$

Here $W_{\text{WKB}} \equiv W^z_{\text{WKB}} dz + W^{\bar{z}}_{\text{WKB}} d\bar{z}$ is the one-form defined as a power series in ζ, with the leading term given by $\sqrt{T}dz/(2\zeta)$. On the other hand, the functions $f_{\pm}^{(1)}$ and $f_{\pm}^{(2)}$ are defined in terms of W^z_{WKB} by

$$f_{\pm}^{(1)} \equiv k_{\text{WKB}} = \sqrt{\frac{\rho - \sqrt{T}\partial\gamma}{T\, W^z_{\text{WKB}}}} , \tag{7.4.30}$$

$$f_{\pm}^{(2)} \equiv \frac{-i}{\sqrt{W^z_{\text{WKB}}}} \left[\pm W^z_{\text{WKB}} + \left(\frac{\sqrt{T}}{2\zeta} - \frac{\rho\cos 2\gamma}{\sqrt{T}} + \frac{\partial \ln k_{\text{WKB}}}{2}\right)\right] . \tag{7.4.31}$$

With this structure in mind, we now introduce an improved notion of the WKB curve, to be called the "exact WKB curve", by writing the exact solutions to the ALP in the form

$$\hat{\psi}^d = \begin{pmatrix} f_{\text{ex}}^{(1)} \\ f_{\text{ex}}^{(2)} \end{pmatrix} \exp\left(\int_{z_0}^{z} W_{\text{ex}}(z, \bar{z}; \zeta)\right) , \tag{7.4.32}$$

where $f_{\text{ex}}^{(1)}$ and $f_{\text{ex}}^{(2)}$ are given by

$$f_{\text{ex}}^{(1)} = \sqrt{\frac{\rho - \sqrt{T}\partial\gamma}{T\, W^z_{\text{ex}}}} , \quad f_{\text{ex}}^{(2)} = \frac{-i}{\sqrt{W^z_{\text{ex}}}} \left[W^z_{\text{ex}} + \left(\frac{\sqrt{T}}{2\zeta} - \frac{\rho\cos 2\gamma}{\sqrt{T}} + \frac{\partial \ln f_{\text{ex}}^{(1)}}{2}\right)\right] . \tag{7.4.33}$$

Note that the expression (7.4.32) is identical in form to (7.4.29) with the plus sign chosen. However, there is an essential difference. While W_{WKB} is given by the asymptotic series

in powers of ζ and is hence ambiguous non-perturbatively, $W_{\rm ex}$ on the other hand is unambiguous as it is defined directly by the exact solution $\hat{\psi}$. Of course, if we expand $W_{\rm ex}$ perturbatively in powers of ζ, the series will coincide with $W_{\rm WKB}$. In this sense, $W_{\rm ex}$ can be regarded as the non-perturbative completion of $W_{\rm WKB}$. Now one of the virtues of the expression (7.4.32) is that we can easily construct another solution satisfying $\langle \hat{\psi}^d \, , \hat{\psi}'^d \rangle = 1$ by choosing the opposite the signs as

$$\hat{\psi}'^d = \begin{pmatrix} f'_{\rm ex}{}^{(1)} \\ f'_{\rm ex}{}^{(2)} \end{pmatrix} \exp\left(- \int_{z_0}^{z} W_{\rm ex}(z, \bar{z}; \zeta) \right) , \tag{7.4.34}$$

where $f'_{\rm ex}{}^{(1)}$ and $f'_{\rm ex}{}^{(2)}$ are given by

$$f'_{\rm ex}{}^{(1)} = \sqrt{\frac{\rho - \sqrt{T}\partial\gamma}{T\, W^z_{\rm ex}}} \, , \;\; f'_{\rm ex}{}^{(2)} = \frac{-i}{\sqrt{W^z_{\rm ex}}} \left[-W^z_{\rm ex} + \left(\frac{\sqrt{T}}{2\zeta} - \frac{\rho \cos 2\gamma}{\sqrt{T}} + \frac{\partial \ln f'_{\rm ex}{}^{(1)}}{2} \right) \right] . \tag{7.4.35}$$

Using the definition (7.4.32), let us now discuss the generalization of the WKB curves. The quantity $\sqrt{T}dz/\zeta$ used to define the original WKB curves is proportional to the leading term in the expansion of $W_{\rm WKB}$. Therefore the most natural generalization of the WKB curves would be to use $W_{\rm ex}$, which is a non-perturbative completion of $W_{\rm WKB}$, to define them as

$$\text{Im} \, \left(W_{\rm ex}(z; \zeta) \right) = 0 \, . \tag{7.4.36}$$

Unfortunately, there is a problem with this definition. Since there are many exact solutions to the ALP, a different choice of the solution $\hat{\psi}^d$ leads to a different $W_{\rm ex}$ and thus to different curves. We can avoid this problem by defining the curves in terms of the small solution s_i (for a general value of ζ) near each puncture z_i. We shall call them the *exact WKB curves* and denote them by $\text{EWKB}_{(i)}$.

The precise definition is given as follows: The exact WKB curves associated to the puncture z_i are defined as the curves satisfying the equation

$$\text{Im} \, \left(W^{(i)}_{\rm ex}(z; \zeta) \right) = 0 \, , \tag{7.4.37}$$

where $W^{(i)}_{\rm ex}$ is the exponential factor for the solution s_i, which is the smaller of the two eigenvectors i_+ and i_-. Explicitly, it is defined through the expression

$$s_i \propto \begin{pmatrix} f^{(1)}_{\rm ex} \\ f^{(2)}_{\rm ex} \end{pmatrix} \exp\left(\int_{z_0}^{z} W^{(i)}_{\rm ex}(z, \bar{z}; \zeta) \right) . \tag{7.4.38}$$

Let us now make several comments. First, it is easy to see that this definition of the exact WKB curves reduces to that of the ordinary WKB curves when ζ is sufficiently small. Second, as in (7.4.34), with a flip of sign in the exponent, we can obtain another solution

$$b_i \equiv \begin{pmatrix} {f'_{\rm ex}}^{(1)} \\ {f'_{\rm ex}}^{(2)} \end{pmatrix} \exp\left(-\int_{z_0}^{z} W_{\rm ex}^{(i)}(z,\bar{z};\zeta) \right) , \tag{7.4.39}$$

which is big near the puncture z_i and satisfies $\langle s_i \, , b_i \rangle = 1$. Such a solution b_i, however, is not guaranteed to be an eigenvector since the eigenvector distinct from s_i is in general given by a linear combination of the form $b_i + cs_i$.

Now the definition of $\text{EWKB}_{(i)}$ given above refers to a specific puncture from which the curves emanate. In order for the notion of the exact WKB curve to be valid for the entire worldsheet, we must guarantee that the definitions of $\text{EWKB}_{(i)}$'s for $i = 1, 2, 3$ are consistent in the region where they overlap. To check this, let us consider the behavior of the small solution s_i as we follow an $\text{EWKB}_{(i)}$. Along such a curve the phase of the exponential factor of s_i stays constant, while its magnitude increases monotonically[34], until it reaches some endpoint. Consider the case in which this endpoint is the puncture at z_j. In such a case, we know that s_i grows exponentially as it approaches z_j and in fact behaves like a big solution b_j, up to an admixture of the exponentially small solution s_j. Thus, with sufficient accuracy, s_i can be expressed in the small neighborhood of z_j as

$$s_i \propto b_j = \begin{pmatrix} {f'_{\rm ex}}^{(1)} \\ {f'_{\rm ex}}^{(2)} \end{pmatrix} \exp\left(-\int_{z_0}^{z} W_{\rm ex}^{(j)}(z,\bar{z};\zeta) \right) . \tag{7.4.40}$$

But since the exponent of the small solution s_j, which is used to define $\text{EWKB}_{(j)}$, is the same as that of b_j except for the sign, we see that by definition the curve we have been following becomes an $\text{EWKB}_{(j)}$ curve in the vicinity of z_j, when z_i and z_j are connected by such a curve. Therefore the definitions of $\text{EWKB}_{(i)}$ and $\text{EWKB}_{(j)}$ are indeed globally consistent.

Let us now make use of the exact WKB curves to determine the analytic properties of the Wronskians. First, by following exactly the same logic as in the case of the ordinary WKB curves, we can immediately conclude that the Wronskian involving two small solutions s_i and s_j must be nonzero if two punctures z_i and z_j are connected by some exact WKB curves. Although this is an extremely useful information, the problem seems to be that, unlike the ordinary WKB curves, we do not know the configurations of the EWKB curves since the exact solutions to the ALP are not available.

[34]Strictly speaking the small eigenvector (7.4.38) also contains a prefactor in front of the exponential. This prefactor, however, does not play a significant role in our discussion since it drops out if we consider the ratio of two solutions s_i/b_i. It is in fact sufficient to know the ratio in order to identify the small solution and the big solution.

Nevertheless, we shall show below that by making use of a characteristic quantity defined locally around each puncture for the EWKB curves, it is possible to fully classify the topology (connectivity) of the curves on the entire worldsheet. The quantity in question is the "number density" of the EWKB curves emanating from a puncture at z_i. To motivate its definition, consider two such curves which emanate from z_i and end at z_j and let the constant phase of $W_{\rm ex}^{(i)}$ along the two curves be ϕ_1 and ϕ_2. Evidently the magnitude of the difference $|\phi_1 - \phi_2|$ is the same around z_i and around z_j, that is, it is conserved. If there is no singularity in the region between these lines, we can draw in more EWKB curves connecting z_i and z_j. Because of the property of the constancy of the phase difference noted above, it is quite natural to draw the curves in such a way that the difference of the phases of the adjacent curves is some fixed unit angle. Going around z_i and counting the number of such lines, we can define the number (density) of the EWKB$_{(i)}$ curves as[35]

$$N_i \equiv \frac{1}{2\pi} \oint_{\mathcal{C}_i} |\mathrm{Im}\ W_{\rm ex}^{(i)}| \,, \tag{7.4.41}$$

where $\mathcal{C}_i$ is an infinitesimal circle around z_i. Although N_i is not an integer in general, we will call it "a number of lines". Actually we can express N_i in a more explicit way. From the asymptotic behavior of $i_\pm$ (7.1.81), we can obtain the form of $W_{\rm ex}^{(i)}$ near z_i as

$$W_{\rm ex}^{(i)} \sim \pm \left(q_i(x) d\tau^{(i)} + i p_i(x) d\sigma^{(i)} \right) \quad \text{as } z \to z_i \,. \tag{7.4.42}$$

Here $(\tau^{(i)}, \sigma^{(i)})$ is the local coordinate defined in (7.1.82), and $+$ or $-$ sign is chosen depending on which of the solutions $i_\pm$ is small. Substituting (7.4.42) into the definition (7.4.41), we obtain a simple expression

$$N_i \equiv |\mathrm{Re}\, p_i(x)| \ . \tag{7.4.43}$$

Since the phase around the puncture is governed by the local monodromy, it is natural that N_i can be expressed in terms of $p_i(x)$.

Before we make use of the concept of N_i in a more global context, let us derive two important properties of the EWKB$_{(i)}$'s which will be necessary for determining their configurations.

The first property will be termed the *non-contractibility*. It can be stated as follows:

> "All the exact WKB curves which start and end at the same puncture are non-contractible."

In other words, such curves must go around a different puncture at least once. The proof is simple. Recall that the Wronskians between small solutions should be nonzero if two

[35] In (7.4.41), we have chosen a convenient normalization of N_i.

punctures are connected by an exact WKB curve. If we apply this statement to the same puncture z_i connected by an EWKB curve, we would conclude that $\langle s_i, s_i \rangle$ is non-zero, which is clearly false. The only way to be consistent with the general assertion above is that the curve is non-contractible and the solution gets transformed by the non-trivial monodromy Ω as it goes around other punctures. In this case the Wronskian is of the form $\langle s_i, \Omega s_i \rangle$, which need not vanish.

The next property is concerned with the endpoints of the exact WKB curves. It can be stated as follows:

" All but finitely many exact WKB curves terminate at punctures. "

The proof can be given as follows. As in the case of the ordinary WKB curves, the possible endpoints are the zeros or the poles of $W_{\rm ex}^{(i)}$. Concerning the former, the number of exact WKB curves flowing into a zero is always finite, as shown in Figure 7.4.1. On the other hand, a pole can be the endpoint of infinitely many curves and thus plays a crucial role in the study of the analyticity of the Wronskians. Now there are three different types of poles for $W_{\rm ex}^{(i)}$. The first is a puncture, at which the vertex operator is inserted. The second type of a pole corresponds to the situation where the small eigenvector s_i develops a singularity at a position different from the puncture. Since we only consider the worldsheet without additional singularities as mentioned in section 7.1.7, such a singularity in s_i should not occur. The last type of divergence for $W_{\rm ex}^{(i)}$ occurs when s_i develops a zero. Indeed, s_i in general has several zeros on the Riemann surface. However, such points cannot be the endpoints of the exact WKB curves for the following reason: At the zeros of s_i, the ratio s_i/b_i of the small and the big solutions must also vanish[36]. But this contradicts the basic property of the exact WKB curve that such a ratio, determined by the exponential factor in (7.4.38), monotonically increases along the exact WKB curve as we move away from z_i. From these considerations, we find that apart from a finite number of curves which can flow into zeros of $W_{\rm ex}^{(i)}$, the rest of the infinitely many exact WKB curves must end at the punctures.

The two properties we have proved above are extremely important for the following reason. They provide certain global restrictions for the EWKB curves for all values of the spectral parameter, about which we only know the local behaviors explicitly in the vicinity of the punctures. Below, they allow us to show that there are essentially two distinct classes of configurations for the exact WKB curves.

These two classes are distinguished by whether the number of lines N_i fully satisfy the

[36]The big solution b_i cannot vanish at such points so as to ensure the normalization condition $\langle s_i\,, b_i \rangle = 1$.

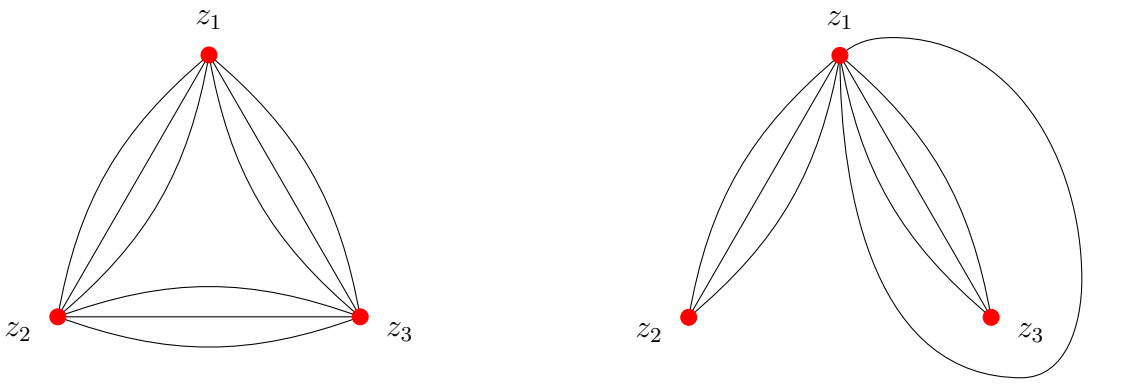

(a) Symmetric case ($N_i + N_j - N_k > 0$) (b) Asymmetric case ($N_2 + N_3 - N_1 < 0$)

Figure 7.4.2: Configuration of the exact WKB curves.

triangle inequalities or not[37]. When N_i's satisfy the relations

$$N_i + N_j - N_k > 0\,, \tag{7.4.44}$$

for all possible combinations of distinct i, j, k, we refer to such a configuration as *symmetric*. It is easy to show that if (7.4.44) is satisfied the number of lines connecting z_i and z_j cannot be zero. As this holds for all the interconnecting lines, the three punctures must be piece-wise connected to each other as in the left figure of Figure 7.4.2.

On the other hand, in the second case, which we shall call *asymmetric*, not all the triangle inequalities are satisfied. For example, one is violated like

$$N_2 + N_3 - N_1 < 0\,. \tag{7.4.45}$$

In this case, one can readily convince oneself that, while all the curves emanating from z_2 and z_3 end at z_1, there must exist a non-contractible curve connecting z_1 to itself. This is depicted in the right figure of Figure 7.4.2.

In this way, we can completely classify the configurations of the exact WKB curves from the local information $N_i = |\mathrm{Re}\, p_i(x)|$. Note that N_i depends on x. In fact it happens that as x changes a symmetric configuration can turn into an asymmetric configuration and vice versa. In an application of the present idea to the classical three-point function in Liouville theory [114], it was checked that such a transition must be taken into account in order to obtain the correct result. Below, we will see explicitly how the patterns of the configurations of the exact WKB curves analyzed above can be used to determine the zeros of the Wronskians.

[37] In the case of the usual WKB curves, $W_{\mathrm{ex}} \sim \sqrt{T(z)}dz$ and hence N_i is proportional to κ_i.

Determination of the zeros of the Wronskians

As an example, let us focus on the factor

$$\sin\left(\frac{p_1+p_2+p_3}{2}\right), \tag{7.4.46}$$

and determine which Wronskians develop a zero when this factor vanishes. (The logic below applies to all the other cases straightforwardly.) From the relations (7.4.9)–(7.4.14), we find that the products of Wronskians that become zero are

$$\langle 1_+\,,2_+\rangle\langle 1_-\,,2_-\rangle\,,\quad \langle 2_+\,,3_+\rangle\langle 2_-\,,3_-\rangle\,,\quad \langle 3_+\,,1_+\rangle\langle 3_-\,,1_-\rangle\,. \tag{7.4.47}$$

For convenience, let us define the following two sets of eigenvectors, namely the set $\mathcal{S}_+ \equiv \{1_+, 2_+, 3_+\}$ and the set $\mathcal{S}_- \equiv \{1_-, 2_-, 3_-\}$. An important feature of the quantities shown in (7.4.47) is that only the Wronskians of the eigenstates in the same group, $\mathcal{S}_+$ or $\mathcal{S}_-$, appear. This is in fact a general feature and holds also for other situations.

Now, let us present two theorems, which will be useful in the determination of the zeros. The first theorem is the following assertion, which we have already proved:

> **Theorem 1.** When two punctures z_i and z_j are connected by an exact WKB curve, the Wronskian between the two small eigenvectors $\langle s_i\,,s_j\rangle$ is non-vanishing.

The second theorem classifies the possibilities of the patterns of the zeros and is stated as follows:

> **Theorem 2.** There are only two distinct possibilities concerning the zeros of the Wronskians in (7.4.47): Either (a) all the Wronskians among the members of $\mathcal{S}_+$ are zero and those among $\mathcal{S}_-$ are nonzero, or (b) all the Wronskians among $\mathcal{S}_-$ are zero and those among $\mathcal{S}_+$ are nonzero.

The proof is as follows. Let us first note that in each product of two Wronskians appearing in (7.4.47), only one of them vanishes. In fact if both factors become zero simultaneously, the product develops a double zero, which contradicts the fact that the zeros of (7.4.46) are all simple zeros. This property implies that in the list given in (7.4.47), at least two of the individual Wronskians which actually vanish must be between the members belonging to the same set, which can be $\mathcal{S}_+$ or $\mathcal{S}_-$. Suppose they belong to $\mathcal{S}_+$. Since $\langle i_+, j_+\rangle = 0$ means that i_+ and j_+ are parallel to each other, vanishing of two such different Wronskians between the states of $\mathcal{S}_+$ implies that in fact all the three states in $\mathcal{S}_+$ are proportional to each other. Therefore the third Wronskian from the set $\mathcal{S}_+$ must also vanish. Obviously the same logic applies to the $\mathcal{S}_-$ case. This proves the theorem.

We can now analyze the zeros of the Wronskians using these theorems. First consider the symmetric case. Since one of the states $i_\pm$ must be a small solution, either $\mathcal{S}_+$ or $\mathcal{S}_-$ must contain two small solutions. For a symmetric configuration, they must be connected by an exact WKB curve. Then by theorem 1 the Wronskian between them must be non-vanishing. Theorem 2 further asserts that all the Wronskians for the members of that set are non-vanishing, while the ones for elements of the other set all vanish.

Next, consider the asymmetric case. For simplicity, let us assume that $N_1 > N_2 + N_3$ is satisfied[38]. In such a case, there exist exact WKB curves which start from z_1, go around z_2 (or z_3), and return to z_1. To make use of the existence of such a curve, consider the following Wronskians:

$$\langle 1_+ \,, \Omega_2 1_+ \rangle \,, \quad \langle 1_- \,, \Omega_2 1_- \rangle \,. \tag{7.4.48}$$

To compute them, we first note that $1_\pm$ can be expressed in terms of $2_\pm$ in the following manner

$$1_\pm = \langle 1_\pm \,, 2_- \rangle 2_+ - \langle 1_\pm \,, 2_+ \rangle 2_- \,. \tag{7.4.49}$$

Then, applying Ω_2 to (7.4.49) and substituting them to (7.4.48), we can express (7.4.48) in terms of the ordinary Wronskians as

$$\langle 1_+ \,, \Omega_2 1_+ \rangle = 2i \sin p_2 \langle 1_+ \,, 2_- \rangle \langle 1_+ \,, 2_+ \rangle \,, \tag{7.4.50}$$

$$\langle 1_- \,, \Omega_2 1_- \rangle = 2i \sin p_2 \langle 1_- \,, 2_- \rangle \langle 1_- \,, 2_+ \rangle \,. \tag{7.4.51}$$

Consider the case where 1_+ is the small solution. Since $\Omega_2 1_+$ can be obtained by parallel-transporting 1_+ along the exact WKB curve which starts and ends at z_1, $\Omega_2 1_+$ must behave as the big solution around z_1. Therefore, the Wronskian $\langle 1_+ \,, \Omega_2 1_+ \rangle$ is non-vanishing in this case. Then from (7.4.50) it follows that $\langle 1_+ \,, 2_+ \rangle$ must also be non-vanishing. Applying the theorem 2, we conclude that the Wronskians between the members of $\mathcal{S}_+$ are non-vanishing and those of $\mathcal{S}_-$ all vanish. In an entirely similar manner, when 1_- is the small eigenvector, we obtain the result where the roles of $\mathcal{S}_+$ and $\mathcal{S}_-$ are interchanged.

Performing similar analyses for the other cases, we obtain the general rules summarized below.

> **Rule 1:** *Decomposition of the eigenvectors into two groups.*
> When a factor of the form $\sin\left(\sum_i \epsilon_i p_i/2\right)$ vanishes, the Wronskians which vanish are the ones among $\{1_{\epsilon_1}, 2_{\epsilon_2}, 3_{\epsilon_3}\}$ or the ones among $\{1_{-\epsilon_1}, 2_{-\epsilon_2}, 3_{-\epsilon_3}\}$.

[38] Generalization to other cases is straightforward.

Rule 2: *Symmetric case.*
When the configuration of the exact WKB curves is symmetric, the Wronskians from the group which contains two or more small solutions are nonzero whereas the Wronskians from the other group are zero.

Rule 3: *Asymmetric case.*
When the configuration of the exact WKB curves is asymmetric and N_i's satisfy $N_i > N_j + N_k$, the Wronskians from the group which contains the smaller of the two solutions $i_\pm$ are nonzero whereas the Wronskians from the other group are zero.

In the next subsection, we will utilize these rules to evaluate the individual Wronskians.

7.4.4 Individual Wronskian from the Wiener-Hopf decomposition

Making use of the data for the analyticity of the Wronskians obtained in the previous subsection, we now set up and solve a Riemann-Hilbert problem to decompose the product of Wronskians and extract the individual Wronskians.The standard method for such a procedure is known as the Wiener-Hopf decomposition, which extracts from a complicated function a part regular on the upper half plane and the part regular on the lower half plane. The typical set up is as follows. Suppose $F(x)$ is a function which decreases sufficiently fast at infinity and can be written as a sum of two components $F(x) = F_\uparrow(x) + F_\downarrow(x)$, where $F_\uparrow(x)$ is regular on the upper half plane while $F_\downarrow(x)$ is regular on the lower half plane. Then, each component, in the region where it is regular, can be extracted from $F(x)$ as

$$F_\uparrow(x) = \int_{-\infty}^{\infty} \frac{dx'}{2\pi i} \frac{1}{x' - x} F(x') \qquad (\mathrm{Im}\, x > 0)\,, \tag{7.4.52}$$

$$F_\downarrow(x) = -\int_{-\infty}^{\infty} \frac{dx'}{2\pi i} \frac{1}{x' - x} F(x') \qquad (\mathrm{Im}\, x < 0)\,. \tag{7.4.53}$$

These equations can be easily proven by first substituting $F(x') = F_\uparrow(x') + F_\downarrow(x')$ on the right hand side and then closing the integration contour for $F_\uparrow(x')$ ($F_\downarrow(x')$) on the upper (lower) half plane. Now when the argument x is not in the region specified in (7.4.52) and (7.4.53), we need to analytically continue the above formulas. For instance, $F_\uparrow(x)$ in the region where $\mathrm{Im}\, x < 0$ should be expressed as

$$F_\uparrow(x) = F(x) - F_\downarrow(x) = F(x) + \int_{-\infty}^{\infty} \frac{dx'}{2\pi i} \frac{1}{x' - x} F(x')\,. \tag{7.4.54}$$

Note that the first term $F(x)$ on the right hand side can be thought of as due to the integral along a small circle around $x' = x$.

To apply this method to the case of our interest, namely to the equations (7.4.9)–(7.4.14), we take the logarithm and represent them in a general form as

$$\ln\langle i_{\epsilon_i}\,,j_{\epsilon_j}\rangle + \ln\langle i_{-\epsilon_i}\,,j_{-\epsilon_i}\rangle = \ln\sin\left(\frac{\epsilon_i p_i + \epsilon_j p_j + p_k}{2}\right) + \ln\sin\left(\frac{\epsilon_i p_i + \epsilon_j p_j - p_k}{2}\right) - \ln\sin p_i - \ln\sin p_j\,. \tag{7.4.55}$$

Here ϵ_i denotes a $+$ or $-$ sign. In this process, we have neglected the contributions of the form $\ln(-1)$, since they only contribute to the overall phase of the three-point functions. Our aim will be to express each of the terms on the left hand side of (7.4.55) in terms of some convolution integrals of the functions on the right hand side. To put it in another way, we wish to decompose each term on the right hand side into contributions coming from each term on the left hand side. Since the quasi-momentum $p_i(x)$ is defined on a Riemann surface with branch cuts, we need to generalize the Wiener-Hopf decomposition formula in an appropriate way, as discussed below.

Separation of the poles

Let us first decompose the terms of the form $-\ln\sin p_i$, which give rise to poles of the Wronskians. As shown in the previous section, which Wronskian develops a pole is determined purely by the sign of the real part of the quasi-momentum $q_i(x)$. Therefore, we should be able to decompose the quantity $-\ln\sin p_i$ by using a convolution integral along the curve defined by $\mathrm{Re}\,q_i = 0$. For the ordinary Wiener-Hopf decomposition, the convolution kernel is given simply by $1/(x-x')$. In the present case, however, we have a two-sheeted Riemann surface and hence we must make sure that the kernel has the simple pole only when x and x' coincide on the same sheet. When they are on top of each other on different sheets, no singularity should occur. The appropriate kernel with this property is given by

$$\widehat{\mathcal{K}}_i(x';x) \equiv \frac{1}{2(x'-x)}\left(\sqrt{\frac{(x-u_i)(x-\bar{u}_i)}{(x'-u_i)(x'-\bar{u}_i)}}+1\right)\,. \tag{7.4.56}$$

When x and x' get close to each other but on different sheets, the square root factor tends to -1 canceling the $+1$ term and hence the kernel is indeed regular. Furthermore, in the limit that x' tends to ∞, the kernel $\widehat{\mathcal{K}}_i(x';x)$ decreases like $(x')^{-2}$, which is sufficiently fast for our purpose.

With such a convolution kernel, we can carry out the Wiener-Hopf decomposition in the usual way. Namely the term $-\ln\sin p_i(x)$ can be decomposed into the contributions of

$\langle i_+ , j_{\epsilon_j} \rangle(x)$ and $\langle i_- , j_{-\epsilon_j} \rangle(x)$ as

$$\langle i_+ , j_{\epsilon_j} \rangle(x) \ni \oint_{\Gamma_{i_+}} \widehat{\mathcal{K}}_i * (-\ln \sin p_i) \,, \tag{7.4.57}$$

$$\langle i_- , j_{-\epsilon_j} \rangle(x) \ni \oint_{\Gamma_{i_-}} \widehat{\mathcal{K}}_i * (-\ln \sin p_i) \,, \tag{7.4.58}$$

where the convolution integral is defined as

$$\int A * B \equiv \int \frac{dx'}{2\pi i} A(x';x) B(x') \,. \tag{7.4.59}$$

As for the contours of integration, Γ_{i_+} is defined by $\mathrm{Re}\ q_i = 0$ and Γ_{i_-} stands for $-\Gamma_{i_+}$. The direction of the contour Γ_{i_+} is defined such that $\langle i_+ , j_{\epsilon_j} \rangle(x)$ does not contain poles in the region to the left of the contour[39].

Now note that under the holomorphic involution $x \to \hat{\sigma} x$, the quasi-momentum $p_i(x)$ and the square-root contained in (7.4.56) simply flip sign. Making use of this property, we can re-express the convolution integrals (7.4.57) and (7.4.58) as integrals only on the first (or the upper) sheet:

$$\langle i_+ , j_{\epsilon_j} \rangle(x) \ni - \oint_{\Gamma^u_{i_+}} \mathcal{K}_i * \ln \sin p_i \,, \tag{7.4.60}$$

$$\langle i_- , j_{-\epsilon_j} \rangle(x) \ni - \oint_{\Gamma^u_{i_-}} \mathcal{K}_i * \ln \sin p_i \,. \tag{7.4.61}$$

Here, $\Gamma^u_{i_\pm}$ denotes the portion of $\Gamma_{i_\pm}$ on the upper-sheet of the spectral curve and the kernel $\mathcal{K}_i(x';x)$ (without a hat) is defined by

$$\mathcal{K}_i(x';x) \equiv \frac{1}{x'-x} \sqrt{\frac{(x-u_i)(x-\bar{u}_i)}{(x'-u_i)(x'-\bar{u}_i)}} \,. \tag{7.4.62}$$

Again we have neglected the factors of the form $\ln(-1)$ arising from the sign flip of $p_i(x)$, as they only modify the overall phase of the Wronskians and the three-point functions.

It is important to note that (7.4.57) and (7.4.58) are valid only when x is on the left hand side of the contours, just as in the case of the ordinary Wiener-Hopf decomposition. When the argument x is on the right hand side of the contour $\Gamma_{i_\pm}$, we must add $-\ln \sin p_i$ to (7.4.57) and (7.4.58), as explained in (7.4.54). Such effects can be taken into account also in (7.4.60) and (7.4.61), if x is on the upper sheet, by adding a small circle encircling $x' = x$ counterclockwise to the integration contours. In what follows, such contributions will be referred to as *contact terms*.

[39] A typical form of the contour is depicted in Figure 7.6.4 in section 7.6, where we study explicit examples.

Separation of the zeros

Next we shall discuss the decomposition of the first two terms on the right hand side of (7.4.55), which are responsible for the zeros of the Wronskians. To perform the decomposition, again we need to determine the appropriate convolution kernel and the integration contour.

Let us first discuss the convolution kernel. As the terms of our focus depend on all the quasi-momenta $p_i(x)$'s, the appropriate convolution kernel must be a function on the Riemann surface which contains all the branch cuts of the $p_i(x)$'s. Such a kernel can be easily written down as a generalization of the expression (7.4.56) and is given by

$$\widehat{\mathcal{K}}_{\rm all} \equiv \frac{1}{8(x'-x)} \prod_{i=1}^{3} \left(\sqrt{\frac{(x-u_i)(x-\bar{u}_i)}{(x'-u_i)(x'-\bar{u}_i)}} + 1 \right) . \tag{7.4.63}$$

Since there are two choices of sign for each square root factor on the right hand side of (7.4.63), $\widehat{\mathcal{K}}_{\rm all}$ is properly defined on the eightfold cover of the complex plane. In what follows, we distinguish these eight sheets as $\{\bullet, \bullet, \bullet\}$-sheet, where the successive entry $\bullet$ is either "u" denoting upper sheet or "l" denoting lower sheet, referring to the two sheets for $p_1(x)$, $p_2(x)$ and $p_3(x)$ respectively. It is clear that the kernel (7.4.63) has a pole with a residue $+1$ at $x' = x$ only when two-points are on the same sheet. Therefore it has a desired property for the Wiener-Hopf decomposition.

Let us next turn to the contour of integration. As discussed in the previous section, the zeros of the Wronskians are determined by the following two properties: (i) The connectivity of the exact WKB-curves and (ii) the relative magnitude of the eigenvectors $i_\pm$. Therefore, curves across which these two properties change can be the possible integration contours. Corresponding to the properties (i) and (ii) above, there are two types of integration contours; the curves defined by $\mathrm{Re}\, q_i(x) = 0$ and the curves defined by $N_i = N_j + N_k$. An important point to bear in mind is that in general only some portions of these curves will be the proper integration contours, since in some cases the analyticity of the Wronskians does not change even when we cross these curves. In order to determine the correct integration contours explicitly, we need to apply the general rules derived in the previous section. However, as the form of the contours determined through such a procedure depends on the specific details of the choice of the external states, we will postpone such an analysis until section 7.6, where we work out some specific examples. Thus, in what follows we will denote the integration contours without specifying their explicit forms as $\mathcal{M}_{\pm\pm\pm}$, where $\mathcal{M}_{\epsilon_1\epsilon_2\epsilon_3}$ denotes the contour we use to determine the contribution of the factor $\sin\left(\sum_i \epsilon_i p_i\right)$ to $\langle i_{\epsilon_i}, j_{\epsilon_j} \rangle$. They are defined such that they flip the orientation if we flip the signs of three indices, for example $\mathcal{M}_{+++} = -\mathcal{M}_{---}$

Employing the kernel and the contours given above, let us perform the decomposition of the product of Wronskians, taking that of $\langle 1_+ , 2_+ \rangle$ and $\langle 1_- , 2_- \rangle$ as a representative example. Applying the Wiener-Hopf decomposition to the relation (7.4.55) with $i = 1, j = 2$ and $\epsilon_1 = +, \epsilon_2 = +$, we obtain

$$\langle 1_+ , 2_+ \rangle \ni$$

$$\oint_{\mathcal{M}_{+++}} \widehat{\mathcal{K}}_{\rm all} * \ln\sin\left(\frac{p_1+p_2+p_3}{2}\right) + \oint_{\mathcal{M}_{++-}} \widehat{\mathcal{K}}_{\rm all} * \ln\sin\left(\frac{p_1+p_2-p_3}{2}\right) , \tag{7.4.64}$$

$$\langle 1_- , 2_- \rangle \ni$$

$$\oint_{\mathcal{M}_{---}} \widehat{\mathcal{K}}_{\rm all} * \ln\sin\left(\frac{p_1+p_2+p_3}{2}\right) + \oint_{\mathcal{M}_{--+}} \widehat{\mathcal{K}}_{\rm all} * \ln\sin\left(\frac{p_1+p_2-p_3}{2}\right) . \tag{7.4.65}$$

As in the case of the ordinary Wiener-Hopf decomposition, the expressions (7.4.64) and (7.4.65) are valid only when x is located to the left of the integration contour. Additional terms, to be discussed shortly, are needed when x is on the other side of the contour.

Let us now show that the kernel $\widehat{\mathcal{K}}_{\rm all}$ used in (7.4.64) and (7.4.65) can be effectively replaced by simpler combinations of the form $(\mathcal{K}_i + \mathcal{K}_j)/8$. To explain the idea, consider the following integral as an example:

$$\oint_{\mathcal{M}_{+++}} \frac{dx'}{2\pi i} \widehat{\mathcal{K}}_{\rm all}(x';x) \ln\sin\left(\frac{p_1+p_2+p_3}{2}\right)(x') . \tag{7.4.66}$$

As the first step, we make a change of integration variable from x' to $\hat{\sigma}_3 x'$, where $\hat{\sigma}_i$ denotes the holomorphic involution with respect to p_i, namely the operation that exchanges the two sheets associated with p_i. Although this clearly leaves the value of the integral intact, the form of the integral changes. One can easily verify that the following transformation formulas for the integrand and the contours hold:

$$\ln\sin\left(\frac{p_1+p_2+p_3}{2}\right)(\hat{\sigma}_3 x') = \ln\sin\left(\frac{p_1+p_2-p_3}{2}\right)(x') , \tag{7.4.67}$$

$$\widehat{\mathcal{K}}_{\rm all}(\hat{\sigma}_3 x';x) = \widehat{\mathcal{K}}^{(3)}_{\rm all}(x';x) , \tag{7.4.68}$$

$$\oint_{\mathcal{M}_{+++}} d(\hat{\sigma}_3 x') = \oint_{\mathcal{M}_{++-}} dx' . \tag{7.4.69}$$

In the second line (7.4.68), the "sign-flipped kernel" $\widehat{\mathcal{K}}^{(3)}_{\rm all}$ is defined by

$$\widehat{\mathcal{K}}^{(3)}_{\rm all} \equiv \frac{1}{8(x'-x)} \left(-\sqrt{\frac{(x-u_3)(x-\bar{u}_3)}{(x'-u_3)(x'-\bar{u}_3)}} + 1 \right) \prod_{\ell=1,2} \left(\sqrt{\frac{(x-u_\ell)(x-\bar{u}_\ell)}{(x'-u_\ell)(x'-\bar{u}_\ell)}} + 1 \right) . \tag{7.4.70}$$

Making such transformations, we can re-express the integral (7.4.66) as

$$\oint_{\mathcal{M}_{++-}} \frac{dx'}{2\pi i} \widehat{\mathcal{K}}^{(3)}_{\text{all}}(x';x) \ln\sin\left(\frac{p_1+p_2-p_3}{2}\right)(x') \,. \tag{7.4.71}$$

Performing similar analysis for all the possible sign-flips, we obtain 2^3 different expressions for (7.4.66). Then averaging over all the 2^3 expressions, we find that the final expressions are given in terms of the kernels $\mathcal{K}_i$ as follows:

$$\begin{aligned}
&\langle 1_+\,, 2_+\rangle \ni \\
&\frac{1}{16}\left(\oint_{\mathcal{M}_{+++}} (\mathcal{K}_1+\mathcal{K}_2) * \ln\sin\left(\frac{p_1+p_2+p_3}{2}\right) + \oint_{\mathcal{M}_{++-}} (\mathcal{K}_1+\mathcal{K}_2) * \ln\sin\left(\frac{p_1+p_2-p_3}{2}\right)\right. \\
&\left. + \oint_{\mathcal{M}_{+-+}} (\mathcal{K}_1-\mathcal{K}_2) * \ln\sin\left(\frac{p_1-p_2+p_3}{2}\right) + \oint_{\mathcal{M}_{-++}} (-\mathcal{K}_1+\mathcal{K}_2) * \ln\sin\left(\frac{-p_1+p_2+p_3}{2}\right)\right) ,
\end{aligned} \tag{7.4.72}$$

$$\begin{aligned}
&\langle 1_-\,, 2_-\rangle \ni \\
&\frac{1}{16}\left(\oint_{\mathcal{M}_{---}} (\mathcal{K}_1+\mathcal{K}_2) * \ln\sin\left(\frac{p_1+p_2+p_3}{2}\right) + \oint_{\mathcal{M}_{--+}} (\mathcal{K}_1+\mathcal{K}_2) * \ln\sin\left(\frac{p_1+p_2-p_3}{2}\right)\right. \\
&\left. + \oint_{\mathcal{M}_{-+-}} (\mathcal{K}_1-\mathcal{K}_2) * \ln\sin\left(\frac{p_1-p_2+p_3}{2}\right) + \oint_{\mathcal{M}_{+--}} (-\mathcal{K}_1+\mathcal{K}_2) * \ln\sin\left(\frac{-p_1+p_2+p_3}{2}\right)\right) .
\end{aligned} \tag{7.4.73}$$

Just as before, we neglected the contributions of the form $\ln(-1)$ as leading to pure phases. Also, the same remarks made below equations (7.4.64) and (7.4.65) on the position of x relative to the contour lines apply to the expressions (7.4.72) and (7.4.73) above.

Finally, for later convenience, let us further re-write the above expressions as integrals performed purely on the $\{u,u,u\}$-sheet. Each contour $\mathcal{M}_{\epsilon_1\epsilon_2\epsilon_3}$ has parts on the eight different sheets denoted by $\mathcal{M}^{u,u,u}_{\epsilon_1\epsilon_2\epsilon_3}, \mathcal{M}^{u,u,l}_{\epsilon_1\epsilon_2\epsilon_3}$, etc., where the superscripts indicate the relevant sheet in an obvious way. Consider for example the first integral in (7.4.72) along the contour $\mathcal{M}_{+++}$. The form as given is for the portion $\mathcal{M}^{uuu}_{+++}$. For the portion denoted by $\mathcal{M}^{ulu}_{+++}$ for example, if we wish to express its contribution in terms of an integral on the $\{u,u,u\}$-sheet, we need to change the sign of $\mathcal{K}_2$ and p_2. Then the integral becomes identical to that of the first term in the second line of (7.4.72), except along $\mathcal{M}^{uuu}_{+-+}$. In similar fashions we can re-express the contributions from the eight parts of $\mathcal{M}_{+++}$ in terms of the integrals on the $\{u,u,u\}$-sheet. After repeating the same procedure for the rest of the three terms in (7.4.72), one finds that the net effect is that each term of (7.4.72) is multiplied by a factor of eight, with each contour

restricted to the $\{u,u,u\}$-sheet. In this way we obtain the representations

$$\langle 1_+\,,2_+\rangle \ni$$
$$\frac{1}{2}\left(\oint_{\mathcal{M}^{uuu}_{+++}}(\mathcal{K}_1+\mathcal{K}_2)*\ln\sin\left(\frac{p_1+p_2+p_3}{2}\right)+\oint_{\mathcal{M}^{uuu}_{++-}}(\mathcal{K}_1+\mathcal{K}_2)*\ln\sin\left(\frac{p_1+p_2-p_3}{2}\right)\right.$$
$$\left.+\oint_{\mathcal{M}^{uuu}_{+-+}}(\mathcal{K}_1-\mathcal{K}_2)*\ln\sin\left(\frac{p_1-p_2+p_3}{2}\right)+\oint_{\mathcal{M}^{uuu}_{-++}}(-\mathcal{K}_1+\mathcal{K}_2)*\ln\sin\left(\frac{-p_1+p_2+p_3}{2}\right)\right)\,, \tag{7.4.74}$$

$$\langle 1_-\,,2_-\rangle \ni$$
$$\frac{1}{2}\left(\oint_{\mathcal{M}^{uuu}_{---}}(\mathcal{K}_1+\mathcal{K}_2)*\ln\sin\left(\frac{p_1+p_2+p_3}{2}\right)+\oint_{\mathcal{M}^{uuu}_{--+}}(\mathcal{K}_1+\mathcal{K}_2)*\ln\sin\left(\frac{p_1+p_2-p_3}{2}\right)\right.$$
$$\left.+\oint_{\mathcal{M}^{uuu}_{-+-}}(\mathcal{K}_1-\mathcal{K}_2)*\ln\sin\left(\frac{p_1-p_2+p_3}{2}\right)+\oint_{\mathcal{M}^{uuu}_{+--}}(-\mathcal{K}_1+\mathcal{K}_2)*\ln\sin\left(\frac{-p_1+p_2+p_3}{2}\right)\right)\,. \tag{7.4.75}$$

The results obtained in this subsection and the previous subsection are both expressed in terms of certain convolution integrals on the spectral curve. Thus, in what follows, we will denote their sum by $\mathsf{Conv}\langle i_\pm, j_\pm\rangle$.

Before ending this subsection, let us make one important remark. Although each convolution integral obtained so far is divergent at $x=\pm 1$, the divergence cancels[40] in the sum $\mathsf{Conv}\langle i_\pm, j_\pm\rangle$. Thus the contribution singular at $x=\pm 1$ must be separately taken into account as we will do in the next subsection.

7.4.5 Singular part and constant part of the Wronskians

In addition to the main non-trivial parts determined by the Wiener-Hopf decomposition described above, there are two further contributions to the Wronskians. One is the contribution singular at $x=\pm 1$, coming from such structure in the connections used in ALP. The other is the possibility of adding a constant function on the spectral curve. In this subsection, we will determine these two contributions.

Let us first focus on terms singular at $x=1$. To determine such terms, we will need the WKB expansions around $x=1$ for all the Wronskians, not just the ones that were discussed in section 7.2.2, namely $\langle i_+\,,j_+\rangle$ and $\langle i_-\,,j_-\rangle$. This is because of the following reason: Although the formulas we obtained for the contribution of the action and that of the

[40] One can confirm this by expanding the convolution integrals around $x=\pm 1$.

wave function appear to contain Wronskians of the type $\langle i_+ , j_+ \rangle$ and $\langle i_- , j_- \rangle$ only, we must understand their behavior when they are followed into the second sheet as well in order to know the analyticity property on the entire Riemann surface. As shown in (7.1.85), when we cross the branch cut associated with $p_i(x)$ into the lower sheet, the eigenfunctions i_+ and i_- behave like i_- and $-i_+$ on the upper sheet, respectively, . Therefore the behavior of $\langle i_+ , j_+ \rangle$ on the $\{u, l, *\}$-sheet can be obtained from the behavior of $\langle i_+ , j_- \rangle$ on the $\{u, u, *\}$-sheet, etc.

Now the WKB expansions of the Wronskians of the type $\langle i_+ , j_- \rangle$ can be obtained from those of $\langle i_+ , j_+ \rangle$ by the use of the following Schouten identities:

$$\langle i_+ , j_- \rangle \langle j_+ , k_+ \rangle + \langle i_+ , j_+ \rangle \langle j_- , k_+ \rangle + \langle i_+ , k_+ \rangle \langle j_- , j_+ \rangle = 0 \,. \tag{7.4.76}$$

Indeed these identities can be regarded as the equations for the six unknown Wronskians of the form $\langle i_+ , j_- \rangle$. If we consider all the combinations of i, j and k in (7.4.76), we obtain three independent equations. Combining them with the equations (7.4.12)–(7.4.14) for the products of the Wronskians, we can completely determine $\langle i_+ , j_- \rangle$'s in terms of $\langle i_+ , j_+ \rangle$ in the following form:

$$\langle 1_+ , 2_- \rangle = e^{-i(p_1+p_2-p_3)/2} \frac{\sin\left(\frac{p_1-p_2-p_3}{2}\right)}{\sin p_2} \frac{\langle 3_+ , 1_+ \rangle}{\langle 2_+ , 3_+ \rangle} \,, \tag{7.4.77}$$

$$\langle 1_- , 2_+ \rangle = e^{i(p_1+p_2-p_3)/2} \frac{\sin\left(\frac{p_1-p_2-p_3}{2}\right)}{\sin p_1} \frac{\langle 2_+ , 3_+ \rangle}{\langle 3_+ , 1_+ \rangle} \,, \tag{7.4.78}$$

$$\langle 2_+ , 3_- \rangle = e^{-i(-p_1+p_2+p_3)/2} \frac{\sin\left(\frac{-p_1+p_2-p_3}{2}\right)}{\sin p_3} \frac{\langle 1_+ , 2_+ \rangle}{\langle 3_+ , 1_+ \rangle} \,, \tag{7.4.79}$$

$$\langle 2_- , 3_+ \rangle = e^{i(-p_1+p_2+p_3)/2} \frac{\sin\left(\frac{p_1+p_2-p_3}{2}\right)}{\sin p_2} \frac{\langle 3_+ , 1_+ \rangle}{\langle 1_+ , 2_+ \rangle} \,, \tag{7.4.80}$$

$$\langle 3_+ , 1_- \rangle = e^{-i(p_1-p_2+p_3)/2} \frac{\sin\left(\frac{-p_1-p_2+p_3}{2}\right)}{\sin p_1} \frac{\langle 2_+ , 3_+ \rangle}{\langle 1_+ , 2_+ \rangle} \,, \tag{7.4.81}$$

$$\langle 3_- , 1_+ \rangle = e^{i(p_1-p_2+p_3)/2} \frac{\sin\left(\frac{-p_1+p_2+p_3}{2}\right)}{\sin p_3} \frac{\langle 1_+ , 2_+ \rangle}{\langle 2_+ , 3_+ \rangle} \,. \tag{7.4.82}$$

From these expressions, we can obtain the WKB-expansion for every Wronskian using the results for $\langle i_+ , j_+ \rangle$.

The singular term of the Wronskians is given simply by the leading term in the WKB expansion. For instance, the singular terms for $\langle i_+ , j_+ \rangle$ and $\langle i_- , j_- \rangle$ at $x = 1$ on the

$\{u,u,u\}$-sheet is determined from the expansion (7.2.35) and (7.2.36) as

$$\ln\langle 1_+\,,2_+\rangle \overset{x\sim 1}{\sim} \frac{2}{1-x}\int_{\ell_{21}}\sqrt{T}dz\,,\qquad \ln\langle 1_-\,,2_-\rangle \overset{x\sim 1}{\sim} \frac{2}{1-x}\int_{\ell_{12}}\sqrt{T}dz\,, \tag{7.4.83}$$

$$\ln\langle 2_+\,,3_+\rangle \overset{x\sim 1}{\sim} \frac{2}{1-x}\int_{\ell_{23}}\sqrt{T}dz\,,\qquad \ln\langle 2_-\,,3_-\rangle \overset{x\sim 1}{\sim} \frac{2}{1-x}\int_{\ell_{32}}\sqrt{T}dz\,, \tag{7.4.84}$$

$$\ln\langle 3_+\,,1_+\rangle \overset{x\sim 1}{\sim} \frac{2}{1-x}\int_{\ell_{\hat{3}1}}\sqrt{T}dz\,,\qquad \ln\langle 3_-\,,1_-\rangle \overset{x\sim 1}{\sim} \frac{2}{1-x}\int_{\ell_{1\hat{3}}}\sqrt{T}dz\,. \tag{7.4.85}$$

Then by using (7.4.77)–(7.4.82) we can determine the singular terms for $\langle i_+\,,j_-\rangle$ on the $\{u,u,u\}$-sheet as

$$\ln\langle 1_+\,,2_-\rangle \overset{x\sim 1}{\sim} \frac{2\pi i(\kappa_1+\kappa_2-\kappa_3)}{1-x}+\frac{2}{1-x}\int_{\ell_{\hat{2}\hat{3}}+\ell_{\hat{3}1}}\sqrt{T}dz\,, \tag{7.4.86}$$

$$\ln\langle 1_-\,,2_+\rangle \overset{x\sim 1}{\sim} \frac{2\pi i(-\kappa_1-\kappa_2+\kappa_3)}{1-x}+\frac{2}{1-x}\int_{\ell_{1\hat{3}}+\ell_{\hat{3}\hat{2}}}\sqrt{T}dz\,, \tag{7.4.87}$$

$$\ln\langle 2_+\,,3_-\rangle \overset{x\sim 1}{\sim} \frac{2\pi i(-\kappa_1+\kappa_2+\kappa_3)}{1-x}+\frac{2}{1-x}\int_{\ell_{21}+\ell_{1\hat{3}}}\sqrt{T}dz\,, \tag{7.4.88}$$

$$\ln\langle 2_-\,,3_+\rangle \overset{x\sim 1}{\sim} \frac{2\pi i(\kappa_1-\kappa_2-\kappa_3)}{1-x}+\frac{2}{1-x}\int_{\ell_{\hat{3}1}+\ell_{12}}\sqrt{T}dz\,, \tag{7.4.89}$$

$$\ln\langle 3_+\,,1_-\rangle \overset{x\sim 1}{\sim} \frac{2\pi i(\kappa_1-\kappa_2+\kappa_3)}{1-x}+\frac{2}{1-x}\int_{\ell_{12}+\ell_{23}}\sqrt{T}dz\,, \tag{7.4.90}$$

$$\ln\langle 3_-\,,1_+\rangle \overset{x\sim 1}{\sim} \frac{2\pi i(-\kappa_1+\kappa_2-\kappa_3)}{1-x}+\frac{2}{1-x}\int_{\ell_{32}+\ell_{21}}\sqrt{T}dz\,. \tag{7.4.91}$$

In order to determine the singular terms completely, we also need to understand the singular behavior on other sheets. As already described, this can be done by utilizing the fact that i_+ and i_- transform into i_- and $-i_+$ respectively as one crosses a branch cut associated to $p_i(x)$. For instance, applying this rule we can easily find that the singular term for $\langle 1_+\,,2_+\rangle$ must behave in the following way on each sheet:

$$\langle 1_+\,,2_+\rangle \overset{x\sim 1}{\sim} \frac{2}{1-x}\int_{\ell_{21}}\sqrt{T}dz \qquad (\text{on the } \{u\,,u\,,*\}\text{-sheet})\,, \tag{7.4.92}$$

$$\langle 1_+\,,2_+\rangle \overset{x\sim 1}{\sim} \frac{2\pi i(\kappa_1+\kappa_2-\kappa_3)}{1-x}+\frac{2}{1-x}\int_{\ell_{\hat{2}\hat{3}}+\ell_{\hat{3}1}}\sqrt{T}dz \qquad (\text{on the } \{u\,,l\,,*\}\text{-sheet})\,, \tag{7.4.93}$$

$$\langle 1_+\,,2_+\rangle \overset{x\sim 1}{\sim} \frac{2\pi i(-\kappa_1-\kappa_2+\kappa_3)}{1-x}+\frac{2}{1-x}\int_{\ell_{1\hat{3}}+\ell_{\hat{3}\hat{2}}}\sqrt{T}dz \qquad (\text{on the } \{l\,,u\,,*\}\text{-sheet})\,, \tag{7.4.94}$$

$$\langle 1_+\,,2_+\rangle \overset{x\sim 1}{\sim} \frac{2}{1-x}\int_{\ell_{12}}\sqrt{T}dz \qquad (\text{on the } \{l\,,l\,,*\}\text{-sheet})\,. \tag{7.4.95}$$

Combining all these results, it is possible to write down the expression on the entire Riemann surface which gives the correct singular behavior on the respective sheet. It is given by

$$\mathsf{Sing}_+\left[\langle 1_+\,,2_+\rangle\right]=\frac{1}{1-x}\sqrt{\frac{(x-u_1)(x-\bar{u}_1)}{(1-u_1)(1-\bar{u}_1)}}\left(\pi i(\kappa_1+\kappa_2-\kappa_3)+2\int_{\ell_{\hat{1}\hat{2}}+\ell_{\hat{2}\hat{3}}+\ell_{\hat{3}1}}\sqrt{T}dz\right)$$
$$+\frac{1}{1-x}\sqrt{\frac{(x-u_2)(x-\bar{u}_2)}{(1-u_2)(1-\bar{u}_2)}}\left(\pi i(-\kappa_1-\kappa_2+\kappa_3)+2\int_{\ell_{23}+\ell_{3\hat{1}}+\ell_{\hat{1}\hat{2}}}\sqrt{T}dz\right)\,. \quad (7.4.96)$$

Here and hereafter, we will use the notation $\mathsf{Sing}_\pm\left[f(x)\right]$ to denote the singular term of $f(x)$ around $x=\pm 1$. In an entirely similar manner, we can determine the terms singular at $x=-1$ as

$$\mathsf{Sing}_-\left[\langle 1_+\,,2_+\rangle\right]=\frac{1}{1+x}\sqrt{\frac{(x-u_1)(x-\bar{u}_1)}{(1-u_1)(1-\bar{u}_1)}}\left(\pi i(-\kappa_1-\kappa_2+\kappa_3)+2\int_{\ell_{\hat{1}\hat{2}}+\ell_{\hat{2}\hat{3}}+\ell_{\hat{3}1}}\sqrt{\bar{T}}d\bar{z}\right)$$
$$+\frac{1}{1+x}\sqrt{\frac{(x-u_2)(x-\bar{u}_2)}{(1-u_2)(1-\bar{u}_2)}}\left(\pi i(\kappa_1+\kappa_2-\kappa_3)+2\int_{\ell_{23}+\ell_{3\hat{1}}+\ell_{\hat{1}\hat{2}}}\sqrt{\bar{T}}d\bar{z}\right)\,. \quad (7.4.97)$$

Singular terms for other Wronskians at $x=\pm 1$ can be determined in a similar manner.

The remaining issue is the ambiguity of adding a constant function to the logarithm of the Wronskian. Such an ambiguity can be fixed by once more utilizing the property that $i_\pm$ that i_+ (i_-) transforms into i_- ($-i_+$) as it crosses the branch cut of p_i. This leads to the following constraint for the Wronskians

$$\langle i_+\,,j_+\rangle(\hat{\sigma}_i\hat{\sigma}_j x)=\langle i_-\,,j_-\rangle(x)\,. \quad (7.4.98)$$

It turns out that all the results obtained so far satisfy (7.4.98). Since this property gets lost upon adding a constant to the logarithm of the Wronskian, it shows that our results are already complete and we should not add any constant functions.

7.5 Complete three-point functions at strong coupling

Up to the last section, we have developed necessary methods and acquired the knowledge of the various parts that make up the three-point functions of our interest. Now we are ready to put them together and see that they combine in a non-trivial fashion to produce a rather remarkable answer.

First in subsection 7.5.1, we obtain the complete result for the S^3 part by putting together the contribution of the action and that of the vertex operators. These two contributions

combine nicely to produce a simple expression in terms of integrals on the spectral curve. Then, adapting the methods developed for the S^3 part, we evaluate in subsection 7.5.2 the $EAdS_3$ part of the three-point function. Our focus will be on the differences between the S^3 and $EAdS_3$ contributions. Finally in subsection 7.5.3, we present the full answer by combining the contributions of the S^3 part and the $EAdS_3$ part. We will see that the structure of the final answer closely resembles that of the weak coupling result. Detailed comparison for certain specific cases will be performed in section 7.6.

7.5.1 The S^3 part

Before we begin the actual computations, let us summarize the structure of the contributions from the S^3 part to the logarithm of the three-point function, which we denote by F_{S^3}. As was already indicated in section 7.1.7, F_{S^3} consists of the contribution of the action and that of the vertex operators, namely

$$F_{S^3} = \mathcal{F}_{\text{action}} + \mathcal{F}_{\text{vertex}} \,. \tag{7.5.1}$$

Each contribution can be further split into several different pieces as

$$\mathcal{F}_{\text{action}} = \frac{\sqrt{\lambda}}{6} + \mathcal{A}_{\varpi} + \mathcal{A}_{\eta} \,, \qquad\qquad \mathcal{F}_{\text{vertex}} = \mathcal{V}_{\text{kin}} + \mathcal{V}_{\text{dyn}} + \mathcal{V}_{\text{energy}} \,. \tag{7.5.2}$$

Among these terms, $\mathcal{A}_{\varpi}$, $\mathcal{V}_{\text{kin}}$ and $\mathcal{V}_{\text{energy}}$ have already been evaluated respectively in (7.2.45), (7.3.60) and (7.3.62). Thus, our main task will be to compute $\mathcal{A}_{\eta}$ and $\mathcal{V}_{\text{dyn}}$. As shown in (7.2.46) and (7.3.61), $\mathcal{A}_{\eta}$ is given by the normal ordered derivatives of the Wronskians, $:\partial_x \ln\langle i_+ \,, j_+\rangle:_{\pm}$, whereas $\mathcal{V}_{\text{dyn}}$ is given by the Wronskians evaluated at $x = 0$ and $x = \infty$, $\ln\langle i_+ \,, j_+\rangle|_{\infty}$ and $\ln\langle i_- \,, j_-\rangle|_0$. From the discussion in section 7.4, we know the Wronskians are comprised of two different parts, the convolution-integral part $\mathsf{Conv}\,[\ln\langle i_* \,, j_*\rangle]$ and the singular part $\mathsf{Sing}_{\pm}\,[\ln\langle i_* \,, j_*\rangle]$. They both contribute to $\mathcal{A}_{\eta}$ and $\mathcal{V}_{\text{dyn}}$. In what follows, we examine these two parts separately and evaluate their contributions to $\mathcal{A}_{\eta}$ and $\mathcal{V}_{\text{dyn}}$.

Contributions from the convolution integrals

We begin with the computation of the convolution integrals. To illustrate the basic idea, let us study $\mathsf{Conv}\,[\ln\langle 2_+ \,, 1_+\rangle]|_{\infty}$, $\mathsf{Conv}\,[\ln\langle 2_- \,, 1_-\rangle]|_0$ and $:\partial_x \mathsf{Conv}\,[\ln\langle 2_+ \,, 1_+\rangle]:_{\pm}$ as representative examples.

To compute the first two quantities, we need to know on which side of the integration contours the points $x = 0$ and $x = \infty$ are located. This is because the convolution integrals derived in subsection 7.4.4 are valid only when x is on the left hand side of the contours.

When x is on the right hand side of the contours, we must include the contact terms, which originate from the integration around $x' = x$. Unfortunately, the form of the contours depend on the specific details of the solutions we use and hence we cannot give a general discussion. We will therefore postpone the discussion of the contact terms until we study several explicit examples in the next section.

Apart from such contact terms, $\mathsf{Conv}\left[\langle 2_+ , 1_+\rangle\right]|_\infty$ and $\mathsf{Conv}\left[\langle 2_- , 1_-\rangle\right]|_0$ can be obtained directly from (7.4.60), (7.4.61), (7.4.74) and (7.4.75) by setting the value of x in the convolution kernels $\mathcal{K}_i(x';x)$ to be 0 and ∞ respectively.

Next, consider the evaluation of the normal-ordered derivative $:\partial_x \mathsf{Conv}\left[\ln\langle 2_+ , 1_+\rangle\right]:_\pm$. This quantity does not receive contributions from the contact terms since the integration contours pass right through $x = \pm 1$ and we can compute $:\partial_x \mathsf{Conv}\left[\ln\langle 2_+ , 1_+\rangle\right]:_\pm$ always on the left hand side of the contour. In addition, since the convolution integrals are nonsingular at $x = \pm 1$, as discussed at the end of section 7.4.4, the normal ordering is in fact unnecessary. Thus, $:\partial_x \mathsf{Conv}\left[\ln\langle 2_+ , 1_+\rangle\right]:_\pm$ can be obtained from (7.4.60) and (7.4.74) by simply replacing $\mathcal{K}_i(x';x)$ with their derivatives $\partial_x \mathcal{K}_i(x';x)|_{x=\pm 1}$.

Applying similar analyses to other Wronskians and using the formulas (7.2.46) and (7.3.61), we can obtain the contributions of the convolution integrals to $\mathcal{A}_\eta$ and $\mathcal{V}_{\rm dyn}$, which will be denoted by $\mathsf{Conv}\left[\mathcal{A}_\eta\right]$ and $\mathsf{Conv}\left[\mathcal{V}_{\rm dyn}\right]$. They are given by

$$\begin{aligned}
\mathsf{Conv}\left[\mathcal{A}_\eta\right] =& \sqrt{\lambda}\left[\int_{\mathcal{M}^{uuu}_{---}} \Big\langle\!\Big\langle \kappa_i\, \partial_x \mathcal{K}_i|_+ - \kappa_i\, \partial_x \mathcal{K}_i|_- \Big\rangle\!\Big\rangle_{123} * \ln\sin\left(\frac{p_1+p_2+p_3}{2}\right)\right. \\
&+ \int_{\mathcal{M}^{uuu}_{--+}} \Big\langle\!\Big\langle \kappa_i\, \partial_x \mathcal{K}_i|_+ - \kappa_i\, \partial_x \mathcal{K}_i|_- \Big\rangle\!\Big\rangle^3_{12} * \ln\sin\left(\frac{p_1+p_2-p_3}{2}\right) \\
&+ \int_{\mathcal{M}^{uuu}_{-+-}} \Big\langle\!\Big\langle \kappa_i\, \partial_x \mathcal{K}_i|_+ - \kappa_i\, \partial_x \mathcal{K}_i|_- \Big\rangle\!\Big\rangle^2_{13} * \ln\sin\left(\frac{p_1-p_2+p_3}{2}\right) \\
&+ \int_{\mathcal{M}^{uuu}_{+--}} \Big\langle\!\Big\langle \kappa_i\, \partial_x \mathcal{K}_i|_+ - \kappa_i\, \partial_x \mathcal{K}_i|_- \Big\rangle\!\Big\rangle^1_{23} * \ln\sin\left(\frac{-p_1+p_2+p_3}{2}\right) \\
&\left. -2\sum_{j=1}^{3}\int_{\Gamma^u_{j_-}} \left(\kappa_j\, \partial_x \mathcal{K}_j|_+ - \kappa_j\, \partial_x \mathcal{K}_j|_-\right) * \ln\sin p_j\right] , \qquad (7.5.3)
\end{aligned}$$

$$
\begin{aligned}
\mathsf{Conv}\,[\mathcal{V}_{\rm dyn}] = &\int_{\mathcal{M}^{uuu}_{---}} \Big\langle\!\!\Big\langle S^i_\infty\, \mathcal{K}_i|_\infty + S^i_0\, \mathcal{K}_i|_0 \Big\rangle\!\!\Big\rangle_{123} * \ln\sin\left(\frac{p_1+p_2+p_3}{2}\right) \\
&+ \int_{\mathcal{M}^{uuu}_{--+}} \Big\langle\!\!\Big\langle S^i_\infty\, \mathcal{K}_i|_\infty + S^i_0\, \mathcal{K}_i|_0 \Big\rangle\!\!\Big\rangle^3_{12} * \ln\sin\left(\frac{p_1+p_2-p_3}{2}\right) \\
&+ \int_{\mathcal{M}^{uuu}_{-+-}} \Big\langle\!\!\Big\langle S^i_\infty\, \mathcal{K}_i|_\infty + S^i_0\, \mathcal{K}_i|_0 \Big\rangle\!\!\Big\rangle^2_{13} * \ln\sin\left(\frac{p_1-p_2+p_3}{2}\right) \\
&+ \int_{\mathcal{M}^{uuu}_{+--}} \Big\langle\!\!\Big\langle S^i_\infty\, \mathcal{K}_i|_\infty + S^i_0\, \mathcal{K}_i|_0 \Big\rangle\!\!\Big\rangle^1_{23} * \ln\sin\left(\frac{-p_1+p_2+p_3}{2}\right) \\
&- 2\sum_{j=1}^{3} \int_{\Gamma^u_{j-}} \left(S^j_\infty\, \mathcal{K}_j|_\infty + S^j_0\, \mathcal{K}_j|_0\right) * \ln\sin p_j\,. \qquad (7.5.4)
\end{aligned}
$$

To simplify the expressions, we have introduced the double bracket notation $\Big\langle\!\!\Big\langle\, \bullet \,\Big\rangle\!\!\Big\rangle$, to denote sum of three terms with designated combinations of signs, defined as

$$
\Big\langle\!\!\Big\langle a_i \Big\rangle\!\!\Big\rangle_{123} = a_1 + a_2 + a_3\,, \quad \Big\langle\!\!\Big\langle a_i \Big\rangle\!\!\Big\rangle^3_{12} = a_1 + a_2 - a_3\,, \quad \text{etc.}\,, \qquad (7.5.5)
$$

Also, we have employed the abbreviated symbols $\partial_x \mathcal{K}_i|_\pm$, $\mathcal{K}_i|_\infty$ and $\mathcal{K}_i|_0$, which are defined by

$$
\partial_x \mathcal{K}_i|_\pm \equiv \partial_x \mathcal{K}_i(x';x)|_{x=\pm 1}\,, \quad \mathcal{K}_i|_\infty \equiv \mathcal{K}_i(x';\infty)\,, \quad \mathcal{K}_i|_0 \equiv \mathcal{K}_i(x';0)\,. \qquad (7.5.6)
$$

It turns out that the two contributions (7.5.3) and (7.5.4) combine to give a remarkably simple expression displayed below. This is due to the crucial relation of the form

$$
\sqrt{\lambda}\kappa_i\, \partial_x \mathcal{K}_i|_+ - \sqrt{\lambda}\kappa_i\, \partial_x \mathcal{K}_i|_- + S^i_\infty\, \mathcal{K}_i|_\infty + S^i_0\, \mathcal{K}_i|_0 = z(x')\frac{dp_i(x')}{dx'}\,, \qquad (7.5.7)
$$

where $z(x)$ on the right hand side is the Zhoukowski variable, defined in (3.2.55). Although this equality can be verified by a direct computation using the explicit form of $p_i(x)$ for the one-cut solutions given in (7.1.25), it is important to give a more intuitive and essential understanding. Note that the right hand side of (7.5.7) is proportional to the integrand of the filling fraction given in (3.2.54). Therefore when integrated over appropriate a-type cycles, it produces the corresponding conserved charges. In other words, it is characterized by the singularities associated with such charges. Now observe that the left hand side precisely consists of terms which provide such singularities. The first two terms are responsible for the singularities at $x = \pm 1$, while the last two terms contain the poles at $x = \infty$ and $x = 0$ associated with the charges S^i_∞ and S^i_0 respectively. Furthermore, it should be emphasized that the formula above *unifies* the contributions in two sense of the word. First, it unites the contributions from the action, represented by the first two terms, and those from the

vertex operators, represented by the last two terms. Only when they are put together one can reproduce all the singularities of the right hand side. Second, the expression obtained on the right hand side is universal in that all the specific data shown on the left hand side, namely κ_i, S^i_∞ and S^i_0, are contained in one quantity $p_i(x)$. As we shall discuss in section 7.5.2, this feature allows us to write down the same form of the result (except for an overall sign) given by the right hand side of (7.5.7) for the contributions from the $EAdS_3$ part, using the quasi-momentum for that part of the string.

Now, applying (7.5.7) we can rewrite the sum $\mathcal{T}_{\rm conv} \equiv \mathsf{Conv}\,[\mathcal{A}_\eta] + \mathsf{Conv}\,[\mathcal{V}_{\rm dyn}]$ into the following compact expression:

$$\begin{aligned}
\mathcal{T}_{\rm conv} = &\int_{\mathcal{M}^{uuu}_{---}} \frac{z(x)\,(dp_1+dp_2+dp_3)}{2\pi i} \ln\sin\left(\frac{p_1+p_2+p_3}{2}\right) \\
&+ \int_{\mathcal{M}^{uuu}_{--+}} \frac{z(x)\,(dp_1+dp_2-dp_3)}{2\pi i} \ln\sin\left(\frac{p_1+p_2-p_3}{2}\right) \\
&+ \int_{\mathcal{M}^{uuu}_{-+-}} \frac{z(x)\,(dp_1-dp_2+dp_3)}{2\pi i} \ln\sin\left(\frac{p_1-p_2+p_3}{2}\right) \\
&+ \int_{\mathcal{M}^{uuu}_{+--}} \frac{z(x)\,(-dp_1+dp_2+dp_3)}{2\pi i} \ln\sin\left(\frac{-p_1+p_2+p_3}{2}\right) \\
&- 2\sum_{j=1}^{3} \int_{\Gamma^u_{j-}} \frac{z(x)\,dp_j}{2\pi i} \ln\sin p_j + \mathsf{Contact}\,. \qquad (7.5.8)
\end{aligned}$$

In the last line, we included the possible contributions from the contact terms, denoted by $\mathsf{Contact}$.

Contributions from the singular part of the Wronskians

We now turn to the computation of the singular part $\mathsf{Sing}_\pm\,[\ln\langle i_*\,,j_*\rangle]$. By substituting the expressions for the singular part of the Wronskians, such as (7.4.96) and (7.4.97), into the formulas (7.2.46) and (7.3.61), we can evaluate the contributions of the singular part in a straightforward manner. From this calculation, we find that a part of the terms contribute only to the overall phase of the three-point functions. For instance, the first and the third term in (7.4.96), which are proportional to $\pm\pi i(\kappa_1+\kappa_2-\kappa_3)$, will only yield an overall phase owing to the factor of πi. Just as before, we will ignore such contributions in this work. Then the contributions of $\mathsf{Sing}_+\,[\ln\langle i_*\,,j_*\rangle]$ to $\mathcal{A}_\eta$ and $\mathcal{V}_{\rm dyn}$, denoted by $\mathsf{Sing}_+\,[\mathcal{A}_\eta]$ and $\mathsf{Sing}_+\,[\mathcal{V}_{\rm dyn}]$,

are obtained as

$$\mathsf{Sing}_{+}\left[\mathcal{A}_{\eta}\right]=\sqrt{\lambda}\left[\left\langle\!\!\left\langle \kappa_i{:}\partial_x\mathcal{K}_i(1;x){:}_{+}-\kappa_i\;\partial_x\mathcal{K}_i(1;x)|_{-}\right\rangle\!\!\right\rangle_{12}^{3}\int_{\ell_{21}}\varpi\right.$$
$$+\left\langle\!\!\left\langle \kappa_i{:}\partial_x\mathcal{K}_i(1;x){:}_{+}-\kappa_i\;\partial_x\mathcal{K}_i(1;x)|_{-}\right\rangle\!\!\right\rangle_{23}^{1}\int_{\ell_{23}}\varpi$$
$$\left.+\left\langle\!\!\left\langle \kappa_i{:}\partial_x\mathcal{K}_i(1;x){:}_{+}-\kappa_i\;\partial_x\mathcal{K}_i(1;x)|_{-}\right\rangle\!\!\right\rangle_{13}^{2}\int_{\ell_{\hat{3}1}}\varpi\right], \tag{7.5.9}$$

and

$$\mathsf{Sing}_{+}\left[\mathcal{V}_{\mathrm{dyn}}\right]=\left[\left\langle\!\!\left\langle S_{\infty}^{i}\;\mathcal{K}_i|_{\infty}+S_{0}^{i}\;\mathcal{K}_i|_{0}\right\rangle\!\!\right\rangle_{12}^{3}\int_{\ell_{21}}\varpi+\left\langle\!\!\left\langle S_{\infty}^{i}\;\mathcal{K}_i|_{\infty}+S_{0}^{i}\;\mathcal{K}_i|_{0}\right\rangle\!\!\right\rangle_{23}^{1}\int_{\ell_{23}}\varpi\right.$$
$$\left.+\left\langle\!\!\left\langle S_{\infty}^{i}\;\mathcal{K}_i|_{\infty}+S_{0}^{i}\;\mathcal{K}_i|_{0}\right\rangle\!\!\right\rangle_{13}^{2}\int_{\ell_{\hat{3}1}}\varpi\right]\Bigg|_{x'=+1}. \tag{7.5.10}$$

Note that in the present case, in contrast to the case of ${:}\partial_x\mathsf{Conv}\left[\ln\langle i_{*}\,,j_{*}\rangle\right]{:}_{\pm}$ discussed previously, the normal ordering in ${:}\partial_x\mathcal{K}_i(1;x){:}_{+}$ is necessary since $\partial_x\mathcal{K}_i(1;x)$ is singular at $x=1$. In an entirely similar manner, the contributions of $\mathsf{Sing}_{-}\left[\ln\langle i_{*}\,,j_{*}\rangle\right]$ to $\mathcal{A}_{\eta}$ and $\mathcal{V}_{\mathrm{dyn}}$, denoted by $\mathsf{Sing}_{-}\left[\mathcal{A}_{\eta}\right]$ and $\mathsf{Sing}_{-}\left[\mathcal{V}_{\mathrm{dyn}}\right]$, are computed as

$$\mathsf{Sing}_{-}\left[\mathcal{A}_{\eta}\right]=-\sqrt{\lambda}\left[\left\langle\!\!\left\langle \kappa_i\;\partial_x\mathcal{K}_i(-1;x)|_{+}-\kappa_i{:}\partial_x\mathcal{K}_i(-1;x){:}_{-}\right\rangle\!\!\right\rangle_{12}^{3}\int_{\ell_{21}}\bar{\varpi}\right.$$
$$+\left\langle\!\!\left\langle \kappa_i\;\partial_x\mathcal{K}_i(-1;x)|_{+}-\kappa_i{:}\partial_x\mathcal{K}_i(-1;x){:}_{-}\right\rangle\!\!\right\rangle_{23}^{1}\int_{\ell_{23}}\bar{\varpi}$$
$$\left.+\left\langle\!\!\left\langle \kappa_i\;\partial_x\mathcal{K}_i(-1;x)|_{+}-\kappa_i{:}\partial_x\mathcal{K}_i(-1;x){:}_{-}\right\rangle\!\!\right\rangle_{13}^{2}\int_{\ell_{\hat{3}1}}\bar{\varpi}\right], \tag{7.5.11}$$

and

$$\mathsf{Sing}_{-}\left[\mathcal{V}_{\mathrm{dyn}}\right]=-\left[\left\langle\!\!\left\langle S_{\infty}^{i}\;\mathcal{K}_i|_{\infty}+S_{0}^{i}\;\mathcal{K}_i|_{0}\right\rangle\!\!\right\rangle_{12}^{3}\int_{\ell_{21}}\bar{\varpi}+\left\langle\!\!\left\langle S_{\infty}^{i}\;\mathcal{K}_i|_{\infty}+S_{0}^{i}\;\mathcal{K}_i|_{0}\right\rangle\!\!\right\rangle_{23}^{1}\int_{\ell_{23}}\bar{\varpi}\right.$$
$$\left.\left\langle\!\!\left\langle S_{\infty}^{i}\;\mathcal{K}_i|_{\infty}+S_{0}^{i}\;\mathcal{K}_i|_{0}\right\rangle\!\!\right\rangle_{13}^{2}\int_{\ell_{\hat{3}1}}\bar{\varpi}\right]\Bigg|_{x'=-1}. \tag{7.5.12}$$

Now just as we did for $\mathsf{Conv}\left[\mathcal{A}_{\eta}\right]+\mathsf{Conv}\left[\mathcal{V}_{\mathrm{dyn}}\right]$, we can make use of the relation (7.5.7) to

rewrite the sum $\mathsf{Sing}_{\pm}[\mathcal{A}_\eta] + \mathsf{Sing}_{\pm}[\mathcal{V}_{\rm dyn}]$ into much simpler forms. The results are

$$\begin{aligned}\mathsf{Sing}_{+}[\mathcal{A}_\eta] + \mathsf{Sing}_{+}[\mathcal{V}_{\rm dyn}] =& :z(x)\left(\frac{dp_1}{dx}+\frac{dp_2}{dx}-\frac{dp_3}{dx}\right):_{+}\int_{\ell_{21}}\varpi \\ &+ :z(x)\left(\frac{dp_1}{dx}-\frac{dp_2}{dx}+\frac{dp_3}{dx}\right):_{+}\int_{\ell_{\hat{3}1}}\varpi \\ &+ :z(x)\left(-\frac{dp_1}{dx}+\frac{dp_2}{dx}+\frac{dp_3}{dx}\right):_{+}\int_{\ell_{23}}\varpi\,, \end{aligned} \tag{7.5.13}$$

and

$$\begin{aligned}\mathsf{Sing}_{-}[\mathcal{A}_\eta] + \mathsf{Sing}_{-}[\mathcal{V}_{\rm dyn}] =& -:z(x)\left(\frac{dp_1}{dx}+\frac{dp_2}{dx}-\frac{dp_3}{dx}\right):_{-}\int_{\ell_{21}}\bar{\varpi} \\ &- :z(x)\left(\frac{dp_1}{dx}-\frac{dp_2}{dx}+\frac{dp_3}{dx}\right):_{-}\int_{\ell_{\hat{3}1}}\bar{\varpi} \\ &- :z(x)\left(-\frac{dp_1}{dx}+\frac{dp_2}{dx}+\frac{dp_3}{dx}\right):_{-}\int_{\ell_{23}}\bar{\varpi}\,. \end{aligned} \tag{7.5.14}$$

The expressions $:z(x)\,dp_i/dx:_{\pm}$ in (7.5.13) and (7.5.14) above can be evaluated using the explicit form of the quasi-momentum, given in (7.1.25), as[41]

$$:z(x)\frac{dp_i}{dx}:_{+} = -2\pi\kappa_i - \pi\kappa_i\Lambda_i\,, \quad :z(x)\frac{dp_i}{dx}:_{-} = 2\pi\kappa_i + \pi\kappa_i\bar{\Lambda}_i\,. \tag{7.5.15}$$

This provides fairly explicit forms for the expressions $\mathsf{Sing}_{\pm}[\mathcal{A}_\eta] + \mathsf{Sing}_{\pm}[\mathcal{V}_{\rm dyn}]$.

Result for the S^3 part

We can now combine the results obtained so far and obtain the net contribution of the S^3 part. Recall that the general structure of the S^3 part of the three-point functions we have computed is of the form

$$\begin{aligned}F_{S^3} =& \frac{\sqrt{\lambda}}{6} + 2\sqrt{\lambda}\sum_{i=1}^{3}\kappa_i^2\ln\epsilon_i + \mathcal{A}_\varpi + \mathcal{V}_{\rm kin} + \mathsf{Conv}[\mathcal{A}_\eta] + \mathsf{Conv}[\mathcal{V}_{\rm dyn}] \\ &+ \mathsf{Sing}_{+}[\mathcal{A}_\eta] + \mathsf{Sing}_{+}[\mathcal{V}_{\rm dyn}] + \mathsf{Sing}_{-}[\mathcal{A}_\eta] + \mathsf{Sing}_{-}[\mathcal{V}_{\rm dyn}]\,. \end{aligned} \tag{7.5.16}$$

Among the various terms shown above, those which can be expressed in terms of the contour integrals of ϖ or $\bar{\varpi}$ can be combined and evaluated using the explicit form of $:z\,dp_i/dx:_{\pm}$

[41] Definitions of Λ_i and $\bar{\Lambda}_i$ are given in (7.2.18) and (7.2.29).

given in (7.5.15). The result is

$$\begin{aligned}\mathcal{T}_{\text{sing}} \equiv & \mathcal{A}_{\varpi} + \mathsf{Sing}_{+}\left[\mathcal{A}_{\eta}\right] + \mathsf{Sing}_{+}\left[\mathcal{V}_{\text{dyn}}\right] + \mathsf{Sing}_{-}\left[\mathcal{A}_{\eta}\right] + \mathsf{Sing}_{-}\left[\mathcal{V}_{\text{dyn}}\right] \\ = & -\frac{\sqrt{\lambda}}{2}\left[(\kappa_1+\kappa_2-\kappa_3)\int_{\ell_{21}}(\varpi+\bar{\varpi}) + (\kappa_1-\kappa_2+\kappa_3)\int_{\ell_{\hat{3}1}}(\varpi+\bar{\varpi})\right. \\ & \left. +(-\kappa_1+\kappa_2+\kappa_3)\int_{\ell_{23}}(\varpi+\bar{\varpi})\right] . \end{aligned} \tag{7.5.17}$$

Since ϖ and $\bar{\varpi}$ behave near the punctures as

$$\varpi \to \frac{\kappa_i}{z-z_i}\,, \quad \bar{\varpi} \to \frac{\kappa_i}{\bar{z}-\bar{z}_i}\,, \quad (z \to z_i) \quad \text{for } i = 1, \bar{2}, 3\,, \tag{7.5.18}$$

the expression (7.5.17) diverges in the following fashion as the regularization parameters ϵ_i's tend to zero:

$$\mathcal{T}_{\text{sing}} \to -2\sqrt{\lambda}\sum_{i=1}^{3}\kappa_i^2 \ln\epsilon_i = -\mathcal{V}_{\text{energy}}\,. \tag{7.5.19}$$

Notice, however, that this divergence is precisely canceled by the second term of (7.5.16). Therefore, the quantity (7.5.16) as a whole is finite in the limit $\epsilon_i \to 0$. This is as expected for correctly normalized three-point functions.

Let us summarize the final result for the logarithm of the three-point functions coming from the S^3 part. It can be written in the form

$$F_{S^3} = \frac{\sqrt{\lambda}}{6} + \mathcal{V}_{\text{energy}} + \mathcal{T}_{\text{sing}} + \mathcal{V}_{\text{kin}} + \mathcal{T}_{\text{conv}}\,, \tag{7.5.20}$$

where $\mathcal{V}_{\text{kin}}$ is the kinematical factor depending only on the normalization vectors given in (7.3.60), $\mathcal{T}_{\text{conv}}$ is the sum of the contributions from the convolution integrals (7.5.8), and $\mathcal{T}_{\text{sing}}$, which is given in (7.5.17), represents the sum of $\mathcal{A}_{\varpi}$ defined in (7.2.45) and the contributions from the singular parts of the Wronskians.

7.5.2 The $EAdS_3$ part

We now discuss the contributions from the $EAdS_3$ part. Since the logic of the evaluation is almost entirely similar, we will not repeat the long analysis we performed for the S^3 part. In fact it suffices to explain which part of the analysis for the S^3 part can be "copied" and which part has to be modified.

Contribution from the action

Let us begin with the contribution from the action integral. Since $EAdS_3$ and S^3 are formally quite similar, the computation of the action integral can be performed in exactly the same manner. There is, however, a simple but crucial difference. It is the overall sign of the integral. The $EAdS_3$-subspace is expressed in terms of the embedding coordinate as

$$X^\mu X_\mu = -1\,, \quad \mu,\nu = -1,1,2,4\,, \tag{7.5.21}$$

$$\eta_{\mu\nu} = \text{diag}\,(-1,1,1,1)\,, \tag{7.5.22}$$

which is related to the Poincaré coordinates as

$$X^{-1} + X^4 = \frac{1}{z}\,, \quad X^{-1} - X^4 = z + \frac{x^r x_r}{z}\,, \quad X^r = \frac{x^r}{z}\,. \tag{7.5.23}$$

In terms of the embedding coordinate, the action is given by

$$S_{EAdS_3} = \frac{\sqrt{\lambda}}{\pi}\int d^2z\left(\partial X^\mu \bar{\partial} X_\mu\right)\,. \tag{7.5.24}$$

For practical purposes, it is useful to express it in a matrix form as

$$\mathbb{X} \equiv \begin{pmatrix} X_+ & X \\ X_- & \bar{X} \end{pmatrix}\,, \tag{7.5.25}$$

where

$$X_\pm \equiv X^{-1} \pm X^4\,,\,, \qquad X \equiv X^1 + iX^2\,, \qquad \bar{X} \equiv X^1 - iX^2\,. \tag{7.5.26}$$

The right current is then defined as

$$\hat{j} \equiv \mathbb{X}^{-1}d\mathbb{X} = \hat{j}_z dz + \hat{j}_{\bar{z}} d\bar{z}\,. \tag{7.5.27}$$

Now compare the expressions of the stress tensors and the action integrals for S^3 and $EAdS_3$, expressed in terms of the respective right current. They are given by

$$T(z) \equiv T_{AdS}(z) = \frac{1}{2}\text{tr}\,(\hat{j}_z\hat{j}_z) = \kappa^2\,, \quad T_S(z) = -\frac{1}{2}\text{tr}\,(j_z j_z) = -\kappa^2\,, \tag{7.5.28}$$

$$S_{AdS_3} = \frac{\sqrt{\lambda}}{2\pi}\int d^2z\,\text{tr}\,(\hat{j}_z\hat{j}_{\bar{z}})\,, \qquad S_{S^3} = -\frac{\sqrt{\lambda}}{2\pi}\int d^2z\,\text{tr}\,(j_z j_{\bar{z}})\,. \tag{7.5.29}$$

This shows that while we have the equality $\text{tr}\,(\hat{j}_z\hat{j}_z) = \text{tr}\,(j_z j_{\bar{z}}) = \kappa^2$, the signs in front of the action integrals are opposite. Therefore all the results for the action integral are formally the same as those for the S^3 case, but with opposite signs. This will lead to various cancellations with the contributions from the S^3 part, as we shall see shortly.

Contribution from the wave function

As for the evaluation of the contribution from the wave function, the basic logic of the formalism developed in section 7.3 for the S^3 still applies. However, there are a few important modifications, as we shall explain below.

In the case of a string in $EAdS_3$ the global symmetry group is $\mathrm{SL}(2,\mathrm{C})_R \times \mathrm{SL}(2,\mathrm{C})_L$ and hence the the raising operators with respect to which we define the highest weight state are the left and the right special conformal transformations given by

$$V_R^{\rm sc} = \begin{pmatrix} 1 & 0 \\ \beta_R & 1 \end{pmatrix}, \qquad V_L^{\rm sc} = \begin{pmatrix} 1 & \beta_L \\ 0 & 1 \end{pmatrix}, \tag{7.5.30}$$

where β_R and β_L are constants. Applying our general argument for the determination of the polarization spinors, we readily find that

$$(V_R^{\rm sc})^t n^{\rm diag} = n^{\rm diag}, \qquad n^{\rm diag} = \begin{pmatrix} 1 \\ 0 \end{pmatrix}, \tag{7.5.31}$$

$$(V_L^{\rm sc})^t \tilde{n}^{\rm diag} = \tilde{n}^{\rm diag}, \qquad \tilde{n}^{\rm diag} = \begin{pmatrix} 0 \\ 1 \end{pmatrix}, \tag{7.5.32}$$

are satisfied for the solution corresponding to the operator inserted at the origin of the boundary. It should be noted that, compared to the S^3 case given in (7.3.21), $n^{\rm diag}$ here for the right sector is the same as $\tilde{n}^{\rm diag}$ for the left sector there and similarly $\tilde{n}$ for the left sector in the present case is identical to $n^{\rm diag}$ for the right sector for the S^3 case. Now the algebraic manipulations for the construction of the wave functions are the same as for the S^3 case up to the computation of the factor $e^{i\Delta\phi}$. Therefore, for the *right* sector, we get the same result for the *left* sector in the S^3 case, given in (7.3.57). For example at z_1 we have

$$e^{i\Delta\phi_{R,1}} = a_1^{-2} = \frac{\langle 1_+, 2_+\rangle\langle 3_+, 1_+\rangle}{\langle 2_+, 3_+\rangle}\bigg|_\infty \frac{\langle n_2, n_3\rangle}{\langle n_1, n_2\rangle\langle n_3, n_1\rangle} \tag{7.5.33}$$

This is the *inverse* of the result for S^3 obtained in (7.3.50) with i_- replaced by i_+. The result for the left sector is similar. What this means is that the wave function for the $EAdS_3$ is obtained from the one for the S^3 case by (i) reversing the sign of the powers and (ii) exchanging i_+ and i_-. Abusing the same notations for the polarization spinors and the eigenvectors as in the S^3 case, we get

$$\Psi_R^{EAdS_3} = \prod_{\{i,j,k\}} \left(\frac{\langle n_i, n_j\rangle}{\langle i_+, j_+\rangle\big|_\infty} \right)^{-(R_i+R_j-R_k)}, \tag{7.5.34}$$

$$\Psi_L^{EAdS_3} = \prod_{\{i,j,k\}} \left(\frac{\langle \tilde{n}_i, \tilde{n}_j\rangle}{\langle \tilde{i}_-, \tilde{j}_-\rangle\big|_0} \right)^{-(L_i+L_j-L_k)}, \tag{7.5.35}$$

where R_i and L_i here are the combinations of the conformal dimension Δ_i and the spin S_i given by

$$R_i = \frac{\Delta_i - S_i}{2}\,, \qquad L_i = \frac{\Delta_i + S_i}{2}\,. \tag{7.5.36}$$

This reversal of power relative to the S^3 case is what is desired. Effectively it is equivalent to employing $e^{+iS\phi}$ as the form of the wave function. As we shall show below, correctness of this power structure becomes obvious when we relate the Wronskian $\langle n_i, n_j\rangle$ to the difference of the coordinates x_i and x_j, where x_i is the position of the i-th vertex operator on the boundary of $EAdS_3$.

Recall now that the embedding coordinates of $EAdS_3$ are taken to be X^μ ($\mu = -1, 1, 2, 4$), which is a vector of $SO(1,3)$ with signature $(-,+,+,+)$, while the Poincaré coordinates are given by $z = 1/(X^{-1} + X^4)$, $x^r = zX^r$, $(r = 1, 2)$, with which $X^{-1} - X^4$ is expressed as $z + (\vec{x}^2/z)$. Consider approaching a point on the boundary $z = 0$ with finite values of x^r. Then the term z in $X^{-1} - X^4$ becomes negligible compared to $\vec{x}^2/z$ and X^μ approaches a null vector, with large components. Such a null vector, to be dented by $\mathcal{X}^\mu$, can be parametrized, up to an overall scale, by the boundary coordinates $\vec{x} = (x^1, x^2)$ as

$$\mathcal{X}^{-1} = \frac{1}{2}(1 + \vec{x}^2)\,, \qquad \mathcal{X}^4 = \frac{1}{2}(1 - \vec{x}^2)\,, \qquad (\mathcal{X}^1, \mathcal{X}^2) = \vec{x}\,, \tag{7.5.37}$$

$$\vec{x}^2 = x^r \eta_{rs} x^s = x^r x_r\,, \qquad \eta_{rs} = (+,+)\,, \quad r, s = 1, 2\,. \tag{7.5.38}$$

As usual, one can map $\mathcal{X}^\mu$ to the matrix $\mathcal{X}^\mu \hat{\Sigma}_\mu$, with $\hat{\Sigma}_\mu = (1, \sigma_1, \sigma_2, \sigma_3)$, which transforms from left under $SL(2,C)$ and from right under $SL(2,C)^*$. Then, it is well-known that for a null vector $\mathcal{X}^\mu$ the matrix elements of $\mathcal{X}^\mu \hat{\Sigma}_\mu$ can be written as a product of spinors (or twistors) as

$$(\mathcal{X}^\mu \hat{\Sigma}_\mu)_{\alpha\dot{\alpha}} = \begin{pmatrix} 1 & x \\ \bar{x} & \vec{x}^2 \end{pmatrix} = (\sigma_1 \tilde{n})_\alpha n_{\dot{\alpha}}\,, \tag{7.5.39}$$

where

$$x \equiv x^1 + ix^2\,, \quad \bar{x} \equiv x^1 - ix^2\,, \tag{7.5.40}$$

$$n = \begin{pmatrix} 1 \\ x \end{pmatrix}\,, \qquad \tilde{n} = \begin{pmatrix} \bar{x} \\ 1 \end{pmatrix}\,. \tag{7.5.41}$$

These spinors can be identified precisely as the polarization spinors characterizing a vertex operator which is placed at $\vec{x}$ on the boundary for the following reasons. First they transform in the correct way: Under the global transformation $X^\mu \hat{\Sigma}_\mu \to V_L (X^\mu \hat{\Sigma}_\mu) V_R$, we have $(\sigma_1 \tilde{n})_\alpha \to (V_L \sigma_1 \tilde{n})_\alpha$ and $n_{\dot{\alpha}} \to (n V_R)_{\dot{\alpha}}$. This is equivalent to $\tilde{n} \to V_L^t \tilde{n}$ and $n \to V_R^t n$,

which are the right transformation laws. Second, these spinors coincide with the polarization spinors given in (7.5.31) and (7.5.32) when we bring the point $\vec{x}$ to the origin of the boundary by the translation by the vector $-\vec{x}$. This is effected by the right and the left translation matrices given by

$$V_R^{\rm tr}(-x) = \begin{pmatrix} 1 & -x \\ 0 & 1 \end{pmatrix}, \qquad V_L^{\rm tr}(-\bar{x}) = \begin{pmatrix} 1 & 0 \\ -\bar{x} & 1 \end{pmatrix}. \tag{7.5.42}$$

Then we get

$$(V_R^{\rm tr})^t n = \begin{pmatrix} 1 \\ 0 \end{pmatrix}, \qquad (V_L^{\rm tr})^t \tilde{n} = \begin{pmatrix} 0 \\ 1 \end{pmatrix}. \tag{7.5.43}$$

Therefore n and $\tilde{n}$ can be identified with the polarization spinors for the vertex operator at $\vec{x}$ on the boundary. Now let n' and $\tilde{n}'$ be similar polarization spinors corresponding to a vertex operator at $\vec{x'}$ on the boundary. Then we immediately get

$$\langle n, n' \rangle = x' - x\,, \qquad \langle \tilde{n}, \tilde{n}' \rangle = \bar{x}' - \bar{x}\,, \tag{7.5.44}$$

$$\langle n, n' \rangle \langle \tilde{n}, \tilde{n}' \rangle = (x' - x)(\bar{x}' - \bar{x}) = (x' - x)^2\,. \tag{7.5.45}$$

In this way, for the $EAdS_3$ the Wronskians formed by the polarization spinors produce the difference of the boundary position vectors. Therefore the relevant part of the wave function becomes

$$\begin{aligned} &\prod_{\{i,j,k\}} \langle n_i, n_j \rangle^{-(R_i+R_j-R_k)} \langle \tilde{n}_i, \tilde{n}_j \rangle^{-(L_i+L_j-L_k)} \\ &= \prod_{\{i,j,k\}} (x_i - x_j)^{-(R_i+R_j-R_k)} (\bar{x}_i - \bar{x}_j)^{-(L_i+L_j-L_k)}\,. \end{aligned} \tag{7.5.46}$$

In particular, for the case of spinless configurations that we are considering, this becomes

$$\prod_{\{i,j,k\}} \frac{1}{|x_i - x_j|^{\Delta_i+\Delta_j-\Delta_k}}\,, \tag{7.5.47}$$

which exhibits the familiar coordinate dependence for the three-point function in such a case.

Total contribution from the $EAdS_3$ part

As we have seen, the structure of the contribution from the $EAdS_3$ part is essentially the same as that from the S^3 case, except for the important reversal of signs in the powers in the contributing factor (or the terms contributing to the the logarithm of the three-point coupling.) This change of sign occurred both for the action and for the wave function. As we

compute the basic Wronskians in exactly the same way as before and use them to compute the contributions to the logarithm of the three-point function from the action part and the wave function part, we again obtain the expression of the form of the left hand side of (7.5.7), with the overall sign reversed. Therefore, we can use the identity (7.5.7) again to obtain the result $-z(x')d\hat{p}_i(x')/dx'$, where $\hat{p}_i$ denotes the quasi-momentum for the $EAdS_3$ part of the string. One can check that in fact this rule of correspondence, namely $p_i(x) \to \hat{p}_i(x)$ and the reversal of sign for the convolution integrals, applies to all the contributions. Thus, combining all the results for the AdS part, the contribution to the logarithm of the three-point function is given by the following expression:

$$F_{EAdS_3} = -\frac{\sqrt{\lambda}}{6} + \hat{\mathcal{V}}_{\text{energy}} + \hat{\mathcal{T}}_{\text{sing}} + \hat{\mathcal{V}}_{\text{kin}} + \hat{\mathcal{T}}_{\text{conv}} \,. \tag{7.5.48}$$

Here, $\hat{\mathcal{V}}_{\text{energy}}$ and $\hat{\mathcal{T}}_{\text{sing}}$ are equal to $-\mathcal{V}_{\text{energy}}$ and $-\mathcal{T}_{\text{sing}}$ respectively, $\hat{\mathcal{V}}_{\text{kin}}$ is the kinematical factor given in (7.5.47), and $\hat{\mathcal{T}}_{\text{conv}}$ is the convolution integrals obtained from the unhatted counterpart for the S^3 case with the substitution rule described above.

7.5.3 Complete expression for the three-point function

We are finally ready to put together the contributions from the S^3 part summarized in (7.5.20) and those from the $EAdS_3$ part given in (7.5.48) and present the full answer for the three-point function. As we have already discussed, the divergent terms cancel with each other for the S^3 part and the $EAdS_3$ part separately. On the other hand, the constant terms proportional to $\sqrt{\lambda}/6$ cancel between S^3 and $EAdS_3$ contributions. Thus we are left with the kinematical factors and the contributions from the convolution integrals which are of the same structure except for the overall sign. Therefore, factoring the kinematical structure as

$$\begin{aligned}\langle \mathcal{V}_1 \mathcal{V}_2 \mathcal{V}_3 \rangle =& \frac{1}{N} \frac{C_{123}}{|x_1 - x_2|^{\Delta_1+\Delta_2-\Delta_3}|x_2 - x_3|^{\Delta_2+\Delta_3-\Delta_1}|x_3 - x_1|^{\Delta_3+\Delta_1-\Delta_2}} \\ & \times \langle n_1 \,, n_2 \rangle^{R_1+R_2-R_3} \langle n_2 \,, n_3 \rangle^{R_2+R_3-R_1} \langle n_3 \,, n_1 \rangle^{R_3+R_1-R_2} \\ & \times \langle \tilde{n}_1 \,, \tilde{n}_2 \rangle^{L_1+L_2-L_3} \langle \tilde{n}_2 \,, \tilde{n}_3 \rangle^{L_2+L_3-L_1} \langle \tilde{n}_3 \,, \tilde{n}_1 \rangle^{L_3+L_1-L_2} \,,\end{aligned} \tag{7.5.49}$$

the logarithm of the structure constant C_{123} is finally given by

$$\ln C_{123} =$$

$$\int_{\mathcal{M}^{uuu}_{---}} \frac{z(x)\,(dp_1+dp_2+dp_3)}{2\pi i}\ln\sin\left(\frac{p_1+p_2+p_3}{2}\right)+\int_{\mathcal{M}^{uuu}_{--+}} \frac{z(x)\,(dp_1+dp_2-dp_3)}{2\pi i}\ln\sin\left(\frac{p_1+p_2-p_3}{2}\right)$$

$$+\int_{\mathcal{M}^{uuu}_{-+-}} \frac{z(x)\,(dp_1-dp_2+dp_3)}{2\pi i}\ln\sin\left(\frac{p_1-p_2+p_3}{2}\right)+\int_{\mathcal{M}^{uuu}_{+--}} \frac{z(x)\,(-dp_1+dp_2+dp_3)}{2\pi i}\ln\sin\left(\frac{-p_1+p_2+p_3}{2}\right)$$

$$-\int_{\hat{\mathcal{M}}^{uuu}_{---}} \frac{z(x)\,(d\hat{p}_1+d\hat{p}_2+d\hat{p}_3)}{2\pi i}\ln\sin\left(\frac{\hat{p}_1+\hat{p}_2+\hat{p}_3}{2}\right)-\int_{\hat{\mathcal{M}}^{uuu}_{--+}} \frac{z(x)\,(d\hat{p}_1+d\hat{p}_2-d\hat{p}_3)}{2\pi i}\ln\sin\left(\frac{\hat{p}_1+\hat{p}_2-\hat{p}_3}{2}\right)$$

$$-\int_{\hat{\mathcal{M}}^{uuu}_{-+-}} \frac{z(x)\,(d\hat{p}_1-d\hat{p}_2+d\hat{p}_3)}{2\pi i}\ln\sin\left(\frac{\hat{p}_1-\hat{p}_2+\hat{p}_3}{2}\right)-\int_{\hat{\mathcal{M}}^{uuu}_{+--}} \frac{z(x)\,(-d\hat{p}_1+d\hat{p}_2+d\hat{p}_3)}{2\pi i}\ln\sin\left(\frac{-\hat{p}_1+\hat{p}_2+\hat{p}_3}{2}\right)$$

$$-2\sum_{j=1}^{3}\int_{\Gamma^u_{j-}} \frac{z(x)\,dp_j}{2\pi i}\ln\sin p_j+2\sum_{j=1}^{3}\int_{\hat{\Gamma}^u_{j-}} \frac{z(x)\,d\hat{p}_j}{2\pi i}\ln\sin\hat{p}_j+\mathsf{Contact}\,, \tag{7.5.50}$$

where Contact stands for the contribution from the contact terms. Truly remarkable is that, in spite of the complexity of both the analysis and the intermediate expressions, the final answer takes such a simple form. Moreover, it exhibits essential similarity to the form of the weak coupling result [92, 93, 115, 116] even before taking any further limits. In the next section, we shall evaluate the structure constant (7.5.50) more explicitly, including the quantity Contact, for several important examples and compare with the weak coupling results more closely.

7.6 Examples and comparison with the weak coupling result

The results obtained in the previous section are quite general and applicable to three-point functions of arbitrary one-cut solutions on $EAdS_3 \times S^3$. In this section we focus on several explicit examples, make some basic checks and discuss the relation with the results at weak coupling.

In subsection 7.6.1, we first explain the basic set-up, which will be used throughout this section. Then, in subsection 7.6.2, we study the correlation functions of three BPS operators and see that the contributions from the S^3 part and the $EAdS_3$ part completely cancel out in this case. The results thus obtained fully agree with the results obtained in the gauge theory. In subsection 7.6.3, we study the behavior of the three-point function under the limit where the charge of one of the operators becomes negligibly small while the other two operators become identical. We confirm that the result reduces to that of the two-point function, as expected. Next, in subsection 7.6.4, we study three-point functions of one non-BPS and two BPS operators, which were studied on the gauge theory side in [115]. We will focus on certain explicit examples and show that the full three-point functions can be

expressed in terms of simple integrals which resemble the semi-classical limit of the results at weak coupling [92, 93, 115, 116]. Then, in subsection 7.6.5, we discuss the Frolov-Tseytlin limit of such three-point functions. In this limit, the integrands in the final expression approximately agree with the ones in the weak coupling, whereas the integration contours are rather different. Lastly, we discuss the possible origin and the implication of this mismatch.

7.6.1 Basic set-up

Before starting the detailed analysis, let us clarify the basic set-ups to be used in this section recalling several necessary facts.

The three-point functions studied extensively on the gauge theory side are those of the following three types of operators (see also (4.1).):

$$\mathcal{O}_1 = \mathrm{tr}\,\left(Z^{l_1-M_1}X^{M_1}\right)+\cdots\,,\quad \mathcal{O}_2 = \mathrm{tr}\,\left(\bar{Z}^{l_2-M_2}\bar{X}^{M_2}\right)+\cdots\,,\quad \mathcal{O}_3 = \mathrm{tr}\,\left(Z^{l_3-M_3}\bar{X}^{M_3}\right)+\cdots\,.$$

As explained in section 7.3.4, such three-point functions vanish unless the conservation laws[42] for the charges (7.3.63) are satisfied. Due to these conservation laws, one cannot in general take the operators to be simple BPS states, such as $\mathrm{tr}\,(Z^l)$ or $\mathrm{tr}\,(\bar{Z}^l)$, which are the highest-weight vectors of the global $\mathrm{SU}(2)_R\times\mathrm{SU}(2)_L$ symmetry. Instead, we need to use descendants of the global symmetry to satisfy the conservation laws when we study three-point functions involving BPS operators [80, 115]. While this can be done without problems on the gauge theory side, it leads to certain difficulty on the string theory side. This is because all the classical solutions of string are known to (or believed to) correspond to some highest-weight states. To circumvent this difficulty, below we will utilize the global transformations to make all three operators to be built on different "vacua". On the string theory side, this corresponds to taking the polarization vectors of the three operators, n_i's and $\tilde{n}_i$'s, to be all distinct. Then no conservation laws will be imposed and we can safely take the limit where some of the operators become BPS while keeping them to be of highest-weight. Since the correlation functions involving descendants can be obtained from the correlation functions involving the highest-weight states by simple group theoretical manipulations, knowledge of the three-point functions for the highest weight states is sufficient. In addition, replacing the highest-weight operator with its descendant only modifies the kinematical factor, $\mathcal{V}_{\mathrm{kin}}$, of our result and the dynamical parts of three-point functions, which are main subjects of study in this section, will not be affected.

After making the global transformations, the operators $\mathcal{O}_1$, $\mathcal{O}_2$ and $\mathcal{O}_3$ can be treated almost on the same footing. However, there is an important difference between $\mathcal{O}_3$ and the

[42] As we have shown in section 7.3, such conservation laws can be derived also on the string theory side.

other two in string theory: As explained in section 7.3.4, the quasi-momenta for the operators $\mathcal{O}_1$ and $\mathcal{O}_2$ contain branch cuts in the $|\mathrm{Re}\, x| > 1$ region, whereas the quasi-momentum for the operator $\mathcal{O}_3$ contains a branch cut in the $|\mathrm{Re}\, x| < 1$ region. This difference is important in the analysis to follow, since the position of the branch cuts affects the contours for the convolution integrals.

7.6.2 Case of three BPS operators

Let us first study the correlation functions of three BPS operators. In order to apply the general formula for the three-point functions of one-cut solutions obtained in the previous section, we need the explicit forms of $p(x)$ and $q(x)$ for the BPS operators, which in particular determine the integration contours. Within the bosonic sector, the characteristic feature of a BPS state is that, as it should correspond to a supergravity mode, it is "point-like", meaning that its two-point function is σ-independent. In the language of the spectral curve, it means the absence of a branch cut, since a branch cut corresponds to a non-trivial string mode with σ-dependence.

Now in fixing the forms of $p(x)$ and $q(x)$, there is a subtle problem with the configuration without a branch cut. In the case of one-cut solutions corresponding to non-BPS operators, the constant parts of $p(x)$ and $q(x)$ are fixed in such a way that they vanish at the branch points. Obviously, for configurations without a branch cut, this prescription cannot be applied. One natural remedy would be to start with a non-BPS solution, apply the usual method above to fix the constants and then shrink the cut to obtain a BPS solution. This idea, however, still does not cure the problem since the resultant $p(x)$ and $q(x)$ depend on the points on the spectral curve at which we shrink the branch cut. The existence of such an ambiguity possibly implies that the semi-classical three-point functions are affected by the presence of infinitesimal branch cuts. Although such an assertion sounds counter-intuitive, it is not totally inconceivable since similar effects were already observed in the study of "heavy-heavy-light" three-point functions[43] in [91].

Below we shall fix the ambiguity by employing a prescription which is quite natural from the viewpoint of the correspondence with the spin chain on the gauge theory side. The prescription is to shrink the branch cuts either at $x = 0$ or at $x = \infty$ in producing BPS operators. This choice is based on the following fact: In gauge theory, adding a small number of Bethe roots at $x = 0$ or $x = \infty$ correspond to performing a small global transformation and keeps the operator to be BPS, whereas adding a small number of Bethe roots at generic points on the spectral curve creates nontrivial magnon excitations and makes the operator non-BPS.

[43] In [91], such effects were called *back reactions*.

Having identified the classical solutions corresponding to BPS operators, let us now determine the integration contours. First we focus on the S^3-part of three-point functions. As discussed in section 7.3.4, for $\mathcal{O}_1$ and $\mathcal{O}_2$, $p_i(x)$ and $q_i(x)$ can have branch cuts only in the the $|\mathrm{Re}\, x| > 1$ region and hence we take the infinitesimal branch cut to be placed at $x = \infty$. Then from the general form of the one-cut solution given in (7.1.25) and (7.1.26), we get

$$p_i(x) = -2\pi\kappa_i \left(\frac{1}{x-1} + \frac{1}{x+1} \right) , \quad q_i(x) = -2\pi\kappa_i \left(\frac{1}{x-1} - \frac{1}{x+1} \right) , \tag{7.6.1}$$

which vanish at $x = \infty$, as desired. On the other hand, for $\mathcal{O}_3$, since the branch cuts can only be in the $|\mathrm{Re}\, x| < 1$ region, we place an infinitesimal branch cut at $x = 0$. Then from (7.1.25) and (7.1.26) we get

$$p_3(x) = -2\pi\kappa_3 \left(\frac{x}{x-1} - \frac{x}{x+1} \right) = -2\pi\kappa_3 \left(\frac{1}{x-1} + \frac{1}{x+1} \right) \tag{7.6.2}$$

$$q_3(x) = -2\pi\kappa_3 \left(\frac{x}{x-1} + \frac{x}{x+1} \right) . \tag{7.6.3}$$

These expressions vanish at $x = 0$.

As discussed in detail in section 7.4, the contours for the convolution integrals consist of two types of curves. The first type are those defined by $\mathrm{Re}\, q_i(x) = 0$, across which the relative magnitude of i_+ and i_- changes. They determine the integration contours $\Gamma^u_{i_-}$ defined in section 7.4.4 and are depicted in Figure 7.6.1. Note that in the present case, the contours $\Gamma^u_{1_-}$ and $\Gamma^u_{2_-}$ coincide since $q_1(x) = q_2(x)$. The second type are the curves defined by $N_i = N_j + N_k$, across which the connectivity of the exact WKB curves changes. Now for a BPS operator, $N_i = |\mathrm{Re}\, p_i(x)|$ is given by a common function $|\mathrm{Re}\, ((x+1)^{-1} + (x-1)^{-1})|$ times the factor $-2\pi\kappa_i$, as shown above. Since κ_i's satisfy the triangular inequalities, this means that $N_i = N_j + N_k$ cannot be satisfied. Hence the second type of curves are absent and the integration contours are determined solely by the first type of curves.

With this knowledge, we can now apply the general rules given at the end of section 7.4.3 to determine the integration contours $\mathcal{M}^{uuu}_{\pm\pm\pm}$. As an example, consider the contour $\mathcal{M}^{uuu}_{---}$, which is used for the convolution integral involving $\sin \frac{1}{2}(-p_1(x) - p_2(x) - p_3(x))$. From the Rule 1, either Wronskians among $\mathcal{S}_- = \{1_-, 2_-, 3_-\}$ vanish or those among $\mathcal{S}_+ = \{1_+, 2_+, 3_+\}$ vanish. Then we must apply Rule 2, since the triangle inequalities are satisfied in the present case. It states that if two of the members of $\mathcal{S}_-$ (resp. $\mathcal{S}_+$) are small solutions, then the Wronskians for the members of $\mathcal{S}_+$ (resp. $\mathcal{S}_-$) vanish. Now consider the curve $\Gamma^u_{1_-}$. From its definition, it is along $\mathrm{Re}\, q_1(x) = 0$ with the direction such that to the left of this curve 1_- is the small solution. The curve $\Gamma^u_{2_-}$ is identical, as we already remarked. These curves are depicted in the left figure of Figure 7.6.1, together with the states which are small in the three regions separated by these curves. Together with the rules mentioned above, we

see explicitly that the analyticity of Wronskians change across such curves and hence we can identify $\Gamma^u_{1_-}(=\Gamma^u_{2_-})$ as the contour $\mathcal{M}^{uuu}_{---}$. Similarly, the curve $\Gamma^u_{3_-}$, identified as $\mathcal{M}^{uuu}_{+--}$, is shown in the right figure of Figure 7.6.1. In this way, we find the contours $\mathcal{M}^{uuu}_{\pm\pm\pm}$ to be given by

$$\begin{aligned}
&\mathcal{M}^{uuu}_{---} = \Gamma^u_{1_-}(=\Gamma^u_{2_-})\,, \quad \mathcal{M}^{uuu}_{+--} = \Gamma^u_{3_-}\,, \\
&\mathcal{M}^{uuu}_{-+-} = \Gamma^u_{3_-}\,, \quad \mathcal{M}^{uuu}_{--+} = \Gamma^u_{1_-}(=\Gamma^u_{2_-})\,.
\end{aligned} \tag{7.6.4}$$

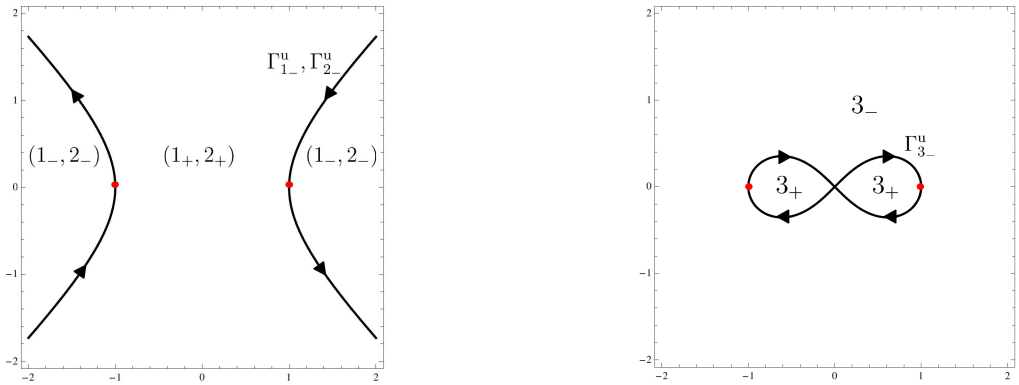

Figure 7.6.1: The contours $\Gamma^u_{i_-}$, defined by $\mathrm{Re}\, q_i = 0$. In each region, we showed which of the eigenvectors is the small solution.

Let us next consider the effects of the contact terms. As argued in section 7.5, such contribution must be taken into account when $x = 0$ ($x = \infty$) is on the left (right) hand side of the integration contours. The effect is most conveniently done by adding a small circle around $x = 0$ ($x = \infty$) to the contour for each integration in (7.5.8). However, in the case of BPS operators, the integration contours terminate right at $x = 0$ or $x = \infty$. Therefore we need to first regularize them by putting a small branch cut slightly away from $x = 0$ or $x = \infty$ and then take the limit where the branch cut shrinks to $x = 0$ or $x = \infty$. An example of such a procedure is depicted in Figure 7.6.2. Since the sine-functions in the convolution integrals (7.5.8) turn out to vanish only on the real axis in the case of BPS operators, we can further deform the contours into those on the unit circle. As a result, we find that the S^3-part of the three-point function is given by

$$\begin{aligned}
&\oint_U \frac{z\,(dp_1+dp_2+dp_3)}{2\pi i} \ln\sin\left(\frac{p_1+p_2+p_3}{2}\right) + \oint_U \frac{z\,(dp_1+dp_2-dp_3)}{2\pi i} \ln\sin\left(\frac{p_1+p_2-p_3}{2}\right) \\
&+ \oint_U \frac{z\,(dp_1-dp_2+dp_3)}{2\pi i} \ln\sin\left(\frac{p_1-p_2+p_3}{2}\right) + \oint_U \frac{z\,(-dp_1+dp_2+dp_3)}{2\pi i} \ln\sin\left(\frac{-p_1+p_2+p_3}{2}\right) \\
&- 2\sum_{j=1}^{3} \int_U \frac{z\,dp_j}{2\pi i} \ln\sin p_j\,,
\end{aligned}$$

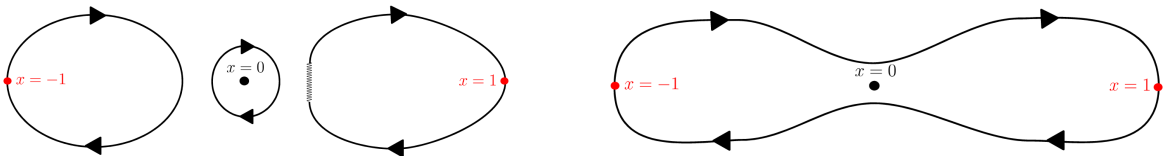

(a) Putting a small branch cut away from $x = 0$.

(b) Shrinking the cut and deforming the contour.

Figure 7.6.2: An example of the contour deformation. The contour depicted in (b) can be further deformed into the contour on the unit circle.

where U denotes the contour which goes around the unit circle clockwise.

Next consider the $EAdS_3$-part of the three-point function. The quasi-momenta and the quasi-energies for the operators without spin in AdS are given in [105] by[44]

$$\hat{p}_i(x) = -2\pi\kappa_i \left(\frac{1}{x-1} + \frac{1}{x+1} \right) , \quad \hat{q}_i(x) = -2\pi\kappa_i \left(\frac{1}{x-1} - \frac{1}{x+1} - 1 \right) . \tag{7.6.5}$$

Then, performing a similar analysis as in the case of S^3-part, we find that the result is again given by the integrals along the unit circle. As the quasi-momenta $p_i(x)$ for the S^3-part and the ones $\hat{p}_i(x)$ for the $EAdS_3$-part coincide in the case of BPS operators, we see from the general formula (7.5.50) that the contributions form these two parts cancel each other completely. Therefore, the three-point function for three BPS operators is given purely by the kinematical factors as

$$\begin{aligned} \langle V_1 V_2 V_3 \rangle = & \frac{1}{|x_1 - x_2|^{\Delta_1+\Delta_2-\Delta_3} |x_2 - x_3|^{\Delta_2+\Delta_3-\Delta_1} |x_3 - x_1|^{\Delta_3+\Delta_1-\Delta_2}} \\ & \times \langle n_1 \, , n_2 \rangle^{R_1+R_2-R_3} \langle n_2 \, , n_3 \rangle^{R_2+R_3-R_1} \langle n_3 \, , n_1 \rangle^{R_3+R_1-R_2} \\ & \times \langle \tilde{n}_1 \, , \tilde{n}_2 \rangle^{L_1+L_2-L_3} \langle \tilde{n}_2 \, , \tilde{n}_3 \rangle^{L_2+L_3-L_1} \langle \tilde{n}_3 \, , \tilde{n}_1 \rangle^{L_3+L_1-L_2} , \end{aligned} \tag{7.6.6}$$

This is consistent with the result in the gauge theory that the three-point functions of BPS operators are tree-level exact and have no dependence on the 'tHooft coupling constant λ.

7.6.3 Limit producing two-point function

Having seen that the BPS three-point functions are correctly reproduced from our general formula, let us next discuss the limit where the three-point functions are expected to reduce to two-point functions. As an example, we take two of the operators $\mathcal{O}_1$ and $\mathcal{O}_2$ to have

[44] The spectral parameter x used in (7.6.5) is related to the spectral parameter ξ used in [105] by $\xi = (x-1)/(x+1)$.

identical quasi-momenta and quasi-energy, while $\mathcal{O}_3$ is a BPS operator with vanishingly small charge[45].

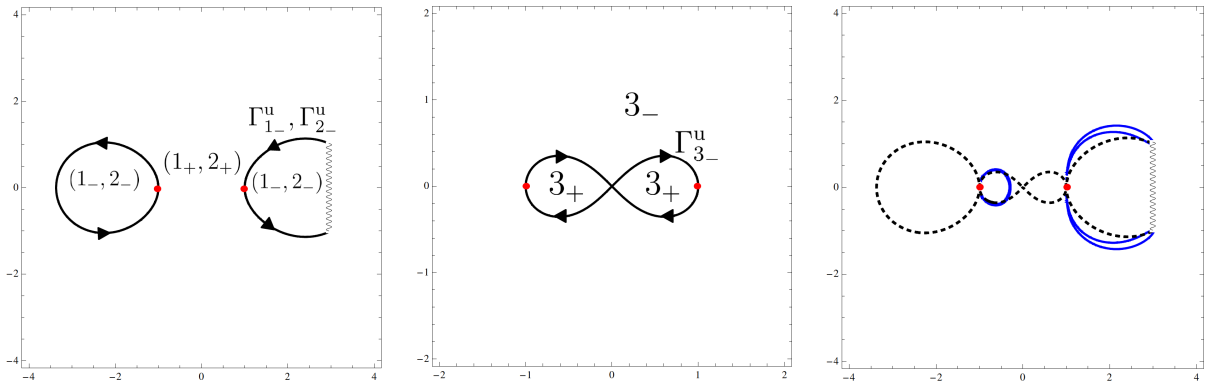

(a) (b) (c)

Figure 7.6.3: The curves which determine the integration contours in the limit where three-point functions reduce to two-point functions. In the left and the middle figures, the contours $\Gamma^{u}_{i_-}$, determined by Re $q_i(x) = 0$ are depicted. The segment represented by a wavy line is the branch cut. In the rightmost figure, the curve defined by $N_3 = N_1 + N_3$ is drawn in blue. For convenienece, we redisplayed the curves in figures (a) and (b) as dotted lines.

To understand what happens in such a limit, let us draw the two types of curves, namely Re $q_i = 0$ and $N_i = N_j + N_k$. The first type of curves are depicted in the first and the second figures of Figure 7.6.3. As for the second type, the only curve we need to consider is the curve given by $N_3 = N_1 + N_2$. This is because the inequalities $N_1 + N_3 \geq N_2$ and $N_2 + N_3 \geq N_1$ are always satisfied since $N_1 = N_2$ in the present case. When the operator $\mathcal{O}_3$ is sufficiently small, the curve defined by $N_3 = N_1 + N_2$ almost vanishes and we can practically ignore the effects of such a curve. Thus the integration contours are given purely by Re $q_1 =$ Re $q_2 = 0$. Applying the rules given in the previous section and taking into account the contact terms,

[45] Although the case considered here appears similar to the one studied in the gauge theory [91] with $\mathcal{O}_3$ taken to be small but nonvanishing, there is a difference: In [91], $\mathcal{O}_1$ and $\mathcal{O}_2$ must have slightly different quasi-momenta in the presence of $\mathcal{O}_3$, due to the conservation law for the magnons. In the present case, however, as we performed the global transformation, no conservation law is imposed and we can take $\mathcal{O}_1$ and $\mathcal{O}_2$ to have identical quasi-momenta.

we find that the convolution integrals for the S^3-part are given by

$$\int_{\Gamma^u_{1\_}+\mathcal{C}_\infty} \frac{z\,(dp_1+dp_2+dp_3)}{2\pi i} \ln\sin\left(\frac{p_1+p_2+p_3}{2}\right) + \int_{\Gamma^u_{1\_}+\mathcal{C}_\infty} \frac{z\,(dp_1+dp_2-dp_3)}{2\pi i} \ln\sin\left(\frac{p_1+p_2-p_3}{2}\right)$$
$$+ \int_{\Gamma^u_{3\_}+\mathcal{C}_0} \frac{z\,(dp_1-dp_2+dp_3)}{2\pi i} \ln\sin\left(\frac{p_1-p_2+p_3}{2}\right) + \int_{\Gamma^u_{3\_}} \frac{z\,(-dp_1+dp_2+dp_3)}{2\pi i} \ln\sin\left(\frac{-p_1+p_2+p_3}{2}\right)$$
$$- 2\sum_{j=1}^{2} \int_{\Gamma^u_{j\_}+\mathcal{C}_\infty} \frac{z\,dp_j}{2\pi i} \ln\sin p_j - 2\int_{\Gamma^u_{3\_}+\mathcal{C}_0} \frac{z\,dp_3}{2\pi i} \ln\sin p_3\,, \tag{7.6.7}$$

where $\mathcal{C}_\infty$ is the contour encircling $x=\infty$ counterclockwise and $\mathcal{C}_0$ is the contour encircling $x=0$ clockwise. Setting $p_1=p_2$ and $p_3=0$ in this formula, we see that in this limit all the terms in (7.6.7) completely cancel out with each other. Similar cancellation occurs also for the $EAdS_3$-part. Therefore the structure constant C_{123} of the three-point function in this limit becomes unity and the result correctly reproduces the correctly normalized two-point function given by

$$\frac{\langle n_1\,,n_2\rangle^{2R}\langle\tilde{n}_1\,,\tilde{n}_2\rangle^{2L}}{|x_1-x_2|^{2\Delta}}\,. \tag{7.6.8}$$

Here, Δ, R and L are, respectively, the conformal dimension, the (absolute values of the) right and the left global charges, which are common to $\mathcal{O}_1$ and $\mathcal{O}_2$.

7.6.4 Case of one non-BPS and two BPS operators

Having checked that our formula correctly reproduces the known results in simple limits, let us now study more nontrivial examples. In this subsection, we take up the three-point functions of one non-BPS and two BPS operators, which were studied on the gauge-theory side in [115]. As in [115], we take $\mathcal{O}_2$ to be non-BPS and $\mathcal{O}_1$ and $\mathcal{O}_3$ to be BPS. In this case, the typical forms of the curves corresponding to $\mathrm{Re}\,q_i=0$ and $N_i=N_j+N_k$, are given in Figure 7.6.4.

To perform a more detailed analysis, we need to specify the properties of the operators more explicitly, since the precise form of the integration contours depend on such details. As we wish to analyze the so-called Frolov-Tseytlin limit and make a comparison with the results in the gauge theory in the next subsection, we will take as a representative example

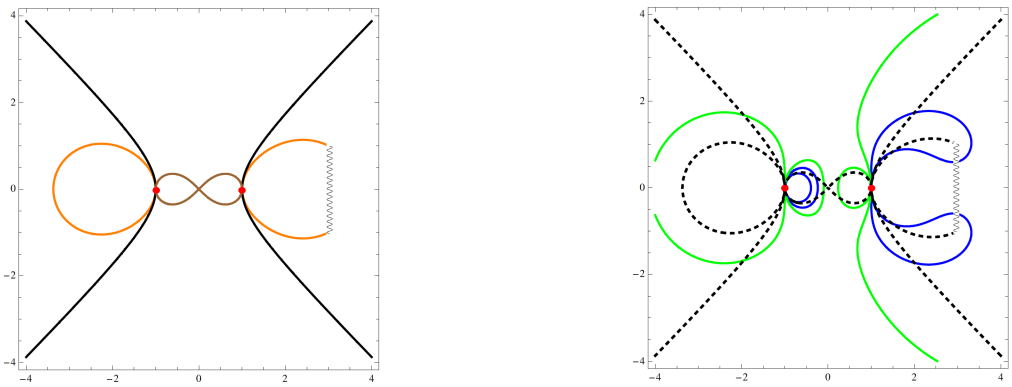

Figure 7.6.4: Typical configuration of the curves produced by the conditions $\mathrm{Re}\, q_i = 0$ and $N_i = N_j + N_k$, for the three-point functions of one non-BPS operator and two BPS operators. In the left figure, $\mathrm{Re}\, q_1 = 0$, $\mathrm{Re}\, q_2 = 0$ and $\mathrm{Re}\, q_3 = 0$ are drawn respectively in black, orange and brown. In the right figure, $N_1 = N_2 + N_3$ is drawn in blue and $N_2 = N_1 + N_3$ is drawn in green.

the following set of operators carrying large conformal dimensions:

$$\begin{aligned} &\mathcal{O}_1 : \text{BPS}\,, \quad 2\pi\kappa_1 = 2500\,, \\ &\mathcal{O}_2 : \text{non-BPS}\,, \quad 2\pi\kappa_2 = 3250\,, \\ &\qquad p(u) - p(\infty^+) = -16\pi\,, \quad p(0^+) - p(\infty^+) = -2\pi\,, \\ &\mathcal{O}_3 : \text{BPS}\,, \quad 2\pi\kappa_3 = 3000\,. \end{aligned} \tag{7.6.9}$$

Here u denotes the position of an end of the branch cut for the non-BPS operator $\mathcal{O}_2$. For these operators, the curves defined by $\mathrm{Re}\ q_i = 0$ and those defined by $N_i = N_j + N_k$ are depicted respectively in Figure 7.6.5 and Figure 7.6.6.

As in the case of the three BPS operators, we must now apply the general rules of section 7.4 to determine the integration contours. As an example, consider the contour $\mathcal{M}^{uuu}_{---}$ in the region where $|\mathrm{Re}\, x| \gg 1$. Focus first on the left figure of Figure 7.6.5. Compared to the typical configuration shown in the left figure of Figure 7.6.4, the curve determined by $\mathrm{Re}\, q_3 = 0$ (shown in brown in Figure 7.6.4) is depicted here as a point in the middle since we are considering the region where $|\mathrm{Re}\, x| \gg 1$. Since the inside of the shrunken region is where 3_+ is small, we have 3_- as the small solution everywhere in this figure. From the direction of the curves Γ^u_{1-} and Γ^u_{2-}, we can easily tell which of the states $1_\pm$ and $2_\pm$ are the small solutions in each of the region separated by these curves.

Now, in distinction to the case of three BPS operators, we must also take into account the possible change of the analyticity of the Wronskians as we cross the lines defined by $N_i = N_j + N_k$. Thus, we must analyze relevant curves drawn in Figure 7.6.6 (a), where the one in green corresponds to $N_2 = N_1 + N_3$ and the one in blue represents $N_1 = N_2 + N_3$.

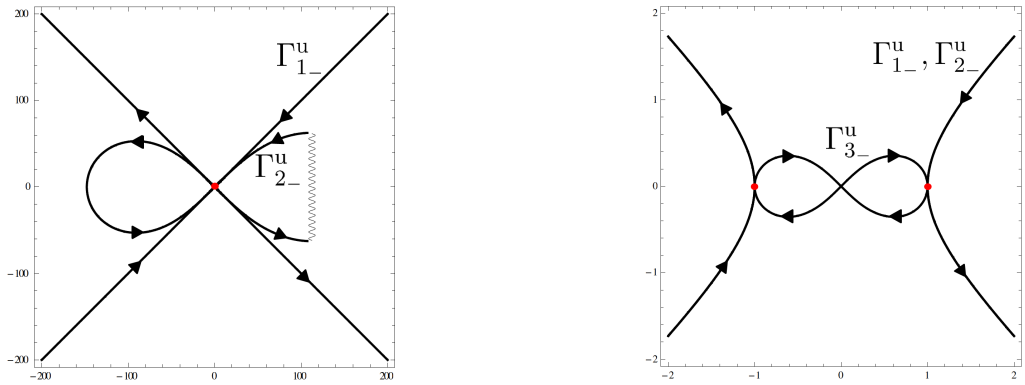

Figure 7.6.5: The contours Γ^{u}_{i-}, defined by $\mathrm{Re}\, q_i = 0$. The left figure shows the configuration of contours in the $|x| \gg 1$ region, where as the right figure depicts the configuration of contours in the $|x| < 1$ region.

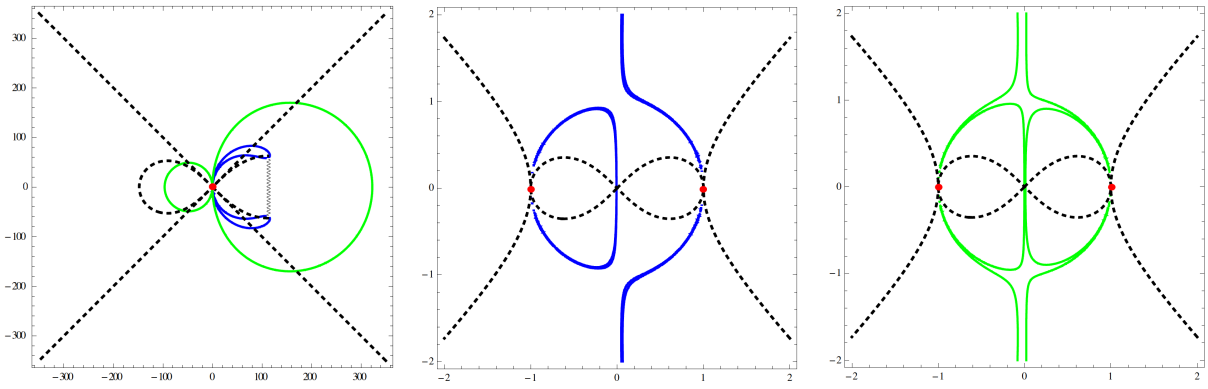

Figure 7.6.6: The curves defined by $N_i = N_j + N_k$. We name the three figures (a), (b) and (c) from the left. The figure (a) shows the configuration of curves in $|x| \gg 1$ region where as the figure (b) shows the configuration of $N_1 = N_2 + N_3$ in $|x| < 1$ region and the figure (c) shows the configuration of $N_2 = N_1 + N_3$ in $|x| < 1$ region. In the present case, the curve $N_3 = N_1 + N_2$ does not exist.

Across these lines the configuration changes from symmetric to asymmetric. Accordingly, the rule to find the non-vanishing set of Wronskians changes from Rule 2 to Rule 3. Let us focus on the green curve, which is re-drawn in Figure 7.6.7, with additional information. It turns out that the configuration is symmetric inside the green circles and asymmetric outside, indicated by the letters S and A respectively. Now in the region outside of the arc of the large green circle bordered by the lines representing $\Gamma^u_{1_-}$, shown in Figure 7.6.7 by the red straight lines, $1_-, 2_+, 3_-$ are the small solutions, as indicated in the figure. As this is the asymmetric region we apply the Rules 1 and 3 and conclude that the Wronskians among the states $\{1_+, 2_+, 3_+\}$ are non-vanishing. As we cross the arc into the shaded region inside of the green circle where the configuration is symmetric, still $1_-, 2_+, 3_-$ are the small solutions but now we must apply the Rules 1 and 2. Then we learn that the Wonskians among the states $\{1_-, 2_-, 3_-\}$ are non-vanishing instead. In other words, the analyticity property of the Wronskians change across this portion of the green line and hence it must serve as a part of the contour for the convolution integral. This explains the portion of the contour along the arc of the large circle shown in the left-most figure in Figure 7.6.8. Now consider what happens when this contour meets the $\Gamma^u_{1_-}$ line. Across this line, the small solution changes from 1_- to 1_+. Thus when we cross this line from inside the large circle, the set of small solutions change from $\{1_-, 2_+, 3_-\}$ to $\{1_+, 2_+, 3-\}$ as shown in Figure 7.6.7. As we are still in the symmetric region, the Rules 1 and 2 apply and hence we learn that set of non-vanishing Wronskians change across this line. Therefore this portion must consitute a part of the contour. This explains the straight red line starting from the the point of intersection with the large circle. In this fashion, we can uniquely obtain the integration contour $\mathcal{M}^{uuu}_{---}$, shown in the leftmost figure of Figure 7.6.8, across which the analyticity property of the Wronskians change. All the other contours $\mathcal{M}^{uuu}_{\pm\pm\pm}$ can also be determined in an entirely similar manner, the result of which are depicted in Figure 7.6.8 and Figure 7.6.9.

The contours shown in Figure 7.6.8 and Figure 7.6.9 can be simplified by continuous deformation as long as we do not make them pass through the singularities of the integrands. We can determine the positions of the singularities numerically and find that most of the singularities lie on the real axis. Avoiding them, we can deform each contour into a sum of the contour along the unit circle and the one which is far from the unit circle. The results of this deformation are summarized as

$$\begin{aligned}
&\mathcal{M}^{uuu}_{---} \longmapsto \left(\mathcal{M}^{uuu}_{---}\right)' + U\,, \quad \mathcal{M}^{uuu}_{--+} \longmapsto \left(\Gamma^u_{2_-}\right)' + U\,,\\
&\mathcal{M}^{uuu}_{-+-} \longmapsto \left(\mathcal{M}^{uuu}_{-+-}\right)' + U\,, \quad \mathcal{M}^{uuu}_{+--} \longmapsto \left(\Gamma^u_{2_-}\right)' + U\,,\\
&\Gamma^u_{1_-} \longmapsto U\,, \quad \Gamma^u_{2_-} \longmapsto \left(\Gamma^u_{2_-}\right)' + U\,, \quad \Gamma^u_{3_-} \longmapsto U\,,
\end{aligned} \tag{7.6.10}$$

where, as before, U denotes the unit circle and the primed contours are as depicted in Figure

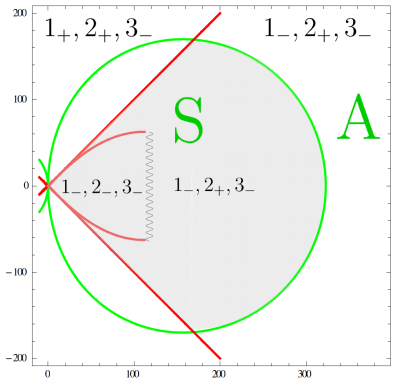

Figure 7.6.7: Magnified view of a part of the figure (a) of Figure 7.6.6, with data necessary for determining the contour of integration. In each region separated by lines and/or the cut (wavy line), the set of "small" eigenvectors are indicated. The green circle separates the symmetric (S) and the assymetric (A) regions, to which different rules of analysis apply. The result is that across the boundary of the shaded area, the analyticity of the Wronskian changes: In the shaded region, the Wronskians among $\{1_-, 2_-, 3_-\}$ are non-vanishing whereas, outside the shaded region, the Wronskians among $\{1_+, 2_+, 3_+\}$ are non-vanishing. For details of the analysis using this figure, see the explanation in the main text.

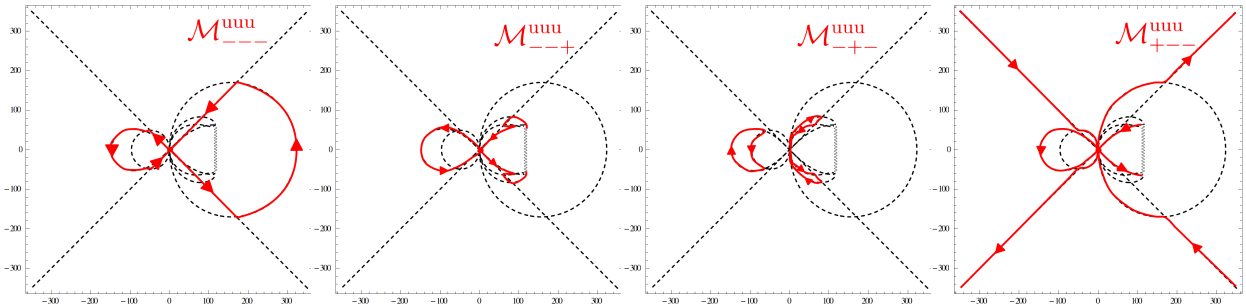

Figure 7.6.8: The integration contours $\mathcal{M}^{uuu}_{\pm\pm\pm}$ in the region $|x| \gg 1$. From left to right, $\mathcal{M}^{uuu}_{---}$, $\mathcal{M}^{uuu}_{--+}$, $\mathcal{M}^{uuu}_{-+-}$ and $\mathcal{M}^{uuu}_{+--}$.

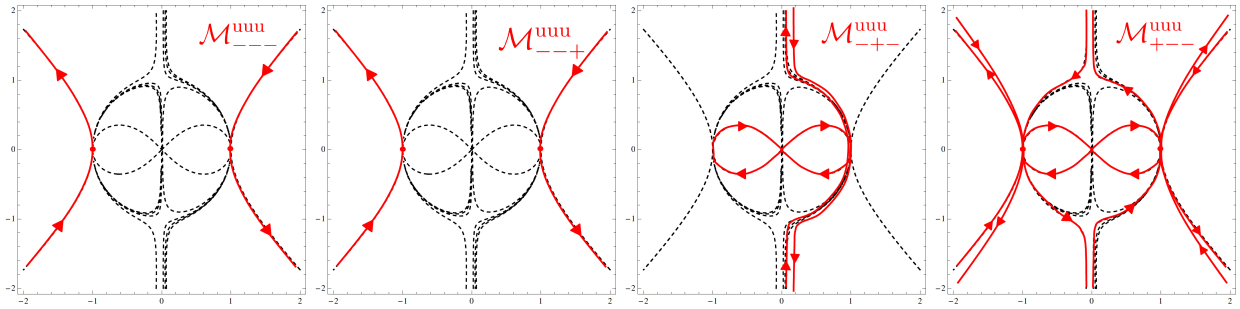

Figure 7.6.9: The integration contours $\mathcal{M}^{uuu}_{\pm\pm\pm}$ in the region $|x| < 1$. From left to right, $\mathcal{M}^{uuu}_{---}$, $\mathcal{M}^{uuu}_{--+}$, $\mathcal{M}^{uuu}_{-+-}$ and $\mathcal{M}^{uuu}_{+--}$.

7.6.10.

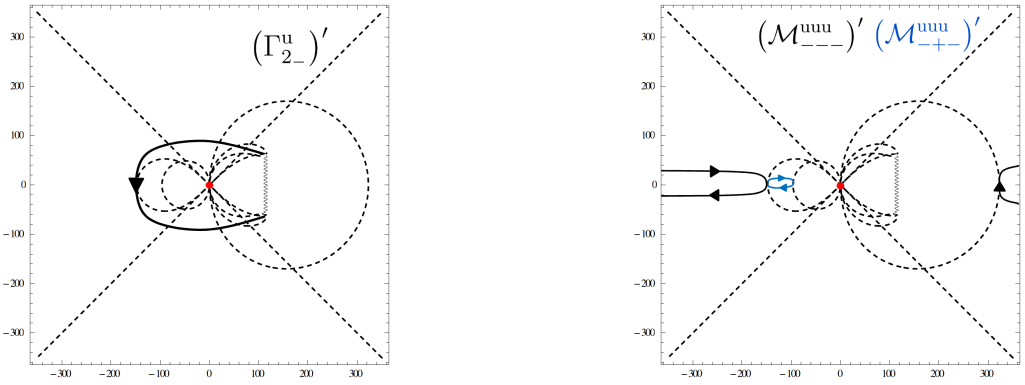

Figure 7.6.10: The contours obtained after the deformation. On the left figure, we depicted $\left(\Gamma^{u}_{2-}\right)'$ and, on the right figure, we depicted $\left(\mathcal{M}^{uuu}_{---}\right)'$ in black and $\left(\mathcal{M}^{uuu}_{-+-}\right)'$ in blue.

Let us make a remark on the separation of the integration contours into the unit circle and the large contours. It is intriguingly reminiscent of the expressions for the one-loop correction to the spectrum of a classical string [37]. In that context, the integration along the unit circle is interpreted as giving the dressing phase and the finite size corrections. Since our results do not include one-loop corrections, it is not at all clear whether our results can be interpreted in a similar way. However, the apparent structural similarity calls for further study.

7.6.5 Frolov-Tseytlin limit and comparison with the weak coupling result

Frolov-Tseytlin limit of the three-point function

We are now ready to discuss the Frolov-Tseytlin limit of the three-point function and compare it with the weak coupling result. Let us briefly recall how such a limit arises. As shown in [46], the dynamics of the fluctuations around a fast-rotating string on S^3 can be mapped to the dynamics of the Landau-Lifshitz model, which arises as a coherent state description of the XXX spin chain. In such a situation, the angular momentum J of the S^3 rotation can be taken to be so large that the ratio $\sqrt{\lambda}/J$ becomes vanishingly small, even when λ is large. For the spectral problem, it has been demonstrated that such a limit is quite useful in comparing the strong coupling result with the weak coupling counterpart. We would like to see if it applies also to the three point functions. For this purpose, we need to know how such a limit is taken at the level of the quasi-momenta. Since the SO(4) charges of the external states are proportional to κ_i, the appropriate limit is to scale all the κ_i to infinity while keeping the mode numbers $\oint_{b_i} dp$ finite. As already indicated, we have chosen the example in the previous subsection to be such that we can readily take such a limit.

Upon taking the Frolov-Tseytlin limit, two simplifications occur in our formula. First, since the branch points are far away from the unit circle, we can approximate $p_2(x)$ on the unit circle by a quasi-momentum for a BPS operator, namely

$$p_2(x) \simeq p_2^{\rm BPS}(x) = -2\pi\kappa_2 \left(\frac{1}{x-1} + \frac{1}{x+1} \right) . \tag{7.6.11}$$

Now recall that the contribution from the $EAdS_3$ part is such that it precisely canceled the S^3 part in the case of the three BPS operators. Since the $EAdS_3$ part is unchanged for the present case, again the same exact cancellation takes place as far as the integrals over the unit circles are concerned. Therefore we can drop such integrals and obtain

$$\begin{aligned}
&\int_{(\mathcal{M}^{uuu}_{---})'+\mathcal{C}_\infty} \frac{z\,(dp_1+dp_2+dp_3)}{2\pi i} \ln\sin\left(\frac{p_1+p_2+p_3}{2}\right) + \int_{\left(\Gamma^u_{2-}\right)'+\mathcal{C}_\infty} \frac{z\,(dp_1+dp_2-dp_3)}{2\pi i} \ln\sin\left(\frac{p_1+p_2-p_3}{2}\right) \\
&+ \int_{(\mathcal{M}^{uuu}_{-+-})'+\mathcal{C}_\infty} \frac{z\,(dp_1-dp_2+dp_3)}{2\pi i} \ln\sin\left(\frac{p_1-p_2+p_3}{2}\right) + \int_{\left(\Gamma^u_{2-}\right)'+\mathcal{C}_\infty} \frac{z\,(-dp_1+dp_2+dp_3)}{2\pi i} \ln\sin\left(\frac{-p_1+p_2+p_3}{2}\right) \\
&- 2\int_{\left(\Gamma^u_{2-}\right)'+\mathcal{C}_\infty} \frac{z\,dp_2}{2\pi i} \ln\sin p_2 \,,
\end{aligned} \tag{7.6.12}$$

Second simplification occurs because on the large contours the integration variable x is of order κ_i. This is precisely the situation where we can approximate the quasi-momenta of the classical strings by the corresponding quantities for the spin-chains. Indeed, as explained in [40], the quasi-momentum for the string can be identified with that of the Landau-Lifshitz model, which describes the spin-chain on the gauge theory side in the above limit. More precisely, we can use the following identification of the quasi-momenta on the large contour:

$$p^{\rm string}(x) \simeq p^{\rm spin}(z(x)) \,. \tag{7.6.13}$$

The use of the Zhukovsky variable $z(x)$ on the right hand side is motivated by the fact that in the all-loop asymptotic Bethe ansatz equation [51, 53], the rapidity of the spin-chain on the gauge theory side is identified with the Zhukovsky variable on the string theory side. In the present situation, however, since $z(x) \simeq x$ for large x, the quasi-momenta in (7.6.12) can be replaced simply with the quasi-momenta for the corresponding spin-chain states at the same value of x.

With such a replacement, the expression (7.6.12) already appears rather similar to the weak-coupling result. To make the resemblance more conspicuous, we can regard the integral of $\sin\left((-p_1+p_2+p_3)/2\right)$ along $(\Gamma^u_{2-})'$ on the upper sheet as the integral of $\sin\left((p_1+p_2-p_3)/2\right)$ along the reversed contour on the lower sheet for p_2, which we denote by $(\Gamma^l_{2-})'$. Combining this with the integral of $\sin\left((p_1+p_2-p_3)/2\right)$ along $(\Gamma^u_{2-})'$ already present and defining

$\left(\Gamma_{2-}\right)'$ to be the sum of $(\Gamma^u_{2-})'$ and $(\Gamma^l_{2-})'$, we can write (7.6.12) as

$$\int_{\left(\Gamma_{2-}\right)'+\mathcal{C}_\infty} \frac{z\,(dp_1+dp_2-dp_3)}{2\pi i}\ln\sin\left(\frac{p_1+p_2-p_3}{2}\right) - \int_{\left(\Gamma_{2-}\right)'+\mathcal{C}_\infty} \frac{z\,dp_2}{2\pi i}\ln\sin p_2 + \mathsf{Mismatch}\,, \tag{7.6.14}$$

where Mismatch is given by

$$\begin{aligned}\mathsf{Mismatch} = &\int_{\left(\mathcal{M}^{uuu}_{---}\right)'+\mathcal{C}_\infty} \frac{z\,(dp_1+dp_2+dp_3)}{2\pi i}\ln\sin\left(\frac{p_1+p_2+p_3}{2}\right)\\ &+\int_{\left(\mathcal{M}^{uuu}_{-+-}\right)'+\mathcal{C}_\infty} \frac{z\,(dp_1-dp_2+dp_3)}{2\pi i}\ln\sin\left(\frac{p_1-p_2+p_3}{2}\right)\,.\end{aligned} \tag{7.6.15}$$

Now the corresponding weak-coupling result obtained in [115] can be re-cast into the following form by the use of integration by parts,

$$\int_{-\mathcal{A}_2} \frac{z\left(dp_1^{\rm spin}+dp_2^{\rm spin}-dp_3^{\rm spin}\right)}{2\pi i}\ln\sin\left(\frac{p_1^{\rm spin}+p_2^{\rm spin}-p_3^{\rm spin}}{2}\right) - \int_{-\mathcal{A}_2} \frac{z\,dp_2^{\rm spin}}{2\pi i}\ln\sin p_2^{\rm spin}\,, \tag{7.6.16}$$

where $\mathcal{A}_2$ is the contour which encircles the branch cut of p_2 counterclockwise. Comparing (7.6.14) and (7.6.16), one notes the following: (i) The terms denoted by Mismatch in the strong coupling result are not present in the weak coupling expression. (ii) The integrands of the rest of the terms are precisely of the same form as for the weak coupling result, but the contours of integrations are different. This makes a difference in the answer since in deforming the contours from those for the strong coupling to those for the weak coupling picks up non-vanishing contributions from the singularities of the integrands. Concerning the three-point functions, there is no firm argument that the Frolov-Tseytlin limit must be universal for all the observables. Therefore the discrepancies that we found above do not immediately imply the breakdown of the duality. However, it is certainly of importance to clarify the origin of these differences. As a part of the possible understanding, below we shall offer a natural mechnism which can change the contours of integration.

A mechanism for modifying the contours

The mechanism that we wish to point out is based on the possibility of having extra singularities on the worldsheet. To see this, let us first recall that in the derivation of the important rules which determine the analyticity of the Wronskians, we have made an important assumption that the only singularities on the worldsheet of the solutions of the ALP occur at the positions of the vertex insertion points. This in turn means that if there exist

extra singularities this assumption breaks down and affects the rules for determining the contours of the convolution integrals[46]. Depending on the number and the positions of the extra singularities, the contours can be modified in various ways and it might be possible to obtain the contour which appear in the weak coupling result.

Now we can provide some arguments which indicate that indeed the existence of additional singularities is not uncommon. First, recall that the usual finite gap method is capable of constructing solutions which correspond to the saddle point configurations for two-point functions. As such they contain only two singularities, normally placed at $\tau = \pm\infty$ in the cylinder coordinates. In such a formalism designed to deal with two-point functions, description of three-point solutions would require additional singularities. In our treatment, due to the inability to construct genuine three-point saddle solutions, we describe the effect of the three vertex operators separately except for imposing the global monodromy condition that reflects the essence of their interaction. However, as already emphasized in section 7.1.6, if we wish to deal properly with the three- and higher-point functions using algebraic curve setup, one should actually start from the infinite gap solutions and then consider the limits where the infinite number of cuts on the spectral curve degenerate to zero size. This process is rather non-trivial and it should be possible to produce some extra singularities on the worldsheet. Although we cannot demonstrate this phenomenon explicitly for the three-point solution, we know that already at the level of two-point solution such a mechanism exists, as discussed in some detail in section 7.1.6. There we saw explicitly that a "one-cut" solution obtained from a multi-cut solution in a certain degeneration limit can produce extra singularities without affecting the infinite number of conserved charges carried by the solution. It is certainly expected that such a mechanism would exist also in the case of higher-point solutions. An interesting question is which of the saddle points, those with extra singularities or those without, describe the correlator of the gauge-theory operators. In any case, further studies are definitely needed to clarify this issue.

[46] A similar mechanism of changing the integration contour by the extra singularities is discussed in the context of the so-called ODE/IM correspondence [117].

Part IV

Conclusion

Chapter 8

Summary and Prospect

The AdS/CFT correspondence has been and will continue to be a source of inspiration for diverse areas of theoretical physics. The prototypical example of such correspondence is the one between $\mathcal{N} = 4$ supersymmetric Yang-Mills theory and type IIB superstring theory in $AdS_5 \times S^5$ spacetime. The aim of this thesis was to uncover the structures of three-point functions on both sides of this correspondence. Below we shall discuss future prospects reviewing what has been achieved in this thesis.

As explained in Part II, three-point functions in the gauge theory can be computed at tree-level by evaluating overlaps of three different states in a certain integrable spin-chain. This is based on the earlier discovery, reviewed in Part I, that the computation of anomalous dimensions in the gauge theory can be mapped to the diagonalization of the Hamiltonian of an integrable spin-chain. For deeper understanding of the AdS/CFT correspondence, of particular importance are three-point functions of operators composed of a large number of fields. When the operators are made up of two complex scalars, the results for such three-point functions were obtained by taking the limit of known determinant formulas of scalar products in the XXX spin-chain. The simple form of the resultant expression strongly indicates the existence of simpler and more physical derivation. The integral expression derived in this thesis is of particular interest in this respect. As discussed in section 5.4, it seems to be possible to derive the semi-classical limit using our expression. It would be important to work out the details and try to understand the physical picture behind the simple expression.

Apart from the semi-classical limit, an important future problem on the gauge theory side is to consider three-point functions of more general operators. Partial results for three-point functions involving operators composed of three complex scalars (*SU(3)-sector*) were obtained in [118]. More recently, partial results for operators containing derivatives (*SL(2)-sector*) were obtained in [119]. However, owing to the lack of determinant formulas for

scalar products in spin-chains with higher-rank symmetry groups, general results are still unavailable. Our integral formula based on Sklyanin's separation of variables may be of use also for this purpose since the separation of variables itself is known to be applicable to theories with higher-rank symmetry groups [120, 121]. What needs to be done is to determine the spectrum of separated variables and derive the integration measure. A naïve guess is that the final result will be given by a certain multiple integral akin to the eigenvalue integrals of quiver matrix models [122]. This, of course, must be validated by the explicit computation. Another important future problem is to consider loop corrections in the gauge theory. There are two sources of loop corrections for three-point functions. The first one is correction to the operators themselves. This can be taken into account if we use loop-corrected Hamiltonians and consider the eigenstates of such Hamiltonians. The other is correction to the contraction of operators. At one loop in the SO(6)-sector, they are given by the insertions of Hamiltonian density at the splitting point of the spin chain. In [32, 33], it was found that the sum of these two corrections can be conveniently taken into account by introducing the inhomogeneities to the spin-chain and performing the differentiation with respect to such inhomogeneities. This procedure is called *Theta-Morphism* and is conjectured to work also at higher loop if operators are sufficiently long. A more physical interpretation of Theta-Morphism was given later in [123]. In [123], a somewhat mysterious success of Theta-Morphism was attributed to the existence of a unitary transformation which maps the long-range spin chain describing higher-loop corrections to the nearest-neighbor spin chain with inhomogeneities. It is important to push on this line of research and try to understand the general structures of three-point functions. In the case of the spectrum problem, two nontrivial structures are known to appear at higher loop: The first one is the scalar factor of the magnon-scattering matrix, called the *dressing phase*. The other is the *finite size corrections*, which originate from the propagation of virtual particles. The results on the string theory side, explained in Part III, suggests that these structures might be present also in three-point functions. It would thus be interesting to understand how these structures make appearance in the calculation on the gauge theory side.

On the string theory side, three-point functions for classical strings are computed by evaluating the action and the vertex operators on the saddle point trajectory. As explained in Part III, such computation can be performed without knowing the explicit form of the saddle point trajectory if we ingeniously utilize the integrability of the string sigma model. One conspicuous feature of our final result (7.5.50) is that even for rather general external states the integrands of the integrals expressing the structure constant exhibit structures quite similar to the corresponding result at weak coupling. This is quite non-trivial since the weak coupling result in the relevant semi-classical regime is obtained from the determinant formula for the inner product of the Bethe states, which is so different from the method employed

for strong coupling. A possible future direction along this line of study is to generalize the method explained in this thesis to strings moving in a larger subspace of $AdS_5 \times S^5$. Our method of calculation is built upon the notion of the WKB curves introduced in [112]. Generalization to a larger subspace would then necessitate the use of the *spectral network*[1] defined in [124]. It would also be important to consider higher-point functions building upon the work [111]. Although higher-point functions in conformal field theories can be computed from two- and three-point functions and do not provide further information of the theories, it is still important to understand how the structures of the operator product expansion (OPE) in the gauge theory are realized in the string theory. A naïve expectation would be that the OPE in the gauge theory is directly realized by the OPE on the worldsheet. This, however, is not correct since the OPE on the worldsheet produce *unphysical* (off-shell) states, which do not correspond to the operators in the gauge theory. To eliminate such unwanted contributions, it would be important to consider the integration over the moduli of the Riemann-surface. In fact, such integration generally produces the propagator of a closed string,

$$\int d\tau e^{-\tau(L_0+\bar{L}_0)} \sim \frac{1}{L_0+\bar{L}_0}\,, \tag{8.0.1}$$

which gives a dominant (divergent) contribution when the state is on-shell. However, in order to eliminate the off-shell contributions completely, we need a supplementary mechanism[2] which replaces the propagator with a delta-functional factor $\delta(L_0+\bar{L}_0)$.

Clarification of such a supplementary mechanism will be important also for deeper understanding of the AdS/CFT correspondence itself. This is because a similar situation is encountered also when we attempt a first-principle derivation of the AdS/CFT correspondence. To see this, let us recall and expand the argument given in the footnote of section 1.1. As explained in section 1.1, the worldsheet of a closed string can have several holes in the presence of D-branes. As is well-known, the effect of such holes can be taken into account by the use of a *boundary state* $|\mathcal{B}\rangle$ as follows[3]:

$$\int \frac{d\rho}{\rho} \rho^{L_0+\bar{L}_0} |\mathcal{B}\rangle\,, \tag{8.0.2}$$

where ρ denotes the size of the hole. Performing the integration with respect to ρ, we generally obtain a propagator,

$$\sim \frac{1}{L_0+\bar{L}_0}|\mathcal{B}\rangle\,. \tag{8.0.3}$$

[1] Since the spectral network is a much less understood object than the WKB curve, such generalization would require considerable effort.

[2] In this regard, there is an interesting work [125], which discusses the connection between the space-time OPE and the worldsheet OPE.

[3] Precisely speaking, we also need to insert zero modes of b ghosts, $b_0+\bar{b}_0$. For details, see [12].

The effect of the holes can be naturally replaced[4] with the deformation of the background geometry if we can project away all the off-shell closed string contributions contained in the boundary state and substitute (8.0.3) with a sum of on-shell vertex operators. However, as mentioned above, such projection is realized only when there is a delta-functional factor $\delta(L_0 + \bar{L}_0)$. In the case of imaginary D-branes, mentioned in section 1.1, such a factor naturally arises from the propagetor as a result of Wick rotation[5]. For other examples, however, we need some additional mechanism, which would be closely related to the one we need for four-point functions.

Another important future direction is to study quantum corrections to the results obtained in this thesis. However, as our method does not provide the explicit forms of saddle-point trajectories, it is not straightforward to compute quantum corrections within our framework. To overcome such difficulty, it would be instructive to study a simpler theory with common features. The most suitable theory for this purpose would be the Liouville field theory. The Liouville field theory is one of a few well-studied irrational conformal field theories and is studied thoroughly in various contexts. The three-point function of this theory was solved completely in [127–129]. Recently, the classical limit of such three-point functions was re-derived in [114] using the techniques explained in this thesis. One of the virtues of studying the Liouville field theory is that we can identify the quantum analogues of the Wronskians $\langle i_\pm \, , j_\pm \rangle$ and utilize them to determine fully quantum three-point functions [130, 131]. Thus, by studying the Liouville field theory further with the integrability-based methods and exploring its similarity with the string sigma model in AdS, we may be able to obtain a new nonperturbative characterization[6] of three-point functions in the AdS/CFT correspondence in the near future. Such a characterization would probably involve the unification of two methods; the method based on the integrability and the conventional method to study 2d CFTs[7]. Once this is achieved, it would also be interesting to see if it is possible to construct novel non-rational 2d CFTs utilizing the integrable structure, such as the solutions to the Yang-Baxter equation.

As a last remark, let us hint a possible connection with the AGT correspondence [135], which is a recently discovered mysterious relation between the four-dimensional $\mathcal{N} = 2$

[4]For a detailed discussion, see the footnote of section 1.1.

[5]Even in general situations, some sort of Wick rotation or analytic continuation seems to be necessary to realize the projection. In this respect, the $i\epsilon$-prescription of the propagator [126] will play an important role because the propagator acquires an imaginary part proportional to $\delta\left(L_0 + \bar{L}_0\right)$ after the introduction of the $i\epsilon$ factor.

[6]In the case of scattering amplitudes, such a nonperturbative characterization was proposed recently in [132, 133].

[7]Certain integrable structures in two-dimensional CFTs were found in their early days [134]. However, to date, the connection with the integrable systems have not been fully explored in the study of 2d CFTs.

supersymmetric gauge theories and the Liouville field theory. In the AGT correspondence, the correlation functions in the Liouville field theory are related to the partition functions of $\mathcal{N} = 2$ gauge theories on a so-called omega-deformed background. In particular, the classical limit of the Liouville field theory corresponds to the special limit of the gauge theory, called Nekrasov-Shatashvili limit [136], where one of the omega-deformation parameters goes to zero. As stated above, the classical correlation functions in the Lioville field theories can be studied by the methods developed in this thesis. On the other hand, it was recently reported [137] that the method used in the study of partition functions in the Nekrasov-Shatashvili limit is effective also in the study of semi-classical limit of scalar products of the XXX spin-chain. These two observations indicate that three-point functions in the $\mathrm{AdS}_5/\mathrm{CFT}_4$ correspondence has a similar mathematical structure as the AGT correspondence. More concretely, it is tempting to speculate on the existence of the following relation:

$$\begin{array}{ccc} \text{Spin chain in } \mathcal{N} = 4 \text{ SYM} & \overset{?}{\longleftrightarrow} & \text{Partition function in } \mathcal{N} = 2 \text{ theories} \\ \text{String theory in } AdS_5 \times S^5 & \overset{?}{\longleftrightarrow} & \text{Liouville field theory} \end{array}$$

Of course, this is just a speculation at the moment and we need to await further developments in both fields to see if there really is such a relation. In any case, we hope the materials explained in this thesis will play a foundational role in future progress.

Part V

Appendices

Chapter A

Details on the integral expression for the scalar products

A.1 Proof of theorem

In this appendix, we shall provide a proof of the theorem in section 5.3, which gives the action of the normal-ordered operators $:A_\epsilon(\hat{x}_k):_\ell$ and $:D_\epsilon(\hat{x}_k):_\ell$ on the SoV bra $\langle \dots, x_k, \dots |$. Essentially, what follows is a pedagogical adaptation of the argument given in [138].

The proof is by mathematical induction in the number of sites ℓ. Begin with the $\ell = 1$ case. The operators $A_\epsilon(u), B_\epsilon(u), C_\epsilon(u), D_\epsilon(u)$ are given by[1]

$$A(u) = u - \theta_1 + iS^z + i\epsilon S^+ , \qquad B(u) = \epsilon(u - \theta_1 - iS^z) + iS^- , \tag{A.1.1}$$

$$C(u) = -\epsilon(u - \theta_1 + iS^z) + iS^+ , \qquad D(u) = u - \theta_1 - iS^z - i\epsilon S^- . \tag{A.1.2}$$

By solving $B(\hat{x}_1) = 0$ for $\hat{x}_1$ and substituting it into $A(u)$ and $D(u)$, we get

$$\hat{x}_1 = \theta_1 + iS^z - i\epsilon^{-1}S^- = \begin{pmatrix} \theta_1 + \frac{i}{2} & 0 \\ -i\epsilon^{-1} & \theta_1 - \frac{i}{2} \end{pmatrix} , \tag{A.1.3}$$

$$:A(\hat{x}_1):_\ell = 2iS^z - i\epsilon^{-1}S^- + i\epsilon S^+ = i \begin{pmatrix} 1 & \epsilon \\ -\epsilon^{-1} & -1 \end{pmatrix} , \tag{A.1.4}$$

$$:D(\hat{x}_1):_\ell = -i(\epsilon + \epsilon^{-1})S^- = -i(\epsilon + \epsilon^{-1}) \begin{pmatrix} 0 & 0 \\ 1 & 0 \end{pmatrix} . \tag{A.1.5}$$

Since $\hat{x}_1$ is lower triangular, its eigenvalues are read off as $\theta_1 \pm \frac{i}{2}$ and the corresponding normalized eigenbras $\langle \pm |$ are given by $\langle + | = (1, 0), \langle - | = (1, \epsilon)/\sqrt{1 + \epsilon^2}$. Then, we can

[1] We have dropped the subscript 1 for S^k for simplicity. Also subscripts ϵ for $A(u), \dots, D(u)$ are suppressed.

compute the action of $:A(\hat{x}_1):_\ell$ and $:D(\hat{x}_1):_\ell$ explicitly and get

$$\langle +|:A(\hat{x}_1):_\ell = i\sqrt{1+\epsilon^2}\langle -|\,, \quad \langle -|:A(\hat{x}_1):_\ell = 0\,, \tag{A.1.6}$$

$$\langle +|:D(\hat{x}_1):_\ell = 0\,, \qquad \langle -|:D(\hat{x}_1):_\ell = -i\sqrt{1+\epsilon^2}\langle +|\,. \tag{A.1.7}$$

This is precisely what the theorem says for $\ell = 1$.

Next, assume that the formulas hold for up to $\ell = N$ and consider $\ell = N+1$ case. The monodromy matrix for $\ell = N+1$ is given by

$$\Omega_{N+1} = KL_1 \cdots L_N L_{N+1}\,, \tag{A.1.8}$$

where K is the twisting matrix given by $K = \begin{pmatrix} 1 & \epsilon \\ -\epsilon & 1 \end{pmatrix}$. Now in order to split this into the monodromy matrix at the Nth level and the subsequent action of the Lax operator at the $(N+1)$th step, we should introduce in the final Lax operator a twisting matrix of a similar form, which we denote as

$$\tilde{K} \equiv \begin{pmatrix} 1 & \eta \\ -\eta & 1 \end{pmatrix}\,, \tag{A.1.9}$$

with η being an arbitrary parameter, just like ϵ. Then we can write $\Omega_{N+1} = \tilde{\Omega}_N L'_{N+1}$, where

$$\tilde{\Omega}_N = (K\tilde{K}^{-1})\tilde{L}_1\tilde{L}_2\cdots\tilde{L}_N\,, \qquad K\tilde{K}^{-1} = \frac{1}{1+\eta^2}\begin{pmatrix} 1+\epsilon\eta & \epsilon-\eta \\ -(\epsilon-\eta) & 1+\epsilon\eta \end{pmatrix}\,, \tag{A.1.10}$$

$$\tilde{L}_i = \tilde{K}L_i\tilde{K}^{-1}\,, \qquad L'_{N+1} = \tilde{K}L_{N+1}\,. \tag{A.1.11}$$

Since the conjugation by $\tilde{K}$ does not affect the structure of the algebra, we may regard $\tilde{\Omega}_N$ as the monodromy matrix for $\ell = N$ for which the theorem holds with the factor $\sqrt{1+\epsilon^2}$ in (5.3.13) and (5.3.14) replaced with $\sqrt{(1+\epsilon^2)/(1+\eta^2)}$. We now write the matrix elements of $\tilde{\Omega}_N$ and L'_{N+1} as

$$\tilde{\Omega}_N(u) = \begin{pmatrix} \tilde{A}_N & \tilde{B}_N \\ \tilde{C}_N & \tilde{D}_N \end{pmatrix}\,, \qquad L'_{N+1} = \begin{pmatrix} a_{N+1} & b_{N+1} \\ c_{N+1} & d_{N+1} \end{pmatrix}\,, \tag{A.1.12}$$

and compute $\Omega_{N+1} = \begin{pmatrix} A_{N+1} & B_{N+1} \\ C_{N+1} & D_{N+1} \end{pmatrix}$. Then B_{N+1} operator is given by

$$B_{N+1}(u) = \tilde{A}_N(u)b_{N+1}(u) + \tilde{B}_N(u)d_{N+1}(u)\,. \tag{A.1.13}$$

Let us now write the SoV basis of bras for $\ell = N+1$ as $\langle x_1, \ldots, x_N; y|$. By the hypothesis of the induction, $\tilde{B}_N(u)$ is diagonal in this basis and also b_{N+1}, which acts only on the $(N+1)$th

site, is diagonal. Explicitly, we have

$$\langle x_1,\dots,x_N;y|\tilde{B}_N(u)=\frac{\epsilon-\eta}{1+\eta^2}\prod_{i=1}^{N}(u-x_i)\langle x_1,\dots,x_N;y|\,, \tag{A.1.14}$$

$$\langle x_1,\dots,x_N;y|b_{N+1}(u)=\eta(u-y)\langle x_1,\dots,x_N;y|\,. \tag{A.1.15}$$

We may now compute the action of $\tilde{B}_{N+1}(u)$ at $u=\hat{x}_k$ and $u=\hat{y}$, where $\hat{y}$ is the root of $b_{N+1}(\hat{y})=0$ given by $\hat{y}=\theta_{N+1}+iS^3_{N+1}-i\eta^{-1}S^-_{N+1}$. Since $\tilde{B}_N(\hat{x}_k)$ and $b_{N+1}(\hat{y})$ vanishes on this state, we get

$$\langle x_1,\dots,x_N;y|B_{N+1}(\hat{x}_k)=\langle x_1,\dots,x_N;y|\tilde{A}_N(\hat{x}_k)b_{N+1}(\hat{x}_k)\,, \tag{A.1.16}$$

$$\langle x_1,\dots,x_N;y|B_{N+1}(\hat{y})=\langle x_1,\dots,x_N;y|\tilde{B}_N(\hat{y})d_{N+1}(\hat{y})\,. \tag{A.1.17}$$

The RHS can be easily computed since $\tilde{A}_N(\hat{x}_k)$ shifts x_k by $-i$, while $d_{N+1}(\hat{y})$ shifts y by $+i$, with certain known factors multiplied. In this way, we obtain the formulas

$$\langle x_1,\dots,x_N;y|B_{N+1}(\hat{x}_k)=\eta\sqrt{\frac{1+\epsilon^2}{1+\eta^2}}(x_k-y)Q^+_{\boldsymbol{\theta}}(x_k)\langle\dots,x_k-i,\dots;y|\,, \tag{A.1.18}$$

$$\langle x_1,\dots,x_N;y|B_{N+1}(\hat{y})=\frac{\epsilon-\eta}{1+\eta^2}\sqrt{\frac{1+\epsilon^2}{1+\eta^2}}(y-\theta_{N+1}-i/2)\prod_{k=1}^{N}(y-x_k)\langle\dots,x_k,\dots;y+i|\,. \tag{A.1.19}$$

Having understood the action of B_{N+1} at $u=\hat{x}_k,\hat{y}$ on the SoV basis, we now wish to deduce the spectrum of $B_{N+1}(u)$ using this information. Let $|\Phi\rangle$ be the state which diagonalizes $B_{N+1}(u)$. Then by taking the inner product with the above two equations, we obtain

$$\beta(x_k)\Phi(x_1,\dots,x_n;y)=\eta\sqrt{\frac{1+\epsilon^2}{1+\eta^2}}(x_k-\eta)Q^+_{\boldsymbol{\theta}}(x_k)\Phi(\dots,x_k-i,\dots;y)\,, \tag{A.1.20}$$

$$\beta(y)\Phi(x_1,\dots,x_N;y)=\frac{\epsilon-\eta}{1+\eta^2}\sqrt{\frac{1+\epsilon^2}{1+\eta^2}}(y-\theta_{N+1}-i/2)\prod_{k=1}^{N}(y-x_k)\Phi(\dots,x_k,\dots;y+i)\,, \tag{A.1.21}$$

where $\Phi(x_1,\dots,x_N;y)\equiv\langle x_1,\dots,x_N;y|\Phi\rangle$ and we have denoted the eigenvalue of $B_{N+1}(u)$ by $\beta(u)$. Now to simplify the analysis of the spectrum, it is convenient to extract a factor $\rho(x_1,\dots,x_N;y)$ from $\Phi(x_1,\dots,x_N;y)$ in the manner

$$\Phi(x_1,\dots,x_N;y)=\rho(x_1,\dots,x_N;y)\Psi(x_1,\dots,x_N;y) \tag{A.1.22}$$

where $\rho(x_1, \ldots, x_N; y)$ satisfies the first order difference equations

$$\rho(x_1, \ldots, x_N; y) = \eta \sqrt{\frac{1+\epsilon^2}{1+\eta^2}} (x_k - \eta) \rho(\ldots, x_k - i, \ldots; y)\,, \tag{A.1.23}$$

$$\rho(x_1, \ldots, x_N; y) = \frac{\epsilon - \eta}{1+\eta^2} \sqrt{\frac{1+\epsilon^2}{1+\eta^2}} \prod_{i=1}^{N} (y - x_k) \rho(\ldots, x_k, \ldots; y + i)\,. \tag{A.1.24}$$

One can easily verify that the solution to these equations is unique[2] up to an overall constant. Now with such a factor removed, the reduced wave function Ψ satisfies the equations

$$\beta(x_k) \Psi(x_1, \ldots, x_N; y) = Q^+_{\boldsymbol{\theta}}(x_k) \Psi(\ldots, x_k - i, \ldots; y)\,, \tag{A.1.25}$$

$$\beta(y) \Psi(x_1, \ldots, x_N; y) = (y - \theta_{N+1} - i/2) \Psi(\ldots, x_k, \ldots; y + i)\,. \tag{A.1.26}$$

It turns out that we can drastically simplify these equations by assuming the factorized form[3] for Ψ, namely

$$\Psi(x_1, \ldots, x_N; y) = \chi(y) \prod_{k=1}^{N} \xi_k(x_k)\,. \tag{A.1.27}$$

The equations for Ψ then get reduced to the following equations for each factor

$$\beta(x) \xi_k(x) = Q^+_{\boldsymbol{\theta}}(x) \xi_k(x - i)\,, \qquad x \in \left\{ \theta_k - \frac{i}{2}, \theta_k + \frac{i}{2} \right\}\,, \tag{A.1.28}$$

$$\beta(x) \chi(x) = (y - \theta_{N+1} - i/2) \chi(x + i)\,, \qquad x \in \left\{ \theta_{N+1} - \frac{i}{2}, \theta_{N+1} + \frac{i}{2} \right\}\,. \tag{A.1.29}$$

Note that we have used the induction hypothesis that the spectrum of each x_k is two-valued as above.

The rest of the analysis is elementary. First consider the equation (A.1.28) and set $x = \theta_k - \frac{i}{2}$. Then due to the presence of the factor $Q^+_{\boldsymbol{\theta}}(x)$ the RHS vanishes and hence we must have $\beta(\theta_k - \frac{i}{2}) \xi_k(\theta_k - \frac{i}{2}) = 0$. If $\xi_k(\theta_k - \frac{i}{2}) \neq 0$, then $\beta(\theta_k - \frac{i}{2})$ must vanish and $\theta_k - \frac{i}{2}$ is in the spectrum. On the other hand suppose $\xi_k(\theta_k - \frac{i}{2}) = 0$. Then $\xi_k(\theta_k + \frac{i}{2})$ cannot vanish since otherwise the whole wave function vanishes. Now set $x = \theta_k + \frac{i}{2}$ in (A.1.28). Then the RHS vanishes and so must the LHS, *i.e.* $\beta(\theta_k + \frac{i}{2}) \xi_k(\theta_k + \frac{i}{2}) = 0$. This leads to $\beta(\theta_k + \frac{i}{2}) = 0$ and hence $x = \theta_k + \frac{i}{2}$ is in the spectrum. Similar arguments for (A.1.29) tells us that $\theta_{N+1} \pm \frac{i}{2}$ are in the spectrum. Thus, for $\ell = N + 1$, we continue to have the same set of spectrum as stated in the theorem.

[2] The uniqueness is guaranteed by the finiteness of the spectrum of $\hat{x}_k$ and $\hat{y}$. One can construct the solution ρ by starting from the end of the spectrum.

[3] This does not miss any solution since the solution is unique.

From this analysis we learn that the finite discrete nature of the spectrum is due to two reasons. One is that the operators $:A(\hat{x}_k):_\ell$ and $:D(\hat{x}_k):_\ell$ are essentially exponentials of the momentum operator and hence they induce a finite shift in x_k. The second ingredient is the presence of the prefactor $Q^+_{\boldsymbol{\theta}}(x)$. Since it vanishes at finite discrete values of x, the shifting must end after a finite number of steps, in the present case just one.

What remains is the determination of the constant of proportionality in the action of the operators $:A(\hat{x}_k):_\ell$ and $:D(\hat{x}_k):_\ell$. As there are only a finite number of states, such a constant can be adjusted rather freely by the change of the normalization of states. Nonetheless, there is a certain constraint coming from the following non-linear relations:

$$:A_{N+1}(\hat{x}_k):_\ell :D_{N+1}(\hat{x}_k):_\ell = (1+\epsilon^2)\prod_{l=1}^{N+1}(\hat{x}_k-\theta_l+i/2)(\hat{x}_k-\theta_l-3i/2)\,, \tag{A.1.30}$$

$$:D_{N+1}(\hat{x}_k):_\ell :A_{N+1}(\hat{x}_k):_\ell = (1+\epsilon^2)\prod_{l=1}^{N+1}(\hat{x}_k-\theta_l-i/2)(\hat{x}_k-\theta_l+3i/2)\,. \tag{A.1.31}$$

These relations can be obtained in the following way. From the commutation relations between $:A_{N+1}(\hat{x}_k):_\ell$, $:D_{N+1}(\hat{x}_k):_\ell$ and $\hat{x}_k$, one can show

$$:A_{N+1}(\hat{x}_k):_\ell :D_{N+1}(\hat{x}_k):_\ell = \det{}_q\Omega_{N+1}(\hat{x}_k-i/2)\,, \tag{A.1.32}$$

$$:D_{N+1}(\hat{x}_k):_\ell :A_{N+1}(\hat{x}_k):_\ell = \det{}_q\Omega_{N+1}(\hat{x}_k+i/2)\,, \tag{A.1.33}$$

where $\det{}_q\Omega_{N+1}(u)$ is the so-called quantum determinant[4] , which is a central element of the Yang-Baxter exchange algebra. Then by using the co-multiplication rule, $\det{}_q(AB) = \det{}_qA\det{}_qB$, one can explicitly compute the RHS and obtain the relations (A.1.30) and (A.1.31). The constant of proportionality chosen in the theorem is compatible with these relations and also to the explicit equations for $\ell = 1$ case shown in (A.1.6) and (A.1.7) obtained for unit-normalized states. This completes the proof of the theorem.

A.2 Relation to Izergin's determinant formula

In this appendix, we give a direct proof that a slight generalization of our new integral expression is equivalent to the Izergin's determinant formula [139] for the domain wall partition function (DWPF) which appears in the six-vertex model. From this DWPF, the original scalar product of our interest can be obtained by sending an appropriate subset of rapidities to infinity as well as requiring half of the remainder to be on-shell.

[4]For a detailed account of the quantum determinant, we refer the reader to [34] and [138].

We begin with the domain wall partition function, which is defined as follows:

$$Z_\ell(\boldsymbol{w}|\boldsymbol{\theta}) \equiv \langle \downarrow^\ell | \prod_{i=1}^{\ell} B(w_i) | \uparrow^\ell \rangle \,. \tag{A.2.1}$$

Note that the number of B operators is equal to the number of sites ℓ and the rapidities $\boldsymbol{w}$ are not restricted to an on-shell configuration. In [139], Izergin gave a determinant expression for this quantity, which reads

$$Z_\ell(\boldsymbol{w}|\boldsymbol{\theta}) = \frac{\prod_{j,k=1}^{\ell}(w_j-\theta_k+\frac{i}{2})(w_j-\theta_k-\frac{i}{2})}{\prod_{l<m}(w_l-w_m)(\theta_m-\theta_l)} \det\left(\frac{i}{(w_j-\theta_k+\frac{i}{2})(w_j-\theta_k-\frac{i}{2})}\right)_{1\le j,k\le \ell} . \tag{A.2.2}$$

In what follows, we shall show that this is equal to the multiple integral formula of the form

$$\begin{aligned}\langle \downarrow^\ell | \prod_{i=1}^{\ell} B(w_i) | \uparrow^\ell \rangle = i^\ell \prod_{j<k}(\theta_j-\theta_k)(\theta_j-\theta_k+i)(\theta_j-\theta_k-i) \\ \times \prod_{n=1}^{\ell} \oint_{\mathcal{C}_n} \frac{dx_n}{2\pi i} \prod_{k<l}(x_k-x_l) \prod_{m=1}^{\ell} \frac{Q_{\boldsymbol{w}}(x_m)}{Q^+_{\boldsymbol{\theta}}(x_m) Q^-_{\boldsymbol{\theta}}(x_m)} \,.\end{aligned} \tag{A.2.3}$$

First, we shall transform the Izergin's formula to a form more convenient for comparison with the integral expression. By a simple decomposition, the determinant in (A.2.2) can be rewritten as a determinant of the difference of two matrices:

$$\det\left(\frac{i}{(w_j-\theta_k+\frac{i}{2})(w_j-\theta_k-\frac{i}{2})}\right)_{1\le j,k\le \ell} = \det\left(M^-_{jk}-M^+_{jk}\right)_{1\le j,k\le \ell} , \tag{A.2.4}$$

$$M^\pm_{jk} = \frac{1}{w_j-\theta_k\pm i/2} \,. \tag{A.2.5}$$

Then from the definition of the determinant, we can expand the RHS of (A.2.4) as

$$\begin{aligned}\det\left(M^-_{jk}-M^+_{jk}\right)_{1\le j,k\le \ell} &= \sum_{\sigma\in P_\ell}(-1)^\sigma (M^-_{1\sigma(1)}-M^+_{1\sigma(1)})\cdots(M^-_{\ell\sigma(\ell)}-M^+_{\ell\sigma(\ell)}) \\ &= \sum_{\epsilon_i=\pm}(-1)^{n_+}\sum_{\sigma\in P_\ell}(-1)^\sigma M^{\epsilon_1}_{1\sigma(1)}\cdots M^{\epsilon_\ell}_{\ell\sigma(\ell)} \,,\end{aligned} \tag{A.2.6}$$

where n_+ is the number of $+$'s in the set $\{\epsilon_i\}$ and the sign $(-1)^{n_+}$ is produced upon expanding the product. Now by using the definition of determinant again to re-express each summand back as a determinant, we obtain

$$\det\left(M^-_{jk}-M^+_{jk}\right)_{1\le j,k\le \ell} = \sum_{\epsilon_i=\pm}(-1)^{n_+}\det\left(M^{\epsilon_j}_{jk}\right)_{1\le j,k\le \ell} \,. \tag{A.2.7}$$

At this point, one can apply the Cauchy's determinant identity,

$$\det\left(\frac{1}{x_j-y_k}\right)_{1\le j,k\le \ell}=\frac{\prod_{1\le j<k\le \ell}(x_j-x_k)(y_k-y_j)}{\prod_{l,m=1}^{\ell}(x_l-y_m)}\,, \tag{A.2.8}$$

to each term $\det\left(M^{\epsilon_j}_{jk}\right)_{1\le j,k\le \ell}=\det\left((w_j-(\theta_k-\epsilon_j i/2))^{-1}\right)_{1\le j,k\le \ell}$. Putting altogether the determinant (A.2.4) in the Izergin's formula can be expressed as

$$\det\left(\frac{i}{(w_j-\theta_k+\frac{i}{2})(w_j-\theta_k-\frac{i}{2})}\right)_{1\le j,k\le \ell}=\sum_{\epsilon_i=\pm}(-1)^{n_+}\frac{\prod_{1\le j<k\le \ell}(w_j-w_k)(\theta_k-\theta_j-i(\epsilon_k-\epsilon_j)/2)}{\prod_{l,m=1}^{\ell}(w_l-\theta_m+i\epsilon_m/2)}\,. \tag{A.2.9}$$

Substituting it into (A.2.2), Izergin's formula is finally transformed into the expression

$$Z_\ell(\boldsymbol{w}|\boldsymbol{\theta})=\sum_{\epsilon_i=\pm}(-1)^{n_+}\prod_{j,k=1}^{\ell}(w_j-(\theta_k+i\epsilon_k/2))\prod_{1\le l<m\le \ell}\frac{(\theta_l-\theta_m-i(\epsilon_l-\epsilon_m)/2)}{\theta_l-\theta_m}\,, \tag{A.2.10}$$

which is no longer of a determinant form.

Now we are ready to prove its equivalence to the multiple integral (A.2.3). This is done essentially by explicitly performing the contour integrals using the residue formula. By picking up the contributions from the zeros of the functions $Q^{\pm}_{\boldsymbol{\theta}}(x_m)$ in the denominator, the integral is evaluated as

$$\begin{aligned}&\prod_{r<s}(\theta_r-\theta_s)(\theta_r-\theta_s+i)(\theta_r-\theta_s-i)\\ &\times\sum_{\epsilon_i=\pm}(-1)^{n_+}\prod_{1\le l<m\le \ell}\frac{(\theta_l-\theta_m+i(\epsilon_l-\epsilon_m)/2)}{(\theta_l-\theta_m)^2(\theta_l-\theta_m+\epsilon_l)(\theta_l-\theta_m-\epsilon_m)}\prod_{j,k=1}^{\ell}(w_j-(\theta_k+i\epsilon_k/2))\,.\end{aligned} \tag{A.2.11}$$

Now note the following relation, which can be checked for every pair (ϵ_l,ϵ_m), with $\epsilon_l=\pm 1$:

$$\frac{(\theta_l-\theta_m+i)(\theta_l-\theta_m-i)}{(\theta_l-\theta_m+i\epsilon_l)(\theta_l-\theta_m-i\epsilon_m)}=\frac{(\theta_l-\theta_m-i(\epsilon_l-\epsilon_m)/2)}{(\theta_l-\theta_m+i(\epsilon_l-\epsilon_m)/2)}\,. \tag{A.2.12}$$

Using this formula, the expression (A.2.11) can be simplified into

$$\sum_{\epsilon_i=\pm}(-1)^{n_+}\prod_{j,k=1}^{\ell}(w_j-(\theta_k+i\epsilon_k/2))\prod_{1\le l<m\le \ell}\frac{(\theta_l-\theta_m-i(\epsilon_l-\epsilon_m)/2)}{\theta_l-\theta_m}\,. \tag{A.2.13}$$

This is exactly the same as (A.2.10), proving the assertion.

As already stated, the original scalar product of our interest can be obtained from this domain wall partition function through certain manipulations. First, by sending $\ell-n$ of

the ℓ rapidities to infinity, thereby decoupling them, one obtains the partial domain wall partition function with n rapidities $\boldsymbol{z}$ (4.3.7) in the following way:

$$Z^{\mathrm{pDWPF}}(\boldsymbol{z}|\boldsymbol{\theta}) = \frac{1}{(\ell-n)!} \lim_{\{w_1,\ldots,w_{\ell-n}\}\to\infty} \left(\frac{Z_\ell(\boldsymbol{z} \cup \{w_1,\ldots,w_{\ell-n}\}|\boldsymbol{\theta})}{iw_1^{\ell-1}\cdots iw_{\ell-n}^{\ell-1}} \right). \tag{A.2.14}$$

If we now set $n = 2M$ and $\boldsymbol{z} = \boldsymbol{u} \cup \boldsymbol{v}$, where either $\boldsymbol{u}$ or $\boldsymbol{v}$ are on-shell, we recover the original scalar product $\langle \uparrow^\ell | \prod_{i=1}^M C(v_i) \prod_{j=1}^M B(u_j) | \uparrow^\ell \rangle$. On the other hand, if we apply the same manipulations to the integral formula (A.2.2), we obtain the multiple integral formula for the scalar product (5.3.46). This proves the equivalence of our formula and the determinant formula derived by Foda and Wheeler [90].

Chapter B

Action-angle variables in the Landau Lifshitz model

In this Appendix, we derive the Poisson-bracket structure of the Landau-Lifshitz model and construct the action-angle variables. Of crucial importance in the discussion is the so-called *classical r-matrix*, which is a classical analogue of the quantum R-matrix reviewed in section 3.1.3. The materials in this Appendix provide a simple and pedagogical toy model to understand why and how Sklyanin's separation of variables works in classical integrable models, which we used in Part III to construct the semi-classical wave functions.

B.1 Poisson brackets

First we derive the Poisson (Dirac) bracket structure of the Lnadau-Lifshitz model. The most straightforward way is to start from the action (3.3.28), regard $\vec{n}$ as the fundamental variable and derive the Dirac bracket. However, it is practically much easier to first parametrize the 2-sphere by θ and ϕ and then derive the Dirac bracket. In terms of θ and ϕ, the action of the Landau-Lifshitz sigma model is

$$S = -\int d\tau d\sigma \left[\frac{1}{4}\left(\cos\theta\partial_\tau\phi + \phi\sin\theta\partial_\tau\theta\right) + \frac{\lambda}{32\pi^2}\left(\partial_\sigma\theta\partial_\sigma\theta + \sin^2\theta\partial_\sigma\phi\partial_\sigma\phi\right)\right]. \tag{B.1.1}$$

From (B.1.1), the conjugate momenta can be determined as

$$\Pi_\phi = -\frac{1}{4}\cos\theta\,, \qquad \Pi_\theta = -\frac{1}{4}\phi\sin\theta\,. \tag{B.1.2}$$

Evidently, these two equations should be regarded as the constraints. The commutation relation of these two constraints is given by

$$\{\Pi_\phi + \frac{1}{4}\cos\theta\big|_\sigma, \Pi_\theta + \frac{1}{4}\phi\sin\theta\big|_{\sigma'}\} = -\frac{\sin\theta}{2}\delta(\sigma-\sigma')\,. \tag{B.1.3}$$

Thus, the Dirac bracket of this system can be defined as

$$\{A,B\}_D = \{A,B\} + \int d\sigma \frac{2}{\sin\theta}\left(\{A,\Pi_\phi+\frac{1}{4}\cos\theta\}\{\Pi_\theta+\frac{1}{4}\phi\sin\theta,B\}-\{A,\Pi_\theta+\frac{1}{4}\phi\sin\theta\}\{\Pi_\phi+\frac{1}{4}\cos\theta,B\}\right). \tag{B.1.4}$$

Using (B.1.1), the commutation relation of $\vec{n}$ can be determined as

$$\{n_i(\sigma)\,,n_j(\sigma')\} = 2\epsilon_{ijk}n_k\delta(\sigma-\sigma')\,, \tag{B.1.5}$$

which is the classical analogue of the commutation relation of spins.

B.2 Classical r-matrix

Having derived the commutation relation of $\vec{n}$, our next task is to derive the Poisson bracket between the Lax matrices. The Poisson bracket between J_σ can be calculated as

$$\begin{aligned}\{J_\sigma(\sigma|x)\overset{\otimes}{,}J_\sigma(\sigma'|y)\} &= -\frac{1}{16\pi^2xy}\{\vec{n}(\sigma)\cdot\vec{\sigma}\overset{\otimes}{,}\vec{n}(\sigma')\cdot\vec{\sigma}\}\\ &= -\delta(\sigma-\sigma')\frac{1}{8\pi^2xy}\epsilon_{ijk}n_k(\sigma)\sigma_i\otimes\sigma_j\,.\end{aligned} \tag{B.2.1}$$

At this point, we can simplify the expression by using the Fiertz identity:

$$(\sigma_a)_{ij}(\sigma_b)_{kl} = \sum_{c,d}\frac{\mathrm{tr}\,(\sigma_c\sigma_a\sigma_d\sigma_b)}{4}(\sigma_c)_{il}(\sigma_d)_{kj}\,, \tag{B.2.2}$$

where σ_0 is defined to be an identity matrix. The essence is that the factor $\epsilon_{ijk}\sigma_i\otimes\sigma_j$ can be re-expressed by the use of the Fiertz identity as

$$\epsilon_{ijk}(\sigma_i)_{\alpha\beta}(\sigma_j)_{\gamma\delta} = \frac{i}{2}\left((\sigma_k)_{\alpha\delta}\delta_{\beta\gamma}-(\sigma_k)_{\beta\gamma}\delta_{\alpha\delta}\right). \tag{B.2.3}$$

Using such formulas, we arrive at the following expression[1] of the Poisson bracket.

$$\{J_\sigma(\sigma|x)\overset{\otimes}{,}J_\sigma(\sigma'|y)\} = \delta(\sigma-\sigma')\left[\mathbf{r}(x-y)\,,-\left(J_\sigma(x)\otimes\mathbf{1}+\mathbf{1}\otimes J_\sigma(y)\right)\right], \tag{B.2.4}$$

where $\mathbf{r}(x)$ is the so-called *classical r-matrix* which, in this case, is defined as follows.

$$\mathbf{r}(x) = \frac{\mathbb{P}}{2\pi x}\,, \tag{B.2.5}$$

[1] To arrive at the expression (B.2.4), we also need to use $(xy)^{-1} = \left(y^{-1}-x^{-1}\right)(x-y)^{-1}$.

where $\mathbb{P}$ is the operator which permutes two spaces in the tensor product: $V_1 \otimes V_2 \longmapsto V_2 \otimes V_1$. The classical r-matrix is an appropriate classical version of the R-matrix used in section (3.1.3).

It is well-known that when the Poisson bracket between Lax matrices can be expressed by the classical r-matrix as (B.2.4), the Poisson bracket between the monodromy matrices can also be expressed by the classical r-matrix as follows.

$$\{\Omega(x) \overset{\otimes}{,} \Omega(y)\} = [\Omega(x) \otimes \Omega(y)\,,\, \mathbf{r}(x-y)]\ . \tag{B.2.6}$$

The proof of (B.2.6) can be found in [34]. In terms of the components,

$$\Omega(x) \equiv \begin{pmatrix} \mathcal{A}(x) & \mathcal{B}(x) \\ \mathcal{C}(x) & \mathcal{D}(x) \end{pmatrix}\ , \tag{B.2.7}$$

the commutation relation (B.2.6) can be expressed as

$$\{\mathcal{A}(x)\,,\mathcal{B}(y)\} = -\frac{1}{2\pi(x-y)}\left(\mathcal{A}(x)\mathcal{B}(y) - \mathcal{A}(y)\mathcal{B}(x)\right)\ , \tag{B.2.8}$$

$$\{\mathcal{A}(x)\,,\mathcal{C}(y)\} = \frac{1}{2\pi(x-y)}\left(\mathcal{A}(x)\mathcal{C}(y) - \mathcal{A}(y)\mathcal{C}(x)\right)\ , \tag{B.2.9}$$

$$\{\mathcal{A}(x)\,,\mathcal{D}(y)\} = \frac{1}{2\pi(x-y)}\left(\mathcal{B}(x)\mathcal{C}(y) - \mathcal{B}(y)\mathcal{C}(x)\right)\ , \tag{B.2.10}$$

$$\{\mathcal{B}(x)\,,\mathcal{C}(y)\} = \frac{1}{2\pi(x-y)}\left(\mathcal{A}(x)\mathcal{D}(y) - \mathcal{A}(y)\mathcal{D}(x)\right)\ , \tag{B.2.11}$$

$$\{\mathcal{B}(x)\,,\mathcal{D}(y)\} = \frac{1}{2\pi(x-y)}\left(\mathcal{B}(x)\mathcal{D}(y) - \mathcal{B}(y)\mathcal{D}(x)\right)\ , \tag{B.2.12}$$

$$\{\mathcal{C}(x)\,,\mathcal{D}(y)\} = -\frac{1}{2\pi(x-y)}\left(\mathcal{C}(x)\mathcal{D}(y) - \mathcal{C}(y)\mathcal{D}(x)\right)\ , \tag{B.2.13}$$

$$\{\mathcal{A}(x)\,,\mathcal{A}(y)\} = \{\mathcal{B}(x)\,,\mathcal{B}(y)\} = \{\mathcal{C}(x)\,,\mathcal{C}(y)\} = \{\mathcal{D}(x)\,,\mathcal{D}(y)\} = 0\,. \tag{B.2.14}$$

These explicit expressions are useful when we construct the action-angle variables below.

B.3 Construction of action-angle variables

Having obtained the explicit expression of the Poisson bracket, we now proceed to the construction of the action-angle variables[2]. In Sklyanin's approach [94], the action-angle variables can be constructed from the poles of the normalized eigenvector of the monodromy matrix:

$$\Omega(x)\vec{\psi}(x) = e^{ip(x)}\vec{\psi}(x)\,, \quad \vec{n}\cdot\vec{\psi} = 1\,. \tag{B.3.1}$$

[2]For the construction of the action-angle variables of string sigma models, see [43] and Appendix B of [17].

Here $\vec{n} \equiv (n_1, n_2)^t$ is the normalization vector[3], which is chosen to be independent of the spectral parameter x and satisfy the normalization condition $n_1^2 + n_2^2 = 1$. To construct the action-angle variables from the poles of $\vec{\psi}(x)$, it is convenient to consider the transformed monodromy matrix $\tilde{\Omega}(x)$ defined by

$$\tilde{\Omega}(x) \equiv \begin{pmatrix} n_1 & n_2 \\ -n_2 & n_1 \end{pmatrix} \Omega \begin{pmatrix} n_1 & -n_2 \\ n_2 & n_1 \end{pmatrix} \equiv \begin{pmatrix} \tilde{\mathcal{A}}(x) & \tilde{\mathcal{B}}(x) \\ \tilde{\mathcal{C}}(x) & \tilde{\mathcal{D}}(x) \end{pmatrix} . \tag{B.3.2}$$

Owing to the symmetry of the Lax pair, the components of $\tilde{\Omega}$ satisfy the same Poisson-bracket relation as the components of Ω. Therefore we can directly use the results obtained in the previous subsection.

At the poles of the Baker-Akhiezer vector, γ_i's, the components of $\tilde{\Omega}$ satisfy the following relation[4].

$$\tilde{B}(\gamma_i) = 0 \,, \quad \tilde{\mathcal{D}}(\gamma_i) = \tilde{\mathcal{A}}(\gamma_i)^{-1} = e^{ip(\gamma_i)} \,. \tag{B.3.3}$$

In the following discussion, we use these relations to derive the commutation relation between γ_i's and $p(\gamma_i)$'s. To derive the relation correctly, we should start from the analysis of $\{\tilde{\mathcal{B}}(x)\,, \tilde{\mathcal{B}}(x')\} = 0$. Since $\tilde{B}$ has zeros at γ_i and γ_j $(i \neq j)$, it can be expressed as $\tilde{\mathcal{B}}(x) = (x - \gamma_i)\mathcal{B}'(x)$ or $\tilde{\mathcal{B}}(x) = (x - \gamma_j)\mathcal{B}''(x)$. The functions $\mathcal{B}'(x)$ and $\mathcal{B}''(x)$ are not known but what is important is that they have the properties $\mathcal{B}'(\gamma_i) \neq 0$ and $\mathcal{B}''(\gamma_j) \neq 0$. Then the commutation relation between $\tilde{\mathcal{B}}(x)$ and $\tilde{\mathcal{B}}(x')$ can be rewritten as

$$\begin{aligned} &(x - \gamma_i)(x' - \gamma_j)\{\mathcal{B}'(x)\,, \mathcal{B}''(x')\} - (x' - \gamma_j)\mathcal{B}'(x)\{\gamma_i\,, \mathcal{B}''(x')\} \\ &- (x - \gamma_i)\mathcal{B}''(x')\{\mathcal{B}'(x)\,, \gamma_j\} + \mathcal{B}'(x)\mathcal{B}''(x')\{\gamma_i\,, \gamma_j\} = 0 \,. \end{aligned} \tag{B.3.4}$$

Now at this stage, we can safely take the limit $x \to \gamma_i$ and $x' \to \gamma_j$. Then the first three terms vanish manifestly and from the last term we obtain the relation

$$\{\gamma_i\,, \gamma_j\} = 0 \,. \tag{B.3.5}$$

Next step is to consider the commutation relation of $\tilde{\mathcal{A}}(x)$ and $\tilde{\mathcal{B}}(x')$. Here again, we should substitute the expansion $\tilde{\mathcal{A}}(x) = \tilde{\mathcal{A}}(\gamma_i) + (x - \gamma_i)\mathcal{A}'(x)$ as well as the ones for $\mathcal{B}'$ and $\mathcal{B}''$.

[3] As we saw in section 7.3.3, the normalization vector is intimately related to the global symmetry structure and is determined by the highest weight condition. However, for the purpose of this section, we do not need to specify it.

[4] To see this, it is helpful to consider the relation between the *normalized* eigenvector and the *unnormalized* eigenvector. The unnormalized eigenvector can be constructed from the normalized eigenvector by $\vec{\psi}_{\text{normalized}} = \vec{\psi}_{\text{unnormalized}}/(\vec{n} \cdot \vec{\psi}_{\text{unnormalized}})$. Therefore the poles of the normalized eigenvector arise when the unnormalized eigenvector satisfy $\vec{n} \cdot \vec{\psi}_{\text{unnormalized}} = 0$. Thus, at the poles of the normalized eigenvector, the vector $(-n_2\,, n_1)^t$, which is orthogonal to $\vec{n}$, becomes the eigenvector of the monodromy matrix. Then, it is easy to see that (B.3.3) follows.

Then similarly to the previous case, the limit $x \to \gamma_i$ and $x' \to \gamma_j$ can be taken easily and, making use of the relation (B.3.5), we can deduce the important relation

$$\{\tilde{\mathcal{A}}(\gamma_i)\,,\gamma_j\} = \frac{\tilde{\mathcal{A}}(\gamma_i)}{2\pi}\delta_{ij}\,. \tag{B.3.6}$$

Finally, similar calculation for $\{\tilde{\mathcal{A}}(x)\,,\tilde{\mathcal{A}}(x')\} = 0$ leads to

$$\{\tilde{\mathcal{A}}(\gamma_i)\,,\tilde{\mathcal{A}}(\gamma_j)\} = 0\,. \tag{B.3.7}$$

From the equations (B.3.5)-(B.3.7), we can obtain the commutation relation for γ_i's and $p(\gamma_j)$'s as

$$\{\gamma_i\,,\gamma_j\} = \{p(\gamma_i)\,,p(\gamma_j)\} = 0\,, \quad \frac{2\pi}{i}\{\gamma_i\,,p(\gamma_j)\} = \delta_{ij}\,. \tag{B.3.8}$$

Therefore we conclude that $(\gamma_i\,,-2\pi i p(\gamma_i))$'s are canonical pairs of variables.

From $(\gamma_i\,,-2\pi i p(\gamma_i))$'s, one can easily construct the action variables a.k.a. the filling fractions as follows[5].

$$S_i \equiv \frac{1}{2\pi i}\oint_{a_i} p(x)dx\,, \tag{B.3.9}$$

where a_i is the cycle on the spectral curve[6]. To construct angle variables ϕ_i's, which are conjugate to S_i's, we need to find the generating function $F\,(S_i\,,\gamma_i)$ which provides the canonical transformation from $(\gamma_i\,,-ip(\gamma_i))$ to action-angle variables. Such a function is defined as follows,

$$\frac{\partial F}{\partial \gamma_i} = -2\pi i p(\gamma_i)\,, \tag{B.3.10}$$

$$\frac{\partial F}{\partial S_i} = \phi_i\,. \tag{B.3.11}$$

In the present context, the first equation should be viewed as the definition of F while the second equation should be regarded as the definition of ϕ_i. Therefore, to determine F, we need to integrate the first equation with S_i fixed. As the filling fractions are given by the integral of $p(x)$ on the spectral curve, fixing all S_i's is equivalent to fixing the functional form of $p(x)$. Therefore, F can be determined as

$$F = -2\pi i\sum_i \int^{\gamma_i} p(x)dx\,. \tag{B.3.12}$$

[5]The normalization of th filling fractions we adopt here is the one used in [40].

[6]Since we are discussing the general formalism in this subsection and *not* focusing on the particular solution, we need to consider the spectral curve with an infinite number of cuts. For details, see section 7.1.4.

(We will not specify here the initial point of integration. As we will show momentarily, the choice of the initial point is not important in the practical calculation.)

Next we compute $\phi_i = \partial F/\partial S_i$. This requires changing S_i with all the other filling fractions fixed. This is precisely equivalent to adding to $p(x)dx$ a one-form whose period integral along a-cycles is non-vanishing only for a_i. Such a one-form should be proportional to a normalized holomorphic differential ω_i, which satisfies the following property.

$$\oint_{a_j} \omega_i = \delta_{ij} \,. \tag{B.3.13}$$

Using such ω_i, the partial derivative $\partial F/\partial S_i$ can be expressed as

$$\phi_i = 4\pi^2 \sum_j \int^{\gamma_j} \omega_i \,. \tag{B.3.14}$$

From the action-angle variables, the wave function can be constructed as follows. (Note that in general the solution has an infinite number of gaps and thus the number of action-angle variables is also infinite.)

$$\Psi\left[\phi_1\,,\phi_2\,,\cdots\right] \equiv \langle \phi_1\,,\phi_2\,,\cdots|\Psi\rangle = \exp\left[i\sum_j S_j\phi_j\right] \,. \tag{B.3.15}$$

It would be interesting to explore the possibility to use the above wave function to derive the semi-classical limit of three-point functions in the gauge theory [92, 93, 115].

Chapter C

Details on the three-point function in the classical string theory

C.1 Details on the one-cut solutions

In this appendix, we will summarize the details on the one-cut solutions.

C.1.1 Parameters of one-cut solutions in terms of the position of the cut

By using the forms of $p(x)$ and $q(x)$ given in (7.1.25) and (7.1.26) one can evaluate the parameters μ_i, m_i and θ_0 explicitly in terms of u. The results depend on the position of the cut. It is convenient to express them in universal forms by introducing two additional sign factors η_1 and $\eta_{0,1}$. Together with the factor ϵ already introduced in (7.1.27), we give their definitions in the following table:

Table. Sign factors to distinguish between the positions of the cut.

	$\mathrm{Re}\, u < -1$	$-1 < \mathrm{Re}\, u < 0$	$0 < \mathrm{Re}\, u < 1$	$1 < \mathrm{Re}\, u$
ϵ	$+$	$-$	$-$	$+$
η_1	$+$	$+$	$+$	$-$
$\eta_{0,1}$	$+$	$+$	$-$	$+$

Then, ν_1 and ν_2 are obtained as

$$\nu_1 = \kappa \left[-\frac{\eta_1 + \eta_{0,1}|u|}{|u-1|} + \epsilon \frac{\eta_1 - \eta_{0,1}|u|}{|u+1|} \right] , \tag{C.1.1}$$

$$\nu_2 = \kappa \left[\frac{\eta_1 - \eta_{0,1}|u|}{|u-1|} - \epsilon \frac{\eta_1 + \eta_{0,1}|u|}{|u+1|} \right] = \epsilon \nu_1(u \to -u) \, . \tag{C.1.2}$$

As for m_i, we can immediately obtain them form ν_i by the substitution $\epsilon \to -\epsilon$, because, as seen in (7.1.25) and (7.1.26), this interchanges $q(x)$ and $p(x)$:

$$m_1 = \nu_1(\epsilon \to -\epsilon)\,, \tag{C.1.3}$$

$$m_2 = \nu_2(\epsilon \to -\epsilon)\,. \tag{C.1.4}$$

Now $\cos^2(\theta_0/2)$ and $\sin^2(\theta_0/2)$ can be deduced from the Virasoro condition (7.1.37) as

$$\cos^2\frac{\theta_0}{2} = \frac{|u| - \eta_1\eta_{0,1}\mathrm{Re}\,u}{2|u|}\,, \qquad \sin^2\frac{\theta_0}{2} = \frac{|u| + \eta_1\eta_{0,1}\mathrm{Re}\,u}{2|u|}\,. \tag{C.1.5}$$

The right and the left charges are obtained from (3.2.40) and (3.2.41) to be

$$R = -\frac{\kappa\sqrt{\lambda}\eta_1}{2}\left(\frac{\mathrm{Re}\,u - 1}{|u-1|} + \epsilon\frac{\mathrm{Re}\,u + 1}{|u+1|}\right)\,, \tag{C.1.6}$$

$$L = \frac{\kappa\sqrt{\lambda}\eta_{0,1}}{2|u|}\left(\frac{|u|^2 - \mathrm{Re}\,u}{|u-1|} + \epsilon\frac{|u|^2 + \mathrm{Re}\,u}{|u+1|}\right)\,. \tag{C.1.7}$$

From the definition of R and L as the Noether charges, they must be expressed in terms of the parameters ν_i and θ_0 in a universal manner independent of the position of the cut. Indeed by using the formulas already obtained for the parameters and the charges in terms of u, we can check the universal expressions

$$\frac{R}{\sqrt{\lambda}} = \frac{1}{2}\left(-\nu_1\cos^2\frac{\theta_0}{2} + \nu_2\sin^2\frac{\theta_0}{2}\right)\,, \tag{C.1.8}$$

$$\frac{L}{\sqrt{\lambda}} = \frac{1}{2}\left(-\nu_1\cos^2\frac{\theta_0}{2} - \nu_2\sin^2\frac{\theta_0}{2}\right)\,. \tag{C.1.9}$$

Finally, let us discuss the signs and the relative magnitudes of the parameters and the charges. The signs and the relative magnitude of ν_i depend on u. From the formulas for ν_i we can check that

$$|\mathrm{Re}\,u| > 1: \qquad \nu_2 < \nu_1 < 0\,, \tag{C.1.10}$$

$$|\mathrm{Re}\,u| < 1: \qquad \nu_1 < 0 < \nu_2\,, (|\nu_1| < \nu_2)\,. \tag{C.1.11}$$

As for the angles, we always have

$$\cos^2\frac{\theta_0}{2} > \sin^2\frac{\theta_0}{2}\,. \tag{C.1.12}$$

The signs of R and L can be checked to be always positive. (R for the case $|\mathrm{Re}\,u| > 1$ and L for the case $|\mathrm{Re}\,u| < 1$ are somewhat non-trivial to check.)

The relative magnitude of R and L can be deduced easily from the difference

$$\frac{1}{\sqrt{\lambda}}(R-L) = 2\nu_2 \sin^2\frac{\theta_0}{2}\,. \tag{C.1.13}$$

As the sign of ν_2 has already been obtained in (C.1.10) and (C.1.11), we immediately get

$$R < L \qquad \text{for} \quad |\mathrm{Re}\, u| > 1\,, \tag{C.1.14}$$

$$R > L \qquad \text{for} \quad |\mathrm{Re}\, u| < 1\,. \tag{C.1.15}$$

C.1.2 Pohlmeyer reduction for one-cut solutions

Let us next consider the variables appearing in the Pohlmeyer reduction, ρ, $\tilde{\rho}$ and γ for one-cut solutions. From their definitions, we can express them in terms of the parameters of the one-cut solution as

$$\cos 2\gamma = \frac{\nu_1^2 - m_1^2}{4\kappa^2} = \frac{\nu_2^2 - m_2^2}{4\kappa^2}\,, \tag{C.1.16}$$

$$\rho = \frac{1}{8}\cos\frac{\theta_0}{2}\sin\frac{\theta_0}{2}\left((\nu_1+m_1)^2 - (\nu_2+m_2)^2\right)\,, \tag{C.1.17}$$

$$\tilde{\rho} = \frac{1}{8}\cos\frac{\theta_0}{2}\sin\frac{\theta_0}{2}\left((\nu_1-m_1)^2 - (\nu_2-m_2)^2\right)\,, \tag{C.1.18}$$

where we used $z = \tau + i\sigma$ coordinate when we compute these quantities[1].

Using the results in the previous subsection, we can re-express (C.1.16), (C.1.17) and (C.1.18) in terms of the branch points u and $\bar{u}$. They are given by

$$\cos 2\gamma = \epsilon\frac{|u|^2-1}{|u^2-1|}\,, \quad \sin 2\gamma = \frac{2\mathrm{Im}\ u}{|u^2-1|}\,, \tag{C.1.19}$$

$$\rho = -\kappa^2\frac{\mathrm{Im}\ u}{|u-1|^2}\,, \quad \tilde{\rho} = \kappa^2\frac{\mathrm{Im}\ u}{|u+1|^2}\,. \tag{C.1.20}$$

The ALP in the Pohlmeyer gauge can be solved in a similar manner and the result is given in (7.1.83) and (7.1.84).

In the case of three-point functions, we can compute these quantities separately for each

[1]Note that γ is invariant under the coordinate change $z \to z' = f(z)$, whereas ρ and $\tilde{\rho}$ transform respectively as $\rho \to \rho' = \rho/(\partial f)^2$ and $\tilde{\rho} \to \tilde{\rho}' = \tilde{\rho}/(\bar{\partial} f)^2$.

puncture as

$$\gamma_i = \frac{1}{2}\arcsin\left(\frac{2\text{Im } u_i}{|u_i^2-1|}\right), \tag{C.1.21}$$

$$\rho_i = -\kappa^2\frac{\text{Im } u_i}{|u_i-1|^2}, \tag{C.1.22}$$

$$\tilde{\rho}_i = \kappa^2\frac{\text{Im } u_i}{|u_i+1|^2}. \tag{C.1.23}$$

They will be used in the computation of three-point functions.

C.1.3 Computation of various integrals

Using the above results, let us compute various integrals which appear in Local and Double in section 7.2. Around a puncture, one can approximate the behavior of the world-sheet by that of the two-point functions. Thus, when three string states are semi-classically described 1-cut solutions, we expect the following asymptotic behavior of the one-forms:

$$\lambda \overset{z\to z_i}{\sim} \kappa_i dw_i\,, \quad \omega \overset{z\to z_i}{\sim} -\frac{\kappa_i\cos 2\gamma_i}{2}d\bar{w}_i + \frac{2\rho_i^2}{\kappa_i^3}dw_i\,, \tag{C.1.24}$$

where w_i is the local coordinate $w_i \equiv \tau^{(i)} + i\sigma^{(i)}$ around the puncture z_i.

Using (C.1.24), one can evaluate various integrals. First, the contour integrals of λ and ω along $\mathcal{C}_i$'s are given by

$$\oint_{\mathcal{C}_i}\lambda = 2\pi i\kappa_i\,, \quad \oint_{\mathcal{C}_i}\omega = 2\pi i\left(\frac{\kappa_i\cos 2\gamma_i}{2}+\frac{2\rho_i^2}{\kappa_i^3}\right) \qquad i=1,\bar{2},3\,. \tag{C.1.25}$$

On the other hand, the double contour integral, which appears in Double can be computed as follows:

$$\begin{aligned}\oint_{\mathcal{C}_i}\omega\int_{z_i^*}^{z}\lambda &= \int_{\sigma=0}^{\sigma=2\pi}\left(-\frac{\kappa_i\cos 2\gamma_i}{2}d\bar{w}_i+\frac{2\rho_i^2}{\kappa_i^3}dw_i\right)\int_{\sigma'=0}^{\sigma'=\sigma}\kappa_i dw_i' \\ &= -\int_0^{2\pi}d\sigma\left(\frac{\kappa_i\cos 2\gamma_i}{2}+\frac{2\rho_i^2}{\kappa_i^3}\right)\kappa_i\sigma \\ &= -2\pi^2\left(\frac{\kappa_i\cos 2\gamma_i}{2}+\frac{2\rho_i^2}{\kappa_i^3}\right)\kappa_i\,.\end{aligned} \tag{C.1.26}$$

These results are used in section 7.2.1 to explicitly evaluate Local and Double .

C.2 Pohlmeyer reduction

In this appendix, we will give some details of the Pohlmeyer reduction for the string on S^3.

In terms of the embedding coordinate Y_I $(I = 1, \ldots, 4)$, S^3 is realized as a hypersurface in R^4 satisfying $\sum_I Y_I^2 = 1$. The basic idea of the Pohlmeyer reduction is to describe the dynamics of the string in terms of a *moving frame* in R^4 consisting of four basis vectors $\{Y_I, \partial Y_I, \bar{\partial} Y_I, N_I\}$, which satisfy the following properties:

$$N^I N_I = 1\,, \quad N^I Y_I = N^I \partial Y_I = N^I \bar{\partial} Y_I = 0\,. \tag{C.2.1}$$

Then, using the equation of motion, $\partial\bar{\partial}Y^I + \left(\partial Y^J \bar{\partial} Y_J\right) Y^I = 0$ and the Virasoro constraints, $\partial Y^I \partial Y_I = -T(z)$ and $\bar{\partial} Y^I \bar{\partial} Y_I = -\bar{T}(\bar{z})$, we can express the derivatives of these basis vectors, $\partial N^I\,, \partial^2 Y^I\,,$ *etc.* again in terms of the basis vectors:

$$\partial N^I = \frac{2\rho}{T \sin^2 2\gamma} \partial Y^I + \frac{2\cos 2\gamma\rho}{\sqrt{T\bar{T}} \sin^2 2\gamma} \bar{\partial} Y^I\,, \tag{C.2.2}$$

$$\bar{\partial} N^I = \frac{2\rho}{\bar{T} \sin^2 2\gamma} \bar{\partial} Y^I + \frac{2\cos 2\gamma\tilde{\rho}}{\sqrt{T\bar{T}} \sin^2 2\gamma} \partial Y^I\,, \tag{C.2.3}$$

$$\partial^2 Y = T Y^I + \frac{\partial \ln\left(T\bar{T}\sin^2 2\gamma\right)}{2} \partial Y^I + \sqrt{\frac{\bar{T}}{T}} \frac{2\partial\gamma}{\sin 2\gamma} \bar{\partial} Y^I + 2\rho N^I\,, \tag{C.2.4}$$

$$\bar{\partial}^2 Y = \bar{T} Y + \frac{\bar{\partial} \ln\left(T\bar{T}\sin^2 2\gamma\right)}{2} \bar{\partial} Y^I + \sqrt{\frac{T}{\bar{T}}} \frac{2\bar{\partial}\gamma}{\sin 2\gamma} \partial Y^I + 2\tilde{\rho} N^I\,, \tag{C.2.5}$$

$$\partial\bar{\partial} Y = -\sqrt{T\bar{T}} \cos 2\gamma Y\,, \tag{C.2.6}$$

where ρ, $\tilde{\rho}$ and γ are defined by

$$\partial Y^I \bar{\partial} Y_I = \sqrt{T\bar{T}} \cos 2\gamma\,, \quad \rho \equiv \frac{1}{2} N^I \partial^2 Y_I\,, \quad \tilde{\rho} \equiv \frac{1}{2} N^I \bar{\partial}^2 Y_I\,. \tag{C.2.7}$$

Using the equation of motion, one can also show that γ, ρ and $\tilde{\rho}$ satisfy the generalized sin-Gordon equation, which is given in (7.1.11).

Let us next derive a flat connection associated with the system of equations (C.2.2)–(C.2.6). For this purpose, it is convenient to introduce the following orthonormal basis:

$$q_1 \equiv Y\,, \quad q_2 \equiv -\frac{i}{\sin 2\gamma} \left[\frac{e^{i\gamma}}{\sqrt{T}} \partial Y + \frac{e^{-i\gamma}}{\sqrt{\bar{T}}} \bar{\partial} Y\right]\,, \tag{C.2.8}$$

$$q_3 \equiv \frac{i}{\sin 2\gamma} \left[\frac{e^{i\gamma}}{\sqrt{\bar{T}}} \bar{\partial} Y + \frac{e^{-i\gamma}}{\sqrt{T}} \partial Y\right]\,, \quad q_4 \equiv N\,, \tag{C.2.9}$$

which satisfy the following normalization conditions:

$$q_1^2 = q_4^2 = 1\,, \quad q_2 q_3 = -2\,. \tag{C.2.10}$$

With these orthonormal vectors, (C.2.2)–(C.2.6) can be re-expressed as the following set of equations,

$$\partial q_1 = \frac{\sqrt{T}}{2}\left[e^{i\gamma}q_2 + e^{-i\gamma}q_3\right] , \tag{C.2.11}$$

$$\partial q_2 = e^{-i\gamma}\sqrt{T}q_1 + i\partial\gamma q_2 - \frac{2i\rho}{\sqrt{T}\sin 2\gamma}e^{i\gamma}q_4 , \tag{C.2.12}$$

$$\partial q_3 = e^{i\gamma}\sqrt{T}q_1 - i\partial\gamma q_3 + \frac{2i\rho}{\sqrt{T}\sin 2\gamma}e^{-i\gamma}q_4 , \tag{C.2.13}$$

$$\partial q_4 = \frac{i\rho e^{-i\gamma}}{\sqrt{T}\sin 2\gamma}q_2 - \frac{i\rho e^{i\gamma}}{\sqrt{T}\sin 2\gamma}q_3 , \tag{C.2.14}$$

$$\bar\partial q_1 = -\frac{\sqrt{\bar T}}{2}\left[e^{-i\gamma}q_2 + e^{i\gamma}q_3\right] , \tag{C.2.15}$$

$$\bar\partial q_2 = -e^{i\gamma}\sqrt{\bar T}q_1 - i\bar\partial\gamma q_2 - \frac{2i\tilde\rho}{\sqrt{\bar T}\sin 2\gamma}e^{-i\gamma}q_4 , \tag{C.2.16}$$

$$\bar\partial q_3 = -e^{-i\gamma}\sqrt{\bar T}q_1 + i\bar\partial\gamma q_3 + \frac{2i\tilde\rho}{\sqrt{\bar T}\sin 2\gamma}e^{i\gamma}q_4 , \tag{C.2.17}$$

$$\bar\partial q_4 = \frac{i\tilde\rho e^{i\gamma}}{\sqrt{\bar T}\sin 2\gamma}q_2 + \frac{i\tilde\rho e^{-i\gamma}}{\sqrt{\bar T}\sin 2\gamma}q_3 . \tag{C.2.18}$$

By expressing the basis in a matrix form,

$$W \equiv \frac{1}{2}\begin{pmatrix} q_1 + iq_4 & q_2 \\ q_3 & q_1 - iq_4 \end{pmatrix} , \tag{C.2.19}$$

we can convert the above equations into the following form:

$$\partial W + B_z^L W + W B_z^R = 0 , \quad \bar\partial W + B_{\bar z}^L W + W B_{\bar z}^R = 0 , \tag{C.2.20}$$

where $B_{z,\bar z}^{L,R}$ are matrices defined by

$$B_z^L \equiv \begin{pmatrix} -\frac{i\partial\gamma}{2} & \frac{\rho e^{i\gamma}}{\sqrt{T}\sin 2\gamma} - \frac{\sqrt{T}}{2}e^{-i\gamma} \\ \frac{\rho e^{-i\gamma}}{\sqrt{T}\sin 2\gamma} - \frac{\sqrt{T}}{2}e^{i\gamma} & \frac{i\partial\gamma}{2} \end{pmatrix} , \tag{C.2.21}$$

$$B_z^R \equiv \begin{pmatrix} \frac{i\partial\gamma}{2} & -\frac{\rho e^{i\gamma}}{\sqrt{T}\sin 2\gamma} - \frac{\sqrt{T}}{2}e^{-i\gamma} \\ -\frac{\rho e^{-i\gamma}}{\sqrt{T}\sin 2\gamma} - \frac{\sqrt{T}}{2}e^{i\gamma} & -\frac{i\partial\gamma}{2} \end{pmatrix} , \tag{C.2.22}$$

$$B_{\bar z}^L \equiv \begin{pmatrix} \frac{i\bar\partial\gamma}{2} & \frac{\tilde\rho e^{-i\gamma}}{\sqrt{\bar T}\sin 2\gamma} + \frac{\sqrt{\bar T}}{2}e^{i\gamma} \\ \frac{\tilde\rho e^{i\gamma}}{\sqrt{\bar T}\sin 2\gamma} + \frac{\sqrt{\bar T}}{2}e^{-i\gamma} & -\frac{i\bar\partial\gamma}{2} \end{pmatrix} , \tag{C.2.23}$$

$$B_{\bar z}^R \equiv \begin{pmatrix} -\frac{i\bar\partial\gamma}{2} & -\frac{\tilde\rho e^{-i\gamma}}{\sqrt{\bar T}\sin 2\gamma} + \frac{\sqrt{\bar T}}{2}e^{i\gamma} \\ -\frac{\tilde\rho e^{i\gamma}}{\sqrt{\bar T}\sin 2\gamma} + \frac{\sqrt{\bar T}}{2}e^{-i\gamma} & \frac{i\bar\partial\gamma}{2} \end{pmatrix} . \tag{C.2.24}$$

(C.2.20) is equivalent to the flatness conditions of the connections B^L and B^R,

$$\partial B^L_{\bar{z}} - \bar{\partial} B^L_z + [B^L_z\,, B^L_{\bar{z}}] = 0\,, \qquad \partial B^R_{\bar{z}} - \bar{\partial} B^R_z + [B^R_z\,, B^R_{\bar{z}}] = 0\,. \tag{C.2.25}$$

Owing to the classical integrability of the string sigma model, we can "deform" the above connection without spoiling the flatness by introducing a spectral parameter $\zeta = (1-x)/(1+x)$ as

$$B_z(\zeta) \equiv \frac{\Phi_z}{\zeta} + A_z\,, \quad B_{\bar{z}}(\zeta) \equiv \zeta \Phi_{\bar{z}} + A_{\bar{z}}\,. \tag{C.2.26}$$

Φ's and A's are defined by[2]

$$\Phi_z \equiv \begin{pmatrix} 0 & -\frac{\sqrt{T}}{2} e^{-i\gamma} \\ -\frac{\sqrt{T}}{2} e^{i\gamma} & 0 \end{pmatrix}\,, \quad \Phi_{\bar{z}} \equiv \begin{pmatrix} 0 & \frac{\sqrt{\bar{T}}}{2} e^{i\gamma} \\ \frac{\sqrt{\bar{T}}}{2} e^{-i\gamma} & 0 \end{pmatrix}\,, \tag{C.2.27}$$

$$A_z \equiv \begin{pmatrix} -\frac{i\partial\gamma}{2} & \frac{\rho e^{i\gamma}}{\sqrt{T}\sin 2\gamma} \\ \frac{\rho e^{-i\gamma}}{\sqrt{T}\sin 2\gamma} & \frac{i\partial\gamma}{2} \end{pmatrix}\,, \quad A_{\bar{z}} \equiv \begin{pmatrix} \frac{i\bar{\partial}\gamma}{2} & \frac{\tilde{\rho} e^{-i\gamma}}{\sqrt{\bar{T}}\sin 2\gamma} \\ \frac{\tilde{\rho} e^{i\gamma}}{\sqrt{\bar{T}}\sin 2\gamma} & -\frac{i\bar{\partial}\gamma}{2} \end{pmatrix}\,. \tag{C.2.28}$$

The deformed connection (C.2.26) evaluated at $\zeta = 1$ or $\zeta = -1$ is related to the original connection $B^{L,R}$ in the following way:

$$B^L = B(\zeta = 1)\,, \quad \left(B^R\right)^t = \sigma_2 B(\zeta = -1)\sigma_2\,. \tag{C.2.29}$$

Furthermore (C.2.26) is related to the usual left/right connection by an appropriate gauge transformation as will be shown in Appendix C.3.

C.3 Relation between the Pohlmeyer reduction and the sigma model formulation

In this appendix, we explain how the Pohlmeyer reduction and the sigma model formulation are related.

C.3.1 Reconstruction formula for the Pohlmeyer reduction

In section 7.1.3 we presented the simple formulas (7.1.32) and (7.1.33) which reconstruct the solution $\mathbb{Y}$ of the equations of motion from the eigenfunctions of the ALP in the sigma model formulation. We now describe a similar formula for the Pohlmeyer reduction and by

[2] (C.2.26) is equivalent in form to the SL(2)-Hitchin system. However, the boundary conditions we impose around the punctures are different from the ones used in the usual analysis of the Hitchin system.

comparing such reconstruction formulas we can relate the two formulations. Consider the left and the right ALP associated with the Pohlmeyer reduction,

$$\left(d + B^L\right)\psi^L = 0\,, \quad \left(d + B^R\right)\psi^R = 0\,, \tag{C.3.1}$$

and let $\psi_1^{L,R}$ and $\psi_2^{L,R}$ be two linearly independent solutions satisfying the normalization conditions

$$\det\left(\psi_1^L\,,\,\psi_2^L\right) = 1\,, \quad \det\left(\psi_1^R\,,\,\psi_2^R\right) = 1\,. \tag{C.3.2}$$

Then, similarly to the sigma model case, the embedding coordinates $\mathbb{Y}$ can be reconstructed by the formula

$$\mathbb{Y} = q_1 = \begin{pmatrix} Z_1 & Z_2 \\ -\bar{Z}_2 & \bar{Z}_1 \end{pmatrix} = \left(\Psi^L\right)^t \Psi^R\,, \tag{C.3.3}$$

where $\Psi^{L,R}$ are 2×2 matrices with a unit determinant, defined by

$$\Psi^L \equiv \left(\psi_1^L\,,\,\psi_2^L\right)\,, \qquad \Psi^R \equiv \left(\psi_1^R\,,\,\psi_2^R\right)\,. \tag{C.3.4}$$

Concerning the property under the global symmetry transformations, we should note the following. Since the Pohlmeyer connections B^L and B^R in the equation (C.3.1) are invariant, Ψ^L and Ψ^R must also be invariant under such transformations acting from left. However, as for transformations from right, they may transform non-trivially. In fact, as we shall see shortly, they must transform covariantly from right so that the solutions of the ALP for the Pohlmeyer and the sigma model formulations are connected consistently by a gauge transformation.

Furthermore, one can check that the quantities q_2 and q_3, which consist of the derivatives of $\mathbb{Y}$, can be reconstructed as

$$q_2 = \left(\Psi^L\right)^t \begin{pmatrix} 0 & 2 \\ 0 & 0 \end{pmatrix} \Psi^R\,, \qquad q_3 = \left(\Psi^L\right)^t \begin{pmatrix} 0 & 0 \\ 2 & 0 \end{pmatrix} \Psi^R\,. \tag{C.3.5}$$

From these formulas the derivatives of $\mathbb{Y}$ can be obtained as

$$\partial\mathbb{Y} = \frac{\sqrt{T}}{2}\left[e^{i\gamma}q_2 + e^{-i\gamma}q_3\right]\,, \qquad \bar{\partial}\mathbb{Y} = -\frac{\sqrt{\bar{T}}}{2}\left[e^{-i\gamma}q_2 + e^{i\gamma}q_3\right]\,. \tag{C.3.6}$$

Note that, in distinction to the case of the sigma model, the reconstruction formulas for the Pohlmeyer reduction does not use the eigenvectors of the monodromy matrices, namely $\hat{\psi}_\pm$. The solutions $\psi_i^{L,R}$ used are simply two linearly independent solutions to the ALP, which are not necessarily the eigenvectors of Ω.

C.3.2 Relation between the connections and the eigenvectors

We now discuss the relation between the connections and the eigenvectors of the the Pohlmeyer reduction and those of the sigma model.

First consider the relation to the right connection of the sigma model. From the formulas for $\partial\mathbb{Y}$ and $\bar{\partial}\mathbb{Y}$ given in (C.3.6), we can form the right connection j as

$$j_z = \sqrt{T}\left(\Psi^R\right)^{-1}\begin{pmatrix} 0 & e^{i\gamma} \\ e^{-i\gamma} & 0 \end{pmatrix}\Psi^R\,, \quad j_{\bar{z}} = -\sqrt{\bar{T}}\left(\Psi^R\right)^{-1}\begin{pmatrix} 0 & e^{-i\gamma} \\ e^{i\gamma} & 0 \end{pmatrix}\Psi^R\,. \tag{C.3.7}$$

Then, comparing (C.3.7) with (C.2.26)–(C.2.28), we find that the following gauge transformation connects the flat connections of the two formulations:

$$\frac{1}{1-x}j_z = \mathcal{G}^{-1}B_z(\zeta)\mathcal{G} + \mathcal{G}^{-1}\partial\mathcal{G}\,, \tag{C.3.8}$$

$$\frac{1}{1+x}j_{\bar{z}} = \mathcal{G}^{-1}B_{\bar{z}}(\zeta)\mathcal{G} + \mathcal{G}^{-1}\bar{\partial}\mathcal{G}\,, \tag{C.3.9}$$

where

$$\mathcal{G} = i\sigma_2\Psi^R\,. \tag{C.3.10}$$

The eigevectors $\psi_\pm$ of the sigma model formulation and those of the Pohlmeyer reduction, denoted by $\hat{\psi}_\pm$, are related as

$$\psi_\pm = \mathcal{G}^{-1}\hat{\psi}_\pm\,. \tag{C.3.11}$$

Note that the factor of i in (C.3.10) is needed to reproduce the correct normalization condition $\langle\psi_+\,,\psi_-\rangle = 1$. Under the global $\mathrm{SU}(2)_R$ transformation U_R, $\psi_\pm$ transform as $\psi_\pm \to U_R^{-1}\psi_\pm$. From the above formulas (C.3.10) and (C.3.11) we see that this corresponds to the transformation $\Psi^R \to \Psi^R U_R$, as remarked previously.

In an exactly similar manner, we can construct the left current l's by

$$l_z = \sqrt{T}\left(\Psi^L\right)^t\begin{pmatrix} 0 & e^{i\gamma} \\ e^{-i\gamma} & 0 \end{pmatrix}\left[\left(\Psi^L\right)^t\right]^{-1}\,, \quad l_{\bar{z}} = -\sqrt{\bar{T}}\left(\Psi^L\right)^t\begin{pmatrix} 0 & e^{-i\gamma} \\ e^{i\gamma} & 0 \end{pmatrix}\left[\left(\Psi^L\right)^t\right]^{-1}\,, \tag{C.3.12}$$

Comparing (C.3.12) with (C.2.26)–(C.2.28), we find that the following gauge transformation connects the two connections:

$$\frac{x}{1-x}l_z = \tilde{\mathcal{G}}^{-1}B_z(\zeta)\tilde{\mathcal{G}} + \tilde{\mathcal{G}}^{-1}\partial\tilde{\mathcal{G}}\,, \tag{C.3.13}$$

$$-\frac{x}{1+x}l_{\bar{z}} = \tilde{\mathcal{G}}^{-1}B_z(\zeta)\tilde{\mathcal{G}} + \tilde{\mathcal{G}}^{-1}\bar{\partial}\tilde{\mathcal{G}}\,, \tag{C.3.14}$$

where

$$\tilde{\mathcal{G}} = \left[(\Psi_L)^t(-i\sigma_2)\right]^{-1} = i\Psi_L\sigma_2\,. \tag{C.3.15}$$

The eigenvectors are related as

$$\tilde{\psi}_\pm = \tilde{\mathcal{G}}^{-1}\hat{\psi}_\pm\,. \tag{C.3.16}$$

Using (C.3.11) and (C.3.16), one can show the equivalence between the reconstruction formulas (7.1.32), (7.1.33) and (C.3.3).

C.4 Exact solution describing a scattering of three spinning strings in flat space and its action-angle variables

Construction of three-pronged solutions in (the subspace of) $AdS_5 \times S^5$ is an important challenging problem. As discussed in section 7.1.5, their analytic structure is expected to be qualitatively quite different from that of the two-point solutions. To give support to this observation, we present below an exact solution describing a scattering of three spinning strings in flat space and analyze its local behavior. This confirms some important structures concerning the action-angle variables.

A solution describing three interacting strings spinning in the x_1-x_2 plane is given by

$$X^\mu = -i\left(k_1^\mu \ln|z| + k_2^\mu \ln|z-1| + k_3^\mu \ln|z-\infty|\right)\,, \quad \mu \neq 1,2\,, \tag{C.4.1}$$

$$X = \frac{w_3}{2i}(z-\bar{z})\,, \quad \bar{X} = \frac{w_1}{2i}\left(\frac{1}{z}-\frac{1}{\bar{z}}\right) + \frac{w_2}{2i}\left(\frac{1}{z-1}-\frac{1}{\bar{z}-1}\right)\,. \tag{C.4.2}$$

Here, as indicated, X^μ denotes the directions other than the plane of rotation, X and $\bar{X}$ stand for $X_1 + iX_2$ and its complex conjugate respectively and the momentum vectors $\vec{k}_i$ and the parameters w_i, which are related to the spins of the prongs, must satisfy the following conservation laws and the on-shell conditions demanded by the Virasoro conditions:

$$\begin{aligned} &\vec{k}_1 + \vec{k}_2 + \vec{k}_3 = 0\,, \quad w_1 + w_2 = w_3\,, \\ &(\vec{k}_1)^2 + w_1 w_3 = (\vec{k}_2)^2 + w_2 w_3 = (\vec{k}_3)^2 + (w_3)^2 = 0\,. \end{aligned} \tag{C.4.3}$$

Let us study its local behavior by focusing on the vicinity of the singularity $z = 0$. The expansion around this point reads

$$X = \frac{w_3}{2i}(z-\bar{z})\,, \quad \bar{X} = \frac{w_1}{2i}\left(\frac{1}{z}-\frac{1}{\bar{z}}\right) - \frac{w_2}{2i}(z-\bar{z}) + O(|z|^2)\,. \tag{C.4.4}$$

This should be compared with the well-known two-point spinning string solution of given by

$$X = \frac{w}{2i}(z - \bar{z}) \,, \quad \bar{X} = \frac{w}{2i}\left(\frac{1}{z} - \frac{1}{\bar{z}}\right) \,. \tag{C.4.5}$$

There are two important differences to be noted. First, the Fourier coefficient in front of the structure $(z - \bar{z})$ and the one in front of $(1/z - 1/\bar{z})$ are different in (C.4.4), while they are the same in (C.4.5). Since the log of the ratio of such Fourier coefficients describes the shift of the angle variable, this means that the presence of the other vertex operator generated a shift of the angle variable in the case of the three-pronged solution. This type of phenomenon was observed also in the case of a string in S^3 analyzed in section 7.3. The second feature is that for (C.4.4) there are an infinite number of additional Fourier modes excited in $\bar{X}$ besides $(1/z - 1/\bar{z})$. However, since there are no corresponding modes in X, these additional excitations do not contribute to the action variable, namely the spin, given by

$$S = \frac{i}{4\pi\alpha'} \int_0^{2\pi} d\sigma (X\dot{\bar{X}} - \dot{X}\bar{X}) \,. \tag{C.4.6}$$

This means that the infinite number of action variables corresponding to such additional Fourier modes must vanish. Therefore, the solution above embodies the general feature expected of the solution for the higher-point functions. Namely, such a solution has (possibly infinitely many) dynamical angle variables for which the conjugate action variables are zero, in addition to those associated with the action variables which are finite. This suggests that solutions for higher-point functions in S^3 may be constructed also by introducing infinitely many additional degenerate cuts on the spectral curve.

C.5 Details of the WKB expansion

In this appendix, we explain the details of the WKB expansion for the solutions to the ALP. We will describe two approaches, each of which has its own merit. First in subsection C.5.1, we will perform a direct expansion in the small parameter ζ, which is useful for clarifying the general structure of the expansion. This method, however, turned out to be not quite suitable for deriving the explicit formulas for the expansion of the Wronskians. Therefore, in subsection C.5.2, we take a slightly different approach based on the Born series expansion. This allows us to derive the expressions for the Wronskians up to the $O(\zeta^1)$ terms with relative ease, with the results given in (7.2.35), (7.2.36), (7.2.38) and (7.2.39).

C.5.1 Direct expansion of the solutions to the ALP

In this subsection, we will perform a direct expansion of the ALP in the "diagonal gauge" introduced in section 7.2.2. In this gauge the ALP equations become

$$\left(\partial + \frac{1}{\zeta}\Phi_z^d + A_z^d\right)\hat{\psi}^d = 0\,, \qquad \left(\bar{\partial} + \zeta\Phi_{\bar{z}}^d + A_{\bar{z}}^d\right)\hat{\psi}^d = 0\,. \tag{C.5.1}$$

Denoting the components of $\hat{\psi}^d$ as

$$\hat{\psi}^d \equiv \begin{pmatrix} \psi^{(1)} \\ \psi^{(2)} \end{pmatrix}\,, \tag{C.5.2}$$

and substituting the expressions for Φ_z^d, A_z^d, etc. given in (7.2.33), the ALP equations above take the form

$$\partial\psi^{(1)} + \frac{\sqrt{T}}{2\zeta}\psi^{(1)} - \frac{\rho}{\sqrt{T}}\cot 2\gamma\psi^{(1)} + i\left(\frac{\rho}{\sqrt{T}} - \partial\gamma\right)\psi^{(2)} = 0\,, \tag{C.5.3}$$

$$\partial\psi^{(2)} - \frac{\sqrt{T}}{2\zeta}\psi^{(2)} + \frac{\rho}{\sqrt{T}}\cot 2\gamma\psi^{(2)} - i\left(\frac{\rho}{\sqrt{T}} + \partial\gamma\right)\psi^{(1)} = 0\,, \tag{C.5.4}$$

and

$$\bar{\partial}\psi^{(1)} - \zeta\frac{\sqrt{\bar{T}}\cos 2\gamma}{2}\psi^{(1)} - \frac{\tilde{\rho}}{\sqrt{\bar{T}}\sin 2\gamma}\psi^{(1)} + i\frac{\sqrt{\bar{T}}\sin 2\gamma}{2}\psi^{(2)} = 0\,, \tag{C.5.5}$$

$$\bar{\partial}\psi^{(2)} + \zeta\frac{\sqrt{\bar{T}}\cos 2\gamma}{2}\psi^{(2)} + \frac{\tilde{\rho}}{\sqrt{\bar{T}}\sin 2\gamma}\psi^{(2)} - i\frac{\sqrt{\bar{T}}\sin 2\gamma}{2}\psi^{(1)} = 0\,. \tag{C.5.6}$$

Let us examine the first two equations (C.5.3) and (C.5.4). To perform the WKB expansion, it is useful to introduce a coordinate w defined by

$$dw = \sqrt{T}dz\,. \tag{C.5.7}$$

By this coordinate transformation we can absorb the factor $\sqrt{T}$ and bring the equations to the simplified form

$$\partial_w\psi^{(1)} + \frac{1}{2\zeta}\psi^{(1)} - \frac{\rho}{T}\cot 2\gamma\psi^{(1)} + i\left(\frac{\rho}{T} - \partial_w\gamma\right)\psi^{(2)} = 0\,, \tag{C.5.8}$$

$$\partial_w\psi^{(2)} - \frac{1}{2\zeta}\psi^{(2)} + \frac{\rho}{T}\cot 2\gamma\psi^{(2)} - i\left(\frac{\rho}{T} + \partial_w\gamma\right)\psi^{(1)} = 0\,. \tag{C.5.9}$$

Let us express $\psi^{(2)}$ in terms of $\psi^{(1)}$ using (C.5.8). We get

$$\psi^{(2)} = -i\left(\frac{\rho}{T} - \partial_w\gamma\right)^{-1}\left[\partial_w\psi^{(1)} + \left(\frac{1}{2\zeta} - \frac{\rho}{T}\cos 2\gamma\right)\psi^{(1)}\right]\,. \tag{C.5.10}$$

Substituting (C.5.10) into (C.5.9), we obtain a second order differential equation for $\psi^{(1)}$ of the form

$$\partial_w^2 \psi^{(1)} - \partial_w \ln\left(\frac{\rho}{T} - \partial_w \gamma\right) \partial_w \psi^{(1)} - A\psi^{(1)} = 0\,, \tag{C.5.11}$$

where A is given by

$$\begin{aligned} A = &\left(\frac{1}{2\zeta} - \frac{\rho}{T}\cot 2\gamma\right)^2 + \partial_w\left(\frac{\rho}{T}\cot 2\gamma\right) + \partial_w \ln\left(\frac{\rho}{T} - \partial_w\gamma\right)\left(\frac{1}{2\zeta} - \frac{\rho}{T}\cot 2\gamma\right) \\ &+ (\partial_w\gamma)^2 - \left(\frac{\rho}{T}\right)^2 . \end{aligned} \tag{C.5.12}$$

We now make the WKB expansion of $\psi^{(1)}$ in powers of ζ in the form,

$$\psi^{(1)} = \sqrt{\frac{\rho}{T} - \partial_w\gamma}\, \exp\left[\frac{W_{-1}}{\zeta} + W_0 + \zeta W_1 + \cdots\right], \tag{C.5.13}$$

and substitute it into (C.5.11). Then, at order ζ^{-2}, we get the equation

$$(\partial_w W_{-1})^2 = \frac{1}{4}\,, \tag{C.5.14}$$

with the solutions given by $\partial_w W_{-1} = \pm 1/2$. At the next order, we get the equation

$$\partial_w^2 W_{-1} + 2\partial_w W_{-1}\partial_w W_0 = \frac{1}{2}\partial_w \ln\left(\frac{\rho}{T} - \partial_w\gamma\right) - \frac{\rho}{T}\cot 2\gamma\,. \tag{C.5.15}$$

From this $\partial_w W_0$ is determined as

$$\partial_w W_0 = \pm\left[\frac{1}{2}\partial_w \ln\left(\frac{\rho}{T} - \partial_w\gamma\right) - \frac{\rho}{T}\cot 2\gamma\right], \tag{C.5.16}$$

where the plus sign is for $\partial_w W_{-1} = +1/2$ and the minus sign is for $\partial_w W_{-1} = -1/2$. Similarly, we can determine $\partial_w W_1$ as

$$\begin{aligned} \partial_w W_1 = &\pm\left[(\partial_w\gamma)^2 - \left(\frac{\rho}{T}\right)^2 + \partial_w\left(\frac{\rho}{T}\cot 2\gamma\right) - \frac{1}{2}\partial_w^2 \ln\left(\frac{\rho}{T} - \partial_w\gamma\right)\right] \\ &- \frac{1}{2}\partial_w^2 \ln\left(\frac{\rho}{T} - \partial_w\gamma\right), \end{aligned} \tag{C.5.17}$$

where the choice of the sign should be the same as in (C.5.16). Continuing in this fashion using (C.5.5) and (C.5.6), we can determine $\bar\partial W_{-1}$, $\bar\partial W_0$ and $\bar\partial W_1$ to be

$$\begin{aligned} &\bar\partial W_{-1} = 0\,, \quad \bar\partial W_0 = \pm\left[\frac{1}{2}\bar\partial \ln\left(\frac{\rho}{T} - \partial_w\gamma\right) - \frac{\tilde\rho}{\sqrt{T}\sin 2\gamma}\right], \\ &\bar\partial W_1 = \pm\left[\frac{\eta}{2} - \frac{1}{2}\bar\partial\partial_w \ln\left(\frac{\rho}{T} - \partial_w\gamma\right)\right] - \frac{1}{2}\bar\partial\partial_w \ln\left(\frac{\rho}{T} - \partial_w\gamma\right). \end{aligned} \tag{C.5.18}$$

The results obtained above can be reorganized into a compact form. In fact we can write the expansion (C.5.13) as

$$\psi^{(1)} = \exp\left[W_{\text{odd}} + W_{\text{even}}\right] , \tag{C.5.19}$$

where W_{odd} (resp. W_{even}) denotes terms which (do not) change sign under the sign-flip of $\partial_w W_{-1}$. Then, by substituting (C.5.19) into (C.5.11) and extracting the terms odd under the above flip of sign, we can obtain the following simple equation expressing W_{even} in terms of W_{odd}:

$$W_{\text{even}} = -\frac{1}{2} \ln \partial_w W_{\text{odd}} . \tag{C.5.20}$$

As is clear from the analysis above, the WKB expansion of W_{odd} is given in terms of the integrals of certain functions of the worldsheet variables, such as γ, ρ and $\tilde{\rho}$. On the other hand, the even part W_{even}, which depends only on the derivatives of W_{odd}, is expressed purely in terms of the local values of the worldsheet variables. With such classifications, we can recast the WKB expansion of the two linearly independent solutions of the ALP into the following form:

$$\hat{\psi}^d = \begin{pmatrix} f_\pm^{(1)} \\ f_\pm^{(2)} \end{pmatrix} \exp\left(\pm \int_{z_0}^{z} W_{\text{WKB}}(z, \bar{z}; \zeta) \right) . \tag{C.5.21}$$

Here we renamed W_{odd} to W_{WKB} and the functions $f_\pm^{(1)}$ and $f_\pm^{(2)}$ are defined in terms of W_{WKB}^z by

$$f_\pm^{(1)} \equiv k_{\text{WKB}} = \sqrt{\frac{\rho - \sqrt{T}\partial\gamma}{T\, W_{\text{WKB}}^z}} , \tag{C.5.22}$$

$$f_\pm^{(2)} \equiv \frac{-i}{\sqrt{W_{\text{WKB}}^z}} \left[\pm W_{\text{WKB}}^z + \left(\frac{\sqrt{T}}{2\zeta} - \frac{\rho \cos 2\gamma}{\sqrt{T}} + \frac{\partial \ln k_{\text{WKB}}}{2} \right) \right] . \tag{C.5.23}$$

C.5.2 Born series expansion of the Wronskians

In this subsection, we will derive the explicit form of the expansion for the Wronskians up to $O(\zeta^1)$ using the Born series method, which turned out to be more convenient compared to the direct expansion described above. In particular, with this method it is much easier to take into account the normalization conditions of the eigenvectors $i_\pm$ given in (7.1.81). Although the method has been described in Appendix B of [111], we will spell out the details of the derivation since several additional considerations are necessary in our case.

To illustrate the basic idea, let us take the Wronskian $\langle 2_+ , 1_+ \rangle$ as an example and discuss its expansion. To compute $\langle 2_+ , 1_+ \rangle$, we need to parallel-transport the eigenvector 1_+, which

is defined originally in the neighborhood of z_1, to the neighborhood of z_2 using the flat connection and compute the Wronskian with 2_+. In the diagonal gauge, this procedure can be implemented in the following way:

$$\langle \hat{2}^d_+ \, , \hat{1}^d_+ \rangle = \langle \hat{2}^d_+(z_2^*) \, , \mathrm{P} \exp \left[- \int_0^1 dt \left(\frac{1}{\zeta} H_0(t) + V(t) \right) \right] \hat{1}^d_+(z_1^*) \rangle \, . \tag{C.5.24}$$

In this expression t parametrizes the curve joining z_1^* (at $t = 0$) and z_2^* (at $t = 1$) and H_0 and V are defined in terms of the connection in the diagonal gauge, given in (7.2.33), as

$$H_0(t) \equiv \tilde{\Phi}_z \dot{z} \, , \quad V(t) \equiv \tilde{A}_z \dot{z} + \tilde{A}_{\bar{z}} \dot{\bar{z}} + \zeta \tilde{\Phi}_{\bar{z}} \dot{\bar{z}} \, , \tag{C.5.25}$$

with $\dot{z}$ and $\dot{\bar{z}}$ standing for dz/dt and $d\bar{z}/dt$ respectively. The equation (C.5.24) is similar in form to the transition amplitude in quantum mechanics, where $H_0(t)/\zeta$ is the unperturbed Hamiltonian and $V(t)$ is the time-dependent perturbation. Therefore we can derive the expansion of (C.5.24) by applying the familiar Born series expansion.

As the first step toward this goal, let us determine the expansion of the "initial states", $\hat{1}^d_+(z_1^*)$ and $\hat{2}^d_+(z_2^*)$. As explained in section 7.1.7, the eigenvectors can be well-approximated near the puncture by those of the corresponding two-point functions. Thus, the expansion of the initial states can be obtained from the explicit form of $\hat{i}^{\mathrm{2pt}}_\pm$ given in (7.1.83) and (7.1.84) as

$$\hat{1}^d_+(z_1^*) \sim \hat{1}^{\mathrm{2pt},d}_+ = \begin{pmatrix} O(\zeta^1) \\ 1 + O(\zeta^2) \end{pmatrix} , \qquad \hat{2}^d_+(z_2^*) \sim \hat{2}^{\mathrm{2pt},d}_+ = \begin{pmatrix} 1 + O(\zeta^2) \\ O(\zeta^1) \end{pmatrix} . \tag{C.5.26}$$

Let us now study the leading terms (*i.e.* the $O(V^0)$ terms) in the Born series expansion of (C.5.24). They can be expressed as

$$1^{(2)}_+(z_1^*) 2^{(1)}_+(z_2^*) \langle \mathbf{e}_2 | e^{-\int_0^1 H_0 dt/\zeta} | \mathbf{e}_2 \rangle - 1^{(1)}_+(z_1^*) 2^{(2)}_+(z_2^*) \langle \mathbf{e}_1 | e^{-\int_0^1 H_0 dt/\zeta} | \mathbf{e}_1 \rangle \, , \tag{C.5.27}$$

where $|\mathbf{e}_1\rangle$ and $|\mathbf{e}_2\rangle$ stand for the unit vectors

$$|\mathbf{e}_1\rangle = \begin{pmatrix} 1 \\ 0 \end{pmatrix} , \quad |\mathbf{e}_2\rangle = \begin{pmatrix} 0 \\ 1 \end{pmatrix} , \tag{C.5.28}$$

and $i^{(1)}_\pm$ and $i^{(2)}_\pm$ are the upper and the lower component of $\hat{i}^d_\pm$ respectively, which can be expressed as

$$\hat{i}^d_\pm = i^{(1)}_\pm |\mathbf{e}_1\rangle + i^{(2)}_\pm |\mathbf{e}_2\rangle \, . \tag{C.5.29}$$

Using (C.5.26), we can evaluate the expression (C.5.27) explicitly as

$$\big(1 + O(\zeta^2)\big) \exp \left(\int_{\ell_{12}} \frac{1}{\zeta} \varpi \right) - O(\zeta^2) \exp \left(- \int_{\ell_{12}} \frac{1}{\zeta} \varpi \right) , \tag{C.5.30}$$

where ℓ_{12} is the contour that connects z_1^* and z_2^*, defined in section 7.2.1. Note that the second term in (C.5.30), which has an overall $O(\zeta^2)$ factor can be safely neglected only when Re $\left(\int_{\ell_{12}} \varpi/\zeta\right)$ is positive so that the exponential exp $\left(-\int_{\ell_{12}} \varpi/\zeta\right)$ becomes vanishingly small. The positivity of Re $\left(\int_{\ell_{12}} \varpi/\zeta\right)$ is guaranteed when the following two conditions are satisfied:

1. The eigenvectors, 1_+ and 2_+, are small solutions.

2. z_1 and z_2 are connected by a *WKB curve* $z(s)$ defined to be satisfying the condition

$$\text{Im}\left(\sqrt{T}\frac{dz}{ds}\right) = 0\,, \tag{C.5.31}$$

   where s parameterizes the curves.

This can be deduced in the following way: First, from the definition (C.5.31), one can show that the real part of the integral $\int \varpi/\zeta$ monotonically increases or decreases along the WKB curve. Second, when 1_+ and 2_+ are both small solutions, Re $\left(\int \varpi/\zeta\right)$ increases as we *move away from* z_1 in the vicinity of z_1 while it increases as we *approach* z_2 in the vicinity of z_2. From these two observations, one can conclude that Re $\left(\int_{\ell_{12}} \varpi/\zeta\right)$ is positive when both of the eigenvectors are small and the punctures are connected by a WKB curve. Actually, in practice the second condition above is inessential. This is because all the punctures are always connected with each other by WKB curves, except at discrete values of Arg (ζ), due to the triangular inequalities, $\Delta_i < \Delta_j + \Delta_k$ (or equivalently $\kappa_i < \kappa_j + \kappa_k$), which hold in all the cases we study in the main text.

Let us now move on to the study of the $O(V^1)$ contributions. When 1_+ and 2_+ are small solutions, the $O(V^1)$ terms in the Born series expansion are given by

$$\begin{aligned}
&- 1_+^{(2)}(z_1^*)2_+^{(1)}(z_2^*)\int_0^1 dt_1 \langle \mathbf{e}_2| e^{-\int_{t_1}^1 H_0 dt/\zeta} V(t_1) e^{-\int_0^{t_1} H_0 dt/\zeta} |\mathbf{e}_2\rangle \\
&- 1_+^{(1)}(z_1^*)2_+^{(1)}(z_2^*)\int_0^1 dt_1 \langle \mathbf{e}_2| e^{-\int_{t_1}^1 H_0 dt/\zeta} V(t_1) e^{-\int_0^{t_1} H_0 dt/\zeta} |\mathbf{e}_1\rangle \\
&+ 1_+^{(2)}(z_1^*)2_+^{(2)}(z_2^*)\int_0^1 dt_1 \langle \mathbf{e}_1| e^{-\int_{t_1}^1 H_0 dt/\zeta} V(t_1) e^{-\int_0^{t_1} H_0 dt/\zeta} |\mathbf{e}_2\rangle\,.
\end{aligned} \tag{C.5.32}$$

Note that we have omitted the terms of the form, $\langle \mathbf{e}_1| * |\mathbf{e}_1\rangle$, since they are proportional to the factor exp $\left(\int_{\ell_{12}} \varpi/\zeta\right)$, which, as discussed above, is exponentially small when 1_+ and 2_+ are small solutions. Since $|\mathbf{e}_1\rangle$ and $|\mathbf{e}_2\rangle$ are the eigenvectors of H_0, we can evaluate (C.5.32)

as

$$
\begin{aligned}
&- 1^{(2)}_{+}(z^*_1)2^{(1)}_{+}(z^*_2)e^{\int_{\ell_{12}}\varpi/(2\zeta)}\int_0^1 dt_1\langle \mathbf{e}_2|V(t_1)|\mathbf{e}_2\rangle \\
&- 1^{(1)}_{+}(z^*_1)2^{(1)}_{+}(z^*_2)e^{\int_{\ell_{12}}\varpi/(2\zeta)}\int_0^1 dt_1\langle \mathbf{e}_2|V(t_1)|\mathbf{e}_1\rangle e^{-\int_0^{t_1}\varpi/\zeta} \\
&+ 1^{(2)}_{+}(z^*_1)2^{(2)}_{+}(z^*_2)e^{\int_{\ell_{12}}\varpi/(2\zeta)}\int_0^1 dt_1\langle \mathbf{e}_1|V(t_1)|\mathbf{e}_2\rangle e^{-\int_{t_1}^1\varpi/\zeta}\,.
\end{aligned}
\tag{C.5.33}
$$

In the limit $\zeta\to 0$, the integral over t_1 in the second term will be exponentially suppressed by the factor $\exp\left(-2\int_0^{t_1}\varpi/\zeta\right)$, except when the interval is short, *i.e.* $0<t_1<O(\zeta^1)$. Thus, to $O(\zeta^1)$, one can take ϖ in $\int_0^{t_1}\varpi/\zeta$ to be constant and replace $V(t_1)$ with $V(0)$. We can thus approximate the second term in (C.5.33) as

$$
-\zeta\, 1^{(1)}_{+}(z^*_1)2^{(1)}_{+}(z^*_2)e^{\int_{\ell_{12}}\varpi/(2\zeta)}\langle \mathbf{e}_2|V(0)|\mathbf{e}_1\rangle\left(\sqrt{T(z^*_1)}\,\dot z(t=0)\right)^{-1}\,. \tag{C.5.34}
$$

Since the factor $1^{(1)}_{+}(z^*_1)$ is of $O(\zeta^1)$, (C.5.34) as a whole is of $O(\zeta^2)$ and thus can be neglected to the order of our approximation. Similarly, one can also show that the third term of (C.5.33) is of $O(\zeta^2)$. Thus, up to $O(\zeta^1)$, the contribution comes only from the first term proportional to

$$
-e^{\int_{\ell_{12}}\varpi/(2\zeta)}\int_0^1 dt_1\langle \mathbf{e}_2|V(t_1)|\mathbf{e}_2\rangle\,. \tag{C.5.35}
$$

Lastly let us examine the $O(V^2)$ terms. The only term which contributes at $O(\zeta^1)$ is

$$
1^{(2)}_{+}(z^*_1)2^{(1)}_{+}(z^*_2)\int_0^1 dt_2\int_0^{t_2} dt_1\langle \mathbf{e}_2|e^{-\int_{t_2}^1 H_0 dt/\zeta}V(t_2)e^{-\int_{t_1}^{t_2}H_0dt/\zeta}V(t_1)e^{-\int_0^{t_1}H_0dt/\zeta}|\mathbf{e}_2\rangle\,. \tag{C.5.36}
$$

Inserting the identity $1=|\mathbf{e}_1\rangle\langle\mathbf{e}_1|+|\mathbf{e}_2\rangle\langle\mathbf{e}_2|$, this quantity can be computed as

$$
\begin{aligned}
1^{(2)}_{+}(z^*_1)2^{(1)}_{+}(z^*_2)e^{\int_{\ell_{12}}\varpi/(2\zeta)}&\left(\frac{1}{2}\left[\int_0^1 dt_1\langle \mathbf{e}_2|V(t_1)|\mathbf{e}_2\rangle\right]^2\right. \\
&\left.+\int_0^1 dt_1\int_0^{t_1}dt_2 e^{-\int_{t_2}^{t_1}\varpi/\zeta}\langle \mathbf{e}_2|V(t_1)|\mathbf{e}_1\rangle\langle\mathbf{e}_1|V(t_2)|\mathbf{e}_2\rangle\right)\,.
\end{aligned}
\tag{C.5.37}
$$

As in the discussion of the $O(V^1)$ terms, we can take ϖ in $\int_{t_2}^{t_1}\varpi/\zeta$ to be constant and replace $V(t_2)$ with $V(t_1)$ in the second term of (C.5.37), thanks to the suppression factor $\exp\left(-\int_{t_1}^{t_2}\varpi/\zeta\right)$. Then (C.5.37) can be evaluated as

$$
e^{\int_{\ell_{12}}\varpi/(2\zeta)}\left(\frac{1}{2}\left[\int_0^1 dt_1\langle \mathbf{e}_2|V(t_1)|\mathbf{e}_2\rangle\right]^2+\zeta\int_0^1 dt_1\frac{\langle \mathbf{e}_2|V(t_1)|\mathbf{e}_1\rangle\langle\mathbf{e}_1|V(t_1)|\mathbf{e}_2\rangle}{\dot z\sqrt{T}}\right)\,. \tag{C.5.38}
$$

Putting together the expressions (C.5.30), (C.5.35) and (C.5.38), we find that the result can be grouped into an exponential in the following way:

$$\langle 2_+\,,1_+\rangle \sim \exp\left(\frac{1}{2\zeta}\int_{\ell_{12}}\varpi - \int_0^1 dt\langle \mathbf{e}_2|V(t)|\mathbf{e}_2\rangle + \zeta\int_0^1 dt_1 \frac{\langle \mathbf{e}_2|V(t)|\mathbf{e}_1\rangle\langle \mathbf{e}_1|V(t)|\mathbf{e}_2\rangle}{\dot{z}\sqrt{T}}\right). \tag{C.5.39}$$

Thus we have obtained the expansion of $\langle 2_+\,,1_+\rangle$ to be given by

$$\langle 2_+\,,1_+\rangle = \exp\left(-\frac{1}{2\zeta}\int_{\ell_{21}}\varpi - \int_{\ell_{21}}\alpha - \frac{\zeta}{2}\int_{\ell_{21}}\eta + O(\zeta^2)\right), \tag{C.5.40}$$

where the one-form α is given by

$$\alpha = -\frac{\rho}{\sqrt{T}}\cot 2\gamma dz - \frac{\tilde{\rho}}{\sqrt{\bar{T}}\sin 2\gamma}d\bar{z}\,. \tag{C.5.41}$$

The expansion of other Wronskians can be worked out in a similar manner leading to (7.2.35) and (7.2.36). Furthermore, we can apply the same argument to the expansion around $\zeta = \infty$ and obtain (7.2.38) and (7.2.39), where the one-form $\tilde{\alpha}$ appearing in the $O(\zeta^0)$ term is given by

$$\tilde{\alpha} = -\frac{\rho}{\sqrt{T}\sin 2\gamma}dz - \frac{\tilde{\rho}}{\sqrt{\bar{T}}}\cot 2\gamma d\bar{z}\,. \tag{C.5.42}$$

C.6 Shift of the angle variables under the global transformation

In this section, we will derive the formula which computes the shift of the angle variables under the global transformation (7.3.5) and (7.3.6).

Let $\psi_\pm^{\rm ref}(x;\tau,\sigma)$ be the eigenvectors of the auxiliary linear problem for the reference solution $\mathbb{Y}^{\rm ref}$. The normalized Baker-Akhiezer vector $h^{\rm ref}(x;\tau)$ is proportional to $\psi_+^{\rm ref}(x;\tau,\sigma=0)$ and satisfies the condition

$$n\cdot h^{\rm ref}(x;\tau) = n_1 h_1^{\rm ref} + n_2 h_2^{\rm ref} = 1\,, \tag{C.6.1}$$

$$n = \begin{pmatrix} n_1 \\ n_2 \end{pmatrix}, \quad h^{\rm ref} = \begin{pmatrix} h_1^{\rm ref} \\ h_2^{\rm ref} \end{pmatrix}. \tag{C.6.2}$$

Now, under the global transformation $\mathbb{Y}\to\mathbb{Y}V$, $h^{\rm ref}$ gets transformed into $V^{-1}h^{\rm ref}$. However, in order to retain the normalization condition (C.6.2), we must rescale it appropriately. This gives

$$h'(x;\tau) = \frac{1}{f(x;\tau)}V^{-1}h^{\rm ref}(x;\tau)\,, \tag{C.6.3}$$

where the rescaling factor f is given by

$$f(x;\tau) = n \cdot \left(V^{-1} h^{\mathrm{ref}}(x;\tau)\right) . \tag{C.6.4}$$

Hereafter, we shall suppress the τ-dependence as our focus will be on the behavior of functions and differentials on the spectral curve parametrized by x.

Let the positions of the poles of h^{ref} and h' on the spectral curve be $\{\gamma_1, \gamma_2, \ldots, \gamma_{g+1}\}$ and $\{\gamma'_1, \gamma'_2, \ldots, \gamma'_{g+1}\}$ respectively[3]. Then, division by f must remove the poles $\{\gamma_1, \gamma_2, \ldots, \gamma_{g+1}\}$ while creating the new poles $\{\gamma'_1, \gamma'_2, \ldots, \gamma'_{g+1}\}$. In other words, the divisor of f is given by

$$(f) = \sum_{i=1}^{g+1} (\gamma'_i - \gamma_i) . \tag{C.6.5}$$

A natural meromorphic differential which encodes this information is

$$\varpi = d(\log f) = \frac{df}{f} . \tag{C.6.6}$$

From (C.6.5) ϖ must have poles at γ'_i and γ_i with residues 1 and -1 respectively. Besides, ϖ may have a holomorphic part, which can be written as a linear combination of the basic holomorphic differentials ω_i for $i = 1 \sim g$. They are assumed to be normalized in the usual way, namely $\int_{a_i} \omega_j = \delta_{ij}$, $\int_{b_i} \omega_j = \Pi_{ij}$, where Π_{ij} is the period matrix. To express this structure, let us introduce the basic abelian differential of the third kind ω_{PQ} characterized by the properties

$$\oint_P \omega_{PQ} = 1 , \quad \oint_Q \omega_{PQ} = -1 , \quad \oint_{a_i} \omega_{PQ} = 0 . \tag{C.6.7}$$

Then, ϖ can be written as

$$\varpi = \sum_{i=1}^{g+1} \omega_{\gamma'_i \gamma_i} + \sum_{j=1}^{g} c_j \omega_j . \tag{C.6.8}$$

The expansion coefficients c_j are determined by the integrals of ϖ over the a_j-cycles. As ϖ is a differential of a logarithmic function, the possible contribution must be of the form

$$\int_{a_j} \varpi = 2\pi i m_j , \qquad m_j \in \mathbb{Z} . \tag{C.6.9}$$

This gives $c_j = 2\pi i m_j$. Next, consider the integrals of ϖ over the b_k-cycles. Again the possible structure is

$$\int_{b_k} \varpi = 2\pi i n_k , \qquad n_k \in \mathbb{Z} . \tag{C.6.10}$$

[3] As the number of poles in the normalized eigenfunction is dictated by the Riemann-Hurwitz theorem, it does not change under the global transformation. See [41] for details.

From (C.6.8) we then get

$$\sum_{i=1}^{g+1}\int_{b_k}\omega_{\gamma_i'\gamma_i}=2\pi i n_k-2\pi i\sum_{j=1}^{g}m_j\Pi_{jk}\,. \tag{C.6.11}$$

Now by using a variant of the Riemann bilinear identity[4], one can rewrite

$$\int_{b_k}\omega_{\gamma_i'\gamma_i}=2\pi i\int_{\gamma_i}^{\gamma_i'}\omega_k\,. \tag{C.6.12}$$

Thus, (C.6.11) becomes

$$\sum_{i=1}^{g+1}\int_{\gamma_i}^{\gamma_i'}\omega_k=n_k-\sum_{j=1}^{g}m_j\Pi_{jk}\,. \tag{C.6.13}$$

Now note that n_k and m_j are integers which take discrete values. On the other hand, the LHS clearly vanishes continuously in the limit $\gamma_i\to\gamma_i'$. Hence, we should set $n_k=m_j=0$ and conclude

$$\sum_{i=1}^{g+1}\int_{\gamma_i}^{\gamma_i'}\omega_k=0\,,\qquad k=1\sim g\,. \tag{C.6.14}$$

What this means is that the angle variables conjugate to the filling fractions $S_k, k=1\sim g$ do not change under the global transformation.

Therefore, the only angle variable left to be examined is the one associated with the differential $\omega_\infty\equiv\frac{1}{2\pi i}\omega_{\infty^+\infty^-}$, namely the one conjugate to the charge R. We will denote it by ϕ_R. This can be studied by considering the integral over the contour b_∞ running from ∞^- to ∞^+. Repeating essentially the same argument made for b_k, except for the evaluation of $\int_{b_\infty}\varpi$, we readily obtain

$$\int_{b_\infty}\varpi=\log\left(\frac{f(\infty^+)}{f(\infty^-)}\right)=2\pi i\sum_{i=1}^{g+1}\int_{\gamma_i}^{\gamma_i'}\omega_\infty\,, \tag{C.6.15}$$

where we used an identity similar to (C.6.12), namely[5] $\int_{b_\infty}\omega_{\gamma_i'\gamma_i}=2\pi i\int_{\gamma_i}^{\gamma_i'}\omega_\infty$. Since the RHS of (C.6.15) expresses the shift $\Delta\phi_R$ multiplied by i (see (7.1.58)), we have an important formula

$$\Delta\phi_\infty=-i\log\left(\frac{f(\infty^+)}{f(\infty^-)}\right)\,. \tag{C.6.16}$$

[4]See Corollary 2.42 of [41].

[5]See Proposition 2.43 of [41].

This can be recognized as the generalization of the formula given in Proposition 8.13 of [41], which was derived for the $U(1)_R$ part of the global transformation. Our master formula above is valid for an arbitrary global symmetry transformation.

Now by expressing h^{ref} as

$$h^{\text{ref}} = \frac{1}{n \cdot \psi_+^{\text{ref}}} \psi_+^{\text{ref}} \,, \tag{C.6.17}$$

and using the relation $\psi_+ = V^{-1}\psi^{\text{ref}}$, it is straightforward to see that the equation (C.6.16) is indeed the same as (7.3.5). By performing a similar analysis for the left sector, we can also obtain (7.3.6).

Bibliography

[1] J.M. Maldacena, "The large-N limit of superconformal field theories and supergravity", Adv. Theor. Math. Phys. **2** (1998) 231, [arXiv:hep-th/9711200].

[2] S.S. Gubser, I.R. Klebanov and A.M. Polyakov, "Gauge theory correlators from non-critical string theory", Phys. Lett. **B 428** (1998) 105, [arXiv:hep-th/9802109].

[3] E. Witten, "Anti-de Sitter space and holography", Adv. Theor. Math. Phys. **2** (1998) 253, [arXiv:hep-th/9802150].

[4] L. Susskind, "The World as a hologram," J. Math. Phys. **36**, 6377 (1995) [hep-th/9409089].

[5] G. 't Hooft, "Dimensional reduction in quantum gravity," [gr-qc/9310026].

[6] R. Gopakumar and C. Vafa, "On the gauge theory / geometry correspondence," Adv. Theor. Math. Phys. **3**, 1415 (1999) [hep-th/9811131].

[7] H. Ooguri and C. Vafa, "World sheet derivation of a large N duality," Nucl. Phys. B **641**, 3 (2002) [hep-th/0205297].

[8] R. Gopakumar, "What is the simplest gauge-string duality?" [arXiv:1104.2386].

[9] R. Gopakumar and R. Pius, "Correlators in the simplest gauge-string duality", JHEP **1303**, 175 (2013) [arXiv:1212.1236]

[10] J. McGreevy and H. Verlinde, "Strings from tachyons: the c = 1 matrix reloaded," JHEP **0312**, 054 (2003) [hep-th/0304224].

[11] D. Gaiotto and L. Rastelli, "A Paradigm of open / closed duality: Liouville D-branes and the Kontsevich model," JHEP **0507**, 053 (2005) [hep-th/0312196].

[12] D. Gaiotto, N. Itzhaki and L. Rastelli, "Closed strings as imaginary D-branes," Nucl. Phys. B **688**, 70 (2004) [hep-th/0304192].

[13] M. B. Green and J. Polchinski, "Summing over world sheet boundaries," Phys. Lett. B **335**, 377 (1994) [hep-th/9406012].

[14] M. Kruczenski, "Summing planar diagrams," JHEP **0810**, 075 (2008) [hep-th/0703218].

[15] Y. Kazama, S. Komatsu and T. Nishimura, "A new integral representation for the scalar products of Bethe states for the XXX spin chain," JHEP **1309**, 013 (2013) [arXiv:1304.5011].

[16] Y. Kazama and S. Komatsu, "On holographic three point functions for GKP strings from integrability," JHEP **1201**, 110 (2012) [arXiv:1110.3949].

[17] Y. Kazama and S. Komatsu, "Wave functions and correlation functions for GKP strings from integrability", [arXiv:1205.6060]

[18] Y. Kazama and S. Komatsu, "Three-point functions in the SU(2) sector at strong coupling", [arXiv:1312.3727], to appear.

[19] H. Goldstein, "Classical mechanics. Vol. 4. Pearson Education India, 1962.

[20] J. D. Brown and M. Henneaux, "Central Charges in the Canonical Realization of Asymptotic Symmetries: An Example from Three-Dimensional Gravity," Commun. Math. Phys. **104**, 207 (1986).

[21] A. Strominger, "Black hole entropy from near horizon microstates," JHEP **9802**, 009 (1998) [hep-th/9712251].

[22] M. Guica, T. Hartman, W. Song and A. Strominger, "The Kerr/CFT Correspondence," Phys. Rev. D **80**, 124008 (2009) [arXiv:0809.4266].

[23] A. Sen, "Black hole entropy function and the attractor mechanism in higher derivative gravity," JHEP **0509**, 038 (2005) [hep-th/0506177].

[24] A. Dabholkar, J. Gomes and S. Murthy, "Quantum black holes, localization and the topological string," JHEP **1106**, 019 (2011) [arXiv:1012.0265].

[25] N. Seiberg, "Supersymmetry and Nonperturbative beta Functions," Phys. Lett. B **206**, 75 (1988).

[26] S. Mandelstam, "Light Cone Superspace and the Ultraviolet Finiteness of the N=4 Model," Nucl. Phys. B **213**, 149 (1983).

[27] J. A. Minahan and K. Zarembo, "The Bethe ansatz for $\mathcal{N} = 4$ super Yang-Mills," JHEP **0303**, 013 (2003) [hep-th/0212208].

[28] N. Y. Reshetikhin, "A Method Of Functional Equations In The Theory Of Exactly Solvable Quantum Systems," Lett. Math. Phys. **7**, 205 (1983).

[29] N. Y. Reshetikhin, "O(n) Invariant Quantum Field Theoretical Models: Exact Solution," Nucl. Phys. B **251**, 565 (1985).

[30] N. Beisert, G. Ferretti, R. Heise and K. Zarembo, "One-loop QCD spin chain and its spectrum," Nucl. Phys. B **717**, 137 (2005) [hep-th/0412029].

[31] J. A. Minahan, "The SU(2) sector in AdS/CFT," Fortsch. Phys. **53**, 828 (2005) [hep-th/0503143].

[32] N. Gromov and P. Vieira, "Quantum Integrability for Three-Point Functions," [arXiv:1202.4103].

[33] N. Gromov, P. Vieira, "Tailoring Three-Point Functions and Integrability IV. Theta-morphism," [arXiv:1205.5288].

[34] V E Korepin, N M Bogoliubov and A G Izergin, "Quantum inverse scattering method and correlation functions," Cambridge University Press (1993)

[35] I. Bena, J. Polchinski and R. Roiban, "Hidden symmetries of the $AdS_5 \times S^5$ superstring," Phys. Rev. D **69**, 046002 (2004), [hep-th/0305116].

[36] N. Beisert, V. A. Kazakov, K. Sakai and K. Zarembo,"The Algebraic curve of classical superstrings on $AdS_5 \times S^5$," Commun. Math. Phys. **263**, 659 (2006),[hep-th/0502226].

[37] N. Gromov and P. Vieira, "The $AdS_5 \times S^5$ superstring quantum spectrum from the algebraic curve," Nucl. Phys. B **789**, 175 (2008) [hep-th/0703191].

[38] R. R. Metsaev and A. A. Tseytlin, "Type IIB superstring action in AdS(5) x S**5 background," Nucl. Phys. B **533**, 109 (1998) [hep-th/9805028].

[39] R. Janik, P. Surowka and A. Wereszczynski, "On correlation functions of operators dual to classical spinning string states", JHEP **05** (2010) 030, [arXiv:1002.4613].

[40] V. A. Kazakov, A. Marshakov, J. A. Minahan and K. Zarembo, "Classical/quantum integrability in AdS/CFT," JHEP **0405**, 024 (2004), [hep-th/0402207].

[41] B. Vicedo, "The method of finite-gap integration in classical and semi-classical string theory," J. Phys. A A **44**, 124002 (2011).

[42] N. Dorey and B. Vicedo,"On the dynamics of finite-gap solutions in classical string theory," JHEP **0607**, 014 (2006) [hep-th/0601194].

[43] N. Dorey and B. Vicedo, "A Symplectic Structure for String Theory on Integrable Backgrounds," JHEP **0703**, 045 (2007) [hep-th/0606287].

[44] S. Frolov and A. A. Tseytlin, "Rotating string solutions: AdS / CFT duality in non-supersymmetric sectors," Phys. Lett. B **570**, 96 (2003) [hep-th/0306143].

[45] V. A. Kazakov and K. Zarembo, "Classical / quantum integrability in non-compact sector of AdS/CFT," JHEP **0410**, 060 (2004) [hep-th/0410105].

[46] M. Kruczenski, "Spin chains and string theory," Phys. Rev. Lett. **93**, 161602 (2004) [hep-th/0311203].

[47] N. Beisert *et al.*, "Review of AdS/CFT Integrability: An Overview," [arXiv:1012.3982].

[48] N. Beisert, "The complete one loop dilatation operator of $\mathcal{N} = 4$ super Yang-Mills theory," Nucl. Phys. B **676**, 3 (2004) [hep-th/0307015].

[49] D. Serban and M. Staudacher, "Planar $\mathcal{N} = 4$ gauge theory and the Inozemtsev long range spin chain," JHEP **0406**, 001 (2004) [hep-th/0401057].

[50] V. I. Inozemtsev, "Integrable Heisenberg-van Vleck chains with variable range exchange," Phys. Part. Nucl. **34**, 166 (2003) [Fiz. Elem. Chast. Atom. Yadra **34**, 332 (2003)] [hep-th/0201001].

[51] N. Beisert, V. Dippel and M. Staudacher, "A Novel long range spin chain and planar N=4 super Yang-Mills," JHEP **0407**, 075 (2004) [hep-th/0405001].

[52] N. Beisert and M. Staudacher, "Long-range psu(2,2|4) Bethe Ansatze for gauge theory and strings," Nucl. Phys. B **727**, 1 (2005) [hep-th/0504190].

[53] N. Beisert, "The SU(2|2) dynamic S-matrix," Adv. Theor. Math. Phys. **12**, 945 (2008) [hep-th/0511082].

[54] R. A. Janik, "The $AdS_5 \times S^5$ superstring worldsheet S-matrix and crossing symmetry," Phys. Rev. D **73**, 086006 (2006) [hep-th/0603038].

[55] N. Beisert, R. Hernandez and E. Lopez, "A Crossing-symmetric phase for $AdS_5 \times S^5$ strings," JHEP **0611**, 070 (2006) [hep-th/0609044].

[56] N. Beisert, B. Eden and M. Staudacher, "Transcendentality and Crossing," J. Stat. Mech. **0701**, P01021 (2007) [hep-th/0610251].

[57] M. Luscher, "Volume Dependence of the Energy Spectrum in Massive Quantum Field Theories. 1. Stable Particle States," Commun. Math. Phys. **104**, 177 (1986).

[58] M. Luscher, "Volume Dependence of the Energy Spectrum in Massive Quantum Field Theories. 2. Scattering States," Commun. Math. Phys. **105**, 153 (1986).

[59] R. A. Janik and T. Lukowski, "Wrapping interactions at strong coupling: The Giant magnon," Phys. Rev. D **76**, 126008 (2007) [arXiv:0708.2208].

[60] C. -N. Yang and C. P. Yang, "Thermodynamics of one-dimensional system of bosons with repulsive delta function interaction," J. Math. Phys. **10**, 1115 (1969).

[61] A. B. Zamolodchikov, "Thermodynamic Bethe Ansatz in Relativistic Models. Scaling Three State Potts and Lee-yang Models," Nucl. Phys. B **342**, 695 (1990).

[62] G. Arutyunov and S. Frolov, "String hypothesis for the $AdS_5 \times S^5$ mirror", JHEP **03** (2009) 152 [arXiv:0901.1417].

[63] G. Arutyunov and S. Frolov, "Thermodynamic Bethe Ansatz for the $AdS_5 \times S^5$ Mirror Model", JHEP **05** (2009) 068 [arXiv:0903.0141].

[64] N. Gromov, V. Kazakov and P. Vieira, "Exact Spectrum of Anomalous Dimensions of Planar $N = 4$ Supersymmetric Yang-Mills Theory", Phys. Rev. Lett. **103** (2009) 131601 [arXiv:0901.3753].

[65] N. Gromov, V. Kazakov, A. Kozak and P. Vieira, "Exact Spectrum of Anomalous Dimensions of Planar N = 4 Supersymmetric Yang-Mills Theory: TBA and excited states", Lett. Math. Phys. **91** (2010) 265 [arXiv:0902.4458].

[66] D. Bombardelli, D. Fioravanti and R. Tateo, "Thermodynamic Bethe Ansatz for planar AdS/CFT: a proposal", J. Phys. A 42 (2009) 375401 [arXiv:0902.3930].

[67] B. Eden, P. Heslop, G. P. Korchemsky, V. A. Smirnov and E. Sokatchev, "Five-loop Konishi in N=4 SYM," Nucl. Phys. B **862**, 123 (2012) [arXiv:1202.5733].

[68] N. Drukker, "Integrable Wilson loops," JHEP **1310**, 135 (2013) [arXiv:1203.1617].

[69] D. Correa, J. Maldacena and A. Sever, "The quark anti-quark potential and the cusp anomalous dimension from a TBA equation," JHEP **1208**, 134 (2012) [arXiv:1203.1913].

[70] N. Gromov, V. Kazakov, S. Leurent and D. Volin, "Quantum spectral curve for AdS_5/CFT_4," [arXiv:1305.1939].

[71] D. E. Berenstein, J. M. Maldacena and H. S. Nastase, "Strings in flat space and pp waves from N=4 superYang-Mills," JHEP **0204**, 013 (2002) [hep-th/0202021].

[72] S. Lee, S. Minwalla, M. Rangamani and N. Seiberg, "Three point functions of chiral operators in D = 4, N=4 SYM at large N," Adv. Theor. Math. Phys. **2**, 697 (1998) [hep-th/9806074].

[73] M. Baggio, J. de Boer and K. Papadodimas, "A non-renormalization theorem for chiral primary 3-point functions," JHEP **1207**, 137 (2012) [arXiv:1203.1036].

[74] K. A. Intriligator and W. Skiba, "Bonus symmetry and the operator product expansion of N=4 SuperYang-Mills," Nucl. Phys. B **559**, 165 (1999) [hep-th/9905020].

[75] P. S. Howe and P. C. West, "Superconformal invariants and extended supersymmetry," Phys. Lett. B **400**, 307 (1997) [hep-th/9611075].

[76] P. J. Heslop and P. S. Howe, "OPEs and three-point correlators of protected operators in N=4 SYM," Nucl. Phys. B **626**, 265 (2002) [hep-th/0107212].

[77] R. Roiban and A. Volovich, "Yang-Mills correlation functions from integrable spin chains," JHEP **0409**, 032 (2004), [hep-th/0407140].

[78] K. Okuyama and L. S. Tseng, "Three-point functions in N = 4 SYM theory at one-loop," JHEP **0408**, 055 (2004), [hep-th/0404190].

[79] L. F. Alday, J. R. David, E. Gava and K. S. Narain, "Structure constants of planar N = 4 Yang Mills at one loop," JHEP **0509**, 070 (2005), [hep-th/0502186].

[80] J. Escobedo, N. Gromov, A. Sever and P. Vieira, "Tailoring Three-Point Functions and Integrability," JHEP **1109**, 028 (2011), [arXiv:1012.2475].

[81] E. D'Hoker, D. Z. Freedman, S. D. Mathur, A. Matusis and L. Rastelli, "Extremal correlators in the AdS / CFT correspondence," In *Shifman, M.A. (ed.): The many faces of the superworld* 332-360 [hep-th/9908160].

[82] H. Liu and A. A. Tseytlin, "Dilaton - fixed scalar correlators and AdS(5) x S**5 - SYM correspondence," JHEP **9910**, 003 (1999) [hep-th/9906151].

[83] G. Vidal, J. I. Latorre, E. Rico and A. Kitaev, "Entanglement in quantum critical phenomena", Phys. Rev. Lett. **90**, 227902 (2003) [quant-ph/0211074].

[84] P. Calabrese and J. Cardy, "Entanglement entropy and quantum field theory," J. Stat. Mech. **0406**, P002 (2004) [hep-th/0405152].

[85] A. Kitaev and J. Preskill, "Topological entanglement entropy," Phys. Rev. Lett. **96**, 110404 (2006) [hep-th/0510092].

[86] M. Levin and X. G. Wen, "Detecting topological order in a ground state wave function," Phys. Rev. Lett. **96**, 110405 (2006) [cond-mat/0510613].

[87] O. Foda, "N=4 SYM structure constants as determinants," JHEP **1203**, 096 (2012), [arXiv:1111.4663].

[88] N. A. Slavnov, "Calculation of scalar products of wave functions and form factors in the framework of the algebraic Bethe Ansatz," Theor. Math. Phys. **79** (1989), 502-508

[89] I. Kostov and Y. Matsuo, "Inner products of Bethe states as partial domain wall partition functions," JHEP **1210**, 168 (2012) [arXiv:1207.2562].

[90] O. Foda and M. Wheeler, "Variations on Slavnov's scalar product," JHEP **1210**, 096 (2012) [arXiv:1207.6871].

[91] J. Escobedo, N. Gromov, A. Sever and P. Vieira, "Tailoring Three-Point Functions and Integrability II. Weak/strong coupling match," JHEP **1109**, 029 (2011) [arXiv:1104.5501].

[92] I. Kostov, "Classical Limit of the Three-Point Function from Integrability," [arXiv:1203.6180].

[93] I. Kostov, "Three-point function of semiclassical states at weak coupling," [arXiv:1205.4412].

[94] E. K. Sklyanin, "Separation of variables - new trends," Prog. Theor. Phys. Suppl. **118**, 35 (1995), [solv-int/9504001].

[95] S. E. Derkachov, G. P. Korchemsky and A. N. Manashov, "Separation of variables for the quantum SL(2,R) spin chain," JHEP **0307**, 047 (2003) [hep-th/0210216].

[96] E. Sobko, "A new representation for two- and three-point correlators of operators from sl(2) sector," [arXiv:1311.6957].

[97] G. Niccoli, "Antiperiodic spin-1/2 XXZ quantum chains by separation of variables: Complete spectrum and form factors," Nucl. Phys. B **870**, 397 (2013) [arXiv:1205.4537].

[98] G. Niccoli, "Form factors and complete spectrum of XXX antiperiodic higher spin chains by quantum separation of variables," [arXiv:1206.2418].

[99] M. Aganagic, A. Klemm, M. Marino and C. Vafa, "Matrix model as a mirror of Chern-Simons theory," JHEP **0402**, 010 (2004) [hep-th/0211098].

[100] K. Zarembo, "Holographic three-point functions of semiclassical states", JHEP **09** (2010) 030, [arXiv:1008.1059].

[101] M.S. Costa, R. Monteiro, J.E. Santos and D. Zoakos, "On three-point correlation functions in the gauge/gravity duality", JHEP **11** (2010) 141, [arXiv:1008.1070].

[102] R. Roiban and A.A. Tseytlin, "On semiclassical computation of 3-point functions of closed string vertex operators in $AdS_5 \times S^5$", Phys.Rev. **D 82** (2010) 106011, [arXiv:1008.4921].

[103] J. A. Minahan, "Holographic three-point functions for short operators," JHEP **1207**, 187 (2012) [arXiv:1206.3129].

[104] T. Bargheer, J. A. Minahan and R. Pereira, "Computing Three-Point Functions for Short Operators," [arXiv:1311.7461].

[105] R. A. Janik and A. Wereszczynski, "Correlation functions of three heavy operators - the AdS contribution," [arXiv:1109.6262].

[106] S. S. Gubser, I. R. Klebanov and A. M. Polyakov, "A Semiclassical limit of the gauge / string correspondence," Nucl. Phys. B **636**, 99 (2002) [hep-th/0204051].

[107] K. Pohlmeyer, "Integrable Hamiltonian Systems and Interactions Through Quadratic Constraints," Commun. Math. Phys. **46**, 207 (1976).

[108] H. J. De Vega and N. G. Sanchez, "Exact integrability of strings in D-Dimensional De Sitter space-time," Phys. Rev. D **47**, 3394 (1993).

[109] R. A. Janik and P. Laskos-Grabowski, "Surprises in the AdS algebraic curve constructions: Wilson loops and correlation functions," [arXiv:1203.4246].

[110] H. M. Farkas and I. Kra, "Riemann surfaces," Springer New York, 1992.

[111] J. Caetano and J. Toledo, "χ-Systems for Correlation Functions", [arXiv:1208.4548]

[112] D. Gaiotto, G. W. Moore and A. Neitzke, "Wall-crossing, Hitchin Systems, and the WKB Approximation", [arXiv:0907.3987].

[113] L.F. Alday, J. Maldacena, A. Sever and P. Vieira, "Y-system for Scattering Amplitudes", J.Phys. **A 43** (2010) 485401, [arXiv:1002.2459].

[114] D. Honda and S. Komatsu, "Classical Liouville Three-point Functions from Riemann-Hilbert Analysis," [arXiv:1311.2888].

[115] N. Gromov, A. Sever and P. Vieira, "Tailoring Three-Point Functions and Integrability III. Classical Tunneling," [arXiv:1111.2349].

[116] D. Serban, "A note on the eigenvectors of long-range spin chains and their scalar products," [arXiv:1203.5842].

[117] V. V. Bazhanov, S. L. Lukyanov and A. B. Zamolodchikov, "Higher level eigenvalues of Q operators and Schroedinger equation," Adv. Theor. Math. Phys. **7**, 711 (2004) [hep-th/0307108].

[118] O. Foda, Y. Jiang, I. Kostov and D. Serban, "A tree-level 3-point function in the $su(3)$-sector of planar $N = 4$ SYM," [arXiv:1302.3539].

[119] P. Vieira and T. Wang, "Tailoring Non-Compact Spin Chains" [arXiv:1311.6404].

[120] E. K. Sklyanin, "Separation of variables in the quantum integrable models related to the Yangian Y[sl(3)]," J. Math. Sci. **80**, 1861 (1996) [Zap. Nauchn. Semin. **205**, 166 (1993)] [hep-th/9212076].

[121] F. A. Smirnov, "Separation of Variables for Quantum Integrable Models Related to $U_q(\widehat{sl}_N)$." Math. Phys. Odyssey 2001: Integrable Models and Beyond: in Honor of Barry M. McCoy 21 (2002): 455 [math-ph/0109013].

[122] R. Dijkgraaf and C. Vafa, "On geometry and matrix models," Nucl. Phys. B **644**, 21 (2002) [hep-th/0207106].

[123] Y. Jiang, I. Kostov, F. Loebbert and D. Serban, "Fixing the Quantum Three-Point Function," [arXiv:1401.0384].

[124] D. Gaiotto, G. W. Moore and A. Neitzke, "Spectral networks," Annales Henri Poincare **14**, 1643 (2013) [arXiv:1204.4824].

[125] O. Aharony and Z. Komargodski, "The Space-time operator product expansion in string theory duals of field theories," JHEP **0801**, 064 (2008) [arXiv:0711.1174].

[126] E. Witten, "The Feynman $i\epsilon$ in String Theory," [arXiv:1307.5124].

[127] H. Dorn and H. J. Otto, "Two and three point functions in Liouville theory," Nucl. Phys. B **429**, 375 (1994) [hep-th/9403141].

[128] A. Zamolodchikov and Al. Zamolodchikov, "Conformal bootstrap in Liouville field theory," Nucl. Phys. B **477**, 577 (1996) [hep-th/9506136].

[129] J. Teschner, "On the Liouville three point function," Phys. Lett. B **363**, 65 (1995) [hep-th/9507109].

[130] L. Chekhov, B. Eynard and S. Ribault, "Seiberg-Witten equations and non-commutative spectral curves in Liouville theory," J. Math. Phys. **54**, 022306 (2013) [arXiv:1209.3984].

[131] D. Honda and S. Komatsu, Work in progress.

[132] B. Basso, A. Sever and P. Vieira, "Space-time S-matrix and Flux-tube S-matrix at Finite Coupling," Phys. Rev. Lett. **111**, 091602 (2013) [arXiv:1303.1396].

[133] B. Basso, A. Sever and P. Vieira, "Space-time S-matrix and Flux tube S-matrix II. Extracting and Matching Data," [arXiv:1306.2058].

[134] G. W. Moore and N. Seiberg, "Classical and Quantum Conformal Field Theory," Commun. Math. Phys. **123**, 177 (1989).

[135] L. F. Alday, D. Gaiotto, Y. Tachikawa, "Liouville Correlation Functions from Four-dimensional Gauge Theories," Lett. Math. Phys. **91**,167 (2010) [arXiv:0906.3219].

[136] N. A. Nekrasov and S. L. Shatashvili, "Quantization of Integrable Systems and Four Dimensional Gauge Theories," [arXiv:0908.4052].

[137] I. Kostov "Three point correlation function in SU(2) sector for heavy fields", talk presented at *Todai/Riken joint workshop on Super Yang-Mills, solvable systems and related subjects.*
E. Bettelheim and I. Kostov, "Semi-classical analysis of the inner product of Bethe states", [arXiv:1403.0358].

[138] E. K. Sklyanin, *Quantum inverse scattering method. Selected topics*, in *Quantum Groups and Quantum Integrable Systems* (Nankai Lectures in Mathematical Physics), ed. Mo-Lin Ge (World Scientific, 1992), pp.63-97, [hep-th/9211111].

[139] A. G. Izergin, "Partition function of the six-vertex model in a finite volume," Sov. Phys. Dokl. **32** (1987), 878-879